

**EVALUATION OF TOPICAL BIOAVAILABILITY IN HUMAN
STRATUM CORNEUM IN VIVO BY TAPE STRIPPING USING
A DIRECT SPECTROSCOPIC METHOD**

Inauguraldissertation

zur

Erlangung der Würde eines Doktors der Philosophie

vorgelegt der

Philosophisch-Naturwissenschaftlichen Fakultät

der Universität Basel

von

Tatiana Fässler Tassopoulos

aus Basel (BS)

Riehen, 2006

Genehmigt von der Philosophisch-Naturwissenschaftlichen Fakultät
auf Antrag von

Herrn Professor Dr. H. Leuenberger

Herrn PD Dr. G. Imanidis

Herrn Professor Th. Rufli

Herrn Professor Dr. C. Surber

Basel, den 14. Februar 2006

Professor Dr. Hans-Jakob Wirz

Dekan

Quidquid agis, prudenter agas et respice finem!

ACKNOWLEDGEMENTS

The following dissertation “Evaluation of Topical Bioavailability in Human Stratum Corneum in vivo by Tape Stripping using a Direct Spectroscopic Method” was based on research carried out in the Institute of Hospital Pharmacy and the Department of Dermatology, Kantonsspital Basel, University Hospital, Basel, Switzerland.

Listed below are the many persons involved who, during the course of this dissertation, helped contribute to its realization and completion.

Special thanks are extended to:

- Prof. Dr. Christian Surber, Institute of Hospital Pharmacy, Kantonsspital Basel for his mentorship, vision and fruitful discussions which stimulated my interest in new advances in dermatopharmacology. I am deeply grateful for having had the privilege of carrying out this work in his Department.
- Prof. Dr. Theo Rufli, Department of Dermatology, Kantonsspital Basel for the opportunity of integrating me into the clinical aspects of dermatology and for agreeing to act as an reviewer of the thesis.
- Dr. Eric Smith, College of Pharmacy, University of South Carolina, USA, for his encouragement and motivation.
- Ms Verena Figueiredo, Institute of Hospital Pharmacy, Kantonsspital Basel, for her analytical expertise and attention to details.
- PD Dr. Georg Imanidis, Department of Pharmacy, University of Basel, for his assistance with various mathematical approaches in the “Membrane-Transport-Seminar” which also gave me the opportunity of exchanging scientific ideas and problems with my PhD student colleagues Dr. Charu Kochhar, Dr. Gabi Betz, Dr. Marc Sutter, Dr. Timo Schmidt, Dr. Melanie Altenbach, Ms Susanne Reitbauer and Mr Heiko Nalenz.
- Prof. Dr. Hans Leuenberger to present this work to the faculty.
- Dr. Micheal Wall for his statistical recommendations for the clinical studies.
- Dr. Hans-Jürgen Weigmann, Prof. Jürgen Lademann and Dr. Ute Lindenmann, all from the Center of Experimental and Applied Cutaneous Physiology, Department of Dermatology, Humboldt University Berlin, Germany, for exchange of knowledge concerning two different approaches to tape stripping in combination with UV/VIS spectroscopy.
- The graduate students Ms Stefanie Mäder and Ms Hoa Vuong for their help in carrying out the clinical studies.

- Mr Horst Westenfelder and Ms Irene Herde, Roche Vitamins Ltd., Kaiseraugst, Switzerland, for allowing me to produce the sunscreen formulations in their laboratories under standardized conditions.
- Spirig Ltd., Egerkingen, Switzerland, for their financial support.
- Dr. Jan Izakovic, Mr Hans-Martin Roffler and Ms Helen Oxley for reading the manuscript.
- Dr. Geraldine D. Shantz for editing the text, tables and figures for scientific comprehension and clarity of this thesis.
- And finally, to my family and to Reto for their continued encouragement and moral support throughout the entire process.

TABLE OF CONTENTS

1	ABSTRACT	10
2	INTRODUCTION	13
3	STRUCTURE AND FUNCTION OF THE HUMAN SKIN	17
3.1	ANATOMY OF THE SKIN	18
3.1.1	<i>Stratum corneum</i>	18
3.1.2	<i>Epidermis</i>	19
3.1.3	<i>Dermis</i>	19
3.2	BARRIER FUNCTION OF THE STRATUM CORNEUM	20
3.3	THE RESERVOIR OF THE STRATUM CORNEUM	22
3.4	LIPID ORGANIZATION WITHIN THE SKIN BARRIER	23
3.5	DESQUAMATION	25
3.6	DRUG PERMEATION ROUTES	27
4	SOLAR RADIATION	27
4.1	ACUTE AND CHRONIC DAMAGE TO THE SKIN DUE TO UV RADIATION	28
4.2	PROTECTIVE MECHANISMS OF THE SKIN	30
5	SUNSCREEN PRODUCTS	31
5.1	SUN PROTECTION FACTOR	31
5.2	SUNSCREENING AGENTS	32
6	TOPICAL BIOAVAILABILITY OF SUNSCREENING AGENTS	33
6.1	DEFINITION	33
6.2	TARGET SITES	33
6.3	FACTORS AFFECTING THE BIOAVAILABILITY OF SUNSCREENING AGENTS	34
6.3.1	<i>Influence of the compound attributes</i>	35
6.3.1.1	Permeation - Mathematical models for the prediction of skin absorption	35
6.3.1.2	Toxicology	37
6.3.2	<i>Influence of the skin</i>	38
6.3.2.1	Age and race	38
6.3.2.2	Anatomical site	38
6.3.2.3	Skin temperature and hydration	39
6.3.2.4	Diseased and damaged skin	39
6.3.2.5	Differences between subjects	40
6.3.3	<i>Influence of application parameters</i>	40
6.3.3.1	Dosing / Application thickness	40
6.3.3.2	Application technique	42
6.3.3.3	Loss of vehicle from the skin surface	44
6.3.4	<i>Influence of the vehicle</i>	45
6.3.4.1	The sunscreen product vehicle	45
6.3.4.2	Substantivity	46

6.3.4.3	The vehicle interactions	47
6.3.4.3.1	Drug-skin interactions	47
6.3.4.3.2	Vehicle-drug interactions	47
6.3.4.3.3	Vehicle-skin interactions	48
6.3.4.3.4	Vehicle-drug–skin interactions	49
6.4	SUNSCREEN PRODUCT OPTIMIZATION	50
7	DRUG MEASUREMENT IN THE STRATUM CORNEUM.....	51
7.1	SKIN SCRAPING	51
7.2	SKIN SURFACE BIOPSY	51
7.3	TAPE STRIPPING	51
7.3.1	<i>Tape stripping technique</i>	51
7.3.2	<i>Application of the tape stripping technique</i>	52
7.3.3	<i>Dermatopharmacokinetics</i>	52
7.3.4	<i>Quantification of stratum corneum removed</i>	53
8	ORIGINAL PUBLICATIONS.....	57
8.1	SIMULTANEOUS SPECTROPHOTOMETRIC DETERMINATION OF A SUNSCREEN AGENT AND RELATIVE STRATUM CORNEUM TISSUE DENSITY IN SKIN TAPE STRIPS. I. VALIDATION OF ANALYTICAL METHODOLOGY.	57
8.2	SIMULTANEOUS SPECTROPHOTOMETRIC DETERMINATION OF A SUNSCREEN AGENT AND RELATIVE STRATUM CORNEUM TISSUE DENSITY IN SKIN TAPE STRIPS. II. APPLICATION OF THE METHOD IN HUMANS	74
8.3	SIMULTANEOUS SPECTROPHOTOMETRIC DETERMINATION OF A SUNSCREEN AGENT AND RELATIVE STRATUM CORNEUM TISSUE DENSITY IN SKIN TAPE STRIPS. III. COMPARISON OF VEHICLE EFFECTS IN HUMANS	86
9	OVERALL CONCLUSION AND FUTURE PERSPECTIVES	98
10	APPENDIX	102
10.1	PHYSICAL AND CHEMICAL DATA FOR 4-METHYLBENZYLIDENE CAMPHOR	102
10.2	UV/VIS SPECTROPHOTOMETER SPECIFICATION	103
10.2.1	<i>Introduction</i>	103
10.2.2	<i>Adaptations of Perkin-Elmer Lambda 35 UV/VIS-Spectrometer</i>	104
10.3	SELECTION OF ADHESIVE TAPE	106
10.3.1	<i>Physicochemical properties of adhesive tapes</i>	106
10.4	VALIDATION	109
10.4.1	<i>UV/VIS Method</i>	109
10.4.1.1	UV/VIS spectrophotometric procedure	109
10.4.1.2	The template	109
10.4.1.3	Specificity	111
10.4.1.3.1	The absorbance spectrum	112
10.4.1.3.2	Influence of skin and time on the 4-MBC absorbance	113
10.4.1.4	Linearity and Range	114
10.4.1.5	Agreement between nominal and measured 4-MBC concentrations	115
10.4.1.6	Exclusion of Matrix Effects in the Low Concentration Range	116
10.4.1.7	Reference Calibration Curve	117
10.4.1.8	Lack-of-Fit Test	118
10.4.1.9	Detection Limit and Quantitation Limit	119
10.4.1.10	Repeatability and intermediate precision	121

10.4.1.11	Accuracy by comparison	122
10.4.2	<i>HPLC Method</i>	122
10.4.2.1	Chromatographic conditions.....	122
10.4.2.2	Specificity	123
10.4.2.3	Linearity and Range	124
10.4.2.4	Detection Limit and Quantitation Limit.....	126
10.4.2.5	Repeatability and Intermediate Precision	127
10.4.2.6	Accuracy by recovery	128
10.5	EXPERIMENT 1.....	130
10.5.1	<i>4-MBC Sunscreen formulation</i>	131
10.5.1.1	Ingredients	131
10.5.1.2	Stability testing	133
10.5.2	<i>Determination of 4-MBC concentration in formulation</i>	134
10.5.2.1	Material	134
10.5.2.2	Method	134
10.5.2.3	Results	134
10.5.3	<i>Study Design for Experiment 1</i>	135
10.5.4	<i>Tape stripping procedure</i>	135
10.5.5	<i>Results</i>	137
10.5.5.1	Correlation of UV/VIS spectroscopy with HPLC (Accuracy by comparison).....	137
10.5.5.2	Stratum Corneum Profiles	140
10.5.5.3	Amount of 4-MBC penetrating the SC (results calculated by the UV/VIS method).....	145
10.6	EXPERIMENT 2.....	147
10.6.1	<i>Vehicles</i>	147
10.6.1.1	Propylene glycol.....	147
10.6.1.2	Mineral oil.....	148
10.6.2	<i>Determination of solubility of 4-MBC in vehicles</i>	149
10.6.2.1	Material	149
10.6.2.2	Method	149
10.6.2.3	Results	150
10.6.3	<i>Study Design for Experiment 2</i>	151
10.6.4	<i>Inclusion Exclusion Criteria</i>	153
10.6.4.1	Inclusion Criteria.....	153
10.6.4.2	Exclusion Criteria	153
10.6.5	<i>Results</i>	154
10.6.5.1	Stratum Corneum Profiles	154
10.6.5.2	Results for Experiment 2: AUC _{conc-sc}	159
10.6.5.3	Statistical analysis of results for Experiment 2	159
10.6.5.4	Number of tapes stripped	160
10.7	EXPERIMENT 3.....	162
10.7.1	<i>Vehicles</i>	162
10.7.1.1	Polyethylene glycol 400.....	162
10.7.1.2	Transcutol®CG	163
10.7.2	<i>Determination of 4-MBC solubility</i>	163
10.7.2.1	Method	163
10.7.2.2	Material	164

10.7.2.3	Results.....	164
10.7.3	<i>Study Design for Experiment 3</i>	165
10.7.4	<i>Results</i>	167
10.7.4.1	Stratum Corneum Profiles.....	167
10.7.4.2	Results for Experiment 3: AUC _{conc-sc}	177
10.7.4.3	Statistical Analysis of results for Experiment 3	177
10.7.4.3.1	Formulation with 10% Transcutol®CG vs formulation with 0% Transcutol®CG	178
10.7.4.3.2	Formulation with 50% Transcutol®CG vs formulation with 0% Transcutol®CG	179
10.8	CALCULATION OF INTRA-INDIVIDUAL VARIANCE FOR DETERMINATION OF NUMBER OF VOLUNTEERS	180
11	REFERENCES	182
12	CURRICULUM VITAE	194

LIST OF ABBREVIATIONS

ANOVA	Analysis of Variance
AUC _{conc-sc}	Area Under the Curve of the concentration in the stratum corneum
CI	Confidence Interval
COLIPA	European Cosmetic Toiletry and Perfumery Association
CV	Coefficient of Variation
D	relevant Difference
δ (delta)	logarithmic value of relevant Difference
Df	Degrees of freedom
DL	Detection Limit
DMAC	Dimethylacetamide
DMFA	Dimethylformamide
DMSO	Dimethylsulfoxide
DNA	Desoxyribonucleic acid
DPK	Dermatopharmacokinetics
f	female
F	Formulation
FDA	Food and Drug Administration
g	gram
h	hour
HPCD	Hydroxypropyl- β -cyclodextrin
HPLC	High Performance Liquid Chromatography
ICH	International Conference on Harmonization of Technical Requirements for Registration of Pharmaceuticals for Human Use
INCI	International Nomenclature of Cosmetic Ingredients
IUPAC	International Union of Pure and Applied Chemistry
λ (lambda)	wavelength
L	Litre
m	male
μ (micro)	micro
4-MBC	4-Methylbenzylidene Camphor

MED	Minimal Erythema Dose
MO	Mineral Oil
n (nano)	nano
PEG 400	Polyethylene Glycol 400
PG	Propylene Glycol
pKa	negativ logarithm of dissociation constant
QL	Quantitation Limit
r	correlation coefficient
rpm	revolutions per minute
σ (sigma)	intra-individual standard deviation
σ^2 (sigma square)	intra-individual variance
SC	Stratum Corneum
SCTE	Stratum Corneum Tryptic Enzyme
SCCE I	Stratum Corneum Chymotryptic Enzyme
SD	Standard Deviation
SLN	Solid Liquid Nanoparticles
SPF	Sun Protection Factor
Sr	Standard error of estimates
s^2_y	residual variance
t	time
TI	Time Interval
TEWL	Transepidermal Water Loss
Transcutol [®] CG	Diethylene glycol monoethyl ether
UV	Ultraviolet
VIS	Visible
vs	versus
v/v	volume over volume
w/w	weight over weight
\bar{x}	arithmetic mean

DEFINITIONS OF TERMS

Percutaneous Absorption	A general term which describes the passage of a compound through the skin but does not necessarily indicate its eventual fate. The process can be subdivided into the following steps. 1. Penetration 2. Permeation
Transdermal formulation	A formulation which after local application to the skin surface allows active drug to reach the systemic circulation.
Topical formulation	A formulation designed for local delivery i.e. after local application to the skin no drug should reach the systemic circulation.
Cosmetics (MESH Term)	Formulations containing compounds designed to remain on the skin surface. Substances designated for application to the human body for cleansing, beautifying, promoting attractiveness or altering the appearance without affecting the skin's structure or functions. Included in this definition are skin creams, lotions, perfumes, lipsticks, fingernail polishes, eye and facial makeup preparations, permanent waves, hair colors, toothpastes and deodorants as well as any material intended for use as a component of a cosmetic product .
Sunscreening agent (MESH Term)	A chemical or physical agent that protects the skin from sunburn and erythema by absorbing or blocking ultraviolet radiation. Synonym: UV filter, sunscreen agent
Sunscreen product	Formulation (emulsion, oil, gel, mousse, aerosol, stick and ointment) that contains sunscreening agents and that is used to protect the skin from excessive ultraviolet radiation.

1 Abstract

The objective of this thesis was to develop a spectrophotometric methodology for simultaneous determination of a sunscreensing agent and relative stratum corneum tissue density in skin tape strips. This methodology was then employed to investigate the effect of different vehicles and their application time on the penetration of the sunscreensing agent into the stratum corneum (SC) and the ability of these vehicles to create a reservoir. Tape stripping of the stratum corneum from the skin is a relatively non-invasive and useful technique used for bioavailability and dermatopharmacokinetic studies of topically-applied drugs.

As model compound the sunscreensing agent 3-(4-Methylbenzylidene)camphor (4-MBC) was chosen because of its high absorbance potential ($A_{1\text{ cm}}^{1\%}$ 930-990 at 299 nm) and its high affinity to the SC which may be inferred by its low solubility in water (0.00013 g in 100 mL). To be able to conduct SC measurements directly on a tape by UV/VIS spectroscopy, a Perkin Elmer UV/VIS spectrophotometer was modified providing a uniform measurement area of 1 cm² to measure the absorbance through the sample as a result of light scattering by the SC on the tapes.

A spectroscopic UV/VIS method determining the model compound 4-MBC and SC simultaneously in skin tape strips was then developed directly on tape strips and validated according to the International Conference on Harmonization of Technical Requirements for Registration of Pharmaceuticals for Human Use (ICH) guidelines. For SC measurements this technique has distinct advantages in terms of facile sample handling procedures when compared with previously described methods such as tape strip weighing, protein determination and extraction procedures which are laborious and are susceptible to analytical artifacts. The validation parameters of the UV/VIS method were compared to those of a conventional solvent extraction/HPLC method. The data of the two analytical methods were found to be equally accurate and precise in determining sunscreen abundance in the corneocyte layers removed by tape stripping. However, the direct spectrophotometric technique obviates the need for any tape extraction process prior to analysis of 4-MBC and SC, and is sensitive enough for the accurate determination of low analyte concentrations on the tape strips since there is no loss of analyte in the sample handling protocol.

The validation was further completed by comparing the data of an in vivo tape stripping

experiment measured by the UV/VIS method and the solvent extraction/HPLC method. For this purpose the tape stripping procedure has been optimized and standardized using a strict protocol to minimize the variability of the tape stripping data. The 4-MBC delivery from a 2% and 4% 4-MBC emulsions was then investigated in vivo using five human volunteers. A dose of 2 mg/cm² was applied to the volar forearm for one hour. The tapes were analyzed by the new UV/VIS method by determining simultaneously the 4-MBC abundance and the relative density of SC. The tapes were then extracted and the 4-MBC concentrations obtained by direct spectrophotometric quantification were verified by HPLC. The linear correlation factor was 0.974 and statistical analysis confirmed that there was no statistical difference ($p > 0.05$) between the two analytical procedures. The total mass of compound delivered from a vehicle was calculated by summing the 4-MBC abundance determined per tape and area of tape strip. Thereby, the first tape was always discarded. The results showed a statistically significant ($p < 0.05$) influence of the dosing strength (2% vs 4%) of the formulations on the penetration of 4-MBC.

This investigation revealed that the newly developed spectroscopic method is rapid, precise and as accurate as a conventional HPLC method for the in vivo determination of sunscreens agent delivery from topical applied formulations.

Finally, the delivery of 4-MBC from several representative vehicles was compared using the direct spectrophotometric determination method and according to GCP procedures. To be able to detect vehicle effects on the penetration of 4-MBC into the SC, all vehicles used in the study were saturated with 4-MBC.

In the first experiment the influence of propylene glycol and mineral oil and of their application time on 4-MBC penetration was investigated in five volunteers. Although the solubility of 4-MBC was approximately 3.5 times lower in propylene glycol than in mineral oil, the 4-MBC delivery into the SC was significantly higher from propylene glycol. This observation can be explained by the ability of propylene glycol to decrease SC permeability. The number of tape strips required to completely remove the SC in the presence of the propylene glycol was significantly lower revealing a loosening of corneocytes and thus a facilitated penetration of 4-MBC into the SC. The application time showed no influence on the 4-MBC penetration.

In a further experiment, PEG 400 vehicles containing 0%, 10% and 50% Transcutol[®]CG were evaluated in ten subjects for their ability to create a reservoir of 4-MBC in the skin. This was evaluated seven hours post vehicle application. The solubility of 4-MBC increased with increasing Transcutol[®]CG concentration in the vehicle. The 4-MBC delivery from the three

vehicles was proportional to the 4-MBC concentration in the vehicle. The vehicles containing 0% and 10% Transcutol[®]CG showed no difference in the 4-MBC amount measured in the SC seven hours post application compared to the 4-MBC amount measured in the SC one hour post application. For PEG 400 containing 50% Transcutol[®]CG the 4-MBC amount remaining in the SC seven hours post application was smaller than one hour post application.

This study clearly demonstrated that this methodology is, therefore, capable of detecting differences in the extent of reservoir formation of the sunscreen when applied to the skin in different delivery vehicles.

2 Introduction

Tape stripping of the stratum corneum from the skin is a relatively non-invasive and useful technique that has been used widely in recent years for bioavailability and dermatopharmacokinetic studies of topically-applied drugs [1]. The numerous problems associated with the standardization of the tape stripping methodology have been documented at length [2, 3]. The general technique used to date involves topical dosing, followed by application and subsequent removal of adhesive tape strips from the skin; corneocytes adhering to the tape strips are thereby removed from the underlying tissue. Each tape used in the stripping process (often 30-50 strips in total from each stripped skin site) is usually then solvent extracted to isolate the analyte of interest, prior to high sensitivity analysis. However, the adhesive tape stripping of the stratum corneum is not a linear process in terms of the thickness of the layer of corneocytes removed from one strip to the next, and is not uniform in thickness across the entire field of each tape area (see electron micrographs) [2]. This procedure, therefore, relates the mass of permeant found on each strip to the tape strip number analyzed, and not (strictly) to stratum corneum depth or volume [4-7]. A modification of this methodology that has been researched involves the weighing of the tape strips on a high-sensitivity balance before and after stripping to obtain a mass of tissue removed with each strip [8-11]. Alternatively, tissue mass on the tape strips has been determined in terms of protein content using the Lowry method [8]. These tape strip weighing, protein determination and extraction procedures are laborious and are susceptible to analytical artefacts (e.g. vaporization of volatile components of the tape matrix, static charges on the tape strip, etc.). Alternatively, a technique has been researched recently that allows the simultaneous analysis of corneocyte density and xenobiotic abundance using ultraviolet and visible (UV/VIS) spectroscopy [12-14]. This technique has distinct advantages in terms of facile sample handling procedures when compared with previously described methods. We have used the principle of this technique as a basis for the fully-validated studies reported here.

The purpose of this research was: firstly, to develop a standardized method for the direct assessment of tapes removed from the skin without the need to conduct any preparative procedures (such as extraction or weighing) that may introduce artefacts into the analysis. Secondly, to develop a method capable of the simultaneous, accurate and simple, UV/VIS spectrophotometric determination of both analyte concentration and relative corneocyte

density on each tape strip. Thirdly, to fully validate both the new, direct UV/VIS analysis of tapes and the conventional sample extraction/HPLC analysis procedure as a reference, according to current guidelines, in order to assure that either technique may be deemed fit for purpose. The new UV/VIS method must be shown to be as good as the HPLC technique if it is to be used for routine analysis.

A validated direct spectrophotometric technique would obviate the need for an extraction process prior to analysis, but would have to be sensitive enough for determination of low analyte concentrations. Moreover, simultaneously obtaining the relative fraction of stratum corneum adhering to each tape would allow the mass of analyte found to be related directly to the relative amount of tissue removed by each tape strip, thereby providing a method for depicting a generalized penetration profile of the analyte into, or retention in, the stratum corneum layers.

Background, Rational and Purpose

In topical bioavailability studies, tape stripping is a simple, useful technique to quantify drugs in the stratum corneum. In addition, it has the further advantage of being non-invasive.

Despite these advantages, High Performance Liquid Chromatography (HPLC) is currently considered the standard method for quantifying the amount of drug on tapes. However, with HPLC, the final results can not be obtained in one step. Here, the stratum corneum (SC) as well as the drugs, must first of all be extracted before they can be quantified.

To date, the extraction procedures employed are not only laborious but also susceptible to analytical artefacts. Thus, it would be both desirable and optimal if the standard multistep method requiring extraction and HPLC analysis of SC and drugs could be replaced by a simple, accurate and reliable one-step method.

Weigmann and Lademann [12] recently developed an ultraviolet/visible (UV/VIS) spectroscopic method for directly determining the amount of SC on tapes. However, to obtain a drug penetration profile of the SC, an extraction of drug from the tapes was required in another step.

Thus, the purpose of the present thesis was to develop a direct, one-step UV/VIS spectroscopic method for quantifying both the SC and sunscreens such as 4-methylbenzylidene camphor (4-MBC) on tapes (Figure 1).

This new, one-step method should not only be simple and efficient but also reliable and reproducible and, in addition, should be equally as sensitive as the standard multistep method.

Validation and Verification of the Method

Chapter 8.1 concerns validation of two methods: - the one-step UV/VIS spectroscopic method and the multistep HPLC method requiring extraction procedures. The validation parameters were performed according to the International Conference on Harmonization of Technical Requirements for Registration of Pharmaceuticals for Human Use (ICH) Guidelines and the Food and Drug Administration (FDA) Guidance for Industry.

Chapter 8.2 concerns verification of drug concentrations obtained from the direct one-step method by the multistep method after topical application of a 2% and 4% 4-MBC formulation.

Influence of Vehicle on Topical Bioavailability of 4-MBC

Chapter 8.3 describes the influence of vehicles such as mineral oil and propylene glycol and their duration of application on the topical bioavailability of 4-MBC.

Chapter 8.3 concerns also a clinical study in which the concentration of Transcutol®CG on the substantivity of 4-MBC was investigated.

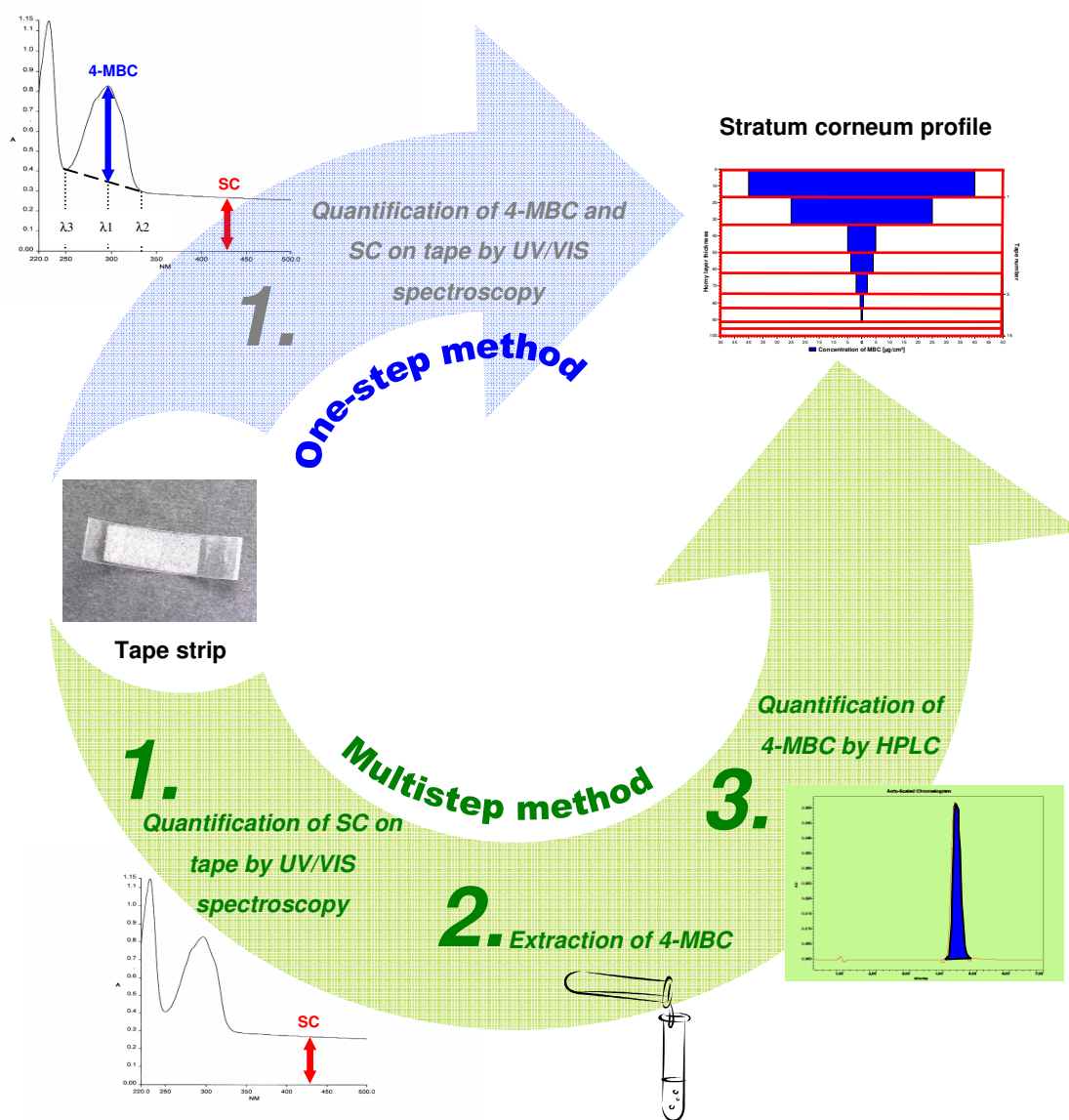


Figure 1 Scheme illustrating distribution of 4-MBC in SC obtained by a new, direct one-step spectroscopic method vs. an established, multistep method.

In the experimental part of this thesis, 4-MBC, a sunscreensing agent, is the drug of interest. Thus, in Chapters 3-7 which describe important aspects of topical bioavailability in relation to the present work examples, whenever possible, are given concerning sunscreensing agents.

3 Structure and function of the human skin

The skin is the largest organ of the body covering 15'000-20'000 cm² and weighing several kilograms. It is the interface of the body with an environment and barrier for minimizing transport of harmful materials into the body. The skin is a highly organized, heterogeneous and multilayered organ. The upper region called the SC, the non-viable part of the epidermis, is between 10-20 µm thick. Underlying this region is the viable epidermis (20-100 µm) and then the dermis (1-2 mm) [15]. The sum of these various layers together with their appendages and underlying microvasculature constitute a living envelope surrounding the body (Figure 2).

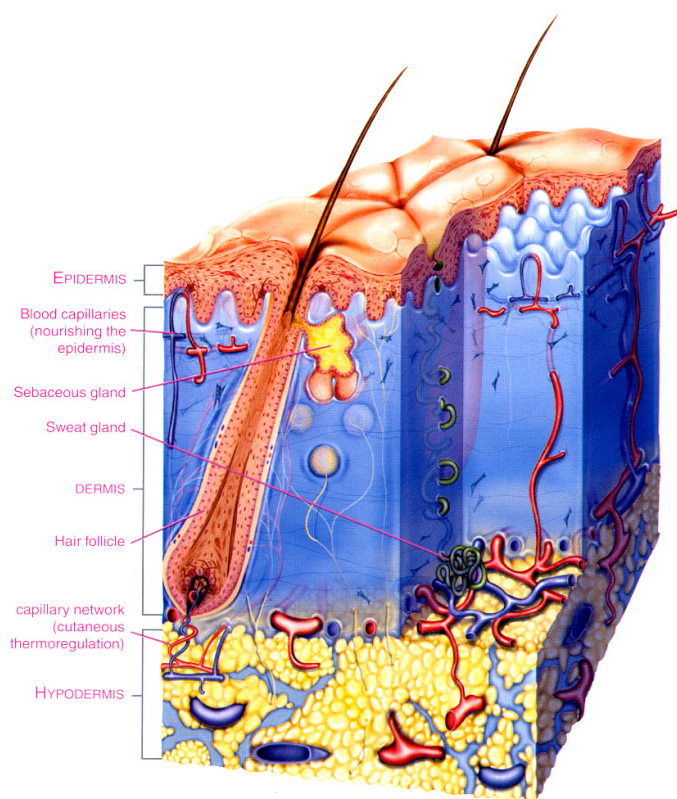


Figure 2. Schematic representation of the structure of the skin.

3.1 Anatomy of the skin

3.1.1 Stratum corneum

The SC is the final product of epidermal differentiation and forms a highly resistant, compact, horny layer made up of approximately 15-25 cell layers. Each day, roughly one layer of the SC is lost in a process termed desquamation and one layer is synthesized by the underlying epidermis.

The main elements of the SC are the corneocytes - flat polyhedral-shaped, enucleated, dehydrated, keratinized cells - which are embedded in a matrix of lipid bilayers often described using the analogy of the bricks and mortar of a brick wall [16]. The corneocytes are approximately 20-40 μm in diameter and differ in their thickness depending on the body site and the location within the stratum corneum [17, 18]. The corneocyte cytosol is filled with keratin filaments and is encased by a chemically resistant yet flexible shell the cornified envelope. This cell envelope is composed and stabilized by cross-linked proteins (involucrin, loricrin) and covalently bound lipids (hydroxyceramides) [19-23].

The structure of the cell envelope consists of two parts: (1) a thick layer adjacent to the cytoplasm and composed of structural proteins and; (2) a thin layer on the exterior of the protein part which is composed of lipids.

The principal factors responsible for maintaining attachment between corneocytes is not the intercellular lipid matrix but corneodesmosomes [24]. These junctions are crucial for the structural integrity of the SC barrier. In the lower SC, called stratum compactum, corneocytes are tightly superimposed and hold together by several corneodesmosomes. Further towards the SC surface, the corneocytes are characterized by a loss of corneodesmosomes. The cells detach at these regions forming a much looser SC structure, the stratum disjunctum, where the corneocytes are in a process of desquamation [25, 26].

The SC is composed of approximately 70% protein, 15% lipid and only 15% water, compared to the average 70% water for the viable epidermis [27, 28]. The water content is variable and is controlled by the environmental conditions and the evaporative flux from lower skin layers. SC is extremely hygroscopic: it can absorb up to 500% of its dry weight in less than 1h following immersion in water, swelling vertically to 4-5 times its original width [29].

3.1.2 Epidermis

The cells of the SC originate in the viable epidermis, a layered epithelium made up of four distinct cell layers which correspond to various stages of epidermal keratinocyte differentiation.

The stratum basale or stratum germinativum is a continuous monolayer consisting of cuboidal keratinocytes. This cell layer constantly divides by mitosis forming daughter cells that are displaced outward and then migrate across successive overlaying layers - the stratum spinosum, the stratum granulosum, the stratum lucidum – to finally enter the SC.

During their migration toward corneocytes, the shape of the keratinocytes changes dramatically. The cells flatten considerably and reduce in volume. This progressive altering of keratinocytes is accompanied by biochemical developments, formation of keratins, formation and hydrolysis of lipids, loss of water and cross-linking of cell envelopes.

Although keratinocytes are the major cells within the epidermis, melanocytes involved in skin pigmentation, Langerhans cells which are important for antigen presentation and the immune response - and Merkel cells, the latter of which are thought to be touch receptors, are also found in the epidermis [15, 30].

3.1.3 Dermis

Below the epidermis lies the dermis, a hydrous connective tissue with collagen fibers and elastin both of which are embedded in glycosaminoglycans networks. This tissue determines the tensile strength and the elasticity of the skin. The dermis contains a sparse cell population; the main cells are fibroblasts which produce the connective tissue components: collagen, laminin, fibronectin and vitronectin. In addition to fibroblasts, mast cells which are involved in the immune and inflammatory responses and melanocytes which are involved in the production of melanin are also present in the dermis. The hair follicles and sweat ducts (skin appendages) originate deep within the dermis and terminate at the external surface of the epidermis. Contained within the dermis is an extensive vascular network providing for skin nutrition, repair and immune responses [15, 30].

Table 1. Characteristics of human skin regions.

Skin region	Thickness	pH	Characteristic cells	Vasculature	Function
SC	10-20 μm	4.2-5.6	Corneocytes	None	Barrier
Viable epidermis	50-200 μm	≤ 7.4	Keratinocytes Melanocytes Langerhans cells Merkel cells	None	Biosynthetic factory Metabolic barrier
Dermis	1000-2000 μm	7.4	Fibroblast Endothelial cells Mast cells Macrophages Lymphocytes Leukocytes	Blood vessels Lymphatics	Connective tissue Support

3.2 Barrier function of the stratum corneum

The barrier function of the skin is strongly attributed to the SC. Removal of SC by tape stripping reveals a dramatic increase in the permeability of water and other compounds [31, 32] (Figure 3).

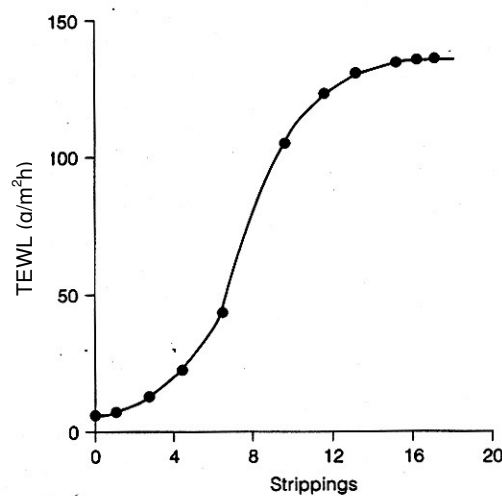


Figure 3. Sequential removal of SC by tape stripping reveals the location of the skin barrier indicated by transepidermal water loss measurements.

The water permeability of the SC is 1000 times lower than most other biological membranes. This is due to the exceptional structural arrangement of the intercellular lipid matrix and the lipid envelope surrounding the corneocytes [33-37]. All the components of the multilamellar lipid matrix present in the SC are produced by keratinocytes in the viable epidermis, essentially in the stratum granulosum. Vesicular structures called lamellar bodies, rich in lipids but also containing various enzymes, fuse with the apical cell membrane of the granular keratinocyte, thus delivering their contents to the interface between the stratum granulosum and the SC. The hydrolytic enzymes start to process their substrates and finally synthesize the SC lipids. The lipids found in the SC are principally ceramides (41%), free fatty acids (9%), cholesterol (27%), cholesteryl esters (10%) and cholesteryl sulfate (2%). Unique to any other known biological membranes, phospholipids are absent [38, 39] (Figure 4). The essential role of the SC lipids in barrier properties has been demonstrated by removal of lipids by solvent extraction, which leads to increased water loss and enhanced skin permeability [40-42].

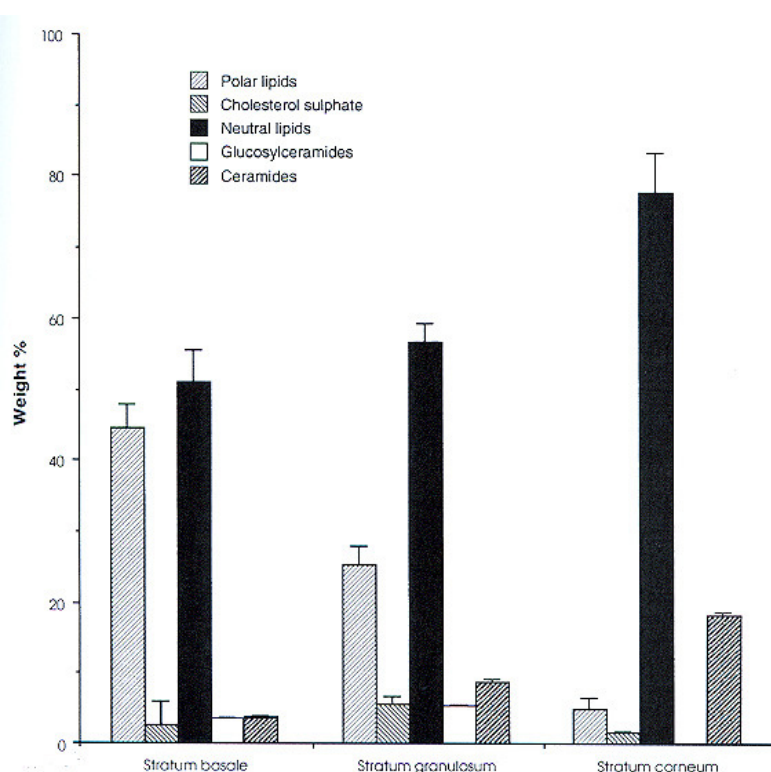


Figure 4. Distribution of lipids in the skin.

Legend. During the course of epidermal differentiation, there are distinct alterations in the distribution of lipid type. Polar phospholipids which are dominant in the basal layer are virtually absent in the outer layers of the stratum corneum. The latter stages of terminal differentiation, the levels of ceramids and neutral lipids increase.

3.3 The reservoir of the stratum corneum

In the literature of the last several decades, the term reservoir has been used to describe the capacity of the skin or the skin layers to store and subsequently deliver, over a prolonged period of time, a xenobiotic to a target site and to other tissues.

Corticosteroids provide the majority of examples for drug reservoir in the skin. Using dermal vasoconstriction as a bioanalytical end point, Vickers [43] showed that corticosteroids remained in the skin for about two weeks after a single, occluded application. This was demonstrated by vasoconstriction from the steroids 7-10 days after topical drug administration (despite washing) by reoccluding the site of application with a plastic.

Barry [44] suggests that the phenomenon is probably a consequence of the high solubility and low diffusivity of the steroids in the SC. Hence, occlusion and penetration enhancers may increase the reservoir of the steroids in the SC. Because of its low diffusivity, the steroid remains trapped in the SC. On reocclusion, diffusivity is promoted and the steroid is absorbed.

It is currently accepted that a reservoir for drugs exists in the SC and that it can be induced by occlusion, increased temperature and humidity [45, 46]. The capacity of a topically applied drug remaining in the SC and thus building a reservoir can be influenced by the nature of the formulation (see section 6.3.4.3). With vasoconstriction as a biomarker, Vickers [47] demonstrated that the vehicle in which the steroid was applied played an important role for drug storage in the SC. The maximum longevity of the reservoir was 9.6 days, which was obtained with an alcoholic solution. With hydrophilic bases, a greater longevity of the reservoir could be achieved than with greasy ointments. In all volunteers, a drug reservoir could be demonstrated after application of the alcohol solution. A diminished longevity of the reservoir obtained with greasy ointments was often not reproducible (Table 2).

Table 2. Effect of vehicle on the development and duration of the reservoir.

Vehicles	Average longevity of the reservoir (days)
Greasy ointment	4.6
Hydrophilic cream	7.4
95% Alcohol	9.6

Legend. Results from 25 volunteers; all were given an adequate dose and the treated skin was occluded; all were previously shown to consistently exhibit drug reservoir.

Stoughton [48, 49] investigated the storage capacity of the SC for hexachlorophen and hydrocortisone. He described the influence of a vehicle containing dimethylacetamide (DMAC) on the deposition of hexachlorophen in the SC. He showed that a vehicle containing 10% DMAC increased the storage capacity of the SC for the drug hexachlorophen by 5 to 25 fold over that of a vehicle without 10% DMAC. Furthermore, the presence of DMAC resulted in a greatly increased biologic activity of the SC. In contrast to the drug hexachlorophen applied in DMAC, the SC reservoir for hexachlorophene was present for 4-5 days whereas after application of hexachlorophen alone no drug was measurable within 24 hours.

In another experiment, Stoughton showed that addition of dimethylsulfoxide to the vehicle established a hydrocortisone reservoir in the SC within a few minutes and increased the longevity of the reservoir to 16 days. Furthermore, the depot of hydrocortisone was resistant to skin cleansing with soap, water and alcohol.

3.4 Lipid organization within the skin barrier

Since lipids form the only continuous region in the SC and substances must diffuse through these lipid areas, the lipid organization of the skin is considered very important. Although the exact structure and physical state of the SC intercellular lipids have not yet been clearly elucidated, studies with mixtures of lipids that mimic SC composition with a diverse range of physical techniques such as x-ray, DSC (Differential Scanning Calorimetry), AFM (Atomic Force Microscopy), NMR (Nuclear Magnetic Resonance) and FTIR (Fourier Transform InfraRed) showed that these lipids are organized in lamellar bilayer structures in which the lipid chains are highly organized [50-56]. These studies also showed that the lipid lamellae are oriented almost parallel to the corneocyte surface with repetitive distances of approximately 6.0-6.4 nm and 13.2-13.4 nm [57-62].

Ceramides play an important role in the lipid organization. To date, eight subclasses of ceramides have been identified in the human SC. Ceramides are sphingolipids that consist of a long chain amino alcohol (sphingosine or one of its derivatives) to which a non-hydroxy fatty acid or an α -hydroxy fatty acid is linked via an amide bond [63] (Figure 5).

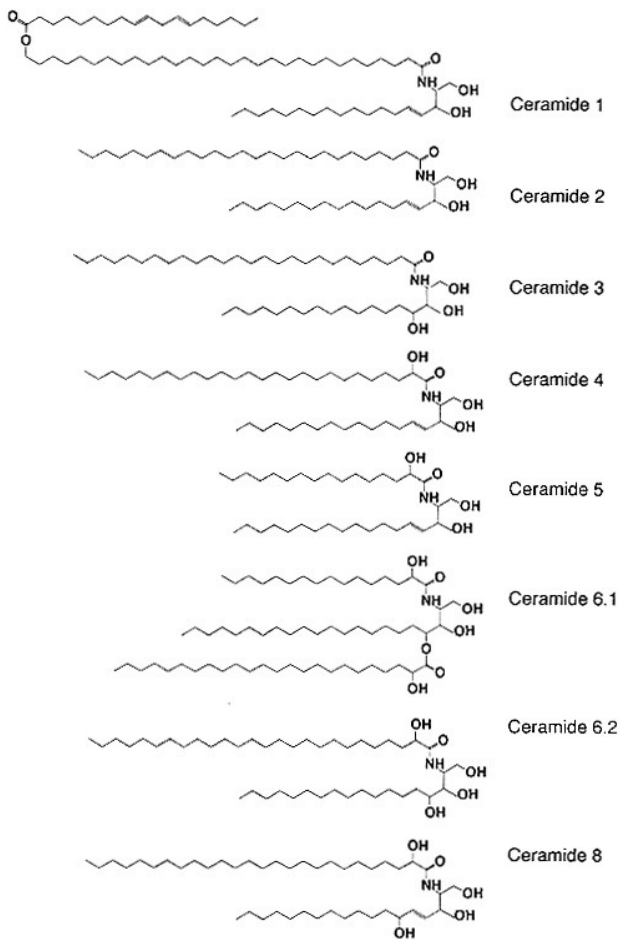


Figure 5. Ceramides of the human stratum corneum intercellular space.

The least polar of the ceramides is designated as ceramide 1, or acylceramide. Ceramide 1 plays an essential role in the formation of the lamellar arrangements. It is thought to function as a molecular rivet, stabilizing the intercellular lipid lamella (Figure 6).

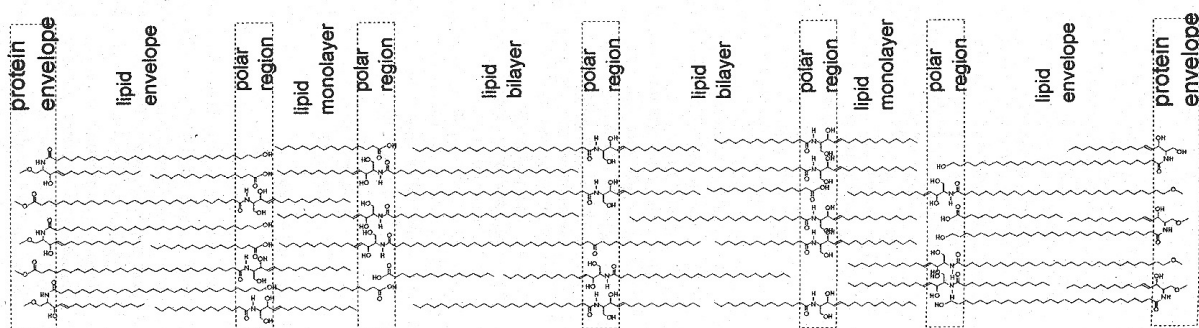


Figure 6. Interpretation of the lipid orientation and interactions that might produce the unique lamellar patterns of the stratum corneum intercellular lamellae.

Wide angle x-ray diffraction studies revealed that in the intercellular lipids several lipid domains coexist which are identified as crystalline, gel and liquid crystalline lipid phases. In the crystalline phase, lipid packing is orthorhombic whereas a hexagonal arrangement is found in the gel phase. In the liquid phase, alkyl chains do not pack into specific arrangements [64-67].

Recently, Norlén [68] postulated a new theoretical model for the structure and function of the skin barrier- the single gel phase model. He proposed that the intercellular lipid within the SC exists as a single and coherent lamellar gel phase. This model differs significantly from earlier models in that it clearly states that phase separation is present, either between liquid crystalline and gel phases or between different crystalline phases with hexagonal and orthorhombic chain packing in the unperturbed barrier structure.

3.5 Desquamation

The barrier function of the skin is facilitated by the continuous desquamation of the horny layer thus preventing lipophilic substances such as sunscreen products from being absorbed into the skin.

The process of desquamation involves the release of intact keratinocytes, presumably after the degradation of the corneodesmosomes, the intercellular adhesive structures between the corneocytes.

The role of the corneodesmosomes was emphasized by Chapman et al. [69] who showed that after sequentially tape stripping the same skin site, the strength of cohesion gradually decreased from the deeper SC towards the skin surface. The decrease of cohesion can be explained by a decrease in the number of corneodesmosomes across the SC.

Suzuki et al. [70] showed that corneodesmosomes are degraded by proteases to liberate corneocytes. Two proteases present in the extracellular spaces of the SC, the SC tryptic enzyme (SCTE) and the SC chymotryptic enzyme (SCCE), are thought to be involved in the proteolysis of the corneodesmosal proteins (desmoglein I, desmocollin, corneodesmosin) [25, 71-74]. In addition, environmental conditions and biochemical factors such as humidity, cholesterol sulfate, calcium ion and pH may also play an important role in desquamation

although how these factors regulate desquamation still remains unknown [72, 75-77] (Figure 7).

A normal desquamation is of crucial importance for maintenance of the function of the SC and for a normal skin appearance. Assuming an entire body surface of $\sim 1.8 \text{ m}^2$ and a corneocyte surface of approximately $1000 \text{ } \mu\text{m}^2$, the entire surface “film” of corneocytes covering the body corresponds roughly to 1.8×10^9 cells. Since the thickness of a corneocyte is $\sim 0.3 \text{ } \mu\text{m}$ with a specific weight of 0.75 kg/m^3 (=protein), these data can be used to calculate a daily loss of about 40 mg of horny cells [78].

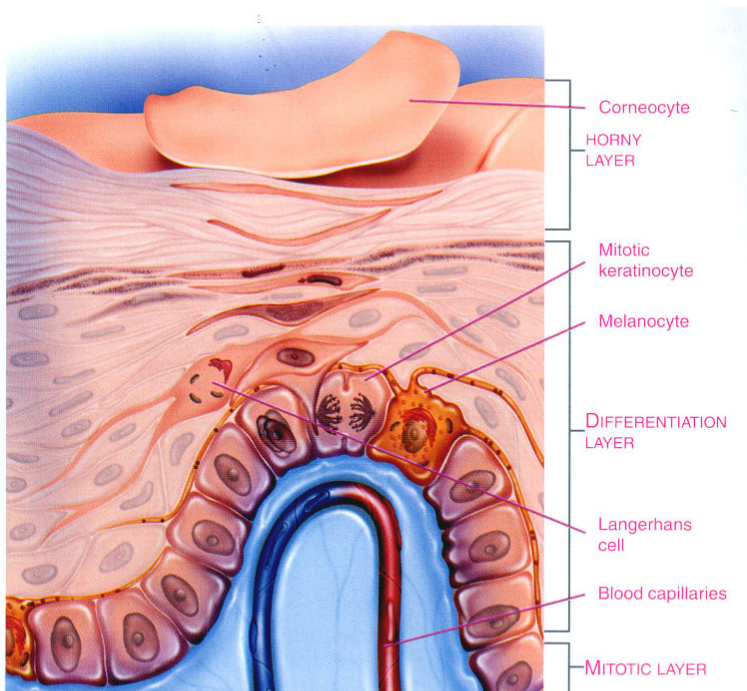


Figure 7. Desquamation process.

Legend. The keratinocytes divide in the basal membrane, the mitotic skin layer, to produce two identical daughter cells. One cell remains in the mitotic layer in order to divide again whereas the other migrates to the upper layers where it will undergo numerous morphological and biochemical changes. The keratinocytes reaching the horny layer are now called corneocytes which are anucleated flattened cells filled with keratin. The corneocytes lose their cohesive properties and thus slough off the surface of the skin upon coming in contact with the proteolytic enzymes (SCTE and SCCE).

At equilibrium, the loss of desquamative cells corresponds to the rate of epidermal cell production. Failure of the SC cells to be shed in a normal manner leads to increased thickening and scaling of the SC (X-linked ichthyosis). Individuals with recessive X-linked ichthyosis lack the enzyme cholesterol sulfatase which catalyzes the reaction of the transformation of cholesterol sulfate to cholesterol and free sulfate. Cholesterol sulfate has

been shown to inhibit pancreatic serin enzyme in vitro and cause scaling on mouse skin in vivo [77].

3.6 Drug permeation routes

The absorption of drugs through the skin is thought to be passive [31]. The permeation of drugs through the skin take place by diffusion through the intact epidermis and through the skin appendages i.e. hair follicles and sweat glands which form shunt pathways through the intact epidermis. However, these skin appendages occupy only 0.1% of the total human skin surface and the contribution of this pathway is usually to be small. As stated above, drug permeation through the skin is usually limited by the SC. Two pathways through the intact barrier may be identified: the intercellular lipid route between the corneocytes and the transcellular route crossing through the corneocytes and the intervening lipids i.e. in both cases the permeant must diffuse at some points through the intercellular lipid matrix which is now recognized as the major determinant of percutaneous transport rate.

4 Solar radiation

Sunlight is composed of radiation with differing wavelengths: Ultraviolet (UV) radiation (5%), visible radiation (39%) and infra-red radiation (56%). UV radiation is of particular interest because it can interact with human skin cells and cause a variety of damaging effects.

UV radiation can be further categorized as UVA (320 to 400 nm), UVB (290 to 320 nm) and UVC (100 to 290 nm). UVA can further be subdivided in UVA-1 (340 to 400 nm) and UVA-2 (320 to 340 nm).

The energetics of the incident radiation is controlled by the fundamental equations:

$$E = h\nu \quad \text{Equation 1}$$

$$\nu = c/\lambda \quad \text{Equation 2}$$

$$E = hc/\lambda \quad \text{Equation 3}$$

where E = Energy (ergs), h = Planck's constant (6.62×10^{-27} erg/s), ν = Frequency (Hz), c = Speed of light (3.0×10^{10} cm/s), and λ = Wavelength (nm).

The shorter the wavelength (λ), the higher the energy level (E) of the light and the more damage it can do. This means that UVC is the most dangerous radiation, but it is mostly absorbed by the ozone layer and does not reach the earth's surface. The remaining UV

radiation that reaches the ground is about 10% UVB and 90% UVA at midday. In contrast to UVB radiation which varies considerably with the time of the day and the seasons, large amounts of UVA are constantly present during daylight hours and throughout the year [79, 80]. Finally, while 90% of UVB radiation is blocked by the SC, over 50% of the UVA radiation received is capable of penetrating deep into the cutaneous structures as far as the dermis.

4.1 Acute and chronic damage to the skin due to UV radiation

UV radiation (290 – 400 nm) has been implicated in the induction of various acute and chronic harmful reactions in the human skin. As t UV light penetrates of the skin, depending on its wavelength, interaction occurs with different cells located in different depths. UV light of shorter wavelengths (UVB, 290-320 nm) is more energetic and is mostly absorbed in the epidermis and predominantly affects epidermal cells, i.e. keratinocytes. Longer wavelength UV light (UVA, 320-400 nm) is of lower energy but penetrates deeper and can interact with both epidermal keratinocytes and dermal fibroblasts (Figure 8).

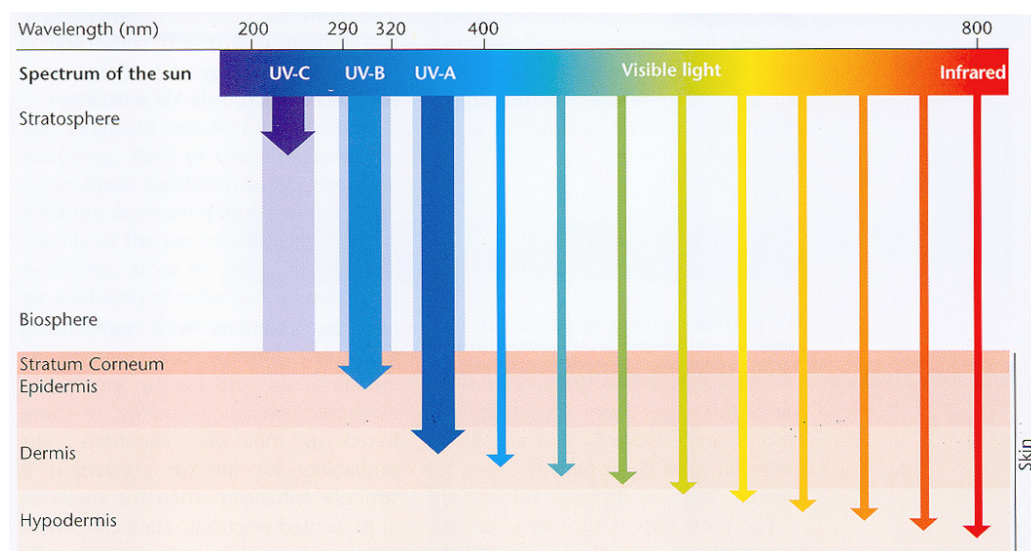


Figure 8. Schematic representation of light penetration into the skin.

The effects of UVB radiation on the skin have become common knowledge and are described in a number of publications. The effects of UVA radiation are supplementary to those of UVB. Recent studies suggest that UVB and UVA may also work synergistically to cause skin damage [81]. In Table 3, the effects caused by UVB and UVA are summarized.

Table 3. Effects of UV radiation on the skin.

Mostly attributed to UVB	Mostly attributed to UVA
Acute erythema	Erythema (high doses of UVA required)
Delayed pigmentation	Immediate pigmentation
Malignant melanoma	Cataract
Basal cell carcinoma (also by UVA)	Phototoxic reactions
Squamous cell carcinoma (also by UVA)	Photoallergies
Potential immunosuppressor	Premature aging / wrinkles
	Potentiate biological effect of UVB

Excessive exposure to UV radiation results in multiple dose- and time-dependent changes in the skin. They include inflammation responses such as erythema [82], epidermal proliferation, apoptosis and hyperpigmentation.

DNA is the principle chromophore in the skin, which absorbs UV radiation. This leads to a variety of adverse effects such as immunosuppression, sunburn cell formation, mutation and, ultimately, carcinogenesis.

Within the DNA, UV radiation induces the formation of pyrimidine dimers. Normally this lesion is repaired. However, if the enzymes are not functional or if the repair system is overloaded, mutations appear in the DNA [83]. Dimer formation is thought to be of crucial importance in the initiation of skin cancer because it has been found to be closely linked to the generation of mutations in tumor suppressor genes (p53) expressed in UV induced skin cancer [84].

In addition, UV radiation is known to generate secondary free radicals and reactive oxygen species which result in DNA damage and alteration in keratinocyte metabolism as well as chemotaxis and activation of cells involved in the inflammation and immune response (Langerhans cells) [85-88]. UV-induced DNA alteration as well as immunosuppression are critical for cutaneous carcinogenesis. UV radiation alters antigen-presenting cell function by directly affecting the number, the morphology and the functionality of Langerhans cells [89, 90]. It also induces the release of immunomodulating cytokines [91] and the isomerization of urocanic acid from the trans- to the cis-form. The cis isomer of urocanic acid is reported to be an important factor in the initiation of photoimmunosuppression [92].

4.2 Protective mechanisms of the skin

The skin adapts to UV radiation exposure by two mechanisms: melanogenesis (tanning) and thickening of the SC.

UVB rays enhance the binding of circulating melanocyte-stimulating hormone to melanocytes. In melanosomes, the melanin synthesizing apparatus of the melanocytes, melanin is formed. Melanin is a compound that absorbs, reflects and scatters UV radiation and acts as a free radical quencher. Melanin is transferred from the dendrites, the melanocyte's cytoplasmic extensions, to the keratinocytes (Figure 9). The keratinocytes' ability to absorb UV radiation is maximal the DNA of basal cells from mutagenic interactions.

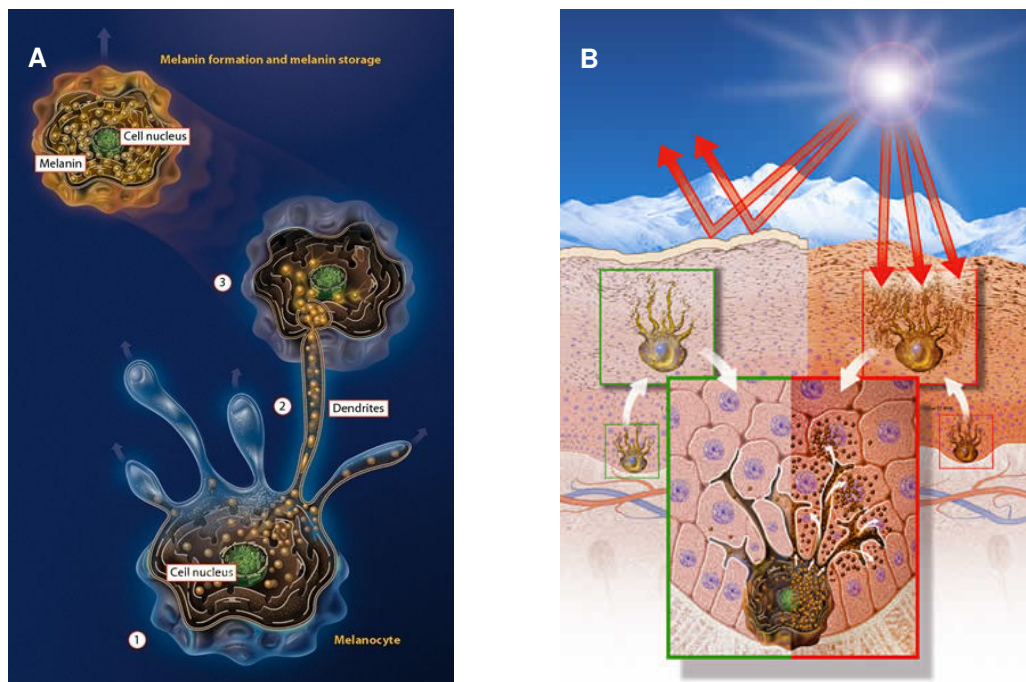


Figure 9. Production and storage of melanin.

Legend. A Melanocytes (1) form dendrites (2), which grow into and through the neighboring keratinocytes (3); B Under influence of UV light, biosynthesis of melanin occurs in the melanosomes. These move toward the cell periphery and into the dendrites. Thus, the keratinocytes fill up with melanin and a coloring of the skin occurs. Applying a sunscreen product provides additionally protection from damaging UV light.

Melanocyte function is able to influence skin color. Although people of all skin types have approximately the same number of melanocytes, there the black race have approximately 400 melanosomes per basal epidermal cell i.e. four times as many as the typical pale Caucasian. This difference reduces UVA and UVB penetration into the dermis by a factor of five in Blacks compared with Caucasians [93].

In response to prolonged UVB exposure, the SC can hypertrophy to six times its original thickness by increased synthesis of keratin by basal keratinocytes. Thickened SC absorbs or reflects 90-95% of UVB so that just 5-10% reaches the basal keratinocytes, melanocytes and superficial dermal vascular system [94].

5 Sunscreen products

The fashion of suntanning began in the 1940s, promoted by Coco Chanel, the French fashion designer [95]. The popularity of suntanning as a symbol of health, wealth and fashion has risen almost unabated since the end of World War II. Only recently, spurred by a rapid rise in skin cancer and decrease in the ozone layer, there has been an attempt to reverse this popularity. The use of sun protection products has increased dramatically and is now universally used by the sunbathing population.

The protection provided by modern sunscreen products against UV induced skin cancer was proven in animal photocarcinogenicity studies and confirmed by numerous in vitro, animal, and human investigations: sunscreens protected p53 tumor suppressor gene from damage [96, 97] and prevented UV-induced immune suppression [98]. Recent studies suggest that sunscreen products protect against precursor lesions of skin cancer such as actinic keratoses. Additional benefits of sunscreens included prevention of photodermatoses such as polymorphic light eruption [99] and possibly photoaging [96, 97].

The efficacy of a sunscreen product preparation is measured by the amount of harmful solar radiation able to be absorbed and/or reflected. The absorption of sunscreens is influenced by a variety of factors such as the components used to constitute the excipient, the pH, the type of emulsion etc..

5.1 Sun protection factor

To assess the efficacy of a sunscreen product in the UVB range of the spectrum the sun protection factor (SPF) is determined.

The SPF is defined as the dose of UV radiation required to produce one minimal erythema dose (MED) on protected skin after application of 2 mg/cm² of product divided by the UVR to produce one MED on unprotected skin.

The generally accepted methods to determine the SPF of a sunscreen product have been described by the United States Food And Drug Administration (U.S. FDA) [100] and by the European Cosmetics and Perfumery Trade Association (COLIPA) [101]. In the COLIPA Guidelines a number of criteria were defined such as: (1) the assessment of MED; (2) the type of skin and number of test volunteers; (3) the amount of product to be applied; (4) UV source to be used and; (5) the statistics for analyzing the data [102, 103].

5.2 Sunscreening agents

Sunscreening agents have traditionally been divided into chemical (organic) absorbers and physical (inorganic) blockers based on their mechanism of action.

Chemical or organic sunscreening agents reduce the amount of UV radiation reaching the skin by absorption. They can be subclassified as either UVB or UVA absorbers depending on the wavelength of their absorption maxima. Chemical sunscreening agents are generally aromatic compounds conjugated with a carbonyl group [104]. These chemicals absorb high energy (250-340 nm) UV rays causing an excitation in the molecule to a higher energy state. As the excited molecule returns to the ground state, longer lower energy (usually above 380 nm) wavelengths are emitted.

Physical or inorganic sunscreen products such as titanium dioxide and zinc oxide are very efficient attenuators of UV radiation. Microfine titanium dioxide primarily absorbs UVB radiation [105] and scatters UVA while zinc oxide absorbs all UV wavelengths. They are used either alone in products designed for children and individuals with sensitive skin or in combination with organic sunscreen products to achieve high levels of broad-spectrum protection. Based on the fact that particles do not penetrate the skin [106], it has been alleged that inorganic sunscreening agents may be safer than organic sunscreening agents.

Modern sunscreen products provide broad-spectrum UV protection and may contain one or several UV filters. A modern sunscreensing agent should be heat and photostable, water resistant, nontoxic and easy to formulate.

The effectiveness of sunscreen products depends upon their UV absorption, their concentration, formulation and their ability to withstand swimming or sweating (substantivity).

6 Topical bioavailability of sunscreensing agents

6.1 Definition

The U.S. FDA defines bioavailability as the rate and extent to which the active ingredient or active moiety is absorbed from a drug product and becomes available at the site of action. For drug products that are not intended to be absorbed into the blood stream, bioavailability may be assessed by measurements intended to reflect the rate and extent to which the active ingredient or active moiety becomes available at the site of action [107].

For determination of topical efficacy, systemic measures of drug availability are irrelevant because the site of action of the drug is located within the skin. Systemically active drugs and their metabolites may, however, raise safety issues.

6.2 Target sites

With a topical product, specific skin sites are targeted. Typical examples are given in Table 4.

Table 4. Skin target sites [108, 109].

Target	Representative function	Examples
Skin surface	Cleaning; protecting; improving skin feel	Soaps, sunscreen products, insect repellents, petrolatum
Stratum corneum	Normalizing SC, treating superficial infection	Moisturizers, antimycotics, sunscreen products
Pilosebaceous unit	Treating acne and other conditions of follicular origin	Retinoids, antibiotics
Sweat duct follicles	Preventing sweating	Antiperspirant aluminum salts
Viable epidermis	Changing mitosis rate; blocking sensory transmission; reducing inflammation	Steroids, local anaesthetics
Epidermal basal cells	Inhibiting cell proliferation	Cytostatic agents (e.g. methotrexate)
Blood	Systemic delivery	Transdermal patches (e.g. nitroglycerin)
Local muscle tissues	Relieving pain	Nonsteroidal anti-inflammatory drugs (NSAID)

For sunscreens agents, localization in the upper layers of the skin is expected to enhance photoprotection as these compounds should absorb or scatter the UV radiation before reaching the deeper, more vulnerable, viable epidermis and dermis. An ideal sunscreen product should contain effective UV absorbers on the skin surface or in the upper SC layers with minimal permeation to the systemic circulation.

6.3 Factors affecting the bioavailability of sunscreens agents

As mentioned above (see section 6.2) the target site of sunscreens agents is the skin surface and the upper layers of the SC. Ideally, a sunscreen product should impregnate the SC and create a barrier against UV radiation but not permeating further into the underlying living tissue. Sunscreens agents that penetrate to deeper skin layers are of minor value since they would leave the skin unprotected. Thus, a concentration of sunscreens agents within the upper layers of the SC are highly desirable, to increase resistance against rubbing and sweat and to avoid safety issues.

The rate and extent to which a chemical compound penetrates the skin depends on a variety of factors i.e. the physicochemical properties of the compound, the formulation, the application, and the type and condition of the skin (Table 5) [110].

Table 5. Factors influencing percutaneous absorption.

Parameter	
Test compound	<ul style="list-style-type: none"> - molecular weight - water / lipid partition coefficient - ionization (pKa value)
Formulation	<ul style="list-style-type: none"> - solubility (thermodynamic activity) / polarity - volatility / occlusion - concentration / thermodynamic activity - distribution in stratum corneum - ingredients - penetration enhancers
Skin	<ul style="list-style-type: none"> - species - age, sex, race - anatomical site - temperature - skin condition and hydration of stratum corneum - metabolism
Application	<ul style="list-style-type: none"> - skin area dose (film thickness) - total skin area in contact with formulation - duration of exposure

^a [110]

6.3.1 Influence of the compound attributes

The capacity of a molecule to enter the skin depends on its ability to penetrate the alternate hydrophobic/hydrophilic barrier layers of the SC. Permeation through the SC depends on many physicochemical parameters such as molecular weight, lipophilicity, polarity, capacity to form hydrogen bonds, solubility and, for acids or bases, the pKa value.

6.3.1.1 Permeation - Mathematical models for the prediction of skin absorption

Sunscreen products are repeatedly and often applied to large body areas. Even low fluxes of sunscreens agents can cause a considerable amount of penetrant to enter the body. Therefore, estimates of percutaneous absorption are required for realistic risk assessment. Mathematical modeling from physicochemical data has suggested that permeation of certain sunscreens agents through the skin may be significant. Several in vitro and in vivo kinetic models for studying percutaneous absorption have been proposed [111-113].

Hagedorn-Leweke and Lippold [112] quantified the transdermal permeabilities and maximum fluxes of various sunscreens agents applied as saturated solutions in a propylene glycol-water mixture applied to human skin in vivo. They found a linear relation between the logarithms of SC/vehicle partition coefficient of the penetrants and the corresponding logarithms of n-octanol/vehicle partition coefficient values. The correlation revealed that even in case of very lipophilic penetrants, no stagnant layers are present in neither the vehicle nor the viable skin in vivo. This model allowed the estimation of the amount of sunscreens agent absorbed after treating the total skin surface (1.8 m²) with a saturated propylene glycol solution for 1 hour (with knowledge of the physicochemical properties of a sunscreens agent). The predicted values ranged from 10 mg for octyl dimethyl p-aminobenzoic acid and to 89 mg for isoamyl-4-methoxycinnamate, respectively (Table 6).

Table 6. Predicted amount of sunscreens agents absorbed after 1h exposure to a saturated propylene glycol solution^a.

Agent (INCI name)	Amount absorbed per hour over the 1.8 m ² skin surface (mg)
Octyl dimethyl p-aminobenzoic acid	10
4-Isopropyl-dibenzoylmethane	15
4-Methylbenzylidene camphor	38^b
Isoamyl-p-methoxycinnamate	57-89
Benzophenone-3	76-80

^a [112]

^b Compound used in the experimental part of the thesis.

Another kinetic model was developed by Watkinson and colleagues [111] to calculate the extent of percutaneous absorption of sunscreens agents. The model uses first order rate constants to describe the processes of transfer and partitioning involved in percutaneous penetration. The authors suggested that systemic absorption of sunscreens agents across large areas of skin could occur at significant levels after long periods of exposure, even for chemicals that are estimated to be absorbed relatively slowly.

In a recent study, Fernandez et al. [113] used two combined non-invasive sampling methods to provide information for predicting the absorption and adsorption of benzophenone-3 in vivo i.e. the 'difference' method and the 'tape stripping' method respectively. They found that after application of benzophenone-3 in acetone and occlusion for 4 hours according to the method of T. Yano [114], the amount of benzophenone-3 crossing the skin was near 35% [113]. With

the tape stripping procedure they found that after a 30 minute application the amount of topically applied benzophenone-3 in the SC was 4% of the applied dose. In the case of benzophenone-3, Hayden and colleagues [115] found that in humans up to 2% of an applied benzophenone-3 dose and its metabolites (glucuronides of 2,4-dihydroxybenzophenone and 2,3,4-trihydroxybenzophenone) were excreted in the urine following topical application of commercially available products and in a further study excretion was reported in breast milk [116].

6.3.1.2 Toxicology

Schlumpf et al. [117] found that five frequently used sunscreens agents increased the activity of breast cancer cells (MCF-7) in vitro by proliferation and expression of estrogen-regulated genes (pS2). Estrogenic in vivo activity of these sunscreens agents was tested by an uterotrophic assay on immature Long-Evans rats that received the chemicals for 4 days in powdered feed. 4-MBC (effective Dose to produce 50% response (ED₅₀) 309 mg/kg/day), octyl-methoxycinnamate (ED₅₀ 935 mg/kg/day), and benzophenone-3 (ED₅₀ 1525 mg/kg/day) increased uterine weight. 4-Methylbenzylidene camphor was the most active compound. The uterine weight also increased after dermal application of 5 % and 7.5% 4-methylbenzylidene camphor in olive oil to immature hairless rats. The uterotrophic assay was repeated by two other investigators [118, 119] that used Sprague-Dawley rats and immature Wistar rats. In both studies the uterotrophic response of the sunscreens agents observed by Schlumpf et al. [117] could not be confirmed.

Despite the importance of sunscreens agents to protect the human epidermis, the majority of the studies are performed in vitro with animal or synthetic membranes and in vivo with animal models. Even although human studies are the critically accepted and desired standard, data available on humans is limited.

However, under real life-conditions the actual applied amount of sunscreen product is in the order of 0.5 mg/cm² i.e. far lower than the assumed 2 mg/cm² [120]. Thus, the actual human systemic exposure to sunscreen products is likely to be minimal to negligible. The duration of exposure offers an additional safety factor. For most people, the duration of whole-body application of sunscreen products is generally limited to 3-4 weeks for the average summer holiday period which is far less than the duration of administration or exposure in animal toxicity studies.

6.3.2 Influence of the skin

The condition of the skin has a considerable influence on the percutaneous absorption. Not only diseased skin conditions but also other factors such as age, race, anatomical location, skin temperature and hydration may affect the absorption.

6.3.2.1 Age and race

Many of the well documented changes that occur in aged skin include: (1) increased SC dryness [121, 122]; (2) reduction in sebaceous gland activity resulting in a decrease in the amount of skin surface lipids [123]; (3) flattening of the dermal-epidermal junction [124] and; (4) atrophy of the skin capillary network resulting in a gradual attenuation of blood supply to the viable epidermis [125]. Although several authors report lower percutaneous absorption of different compounds in the elderly (>65 years), the effect of ageing on percutaneous absorption has not been evaluated in sufficient detail to permit any generalization to be made. The influence of age is thought to be relatively minor compared to all the other variables [126] with the exception of premature infants (< 32 weeks) where the skin is approximately 2.5 times more permeable than full term or adult skin [15].

Racial differences in physicochemical properties of the skin have been reported. In Blacks, there is increased resistance to tape stripping [127], electrical resistance [128], increased lipid content [129], and increased TEWL [130]. Except for one study with nitroglycerin percutaneous absorption [131], one may state that if any racial differences exist, they are below the limit of detection for currently established methods.

6.3.2.2 Anatomical site

Depending on the area of the human body, there are considerable differences in the barrier function of the skin [132]. Feldmann and Maibach [133] were the first to demonstrate a regional influence on percutaneous absorption in humans using hydrocortisone as a model compound. Depending upon the anatomical site, a difference by a factor of 100 was found with ranking as follows: scrotal skin > jaw angle > forehead > axilla > scalp > back > forearm > palm > plantar pedis. A simple correlation between percutaneous absorption and SC thickness was not observed. The barrier function of the forehead was 4 times lower than that of the upper arm although the SC appeared to be the same [134]. Thus, anatomical site is

important and most in vivo human studies on topical application utilize the forearm of human volunteers as the primary testing site. The use of the volar forearm offers the advantage of accessibility to the anatomical region. Additionally, it was a relatively low density of hair and sebaceous glands.

6.3.2.3 Skin temperature and hydration

Changes in skin temperature are always accompanied by other physiological reactions such as increased blood flow or increased moisture content of the SC. These factors can contribute to higher percutaneous absorption. Furthermore, increase in temperature increases drug solubility in both the vehicle and the SC and increases diffusivity, both of which lead to a further increase in percutaneous absorption [135, 136]. For this reason, it is important that the skin temperature is controlled in experiments.

Hydration of the skin is an important factor affecting the rate and extent of percutaneous absorption. It may reduce the barrier integrity thus increasing the rate of percutaneous absorption. The most common method of increasing skin hydration is by occlusion which prevents surface evaporation of endogenous water thereby increasing the water content of the SC up to 50% [137], the temperature from 32°C to as much as 37°C, and the skin pH from 5.6 to 6.7 [138]. An assessment of the degree of hydration can be made by monitoring the permeability of the SC to water through measurements of the transepidermal water loss (TEWL). Occlusion can be achieved by means of plastic films or different types of dermal patches. Partial occlusion may be obtained with topical formulations based on petrolatum or paraffin, ointments and creams.

Both hydration and occlusion have increased the percutaneous absorption of different topically applied drugs such as hydrocortisone [139], nicotinic acid, salicylic acid [140, 141] and parathion [142]. It has been postulated that the SC hydration alters the SC-viable epidermis partitioning so that the effective partition coefficient of the penetrant between SC and the viable epidermis is reduced. This effect is usually more important for nonpolar than for polar molecules [143] and becomes greater as the lipophilicity of the absorbing molecule increases.

6.3.2.4 Diseased and damaged skin

Skin condition has a major influence on barrier integrity. Skin diseases such as ichthyosis, psoriasis and atopic dermatitis, tend to change the skin barrier properties.

Exposure to UV radiation provokes changes in the composition and thus in the barrier properties of the skin. Acute exposure to UV radiation results in an increased rate of epidermal proliferation and desquamation. In addition, acute exposure to damaging levels of radiation leads to decreased barrier function [144].

6.3.2.5 Differences between subjects

Large differences exist in percutaneous absorption between subjects [145] due to drug-vehicle-skin interactions. This can result in subject-formulation interactions so that the bioavailability of a test product relative to that of a reference product may be consistently different between individuals [146].

6.3.3 Influence of application parameters

6.3.3.1 Dosing / Application thickness

Beside the UV filter concentration, the efficacy of a sunscreen product is dependent on adequate application; the sunscreen product must be applied evenly and in sufficient amounts to achieve adequate protection [147-149]. Several factors affect the thickness of sunscreen product applied to the skin such as the texture of the skin, the application technique, type of container and the sunscreen formulation product itself.

The protection offered by a sunscreen product – defined by its SPF – is assessed after it is phototested in vivo at an internationally agreed application thickness of 2 mg/cm² (or 2 µL/cm² assuming a specific gravity of 1). To achieve the rated SPF over the whole body, an adult with a surface area of 1.73 m² would therefore need to apply 35 mL of sunscreen product. Yet a number of studies have shown that consumers apply much less than this, typically 0.39 to 1.5 mg/cm² [120, 149, 150]. Consequently the SPF varies considerably. The **theoretical** relation between the sunscreen product thickness and resulting effective SPF when using different SPFs is depicted in Figure 10 and summarized in Table 7 [151].

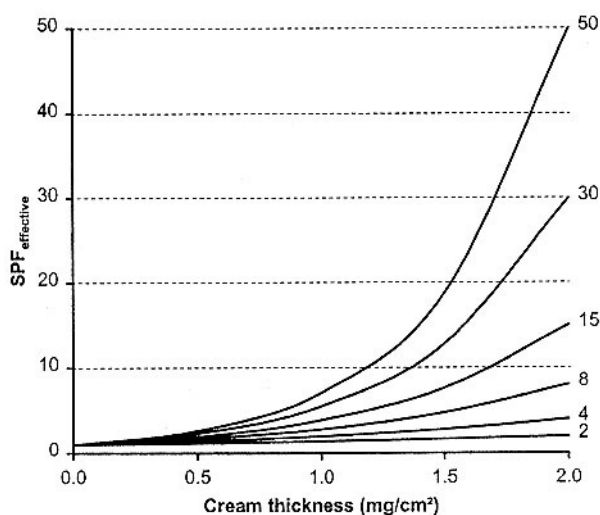


Figure 10. Relation between applied sunscreen thickness and resulting effective SPF with sunscreens of different sun protection factors (SPF) [152].

Table 7. Theoretical SPF with application of a sunscreen product layer thinner than that prescribed by the FDA (2 mg/cm²)^a.

FDA	2.0 mg/cm ²	1.5 mg/cm ²	1.0 mg/cm ²	0.5 mg/cm ²
2	2.0	1.7	1.4	1.2
4	4.0	2.8	2.0	1.4
8	8.0	4.8	2.8	1.7
15	15.0	7.6	3.9	2.0
30	30.0	12.8	5.5	2.3
50	50.0	18.8	7.1	2.7

^a [152]

The layer thickness for sunscreen products with a high versus a low SPF has a greater influence on the effective SPF. The protection from a thin layer of sunscreen product cannot be increased by using a product with a higher SPF. The effective SPF cannot exceed 3 when 0.5 mg/cm² is used and 10 if 1 mg/cm² is used. These prognoses may not always be confirmed in a real life testing situation probably because irregularities of the skin lead to uneven sunscreen product thickness which does not exactly fit the ideal mathematical model [152].

Stenberg's data indicated that the SPF under ad libitum application (1.01 mg/cm²) was approximately 50% of that which would be achieved by applying the standard thickness of 2 mg/cm² used in testing SPF's. These results are not in agreement with the results of Gottlieb et al. [153] who found that applying less than 2 mg/cm² would not diminish the SPF,

at least with the lower SPF sunscreen products. Gottlieb [153] also investigated the influence of the consistency of a sunscreen product on the application thickness. With exception of a gel, which was applied in slightly greater amount compared with that of other vehicles, they found that varying consistencies for different sunscreen products did not appear to play a role in application thickness. Diffey and Grice [150] observed that the amount of sunscreen product varied depending on the physical characteristics of the formulation - chemical (organic) or physical (inorganic) sunscreen product. With the organic sunscreen product which is easier to spread, up to 30% more was applied than the inorganic sunscreen product (1.48 and 0.94 mg /cm², respectively). In a recent study Autier et al. [154] showed that the median quantity of sunscreen products applied by students from different European countries was 0.39 mg/cm². These investigators also examined factors influencing quantities of sunscreen product applied to the skin such as gender, SPF, skin phototype and study place (Lyon, Lausanne, Paris, Thionville, Brussels). They found no statistically significant differences in quantity of sunscreen product applied according to any of the above mentioned factors. An additional factor that influences the amount of formulation applied is the type of dispenser [155]. Investigators found that a cream, contained in a jar was more readily applied than the same cream from a tube 1.7 mg/cm² vs. 0.71 mg/cm² respectively.

6.3.3.2 Application technique

The application technique is an essential factor in the variability of protection over the skin surface [156]. By employing an ultraviolet fluorescent photographic technique with sunscreen products known to exhibit fluorescent characteristics, Grecis et al. [157] showed that in many instances sunscreen products are not applied in an even layer. The SPF for a product may therefore not be achieved over the entire area of skin that was intended for protection by the user. Lynnfield and Schechter [155] found that the areas skipped most often excluded by volunteers were the back, the extremities, the ears and the areas immediately adjacent to the bathing suit. Loesch [158] and Azurdia [159] observed that even on the face, coverage by sunscreen product was incomplete (Figure 11).

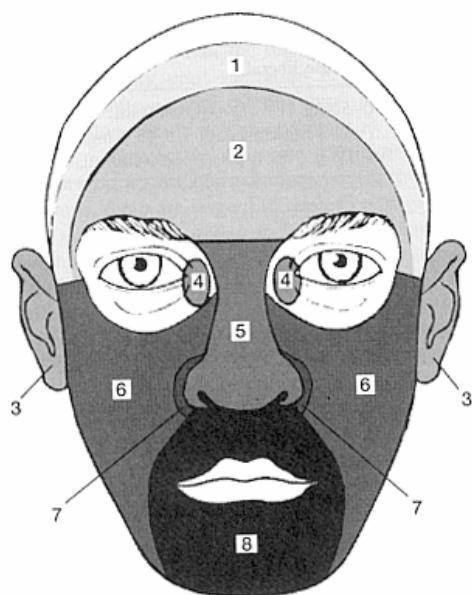


Figure 11. Sunscreen application pattern (from Lit. [158]).

Legend. Anatomic regions: (1) hairline, (2) forehead, (3) ears, (4) periorbital, (5) nose, (6) cheeks, (7) nasolabial, and (8) perioral. A denser shading indicates better coverage with sunscreen e.g. dark (8) good coverage, light grey (1) incomplete coverage.

The consequences of different application techniques were examined [103, 156]. Sayre et al. [103] found that rubbing the product into the skin appears also to remove it from the skin and thus affects the SPF. When cream was rubbed into the skin, at the standard amount of 2 mg/cm^2 , the SPF had a tendency (not always confirmed statistically) to be decreased compared to the situation where the cream was not rubbed in.

The application technique appears to be an important parameter in the determination of the actual SPF and thus needs to be rigorously controlled in SPF test protocols.

Reapplication

A recent Australian study [160] showed that when sunscreen product is applied prior to sun exposure and subsequently reapplied after a period of controlled exposure, a 2-3 fold increase in protection from sunburn can be expected.

Recommendations

For the application of sunscreen products a variety of recommendations have been published. They are helpful to advise the consumer to use the product optimally. Nonetheless, some of the recommendations are not scientifically proven.

- application of sunscreen product 15-20 minutes before sunbathing
- the rule of nines [161]
- teaspoon rule [162] (Figure 12)

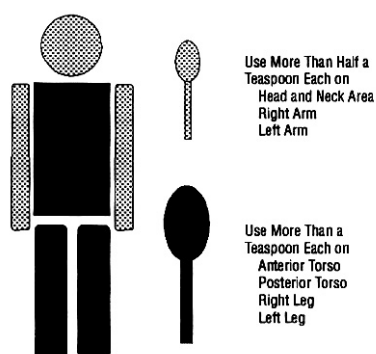


Figure 12. Variation in the optimal amount of sunscreen needed for different body areas to obtain approximately 2 mg/cm^2 .

6.3.3.3 Loss of vehicle from the skin surface

Loss of product from skin due to rubbing, perspiration, water contact, transfer to clothing and absorption can hardly be avoided, particularly in the case of longer exposure.

Using a mathematical model of dermal absorption Auton et al. [163] described removal processes on the surface of the skin, including the effects of washing and rubbing off onto clothing. In this study, different doses of an aqueous solution of a herbicide (fluazifop-butyl) were applied on the backs of human volunteers. Eight hours after application, the skin was washed with distilled water and then the volunteers clothed themselves in a cotton T-shirt for the next 16 hours. The recovery of the herbicide in T-shirts and water washes were 43-48% and 25-34%, respectively. In a further investigation five daily doses of $25 \mu\text{g/cm}^2$ were applied. Contact with a T-shirt as soon as the aqueous formulation had dried on the back of the volunteer removed approximately 52% of the applied dose. Only 10% of the dose was found in the 8hour wash. These results demonstrate that considerable amounts of the chemical were removed by washing or by the clothing. Only a small amount of the dose remained on the skin and was absorbed.

6.3.4 Influence of the vehicle

Under conditions of actual exposure, the bioavailability of sunscreens agents will not only be determined by their physicochemical properties, but may also be strongly influenced by the vehicle in which they are applied.

6.3.4.1 The sunscreen product vehicle

In one case the vehicle may have a solubilizing effect on the sunscreens agent or alternatively the vehicle's nature may modify properties of the SC (e.g. increased hydration, decrease in diffusional resistance), which could influence the penetration profile of sunscreens agents [164]. Various authors [6, 165-169] describe oil/water (o/w) or water/oil (w/o) emulsions, gels, lotions or hydroalcoholic formulations which were investigated in vitro and in vivo. They all found that the vehicle is a factor influencing percutaneous absorption; it may enhance or block the movement of the sunscreens agent in the skin. Jiang et al. [170] demonstrated that the skin penetration and retention of sunscreens agents of commercial products can differ significantly between the formulations used. Therefore, vehicles used for sunscreen products should be optimized to maximize the sunscreens agents variability to be retained in the SC and to minimize their absorption.

Not only skin penetration and skin retention properties of sunscreens agents are influenced by the vehicle but also the SPF can be significantly modulated. It is known that in an o/w emulsion the attained SPF is higher than in a w/o emulsion containing an identical concentration and combination of sunscreens agents. Treffel and Gabard [6] demonstrated that the protection afforded by an emulsion gel formulation was much higher than that of petroleum jelly. Even after removal of the excess emulsion gel formulation, an SPF was measured that demonstrated the ability of the sunscreens agents to penetrate and react within the SC. The authors suggest that the spreadability as well as changes occurring in the formulation due to application such as evaporation (vehicle metamorphosis) probably concentrated the sunscreens agents in a thin layer in the skin surface, thus improving their efficiency to absorb UV light. Rapid evaporation of the volatile vehicle components resulted in an appreciable increase in concentration of the sunscreens agents in the vehicle, acting directly on their thermodynamic activity and thus increasing their skin penetration.

The choice of a vehicle for a sunscreen product is important for several further reasons. A solvent may modify the sunscreens agent because of its polarity and thereby dramatically shift the absorption spectrum of the agent toward or away from the desired range [171] thus profoundly influencing the effectiveness of a sunscreen product formulation.

The wrong vehicle can act as a skin irritant, induce a phototoxic or photoallergic reaction, or may be comedogenic. Finally, especially in recent years, the sunscreen product vehicle has an important function, acting as a protective layer on the skin against external potentially damaging factors that could come into contact with the body. Recently, there has been an increase in various external harmful factors or, at least, a higher awareness about them (e.g. air pollution, UV radiation).

6.3.4.2 Substantivity

To be effective, sunscreens agents must remain on the surface or in the outermost layers of the skin [172]. The overall ability of a sunscreen product to remain on the surface or in the outermost layers of the skin and thus to resist removal is termed substantivity. Substantivity has been defined as the ability of a penetrant to adhere to keratinous substrates in the upper skin layers by chemical conjugation with proteins, thereby resisting removal, especially, when in contact with water. According to the FDA, a sunscreen product is declared water-resistant if it can maintain its original SPF after two 20-min immersions [173].

With increasing substantivity the sunscreen product remains in the skin longer resulting in higher efficacy and safety due to a reduced need for frequent reapplication and delayed percutaneous absorption [174, 175]. Willis and Kligman [176] classified sunscreen products into two types: external (residing on the skin surface) and; reservoir (diffusing into and remaining within the SC) types, depending on their capacity to diffuse into the SC, therefore resisting washing off.

The location of an absorbed substance within the skin is complex. Goddard [177] reported about two main driving forces which may lead to drug accumulation in keratin. First, distribution processes, which are strictly governed by the lipophilicity (partition coefficient) of the penetrant. Secondly, adsorption can occur. Here, distinction is possible between specific adsorption caused by strong physicochemical attraction e.g. ion-ion interactions and, additionally, unspecific adsorption on the basis of van der Waals forces or hydrophobic interactions. Hagedorn-Leweke and Lippold [178] investigated the affinity of non-ionic compounds to animal keratin and to human callus and studied the influence of the skin lipids

on their uptake. They found that the keratin affinity was directly related to the lipophilicity of the penetrant in terms of the octanol-vehicle partition coefficients and solubility in the vehicle. Therefore, they suggested that genuine substantivity, associated with specific adsorption, does not seem to occur for these solutes.

6.3.4.3 The vehicle interactions

The potential for large differences in the extent of absorption between topical formulations is due to the complex interactions between the drug, the vehicle and the skin which control partitioning into and diffusion through the skin barrier.

6.3.4.3.1 Drug-skin interactions

Drug-skin interactions include binding of the drug by the skin. In the optimization of substantivity, attempts have been made to introduce groups with positive electric charges into UV-absorbing molecules [175, 179, 180]. These functional groups are able to interact with negative charges of the protein chains of the keratin and consequently a fraction of such molecules will be retained by the upper skin layers, at least for a certain period of time. However, introduction of ionic groups into the chemical structure of a sunscreens agent may reduce its ability to absorb UV radiation and thereby compromise its efficacy [179].

6.3.4.3.2 Vehicle-drug interactions

On the other hand, various authors have shown that the choice of the vehicle plays an important role in the optimization of a sunscreens products substantivity. Lorenzetti and coworkers [181] showed an improved substantivity of para-aminobenzoic acid by using an ethanolic protein vehicle. They suggested a retarded penetration due to binding between para-aminobenzoic acid molecules and the protein.

Recently, Felton et al. [182] investigated the influence of HPCD (hydroxypropyl- β -cyclodextrin) concentration on the transdermal permeation and accumulation of benzophenone-3 in the skin. The HPCD-benzophenone complexation significantly augmented the aqueous solubility of benzophenone-3, thereby increasing transdermal permeation. Maximum flux occurred at 10% HPCD when sufficient HPCD was added to solubilize all benzophenone-3. Increasing the HPCD concentration up to 20% shifted the theoretical equilibrium of the complexation reaction towards the complexed form and hence

reduced the penetration. The authors conclude that at higher HPCD concentrations a benzophenone-3 reservoir may be created on the skin surface.

6.3.4.3.3 Vehicle-skin interactions

Vehicle-skin interactions include the broad field of permeation/penetration enhancers. Basically these are vehicle components which interact with the SC to increase drug solubility or drug diffusion or both. Penetration enhancers are substances which increase the percutaneous penetration of a chemical. It is presumed that they disrupt the organization of the SC barrier. Figure 13 is a schematic representation of models to show how an enhancer intercalates itself into the closely packed hydrocarbon chains of the SC lipids.

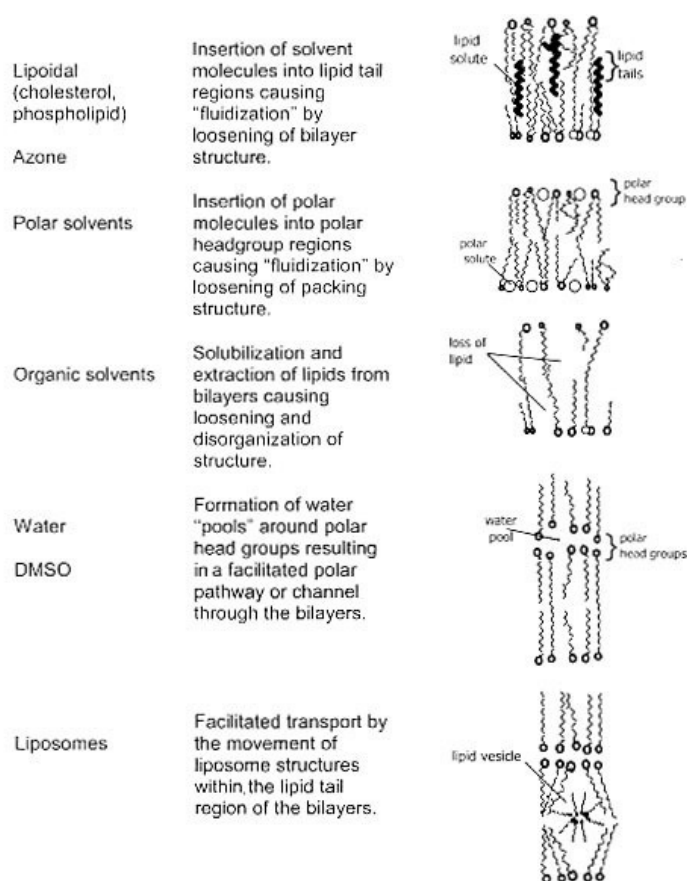


Figure 13. Schematic representation of the possible mechanisms of action of skin penetration enhancers [183].

Different experiments have indicated that vehicles which enhance penetration also increase the quantity and longevity of material retained in the skin [48, 184-189]. Such solvents noted are DMSO (dimethylsulfoxide), DMAC (dimethylacetamide), DMFA (dimethylformamide), Azone[®] and Transcutol[®]CG (diethylen glycol monoethyl ether).

Transcutol®CG is a vehicle used as a solvent/cosolvent in cosmetic and topical preparations and has been shown to form a cutaneous depot in the skin with corticosteroids [186], griseofulvin [190] and ivermectine [188].

The mechanism behind the increased accumulation of a drug in the skin with the use of Transcutol®CG is thought to be a swelling of the SC lipids, thus enabling drugs (especially lipophilic compounds) to form a deposit [186]. A recent study [185] investigated the influence of the Transcutol®CG concentration on the transdermal permeation and skin accumulation of two sunscreens agents, benzophenone-3 and octyl methoxycinnamate. The accumulation of both sunscreens agents in the skin was significantly increased by adding 50% Transcutol®CG in the formulation. However, transdermal permeation was not increased.

A study performed in vitro revealed that Azone® and Transcutol®CG increased the flux of cyanophenol, a model compound, by a factor of 2 [187]. ATR-FTIR (Attenuated Total Reflection Fourier Transform InfraRed) spectroscopy revealed that these enhancers act by different mechanisms. Azone® reduced diffusional resistance of the SC through direct interaction with SC lipids leading to a increased fluidity. Transcutol®CG acted by increasing the solubility of the penetrant in the SC. The transport of Transcutol®CG itself through the skin also improved the skin skin/vehicle partitioning for the drug. As a result, retention and formation of a deposit of the drug was observed [188]. However, evidence for the mechanism by which Transcutol®CG enhances is still limited.

Nannipieri and colleagues [191] analyzed vehicle-skin interaction in vitro. They found that the vehicle used had an effect on the resistance of the SC or of the viable tissues to the permeation of benzophenone-3. The decreasing effect of the SC resistance with several tested vehicles was partially or totally concealed by an opposite effect on the viable tissue resistance.

With sunscreen products, external factors such as contact with clothing, washing with soap or bathing and sweating are more influential and critical for the substantivity, than the sunscreen product formulation itself.

6.3.4.3.4 *Vehicle-drug–skin interactions*

Formulations in which significant vehicle-drug-skin interactions occur are probably the most common. Many pharmaceutical solvents such as propylene glycol are known to have modest

effect on reducing the skin barrier function (vehicle-drug interaction) as well as influencing the solubility of the drug in the delivery vehicle and converting the partitioning of the drug from the vehicle into the SC (vehicle-skin interaction).

6.4 Sunscreen product optimization

The recently developed sunscreens agents are generally more lipophilic substrates having high affinity for the skin compared to older agents. Different U.S. patents [192-194] describe the use of film-forming polymer compositions which, due to their very high molecular weight, maintain active agents on and near the skin surface with a minimum of skin penetration. Polymers are believed to enhance the water-resistant properties of a sunscreen product by maintaining the sunscreens agents on the target sites within the upper layers of the SC. Hence, removal of the active agents will only occur by the natural sloughing (desquamation) of the upper layers of the SC.

Another approach in the optimization of sunscreen products is the use of a specialized delivery system such as liposomes (liquid encapsulation system), and microspheres (solid entrapment system e.g. solid lipid nanoparticles (SLN)). A recent study [195] reported on incorporation of tocopherol acetate into SLN. The SLN dispersion was at least twice as effective as the reference emulsion. The results showed that the incorporation of a sunscreens agent in SLN prevents chemical degradation and increases the UV-blocking capacity.

7 Drug measurement in the stratum corneum

7.1 Skin scraping

The surface topography and the cellular details are not assessed with skin scraping. Large amounts of corneocytes can be harvested by curetting the SC from the surface with an open dermal steel curette. Usually superficial (-20 μm), and with more vigorous scraping midlevel (20-40 μm) SC can be collected [196, 197]. This technique has also been successfully employed by Faergemann et al. to determine drug concentration (terbinafine, fluconazole) in the SC [198-200]. The degree of superficial sebum and contamination of the SC by sweat may influence the amount of drug found in the SC.

7.2 Skin surface biopsy

The SC can also be removed by the so called skin surface biopsy. The skin surface biopsy technique using cyanoacrylate contact cement was employed for the diagnosis and study of superficial mycoses. The glue is applied to a glass slide and pressed onto the skin surface. Then the slide is removed after the glue has polymerized [201, 202]. This technique allows the quantification of drug found in the SC after various application durations [196]. Because the hair follicle content is also removed with this method, a distinction between the transepidermal and the transfollicular routes of absorption is not possible.

7.3 Tape stripping

7.3.1 Tape stripping technique

Tape stripping is a technique that has been found useful in dermatopharmacological research for selectively and, at times, exhaustively removing the skin's outermost layer, the SC. Typically an adhesive tape is pressed onto the skin and is abruptly removed. The application and removal procedure may be repeated 10 to more than 100 times [203, 204].

Tape stripping is widely used in various fields of cutaneous biology, namely for the study of the barrier function and the reservoir of the skin [205-207], epidermal growth kinetics [208-211], and various aspects of skin permeability [32, 212, 213]. Differences in the permeability of intact and fully stripped skin have provided information about the diffusional resistance of the skin [214]. It has been recognized that to reach the point of barrier disruption 30-67 tapes are required, depending on the subject's skin type [215]. Öhman et al. showed that after 100 tape strippings the entire SC could be removed [204]. However, no permeation data through such completely stripped skin exists.

7.3.2 Application of the tape stripping technique

The stripping technique has been extended as a means of predicting systemic absorption following topical application [216].

Dupuis, Lotte, Rougier, and coworkers [151, 164, 217] determined the concentration of four different chemicals (benzoic acid, benzoic acid sodium salt, caffeine, acetylsalicylic acid) in the SC at 30 min after topical application. They found a linear relationship between the SC reservoir content and in vivo absorption of the four compounds at various sites in human subjects measured by the traditional urinary excretion method [218-220]. They could also show for a variety of simple pharmaceutical vehicles that the percutaneous absorption of benzoic acid is vehicle dependent and can be predicted from the amount of drug within the SC at 30 min after topical application. The tape stripping technique offers the advantages that it is essentially non-invasive and that the testing of urine and faecal excretion to determine percutaneous absorption can be eliminated. Existing data indicates that there is a good and valid correlation between percutaneous absorption and SC reservoir.

7.3.3 Dermatopharmacokinetics

Tape stripping has been proposed as a method for evaluating bioavailability and bioequivalence of topical dermatological dosage forms as an alternative approach in clinical trials, analogous to the use of concentration-time curves for systemically administered drugs [221]. By sampling different skin sites at progressive application times, it is possible to derive kinetic uptake metrics for local bioavailability evaluation thus providing a means for assessing the bioequivalence of two dermatological drug products. In the same way, a fixed treatment time for all skin sites followed by sequential tape stripping at incremental post-treatment

removal allows the clearance of the drug from the SC to be assessed. This in vivo approach is also known as “dermatopharmacokinetics” (DPK). DPK studies include validation of both analytical methods and tape stripping techniques. The U.S. FDA is seriously considering this method for regulatory purposes, and after much discussion [221-225] a draft guidance reviewing this procedure has been published [226]. However, further validation is necessary in order to assess the feasibility of the approach.

7.3.4 Quantification of stratum corneum removed

Currently, xenobiotics (e.g. drugs, sunscreens agents) are extracted from a single or combined tape strip and the concentration in the extracted solution is determined by an appropriate analytical method e.g. HPLC, fluorescence spectroscopy etc. [227-229]. Individual analysis of the tape strips allows the SC distribution of the molecule to be displayed as a concentration to tape-strip number or concentration to SC depth profile, which is an instantaneous and static picture of the drug penetration at a given time. Many studies report the mass of penetrating xenobiotic as a function of tape strip number. Although profiles of drug levels versus tape strip number give an estimate of the local SC bioavailability, they are based upon the assumption that each tape strip removes a constant and reproducible amount of SC if the procedure is standardized (e.g. by applying a constant pressure over a given time). Van Der Valk and Maibach [230] demonstrated that the amount of SC removed can change from approximately < 5-30%. The number of strips does not correlate linearly with depth within the SC. The first few corneocyte layers are loosely attached so that relatively large quantities of horny tissue patches are removed by the first pieces of tape. Each successive strip removes smaller quantities. Thus, the amount of SC removed by each tape strip generally decreases with increasing depth [231]. Furthermore, during the tape stripping procedure, clusters of corneocytes are removed, rather than perfect layers, and furrows are obviously not evenly removed with the superficial tape strips [232]. Additionally, the applied vehicle may variably influence both the cohesion of the corneocytes tape as well as the adhesive properties of the tape [233 in preparation]. Swelling by skin hydration provoked by emollient or occlusive formulations results in the removal of non-reproducible amounts of SC [234]. This may be especially true for long application times. It is also probable that the particular tape, the pressure applied on the tape and the peeling force applied for the removal of the tape will affect SC removal [200]. Determining the amount of

SC removed by each single tape strip both intra-individual and inter-individual variability in SC thickness is taken into account.

In order to overcome these problems, it is necessary to express the amount of drug measured as a function of the amount of SC removed by each individual tape strip.

Several methods have been proposed to quantify the amount of SC removed by tape stripping. These include: (a) gravimetric analysis (weighing); (b) spectroscopic determination of the protein absorption of the SC and; (c) measurements of the TEWL.

Weighing is the preferred method [235] but it is a time consuming procedure necessitating a micro balance. Artefacts are sometimes observed due to absorption and desorption of moisture due to weighing of the tape before and after stripping [8-10]. Furthermore, the weight of SC is disturbed by topically applied formulations of sebaceous components of the skin [12].

Some more rapid and less tedious alternatives include spectroscopic measurements. Different spectroscopic methods for measuring the protein absorption of SC have been applied. Marttin et al. [10] used the characteristic protein absorption band in the UV range to determine the SC amount on each tape. Unfortunately, this method is not very reliable because the light scattering by the SC exceeds the light absorption of proteins. Dreher and coworkers [8] proposed quantifying SC by a protein assay. This method is limited because the tape strips are destroyed and thus are unavailable for subsequent determination of the drug concentration on the tape strips. Recently, Weigmann et al. [12] developed a method to determine the SC amount directly on tape strips by measuring the skin in the visible spectral range. The absorption measured is determined by reflection, scattering and diffraction properties of the corneocytes and is taken as a measure of the amount of corneocytes on the individual tape. A sum of the absorption which reflects the total SC mass removed during the tape stripping procedure is obtained. A correlation of the absorption of each single tape to the sum total yields the relative amount of corneocytes in relation to the total amount of SC. Therefore, the entire SC has to be removed during the tape stripping procedure.

A further normalization - as relative instead of absolute SC depth - was proposed by Kalia and coworkers [236, 237]. They measured transepidermal water loss during sequential tape stripping. The theoretical barrier function at the base of the SC can be deduced by this

methodology and the total thickness of the layer may be extrapolated thus permitting the relative depth to be obtained.

In penetration studies, the first strip is often discarded [238, 239]. The first strip, however, is not irrelevant because also a large quantity of SC material is removed. Furthermore, it is the strip that removes the greatest quantity of SC material. In order to obtain reliable concentration to depth profiles of drugs penetrating into the SC, it is important to determine the amount of SC removed by each tape including the first tape strip [10].

Most research papers rarely describe the use of a template to assure accurate and consistent removal of the SC from the target treatment area. Without such a template, consistency in terms of the SC removal area is not assured and thus DPK studies may become questionable.

One unresolved issue of the tape stripping technique is that the skin surface is not flat. The topography of the skin presents unique challenges to validate tape stripping. The skin possesses innumerable macroscopic furrows [240]. A histological section of the skin that was tape-stripped twenty times clearly showed non-stripped skin in the furrows, indicating an incomplete tape stripping [232]. Indeed, after removing forty tape strips the furrows were still present. On one tape removed from the skin surface, SC cells were obtained and also unabsorbed drug from the skin furrows thus distorting the interpretation of the tape stripping study (Figure 14).

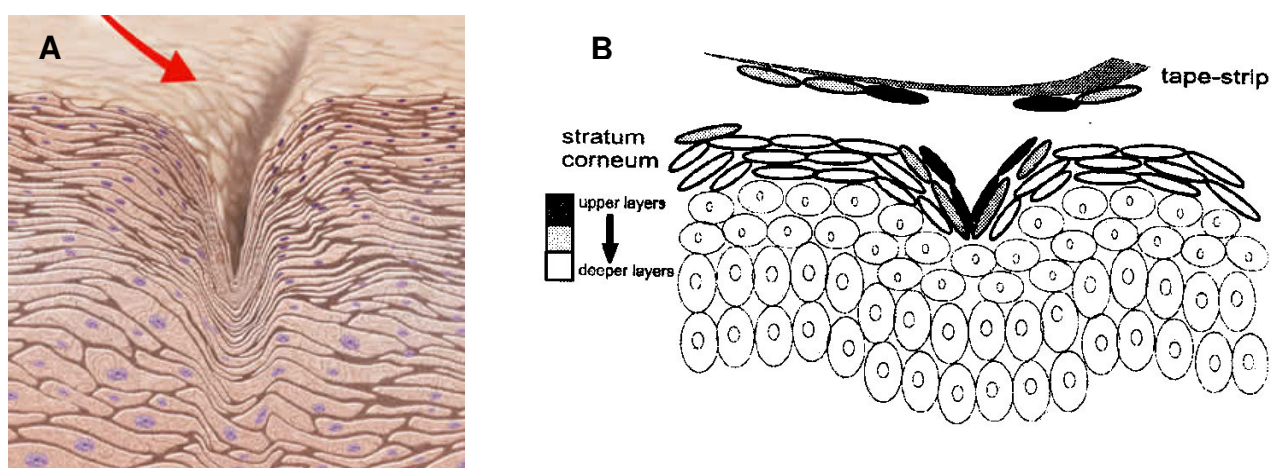


Figure 14. A macroscopic furrow of the skin.

Legend. A macroscopic furrow of the skin

B Schematic drawing of the tape stripping technique. Superficial corneocytes still present in the furrow after tape stripping are removed with later tape strips. In this way, tape strips are obtained containing corneocytes which originate from different layers of the stratum corneum.

It is obvious that the removal of the drug from the skin surface before stripping is a procedure that is important and that has a large influence on the tape stripping study. Residual material can be removed by washing the skin with ethanol followed by distilled water and drying with a cotton swab [7, 151, 241, 242] or simply gently wiping the skin with dry cotton applicators [243]. Wester and [244] demonstrated that the addition of soap reverses the partitioning of the compound into the SC. Such cleaning procedures might even damage the skin or enhance penetration of the applied compound. The removal procedure should only remove excess drug from the SC surface and should not affect drug concentrations in the SC.

Even though tape stripping is considered to be essentially non-invasive, it locally disrupts the barrier function and results in skin glistening and erythema. In certain dark-skinned individuals the stripped sites may remain pigmented for several months after healing. This effect should be communicated to the volunteers before their enrolment in a study.

8 Original publications

8.1 Simultaneous spectrophotometric determination of a sunscreen agent and relative stratum corneum tissue density in skin tape strips. I. Validation of analytical methodology.¹

INTRODUCTION

Tape stripping of the stratum corneum from the skin is a relatively non-invasive and useful technique that has been used widely in recent years for bioavailability and dermatopharmacokinetic studies of topically-applied drugs [1]. The numerous problems associated with the standardization of the tape stripping methodology have been documented at length [2, 3]. The general technique used to date involves topical dosing, followed by application and subsequent removal of adhesive tape strips from the skin; corneocytes adhering to the tape strips are thereby removed from the underlying tissue. Each tape used in the stripping process (often 30-50 strips in total from each stripped skin site) is usually then solvent extracted to isolate the analyte of interest, prior to high sensitivity analysis. However, the adhesive tape stripping of the stratum corneum is not a linear process in terms of the thickness of the layer of corneocytes removed from one strip to the next, and is not uniform in thickness across the entire field of each tape area (see electron micrographs) [2]. This procedure, therefore, relates the mass of permeant found on each strip to the tape strip number analyzed, and not strictly to stratum corneum depth or volume [4-7]. A modification of this methodology involves the weighing of the tape strips on a high-sensitivity balance before and after stripping to obtain a mass of tissue removed with each strip [8-11]. Alternatively, tissue mass on the tape strips has been determined in terms of protein content using the Lowry method [9]. These tape strip weighing, protein determination and extraction procedures are laborious and are susceptible to analytical artefacts (e.g. vaporization of volatile components of the tape matrix, static charges on the tape strip, etc.). Furthermore, a technique has been researched recently that allows the simultaneous analysis of corneocyte density and xenobiotic abundance using ultraviolet and visible (UV/VIS) spectroscopy [12-14]. This technique has distinct advantages in terms of facile

¹ Text submitted for publication: Tassopoulos T, Figueiredo V, Imanidis G, Smith EW, Surber C 2006. Simultaneous Spectrophotometric Determination of a Sunscreen Agent and Relative Stratum Corneum Tissue Density in Skin Tape Strips. I Validation of Analytical Methodology. *J Pharm Sci.* (Note that the in-text citations are referred to in the bibliography at the end of this section.)

sample handling procedures when compared with previously described methods. We have used the principle of this technique as a basis for the fully-validated studies reported here.

The purpose of this research was: firstly, to develop in our laboratories a standardized method for the direct assessment of tapes removed from the skin without the need to conduct any preparative procedures (such as extraction or weighing) that may introduce artifacts into the analysis. Secondly, to establish in our laboratories a method capable of the simultaneous, accurate and simple, UV/VIS spectrophotometric determination of **both** analyte amount and relative corneocyte density on each tape strip. Thirdly, to fully validate both the new, direct UV/VIS analysis of tapes and the conventional sample extraction/HPLC analysis procedure as a reference, according to current guidelines, in order to assure that either technique may be deemed fit for purpose. A validated direct spectrophotometric technique would obviate the need for an extraction process prior to analysis, but would have to be sensitive enough for determination of low analyte concentrations. The new UV/VIS method must be shown to be as good as the HPLC technique if it is to be used for routine analysis.

MATERIAL AND METHODS

Materials and Reagents

The UV filter 3-(4-Methylbenzylidene)-camphor (MBC) (Eusolex[®] 6300) with a purity of > 99.5%; and glacial acetic acid 100%, analysis grade, were obtained from Merck KgaA, Darmstadt, Germany. Methanol, gradient HPLC grade, was obtained from Scharlau Chemie S.A., Barcelona, Spain. Water for HPLC analysis was purified by reverse osmosis (Osmostil LN 4/2 PH - Septron 500 PH, Christ Aqua ecolife AG, Aesch, Switzerland). Tesa Multi-Film Kristall-Klar[®] 57315 tape was obtained from Tesa, Beiersdorf, Hamburg, Germany. Working solutions of MBC were freshly prepared from a methanolic stock solution of concentration 1 mg/mL. Methanolic extraction solutions were filtered through a 0.45 µm membrane (Nylon GyroDisc, Orange Scientific, Braine l'Alleud, Belgium).

UV/VIS Spectrophotometric Procedure

The analytical technique monitors the absorbance/transmission behavior of UV and visible wavelength light as this radiation passes through the tape/corneocyte sample. The proteins

and lipids of the stratum corneum are relatively weak chromophores and do not absorb UV light to any appreciable extent [10]. This is not the case for certain xenobiotics (e.g. UV filters) that penetrate the skin after topical administration: the presence of these chemicals in the layers of the skin present relatively strong absorbing chromophores to the incident UV light, and result in appreciable absorbance measurements. On the other hand, the physical structures of the corneocytes and other stratal components of the skin present formidable barriers to the passage of visible-wavelength light, resulting in appreciable reflectance and scattering of the incident radiation. In practical terms, this scattering of the visible light is measured as a decrease in the transmission through the sample or is monitored as an “absorbance” in the non-classical sense. The analytical usefulness of this phenomenon is that the degree of visible light scatter is proportional to the density of the corneocytes in the path of the light. Therefore, it is possible to obtain a percentage abundance of corneocytes on each tape strip, as a function of the total abundance on all strips, by monitoring the degree of absorbance taking place in the visible wavelength region. A single absorbance spectrum measurement between 220 and 500 nm of each tape strip removed from the skin is, therefore able to yield analytical data of both the sunscreen concentration in the stratal layers removed, and the relative amount of skin tissue adhering to the strip.

Spectrophotometric measurements of MBC on the tape matrix were made using an UV-Spectrophotometer (Lambda 35, Perkin Elmer, Ueberlingen, Germany); which was controlled by UV WinLab Software (v 2.85). The optics of the spectrophotometer were modified by the manufacturer to enable monitoring of a square incident light beam of 1 cm² area, instead of a narrow slit (Measurements to assess sunscreen efficacy in industrial research, EU-project; contract no. SMT-CT 97-2152, 01.12.1997 – 30.11.2000). Continuous spectra of each tape were recorded between 220 and 500 nm as shown in Figure 1. The baseline “absorbance” value of the spectrum depends on the relative amount of corneocytes adhering to the tape strips. The relative abundance of corneocytes is, therefore, represented by the plateau absorbance value in the visible range when compared with the spectra of reference tapes without adhering corneocytes (approximating λ_2). The absorbance spectrum of MBC on the corneocyte tape strips showed a λ_{MAX} at 297 nm, however the absorbance was always recorded at three different wavelengths (peak start (λ_3), λ_{MAX} (λ_1) and peak end (λ_2) as shown in Figure 1), in order to calculate the total absorbance due to MBC alone by using Equation 1.

$$A_{\text{xenobiotic}} = A(\lambda_1) - \frac{[A(\lambda_2) - A(\lambda_3)](\lambda_1 - \lambda_3)}{(\lambda_2 - \lambda_3)} - A(\lambda_3)$$

Equation 1. Calculation of MBC absorbance by three-wavelength analysis.

Legend. A = Absorbance units; for wavelength λ_1 , λ_2 and λ_3 see legend Figure 1.

HPLC Procedure

MBC concentrations were assayed by HPLC using an Alliance HPLC System (2690 Separations Module, 996 Photodiode Array Detector, Millenium³² Software), and a Symmetry Shield RP18 (2.1x 100 mm, 3.5 μm particle size) column (all Waters Corporation, Millford, Massachusetts, USA). The mobile phase consisted of 75% (v/v) methanol and 25% (v/v) water with pH adjustment to 4.8 using glacial acetic acid (approximately 0.01% v/v); the flow rate was set at 0.4 mL/min. The analytical column temperature was set at 35°C, sample aliquots of 10 μL were injected into the chromatograph and the principal detection wavelength was set at 305 nm (the maximum absorbance wavelength of MBC).

VALIDATION PROCEDURES AND RESULTS

Method validation is a process of proving that a quantitative research method (or set of methods) is acceptable for its intended purpose. Usually validation is conducted in parallel with the method development. Each analytical procedure to be used in this research (the UV/VIS spectrophotometric and HPLC methods) had to be validated as a stand-alone analytical tool. The guidelines of the International Conference on the Harmonization of Technical Requirements for the Registration of Pharmaceuticals for Human Use (ICH) were applied for this purpose [15]. These guidelines recommend a set of tests and procedures to be followed (e.g. specificity, linearity, detection limit, quantitation limit, repeatability, accuracy and other evaluations) for validating quantitative analytical procedures.

Furthermore, the validation of the entire set of methods, when used together in this investigation, includes the verification of the following correlations:

- Relative mass of corneocyte tissue adhering to each tape strip as assessed by weighing on a balance or by protein analysis, and as determined by the UV/VIS spectroscopy method. This has previously be validated by Lademann and coworkers [12-14].

- Abundance of the analyte of interest on each tape strip as determined by the UV/VIS spectroscopy method and as assessed by solvent tape extraction/HPLC analysis.

In this manner the technique would be documented to be at least as good as previously-used HPLC methods in determining analyte concentrations in the skin strata, but with the major advantage of simplicity in sample handling and analysis.

Statistical analysis of validation data was carried out using Method Validation in Analytics (MVA) software (Novia GmbH, Saarbrücken, Germany), which is based on the ICH guidelines. Regression analysis and test result evaluations were carried out using the appropriate methods in Statgraphics PLUS 5 software (Manugistic, Inc., Rockville, Maryland, USA).

UV/VIS Spectroscopy Method

Specificity

To assure that there is no interference of matrix components of the tape (e.g. the polymer film or adhesive) with MBC, tapes were spiked with 25 μL of pure methanol and with 25 μL aliquots of standard methanolic MBC solutions to yield loading doses of 1.0 and 35.0 $\mu\text{g}/\text{cm}^2$ on the tapes. In addition, to demonstrate that the specificity of the analytical methods is unaffected by the presence of corneocytes, tapes stripped from human forearm skin were similarly spiked. In each case the methanol was allowed to evaporate completely under ambient conditions after spiking, the tapes were mounted on the spectrophotometer recording frame and an absorbance spectrum was recorded between 220 and 500 nm. In this manner absorbance spectra of: a) untreated tapes, b) untreated tapes stripped from the skin, c) methanol-spiked tapes, d) methanol-spiked tapes stripped from the skin, e) MBC/methanol-spiked tapes, and f) MBC/methanol-spiked tapes stripped from the skin were compared. Analyte specificity would require that none of these handling procedures influence the quantitative dose of MBC found on the tape strips by UV/VIS assessment. Full spectral analysis (as in Figure 1) indicated that there is no interference between MBC and either the tape matrix components, or the tape matrix components/corneocytes, thereby validating the specificity of the technique.

Linearity and Range

A linear relationship between analyte concentration and measured signal (analytical response) exists for many methods used in pharmaceutical analysis. Linear regression

models of absorbance *versus* concentration are simple to implement, when compared with quadratic or polynomial regression models, and the former are preferred over the latter models if equivalent results can be achieved. However particular caution should be taken in order to demonstrate the linearity of the analytical response when the analyte of interest may interact with a matrix (e.g. tape or corneocytes). Usually, UV/VIS spectroscopy is used for the determination of xenobiotics in solution. In most cases the solute concentration can be adjusted to the validated, linear range (low concentration) of analytical quantification by dilution of the working solutions. In contrast, in this methodology the solute is determined on tape strips where the xenobiotic concentration cannot be adjusted to an ideal concentration range. It was anticipated that a few samples of high concentration and many samples of low concentration would be expected in the present investigation, based on preliminary studies and literature data [12]. Therefore, linearity of the assay would, ideally, have to be shown over a wide range of analyte abundance. Theory would suggest that two calibration curves be established for the analysis in this situation; one curve for the high-abundance samples, and one curve for the multiple, low-abundance tape samples. This would allow greater accuracy in determining the (more important) lower concentrations, by not introducing linear skew artifacts from the (less important) high-abundance points that may occur if all concentrations were used in establishing a single curve.

Therefore, to assess the linearity and range of detection for the UV/VIS method, two methanolic solutions of 1.2 and 2.4 mg/mL MBC were freshly prepared. Appropriate dilutions of these solutions gave concentrations of 0.024 mg/mL to 4.7 mg/mL (0.024, 0.12, 0.24, 0.36, 0.48, 0.60, 1.20, 1.80, 2.40, 3.00, 3.60, 4.20 and 4.68 mg/mL). Aliquots of 25 μ L of these solutions were dosed onto an area of 3 cm² (delineated by a template) on the tapes, in triplicate, yielding loading doses of 0.2, 1.0, 2.0, 3.0, 4.0, 5.0, 10.0, 15.0, 20.0, 25.0, 30.0, 35.0 and 39.0 μ g/cm². Two calibration curves (curve 1 and 2) were established ranging from 24 to 600 mg/mL and 0.6 to 4.68 mg/mL, to be used with tape doses of 0.2–5.0 μ g/cm² and 5.0–39.0 μ g/cm², respectively. Spectral analysis was carried out and MBC absorbance was calculated for each prepared tape in order to assess the linearity of the detector response in both concentration ranges.

The two concentration/absorbance plots were analyzed with different linear regression models (unweighted, 1/x weighted and 1/x² weighted) to test for optimal linearity parameters. These linearity parameters were compared by means of the Mandel fitting test (DIN 38402

1986), which compares the three linear regression models to a quadratic model in order to determine which models are closest to the quadratic descriptor. All linear regression models (i.e. the unweighted, $1/x$ and $1/x^2$ weighted) can be accepted at a 95% confidence level for calibration curve 1. However, only the $1/x^2$ weighted linear model can be accepted at a 95% confidence level for calibration curve 2. Therefore, to standardize the methodology, only the $1/x^2$ weighted linear models for curves 1 and 2 were selected for further validation.

Accuracy

Accuracy of the UV/VIS method was determined by analyzing tapes spiked with methanolic solutions of MBC, using the linear calibration curve established above. Three concentrations were used for accuracy determination (0.2, 5.0 and 39.0 $\mu\text{g}/\text{cm}^2$). Five independent solutions were made up at each concentration, and 2 tapes were spiked with each solution. The accuracy values were expressed as relative percentage error (Er %) and were found as follows: at 0.2 $\mu\text{g}/\text{cm}^2$ Er = 97.2%, at 5.0 $\mu\text{g}/\text{cm}^2$ Er = 99.1% and at 39.0 $\mu\text{g}/\text{cm}^2$ Er = 96.4% (overall Er = 97.6%). These parameters demonstrate sufficient accuracy in the UV/VIS methodology for quantitative measurements.

Exclusion of Matrix Effects in the Low Concentration Range

Theoretically, a calibration curve for low analyte concentrations must pass through the origin (zero). In cases of matrix effects that cannot be corrected by a reference sample, a calibration curve may not pass through zero, indicating systematic errors in the methodology. If systematic errors are negligibly small, then the confidence interval range for the y-intercept of the calibration curve must include zero and the intercept should statistically not be distinguishable from zero at the defined level of confidence. This requirement is met for calibration curve 1 (lower range) at a 95% confidence interval with an intercept range from $-1.97\text{E}-03$ to $1.27\text{E}-03$ (including zero). It can therefore be assumed that there are no systematic errors in the methodology at low MBC concentrations.

Reference Calibration Curve

In contrast to HPLC procedures where there is a need to establish daily calibration curves, UV/VIS spectrophotometry is negligibly susceptible to instrument based interferences. It is therefore feasible to establish a single, representative calibration curve for the instrument to determine MBC concentrations on tape strips for use over the entire experimental period. Five calibration curves were constructed over a 4 week period (low and high abundance

range), each having six standards for calibration curve 1, eight standards for calibration curve 2, $n=3$ for each level. The average regression parameters for all five curves were determined using the MVA software package (Table 1).

To investigate the homogeneity of the variance of all data points across the entire range of the mean, $1/x^2$ -weighted calibration curves 1 and 2, the Cochran's C test was applied to the merged data from the five calibration constructions. The null hypothesis assumes that the variances are equal (homoscedastic) at each concentration value across the entire data range. The Cochran's C test confirmed homogeneity of variances for calibration curves 1 and 2 over the entire concentration range (P-value curve 1 = 0.09, P-value curve 2 = 1.0 where P-values > 0.05 indicate that variances are not significantly different). Therefore, the mean reference calibration curves 1 and 2 were used for all further analytical measurements.

Detection Limit (DL) and Quantitation Limit (QL)

According to the ICH recommendations, several methods could be used for determining the DL and QL, these include:

1. calculation from noise ($DL=3.3 \cdot x_{\text{noise}}$, $QL=10 \cdot x_{\text{noise}}$),
2. calculation from standard deviation (SD) of the blank ($DL=3.3 \cdot SD_{\text{blank}}/\text{slope}$, $QL=10 \cdot SD_{\text{blank}}/\text{slope}$),
3. calculation from standard deviation of the y-intercept ($DL=3.3 \cdot SD_{\text{intercept}}/\text{slope}$, $QL=10 \cdot SD_{\text{intercept}}/\text{slope}$),
4. calculation from the standard error of the estimate (S_r) of the calibration line ($DL=3.3 \cdot S_r/\text{slope}$, $QL=10 \cdot S_r/\text{slope}$).

As outlined in Table 2, DL and QL results for the reference calibration curve 1 and QL for reference calibration curve 2 were dependent on the calculation method applied.

Method 4 (worst case scenario) was chosen to define the detection and quantification limits for the assay when used for quantitative investigations. This offers the highest confidence when applying the UV/VIS method for evaluating MBC concentration in the tapes.

Precision

The data from the five calibration curves constructed over the period of four weeks were used for the estimation of repeatability (intra-day variation) and intermediate precision (inter-day

variation) of the UV/VIS method. In the construction of each calibration curve, three samples were analyzed at each concentration level (6 concentration levels for calibration curve 1 and for 8 concentration levels for calibration curve 2). Therefore, the precision parameters were estimated at each concentration by 15 data points collected on five occasions over a four-week period. The precision parameters were calculated for the ratio of absorbance and concentration (sensitivity, response factor), by analysis of variance considering the contributions of intra-series and of inter-series effects. There was no significant difference of the means at a 95% confidence level for the two calibration curves. Calibration curve 1: the coefficients of variation for the different series were lower or equal to 6.2%, the repeatability and the intermediate precision were 4.3% and 4.4%, respectively. Calibration curve 2: the coefficients of variation for the different series were lower or equal to 5.9%, the repeatability and the intermediate precision were 5.3% and 5.3%, respectively.

Therefore, the parameters described above fully validate the UV/VIS methodology and give credence for the use of the technique in tape strip analysis.

HPLC Methodology

In the previous section (see UV/VIS Spectroscopy Method) the validation procedures and results for the UV/VIS spectroscopy method has been described at length. The HPLC methodology has been validated. In a similar way, however, since HPLC validation is a routine laboratory procedure, the technical descriptions have been abbreviated here.

Specificity

To determine HPLC specificity, tapes spiked by the same procedure as described in section UV/VIS Spectroscopy Method, Specificity were extracted for 16 h with 2.0 ml methanol in stoppered 50 ml-volumetric flasks, and aliquots of this extraction solution were injected into the HPLC system without further dilution. The eluent peak diode array spectra obtained from these injections were compared with spectra from an authenticated MBC sample. The retention time of MBC was recorded at 4.33 ± 0.01 min (Figure 2). The chromatograms of the extracts indicated that there is no interference between MBC and the tape matrix components or the tape matrix components/corneocytes.

Linearity and Range

A stock solution was prepared in triplicate by dissolving 100 mg of MBC in 100 mL methanol.

Appropriate dilutions of the stock solution gave standard solutions with concentrations of 0.5, 1.0, 2.5, 5.0, 7.5 and 10.0 µg/mL. These standard solutions were injected in triplicate into the HPLC system to evaluate linearity. Data were analyzed as described in section UV/VIS Spectroscopy Method, Linearity and Range, which yielded a linear relationship between the peak area and the concentration. The results of the Mandel's fitting test showed that the $1/x$ weighted and $1/x^2$ weighted linear regression model can be accepted at a 95% confidence level. Theoretically, the calibration curve must pass through the origin; this requirement is met at a 95% confidence interval with a range of values from $-2.06E03$ to $3.16E03$, including zero. The Cochran's C test was used to assess the homogeneity of the variance over the range of the $1/x$ -weighted calibration curve. The P-value was found to be higher than 0.05 (P-value = 0.12) indicating that there are no statistically significant differences among the variances over the concentration range at the 95% confidence level. Therefore, the $1/x$ -weighted regression model was used for further validation of the calibration curve and for analytical HPLC determination of MBC from tape extracts.

Accuracy

Accuracy of the HPLC system was determined by analyzing independent, known methanolic solutions of MBC, using the linear calibration curve established above. Three concentrations were used for accuracy determination (0.5, 5.0 and 10.0 µg/mL). Five independent solutions were made up at each concentration, three replicates were injected for each solution. The accuracy values were expressed as relative percentage error (Er %) and were found as follows: at 0.5 µg/mL Er = 101.2%, at 5.0 µg/mL Er = 97.6% and at 10.0 µg/mL Er = 103.4% (overall Er = 100.7%). Therefore, according to the ICH guidelines the accuracy of the HPLC techniques was found to be acceptable for analytical determinations.

Detection Limit (DL) and Quantitation Limit (QL)

The four methods described in section UV/VIS Spectroscopy Method, Detection Limit and Quantitation Limit were used to determine the DL and QL of the HPLC system. The noise of the HPLC method was measured between the highest and the lowest signal of a blank (methanol) injection. The DL and QL calculated from the standard error of the estimate of the calibration line (method 4: $DL=3.3*S_r/slope$, $QL=10*S_r/slope$) gave the greatest values and was therefore used for quantitative analysis ($DL = 1.64E-01$ µg/mL, $QL = 4.98E-01$ µg/mL). As previously, the worst case scenario was chosen to define the detection and quantification limits as this offers the highest confidence when applying the HPLC methodology to the

evaluation of MBC concentrations in the tapes.

Precision

The data from three calibration curves constructed on three different days were used for the estimation of repeatability (intraday variation), and intermediate precision (interday variation). Three replicates of each concentration of the calibration curve were injected into the HPLC. There was no significant difference of the means at a 95% confidence level for the calibration curves. The coefficients of variation for the different series were lower or equal to 4.8%. The repeatability and the intermediate precision were 3.4% and 3.4%, respectively. Therefore, the precision of the HPLC methodology is shown to be acceptable for analytical purposes.

Determination of Extraction Recovery

The extraction recovery was determined by spiking skin-stripped tapes with methanolic solutions at three different MBC doses (1, 5 and 35 $\mu\text{g}/\text{cm}^2$). After solvent evaporation, MBC was extracted by methanol as described in section HPLC Methodology, Specificity and, after appropriate dilution, the solute concentrations in the extracts were determined by the HPLC procedure described above. The analyte recovery was calculated from the MBC concentration determined with the calibration curve and compared with the dose spiked on the tapes with corneocytes. The mean recovery for MBC was 91.9% at a concentration of 1 $\mu\text{g}/\text{cm}^2$, 96.1% at a concentration of 5 $\mu\text{g}/\text{cm}^2$ and 90.9% at a concentration of 35 $\mu\text{g}/\text{cm}^2$. Therefore, the average recovery over the entire analytical range is 93.0%. A recovery value may not be a 100% of the nominal MBC concentration. If the average recovery is known (93%), the analytically-measured concentration in routine sample analysis can be corrected to obtain the theoretical 100% nominal concentration. Sample extracts measured by HPLC may therefore be corrected by a factor of 1.075 to yield true concentrations.

Comparison of HPLC and UV/VIS Data

To compare the MBC concentration measured by UV/VIS with the MBC concentration measured by HPLC, tapes were spiked by the same procedure as described in section UV/VIS Spectroscopy Method, Specificity, at loading doses of approximately 1, 5 and 35 $\mu\text{g}/\text{cm}^2$. After evaporation of the methanol, an absorbance spectrum was recorded between 220 and 500 nm and the MBC concentration was determined by the mean regression equation (see Table 1). The same tapes were methanol extracted as described in section HPLC Methodology, Specificity, and the extracted solutions were assayed by the HPLC

system described above. The results found by HPLC were corrected by the factor of 1.075 (see section Determination of Extraction Recovery). The MBC concentrations found by UV/VIS and HPLC were compared to each other in terms of recovery (Table 3).

A t-test was performed to compare the HPLC data with the UV/VIS data. The computed p value was 0.51, indicating that there was no statistically significant difference in the amount of MBC found by both methods at a 95% confidence interval. This clearly demonstrates that analytical data from both methods are equivalent in quality.

DISCUSSION AND CONCLUSIONS

In an attempt to accurately and reproducibly quantify the mass of a sunscreen agent that penetrates into the stratum corneum after topical application, we have independently validated a direct UV/VIS analysis and a solvent extraction/HPLC analytical method for skin tape strips. Each procedure has independently been shown fit for purpose according to the currently-accepted laboratory guidelines. In addition, we have compared the data from the two analytical methods and found them to be equally accurate and precise in determining sunscreen abundance in the corneocyte layers removed by tape stripping. However, the direct spectrophotometric technique obviates the need for any tape extraction process prior to analysis, and is sensitive enough for the accurate determination of low analyte concentrations on the tape strips since there is no loss of analyte in the sample handling protocol. The simplicity of the direct spectrophotometric method, combined with its accuracy and precision, make this an ideal analytical tool for rapidly processing the large data sets involved in dermatopharmacokinetic testing of sunscreen agents, contained in a variety of delivery systems.

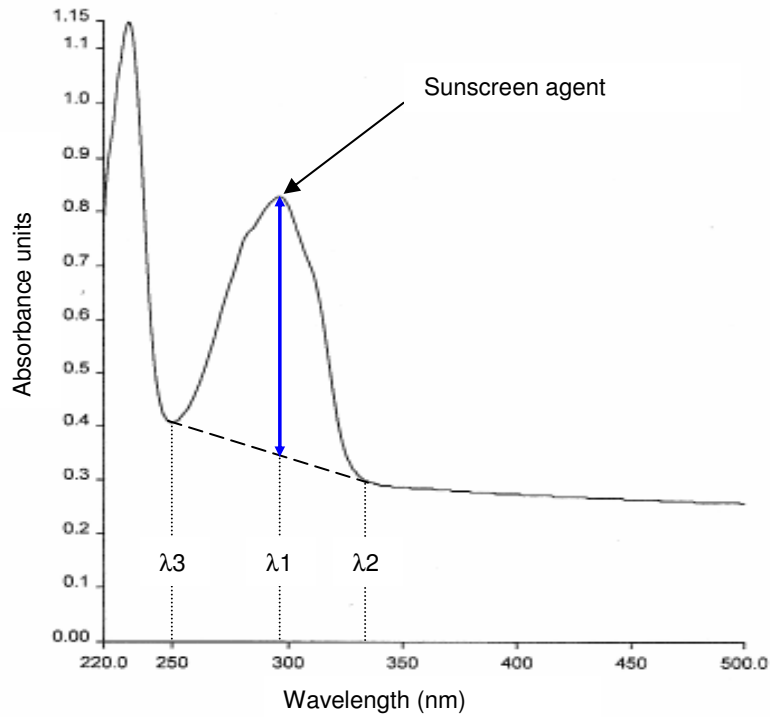
The essential scientific prerequisites for a critical comparison of the quantitative data obtained from the two methods have therefore been established; the application of these validated analytical techniques to in vivo human studies will be described in the second paper in this series.

REFERENCES

1. Draft - Guidance for Industry. Topical dermatological drug product NDAs and ANDAs- In vivo bioavailability, bioequivalence, in vitro release, and associated studies. Center for Drug Evaluation and Research, Food And Drug Administration, U.S. Department of Health and Human Services, 1998, p 1-19.
2. Surber C, Schwarb FP, Smith EW. Tape-Stripping technique. In: Bronaugh RL, Maibach HI, eds. Percutaneous Absorption. Third, Revised and Expanded ed. New York, Basel: Marcel Dekker; 1999. p. 395-409.
3. Bashir SJ, Chew A-L, Anigbogu A, Dreher F, Maibach HI. Physical and physiological effects of stratum corneum tape stripping. *Skin Res Technol* 2001;7:40-48.
4. Henn U, Surber C, Schweitzer A, Bieli E. D-Squame adhesive tapes for standardized stratum corneum stripping. In: Brain KR, James VJ, Walters KA, eds. Prediction of Percutaneous Penetration; 1993; La Grande Motte, Languedoc, France: STS Publishing; 1993. p. 477-481.
5. Caron D, Queille-Roussel C, Shah VP, Schaefer H. Correlation between the drug penetration and the blanching effect of topically applied hydrocortisone creams in human beings. *J Am Acad Dermatol* 1990;23(3):458-462.
6. Treffel P, Gabard B. Skin penetration and sun protection factor of ultra-violet filters from two vehicles. *Pharm Res* 1996;13(5):770-774.
7. Lotte C, Wester RC, Rougier A, Maibach HI. Racial differences in the in vivo percutaneous absorption of some organic compounds: a comparison between black, Caucasian and Asian subjects. *Arch Dermatol* 1993;284:456-459.
8. Tsai J-C, Weiner ND, Flynn GL, Ferry J. Properties of adhesive tapes used for stratum corneum stripping. *Int J Pharm* 1991;72:227-231.
9. Dreher F, Arens A, Hostynek JJ, Mudumba S, Ademola J, Maibach HI. Colorimetric method for quantifying human stratum corneum removed by adhesive-tape-stripping. *Acta Derm Venereol* 1998;78:186-189.
10. Martin E, Neelissen-Subnel MTA, De Haan FHN, Boddé HE. A critical comparison of methods to quantify stratum corneum removed by tape stripping. *Skin Pharmacol* 1996;9(1):69-77.
11. Kalia YN, Alberti I, Sekkat N, Curdy C, Naik A, Guy RH. Normalization of stratum corneum barrier function and transepidermal water loss in vivo. *Pharm Res* 2000;17(9):1148-1150.
12. Weigmann H-J, Lademann J, Meffert H, Schaefer H, Sterry W. Determination of the horny layer profile by tape stripping in combination with optical spectroscopy in visible range as a prerequisite to quantify percutaneous absorption. *Skin Pharmacol Appl Skin Physiol* 1999;12(1-2):34-35.
13. Lindemann U, Weigmann H-J, Schaefer H, Sterry W, Lademann J. Evaluation of the pseudo-absorption method to quantify human stratum corneum removed by tape stripping using the protein absorption. *Skin Pharmacol Appl Skin Physiol* 2003;16(4):228-236.
14. Weigmann H-J, Lindemann U, Antoniou C, Tsirikas GN, Stratigos AI, Katsambas A, et al. UV/VIS absorbance allows rapid, accurate, and reproducible mass determination of corneocytes removed by tape stripping. *Skin Pharmacol Appl Skin Physiol* 2003;16(4):217-227.

15. Guidance for Industry. Q2B Validation of analytical procedures: Methodology. International Conference on the Harmonization of Technical Requirements for the Registration of Pharmaceuticals for Human Use, Center for Drug Evaluation and Research, Center for Biologics Evaluation and Research, Food And Drug Administration, U.S. Department of Health and Human Services, 1996, p 1-10.

Figure 1: UV spectrum of a tape strip removed from the skin after treatment with a MBC formulation.



Legend. $\lambda 1$ = wavelength at maximum absorbance
 $\lambda 2$ = wavelength at end of peak
 $\lambda 3$ = wavelength at start of peak

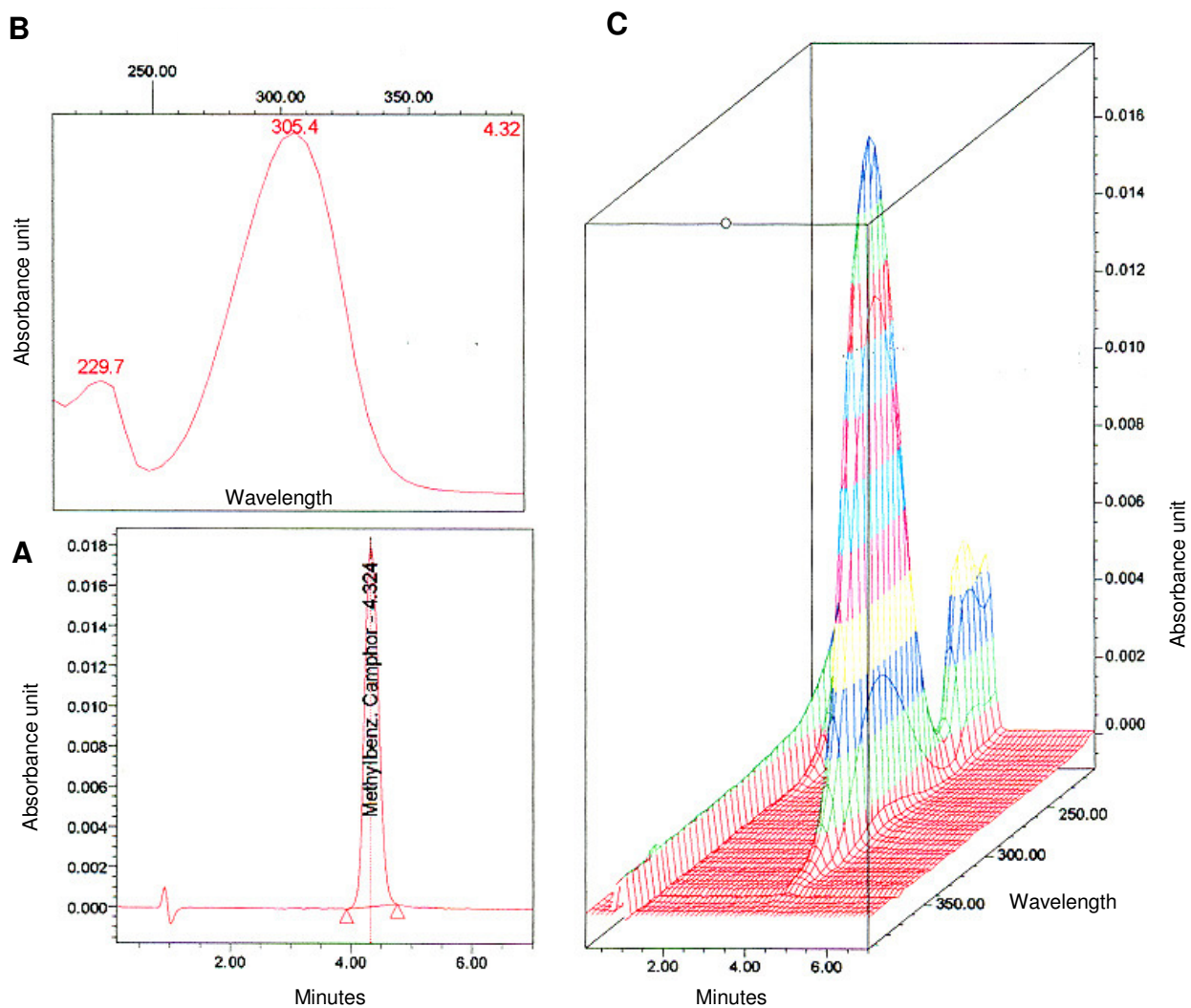
Figure 2: A Chromatogram; B Spectrum index plot and; C 3D plot of MBC.

Table 1: Mean Reference Calibration Curve for UV/VIS Method

	Mean Regression Equation ^a	r^b	S.D. ^c		S_r^d
			Slope	Intercept	
Calibration Curve 1	$y=0.0796 x - 7.205E-4$	0.999	7.561E-4	3.600E-4	1.609E-3
Calibration Curve 2	$y=0.0728 x + 0.0510$	0.998	7.010E-4	8.020E-2	3.185E-2

a Calculated absorbance y versus appropriate abundance x , in $\mu\text{g}/\text{cm}^2$; 90 data points for calibration curve 1, 120 data points for calibration curve 2.

b Correlation coefficient

c Standard deviation of slope / intercept

d Standard error of estimate

Table 2: Detection and quantitation limit of MBC by the UV/VIS method according to the ICH guidelines.

Calculation Method	Reference Calibration Curve 1		Reference Calibration Curve 2
	DL ^a	QL ^b	QL ^b
1	1.76E-03	5.33E-03	5.33E-03
2	1.73E-03	5.23E-03	5.23E-03
3	2.43E-02	7.37E-02	2.94
4	4.86E-02	1.47E-01	5.22

^a Detection limit in $\mu\text{g}/\text{cm}^2$, ^b Quantitation limit in $\mu\text{g}/\text{cm}^2$

Table 3: Method comparison in terms of recovery at 3 different levels of MBC concentration

Approx. Concentration Level (n=5)	% Recovery \pm SD	
	UV/VIS method	HPLC method
1 (1.17) $\mu\text{g}/\text{cm}^2$	100.18 \pm 2.84	98.98 \pm 1.13
5 (4.66) $\mu\text{g}/\text{cm}^2$	98.88 \pm 2.23	103.93 \pm 1.41
35 (34.97) $\mu\text{g}/\text{cm}^2$	100.11 \pm 0.75	98.24 \pm 2.20

8.2 Simultaneous spectrophotometric determination of a sunscreen agent and relative stratum corneum tissue density in skin tape strips. II. Application of the method in Humans²

INTRODUCTION

One of many self-evident prerequisites for investigations in man are well developed analytical methodologies that have been proven fit for purpose. In a previous publication [1] we have detailed the independent validation of: a) the direct UV/VIS spectrophotometric determination of a sunscreen agent on tapes stripped from the skin; and b) an HPLC method for analysis of the sunscreen when solvent extracted from the skin tape strips. These two analytical methods were fully validated as stand-alone procedures according to current guidelines of the International Conference on the Harmonization of Technical Requirements for the Registration of Pharmaceuticals for Human Use (ICH) [2]. In the current paper we report on the comparison of analytical data from the two methods when evaluated in vivo using human volunteers. A standardized tape skin stripping procedure has been developed for this purpose. It has been optimized in terms of methodological shortcomings previously reported for the technique [3-6]. The aim of the research presented here is to minimize the variability of the tape stripping data by optimization and standardization of the methodology, and to complete the validation of the direct spectrophotometric procedure by comparing the quality of the data from UV/VIS and solvent-extracted HPLC analyses, when applied to an in vivo situation where there is an added parameter of a complex topical delivery vehicle.

MATERIAL AND METHODS

Emulsion Formulation

The emulsion formulation used as the delivery vehicle for the sunscreen in these experiments was a modified P3 standard formulation from the European Cosmetic, Toiletry, and Perfumery Association (COLIPA) guidelines [7]. The ingredients of the emulsion were: Tegosoft TN (C12-15 Alkyl benzoate) 15 g, Emulgade F (cetearyl alcohol, PEG-40, castor oil

² Text submitted for publication: Tassopoulos T, Figueiredo V, Imanidis G, Smith EW, Surber C 2006. Simultaneous Spectrophotometric Determination of a Sunscreen Agent and Relative Stratum Corneum Tissue Density in Skin Tape Strips. II Application of the Method in Humans. *J Pharm Sci.* (Note that the in-text citations are referred to in the bibliography at the end of this section.)

and sodium cetearyl sulfate) 3.15 g, Carbopol 934 (carbomer) 0.3 g, ethanol 8.0 g, KOH solution 10% 1.5 g, Eusolex 6300 3-(4-Methylbenzylidene)-camphor (MBC) 2.0 g or 4.0 g, and water q.s. 100g. The MBC and potassium hydroxide were obtained from Merck KgaA, Darmstadt, Germany. Tegosoft TN was obtained from Goldschmidt AG, Essen, Germany. Emulgade F was obtained from Cognis Deutschland GmbH, Düsseldorf, Germany. Carbopol 934 was obtained from Noveon Inc., Cleveland, Ohio, USA. Absolute ethanol was obtained from Fluka, Buchs, Switzerland.

All the components of the oil phase (MBC, Emulgade F and Tegosoft TN) were melted together at 90 °C over a water bath. The carbopol was dispersed in water for approximately 30 seconds with an Ultra Turrax agitator (IKA Ultra Turrax T25 Basic with IKA disperser S25N25F) set at 16 000 rpm and was also warmed to 90 °C using a water bath. The aqueous solution was then slowly added to the oil phase with continuous stirring (200 rpm) using a stirring motor (type IKA Eurostardigital / IKA RW 28 Basic). The ethanol was added when the emulsion had cooled to a temperature of 40 °C. The emulsion was then homogenized with the Ultra Turrax (16 000 rpm) for one minute and finally stirred (50 rpm) for 30 minutes until room temperature was reached. The mass of the final formulation was checked and adjusted to the datum with water during the final stirring phases. All production steps were carried out under GMP conditions. The emulsion phase stability was verified through stress-testing by means of centrifugation (15 min at 5'000rpm). The microscopic aspect and pH of the formulations were tested. The emulsions for both dosing strength were stable (droplet size, pH) throughout this investigation.

Subjects

A standardized clinical protocol was developed for volunteer processing, according to international GCP guidelines and was approved for implementation by the Internal Review Board of the institution [8]. Five volunteers (2 female, 3 male), aged from 24 to 29 years, participated in the study. All subjects were in good general health and had no history of dermatological diseases. Informed consent was obtained from all the participants. The volunteers were asked not to apply detergents or emollients to the forearm on the day of the experiment. The subjects rested 30 min before the experiment at constant environmental conditions of 24 °C room temperature and 40% relative humidity.

Tape Stripping Procedure

A rectangular formulation application area was delineated on the volar surface of each arm by dermatological pen to yield a site of 45 cm². The compounded emulsions containing MBC were randomly applied to the demarcated application sites, one arm of each subject was treated with 2% formulation and the other arm with 4% formulation. In each case, 90 mg of the product was applied to the skin by the portion with a 1 ml syringe and the formulation spread evenly over the demarcated area with a gloved finger, to yield a topical application dose of 2 mg/cm². This application modality ensures a homogenous and accurate distribution and dosing of the formulation.

The dosed skin sites were stripped one hour after formulation application. The central area of the application site to be tape stripped was demarcated by fixing a flexible, grease-proof paper template to the skin with adhesive tape. The template had a rectangular aperture of 1.3 cm x 3.3 cm, thereby exposing a constant skin area (4.29 cm²) for each sequential tape stripping, and ensuring consistent removal of stratum corneum from exactly the same formulation application site. The long axis of the template was fixed along the midline of the forearm to ensure intimate contact with the skin and to simplify the subsequent stripping procedure.

Tape stripping was carried out with Tesa tape (Multi-Film Kristall-Klar[®] 57315 tape, Tesa, Beiersdorf, Hamburg, Germany) of width 1.5 cm. A strip of adhesive tape (longer than the aperture of the template) was placed over the skin area exposed through the template aperture. Pressure was then applied perpendicularly to the adhering tape in a uniform manner using a hand roller that supplied a gravitational weight of 140 g/cm² to the skin. The roller was uniformly passed over the tape 10 times at each stripping, thereby addressing the inconsistency issues of pressure application as described in previous papers [5, 6]. The tape (with adhering corneocytes) was then manually removed from the skin by pulling, using firm, rapid and uniform tension. The direction of tape removal (elbow-to-wrist or wrist-to-elbow) was alternated with each tape in order to strip the stratum corneum in a consistent manner (Figure 1).

This standardized procedure was developed and optimized from previous experience [9], with the intention of addressing as many of the adverse issues as possible that had previously been reported with the tape stripping methodology. These issues centered mainly

on the adhesivity of the tape used, the pressure of tape application, the reproducibility of locating each sequential tape strip on exactly the same skin site, and the uniformity of the process of tape removal from the skin. The permanent template fixed to the skin in the procedure described here ensures exact placement of every tape and the weighted roller provides uniformity of pressure application on the tapes. There may certainly still be some variability in the manual removal of the tapes after adhesion, however, with experience and repetition of this process, variability is presumed to be acceptably low when assessed in relation to the overall experimental protocol.

Tape Strip Assessment

Once removed from the skin, each tape was fixed across a photographic slide frame, exposing the tape and adhering corneocytes through the frame aperture (Figure 1D). This frame could easily be accommodated in the solid-sample holder of the spectrophotometer (Lambda 35, Perkin Elmer, Ueberlingen, Germany) with custom modification to monitor an incident light path area of 1 cm² [1]. Each frame was stored under controlled conditions pending analysis.

Stripping with sequential tapes was carried out in this manner at each skin test site to remove the entire stratum corneum layer. The absorbance of every tenth tape/corneocyte sample was measured at 430 nm immediately after removal from the application site, to determine the transmission through the specimen in relation to blank tape. The absorbance (transmission) measured at 430 nm was taken as the relative abundance of stratum corneum material on the sample. Typically the absorbance value recorded at 430 nm is large initially, representing the large percentage of stratum corneum adhering to the first and initial series of strips. Thereafter the absorbance at 430 nm declines as fewer corneocytes adhere to each subsequent tape. Stripping of the skin was stopped when transmission at 430 nm approached 97% (representing almost complete removal of the stratum corneum). In this evaluation the average number of tapes required to remove the entire SC was 62 ± 12 tapes.

Each tape was scanned for absorbance potential between 220 and 500 nm (in order to quantify the sunscreen and relative abundance of corneocytes). Additionally, a blank tape reference was sampled sequentially from the stock roll of Tesa tape after every five skin strip tapes and included in the sample series for analysis. These reference blank tapes served as a baseline control for comparison of the corneocyte/tape data, and sequential inclusion of

multiple blanks allowed continuous correction for any irregularities in the optical properties of the tape from the start to the end of the roll. A typical UV/VIS scan from a tape manipulated in this manner has been presented earlier which shows the strong absorbance at 297 nm, due to the presence of MBC in the sample, and the plateau absorbance value in the visible range due to the presence of corneocytes adhering to the tape [1].

In addition, after being spectrophotometer-analyzed in this manner, each tape was solvent extracted for HPLC analysis as described previously [1]. In this manner the quantitative data from the direct spectrophotometric method and from the conventional solvent extraction/analysis method could be compared.

Statistical Analysis

Validation assessments were conducted using MVA[®] software (Method Validation in Analytics, Novia GmbH, Saarbrücken, Germany), which is based on the guidelines of the ICH. Regression analysis and test result evaluations were made using the appropriate statistical methods within Statgraphics[®] PLUS 5 software (Manugistic, Inc., Rockville, Maryland, USA).

RESULTS

Direct Spectrophotometric Analysis

The MBC and the corneocytes adhering to the tapes were assessed by scanning the tapes spectrophotometrically after stripping from the skin. The absorbance value at 297 nm (Equation 1) [1] was used to determine the abundance of MBC in $\mu\text{g}/\text{cm}^2$ by interpolation of either calibration curve 1 (0.2–5.0 $\mu\text{g}/\text{cm}^2$) or calibration curve 2 (5.0–39.0 $\mu\text{g}/\text{cm}^2$). The plateau absorbance value at 430 nm, when compared with the next blank tape in the series, gave an indication of the relative amount of corneocyte material adhering to each strip.

Each tape strip analyzed in this manner therefore yields information about the abundance of the sunscreen analyte within the skin tape strip, and the relative amount of stratum corneum adhering to each tape (see section Tape Strip Assessment). As exemplified in Figure 2 data can thus be presented in terms of sunscreen abundance versus either the tape strip number or the relative fraction of stratum corneum removed from the epidermis [10].

To determine the total amount of MBC that has entered the SC, the MBC abundance determined per tape and area of tape strip was summated yielding information of the total mass of compound delivered from a specific formulation. The largest abundance of MBC was always found in the initial tape strips, which also removed the largest amount of corneocyte matrix. The first tape removes not only SC with penetrated MBC, but also un-penetrated MBC remaining on the skin surface with residual vehicle. Therefore, data from the first tape was always ignored when the total mass of compound delivered from a vehicle was calculated. The individual and average data for all the subjects tested are depicted in Figure 3. In each subject, delivery is greater from the 4% than from the 2% formulation. Differences between the mass penetrated from the two formulations were analyzed with ANOVA at a 95% confidence level. The results show that the dosing strength of the formulations has a statistically significant ($p < 0.05$) influence on the penetration of MBC (no statistically significant influence of the volunteers on the data).

Comparison of UV/VIS and HPLC Analysis

After the direct determination of MBC on the tapes by UV/VIS spectroscopy, the MBC was extracted from each tape by methanol and, after appropriate dilution, the concentration in the extracts of each tape was assayed by HPLC as described previously [1]. In this manner the analytical data from the UV/VIS and HPLC methods could be compared directly. To this end, all the concentrations obtained by direct spectrophotometric quantification were plotted against the MBC concentrations measured by HPLC (Figure 4) [1]. The data of 2 outliers were included (subject 3, tape 2, formulation MBC 4% and subject 2, tape 1, formulation MBC 4%). The linear correlation factor was 0.974. The value of the slope of the curve is 0.978 with a 95% confidence interval of 0.953 – 1.002. This confirms statistically that the MBC concentration found by UV/VIS method correlates directly with the MBC concentration measured by HPLC after extraction. A paired-sample hypothesis test confirmed that there is no significant difference ($p > 0.05$) between the two analytical procedures.

DISCUSSION AND CONCLUSIONS

In the present research the validation of a direct spectrophotometric procedure was completed by comparing *in vivo* data from a UV/VIS assessment and from HPLC analysis following solvent extraction of MBC from tapes strips harvested from skin treated with a

complex topical delivery vehicle. A highly standardized tape skin stripping procedure has been developed for this purpose to overcome methodological shortcomings previously reported for the technique [9]. A direct correlation has been found for the data from the two methods. Therefore, the validations presented here verify that the direct spectrophotometric analysis of MBC on skin tape strips is equally valid to the more laborious solvent extraction/HPLC analysis.

The results show furthermore that the dosing strength (2% vs 4%) of the formulations has a statistically significant ($p < 0.05$) influence on the penetration of MBC (no statistically significant influence of the volunteers on the data) into stratum corneum. This is clear evidence that the tape-stripping technique is sensitive and reliable enough to be used for developing new or improving old formulations including topical sun protection products.

This experimental evaluation completes the full validation of the optimized and standardized tape stripping methodology and gives credence to the use of this technique for the *in vivo* determination of sunscreen delivery to the skin from topical delivery vehicles. The delivery of sunscreen from a representative sample of vehicles, using the direct spectrophotometric determination method, is compared in paper three of this series [11].

REFERENCES

1. Tassopoulos T, Figueiredo V, Imanidis G, Smith EW, Surber C. Simultaneous spectrophotometric determination of a sunscreen agent and relative stratum corneum tissue density in skin tape strips. I. Validation of analytical methodology. Submitted. J Pharm Sci 2005.
2. Guidance for Industry. Q2B Validation of analytical procedures: Methodology. International Conference on the Harmonization of Technical Requirements for the Registration of Pharmaceuticals for Human Use, Center for Drug Evaluation and Research, Center for Biologics Evaluation and Research, Food And Drug Administration, U.S. Department of Health and Human Services, 1996, p 1-10.
3. Tsai J-C, Weiner ND, Flynn GL, Ferry J. Properties of adhesive tapes used for stratum corneum stripping. Int J Pharm 1991;72:227-231.
4. Bashir SJ, Chew A-L, Anigbogu A, Dreher F, Maibach HI. Physical and physiological effects of stratum corneum tape stripping. Skin Res Technol 2001;7:40-48.
5. Lademann J, Weigmann H-J, Lindemann U, Audring H, Antoniou C, Tsirikas G, et al. Investigations on the influence of furrows and wrinkles when quantifying penetration of drugs and cosmetics by tape stripping. In: Brain KR, Walters KA, eds. Perspectives in Percutaneous Penetration; 2002; Juans-Les Pins, Antibes; 2002. p. 49.

6. Loffler H, Dreher F, Maibach HI. Stratum corneum adhesive tape stripping: influence of anatomical site, application pressure, duration and removal. *Br J Dermatol* 2004;151(4):746-752.
7. COLIPA Sun protection factor test method. European Cosmetic, Toiletry, and Perfumery Association (COLIPA). Brussels, Belgium, 1994, p 1-72.
8. Guidance for Industry. E6 Good Clinical Practice: Consolidated Guidance. International Conference on the Harmonization of Technical Requirements for the Registration of Pharmaceuticals for Human Use, Center for Drug Evaluation and Research, Center for Biologics Evaluation and Research, Food and Drug Administration, U.S. Department of Health and Human Services, 1996, p 1-63.
9. Surber C, Schwarb FP, Smith EW. Tape-Stripping technique. In: Bronaugh RL, Maibach HI, eds. *Percutaneous Absorption*. Third, Revised and Expanded ed. New York, Basel: Marcel Dekker; 1999. p. 395-409.
10. Jacobi U, Meykadeh N, Sterry W, Lademann J. Effect of the vehicle on the amount of stratum corneum removed by tape stripping. Einfluss der Salbengrundlage auf die mittels der Abrissmethode entnommene Menge an Stratum corneum. *J Deut Dermatol Gesell* 2003;1(11):884-889.
11. Tassopoulos T, Figueiredo V, Imanidis G, Smith EW, Surber C. Simultaneous spectrophotometric determination of a sunscreen agent and relative stratum corneum tissue density in skin tape strips. III. Comparison of vehicle effects in Humans. Submitted. *J Pharm Sci* 2005.

Figure 1: Tape stripping procedure. A strip of adhesive tape was placed over the skin area exposed through the template aperture (B, C). Pressure was then applied perpendicularly to the adhering tape in a uniform manner using a hand roller that supplied a gravitational weight of 140 g/cm^2 to the skin (A). The roller was uniformly passed over the tape 10 times at each stripping. The tape (with adhering corneocytes) was then manually removed from the skin by pulling, using firm, rapid and uniform tension (C). The direction of tape removal (elbow-to-wrist or wrist-to-elbow) was alternated with each tape in order to strip the stratum corneum in a consistent manner. Once removed from the skin, each tape was fixed across a photographic slide frame, exposing the tape and adhering corneocytes through the frame aperture (D). Each frame was stored under controlled conditions pending analysis.

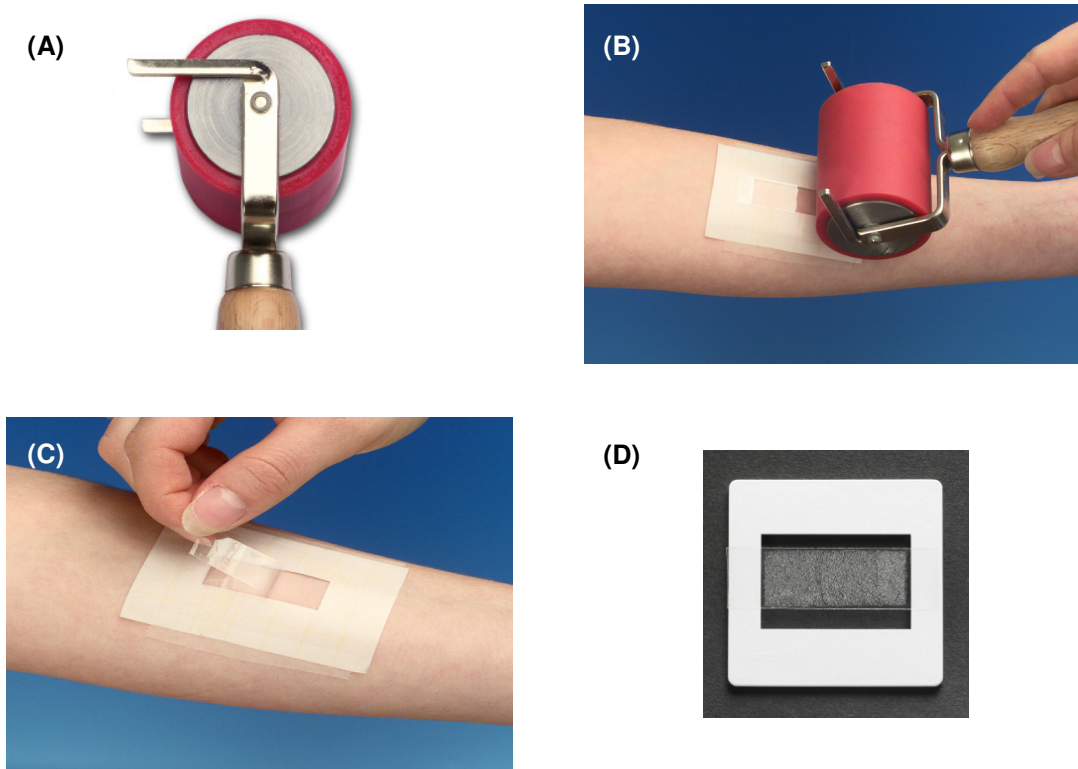


Figure 2: Typical stratum corneum profile of MBC from the (A) 2% formulation and the (B) 4% formulation from an individual. Data is presented in terms of sunscreen abundance versus either tape strip number (left axis) or relative fraction of stratum corneum removed from the epidermis (right axis).

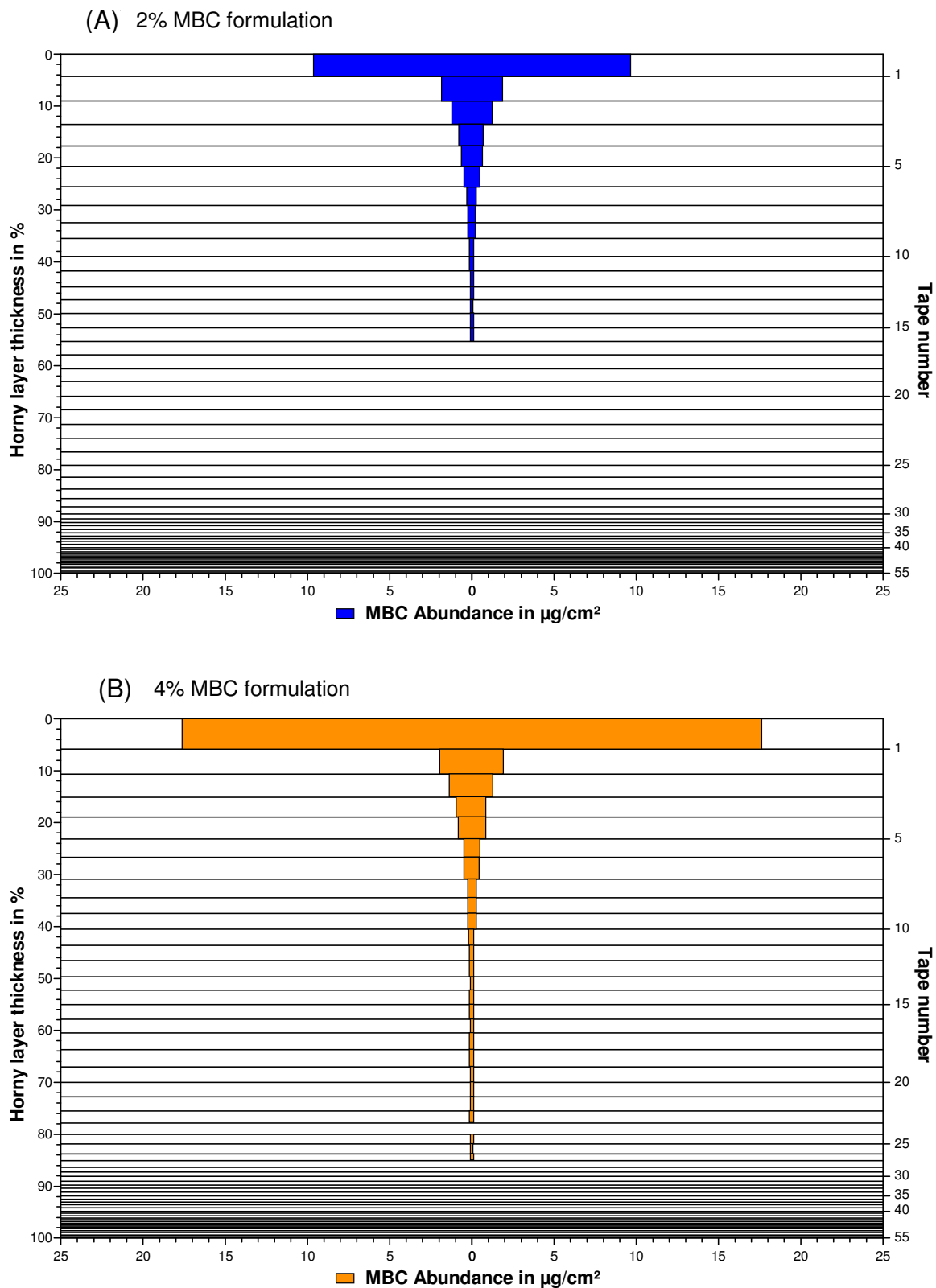


Figure 3: Total mass (μg) of MBC determined by direct spectrophotometric analysis delivered from the 2% and 4% formulations: individual subjects (A), and average data for all subjects (B). Dosing strength of the formulations has a statistically significant ($p < 0.05$) influence on the penetration of MBC.

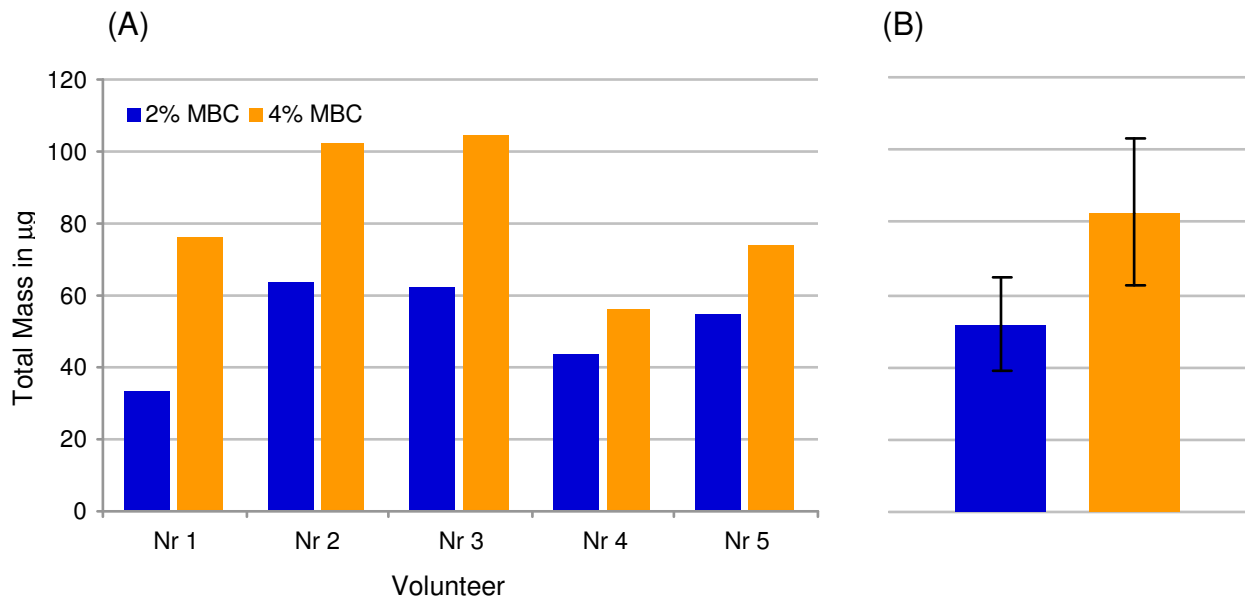
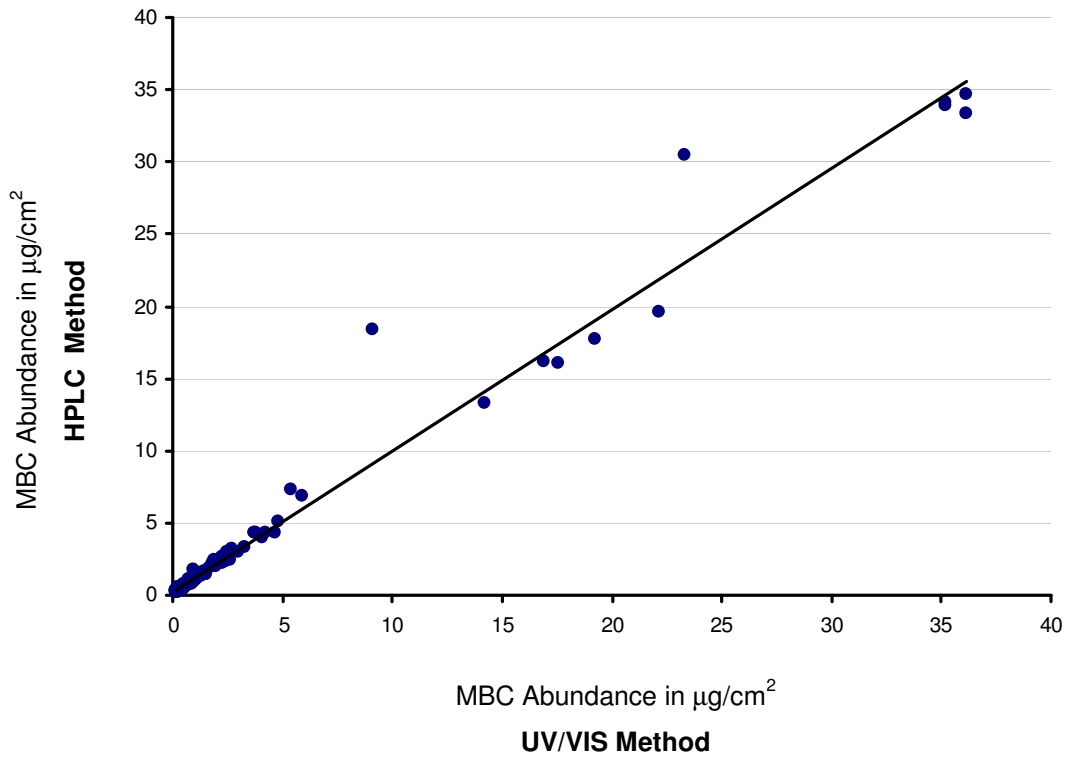


Figure 4: Correlation of the MBC concentrations measured by UV/VIS spectroscopy and the concentrations measured by HPLC. Regression equation: $y = 0.978x + 0.193$, $R^2 = 0.974$. Information on outliers see section Comparison of UV/VIS and HPLC Analysis.



8.3 Simultaneous spectrophotometric determination of a sunscreen agent and relative stratum corneum tissue density in skin tape strips. III. Comparison of vehicle effects in Humans³

INTRODUCTION

It is a well established phenomenon in topical and transdermal formulation development that the vehicle into which the active is incorporated has a marked influence on the rate and extent of drug delivery [1-3]. Moreover, we have already shown the importance in the drug delivery process of not only the chemical composition of the delivery formulation, but also the three-dimensional structural matrix that is formed on manufacture [4]. This concept is currently being investigated at length for physical matrices such as microemulsions and solid lipid nanoparticles [5]. The influence of the delivery vehicle is therefore an important parameter that must be evaluated and validated in the development of a new analytical procedure. Any analytical process that is adopted for routine use in the pharmaceutical industry must be shown to be sensitive and accurate in the presence of diverse delivery matrices. Moreover, if the analytical procedure is quantifying bioavailability parameters, then the protocol must be able to show significant difference in the rate and extent of topical drug delivery if these differences exist.

A previous publication [6] has described the quantitative comparison and analytical validation of 3-(4-Methylbenzylidene)-camphor (MBC) data from an optimized human skin tape stripping procedure. This data has been obtained from the tape matrix by both conventional solvent extraction/HPLC means, and directly assessed by our fully-validated UV/VIS methodology. This data was found to be equally accurate and precise, regardless of the means of analysis. The convenience and facilitated sample handling of the UV/VIS methodology make this the method of choice for further study. Therefore, in this paper we describe the application of the direct UV/VIS technique to the *in vivo* determination of sunscreen delivery to the skin from different topical delivery vehicles, in an attempt to validate the usefulness of the direct UV technique in assessing complex vehicle effects in topical drug delivery.

³ Text submitted for publication: Tassopoulos T, Figueiredo V, Imanidis G, Smith EW, Surber C 2006. Simultaneous Spectrophotometric Determination of a Sunscreen Agent and Relative Stratum Corneum Tissue Density in Skin Tape Strips. III. Comparison of Vehicle Effect in Humans. *J Pharm Sci*. (Note that the in-text citations are referred to in the bibliography at the end of this section.)

MATERIAL AND METHODS

Chemicals

The UV filter 3-(4-Methylbenzylidene)-camphor (MBC) was obtained from Merck KgaA, Darmstadt, Germany. Propylene glycol and polyethylene glycol 400 (Macrogol 400) were purchased from Hänseler AG, Herisau, Switzerland. Mineral oil (paraffinum liquidum) was purchased from Siegrfried Ltd., Zofingen, Switzerland. Transcutol®GC (diethylene glycol monoethyl ether) was obtained from Gattefossé S.A., Saint Priest, France. Tesa Multi-Film Kristall-Klar® 57315 tape was obtained from Tesa, Beiersdorf, Hamburg, Germany. Methanol, HPLC grade, was obtained from Scharlau Chemie S.A., Barcelona, Spain.

Instrumentation, Equipment and Statistical Analysis

Leopold glass application chambers (Figure 1) [7] were used to apply and contain the liquid delivery vehicles on the skin. Spectrophotometric measurements of MBC on the tapes stripped from the skin were made using a custom-modified UV-Spectrophotometer (Lambda 35, Perkin Elmer, Ueberlingen, Germany); which was controlled by UV WinLab Software (v 2.85) [6, 8]. Skin strips collected from the vehicle-treated sites were analyzed for MBC content and corneocyte abundance according to a fully validated UV/VIS method described in detail previously [6, 8]. Data were evaluated for statistically significant differences ($p < 0.05$) using analysis of variance (ANOVA) procedure in Statgraphics® PLUS 5 software (Manugistic, Inc., Rockville, Maryland, USA).

Subjects

A standardized clinical protocol was developed for volunteer processing, according to international GCP guidelines [9] and was approved for implementation by the Internal Review Board of the institution. Fifteen volunteers (7 female, 8 male), aged from 25 to 35 years, participated in the studies. All subjects were in good general health and had no history of dermatological diseases. Informed consent was obtained from all the participants. The volunteers were asked not to apply detergents or emollients to the forearm on the day of the experiment. The subjects rested for 30 min before the experiment at constant environmental conditions of 24 °C room temperature and 40% relative humidity.

Vehicle Formulations

The delivery vehicles were prepared according to cGMP Guidelines. The following five vehicles were used: propylene glycol, mineral oil, PEG 400, PEG 400 containing 10% Transcutol[®]GC, and PEG 400 containing 50% Transcutol[®]GC. To ensure comparable thermodynamic activity of MBC in the different vehicles, all formulations were saturated with MBC. Saturation solubility of MBC was achieved by adding an excess amount of the sunscreen to each vehicle in a 50 mL flask, and the solution was equilibrated for 24 hours in a water bath at $33 \pm 1^\circ\text{C}$ with continuous stirring. After centrifugation of the mixture (Labofuge I, Haereus Christ, Laborgeräte AG, Zürich, Switzerland, 10 min., 4000 rpm) the solution was maintained at 33°C until used for subject application. The MBC saturation solubility in the different formulations was determined by simple UV/VIS spectroscopy and these values are shown in Table 1.

Vehicle Application

Two or three sites on the ventral surface of each forearm of each volunteer were treated (four or six total sites per subject dependent on the protocol). The glass chamber was fixed to the application site with straps and an aliquot of the delivery vehicle was introduced through the side-port. At the end of the vehicle-skin contact time, the residual formulation was removed at each site with four, sequential, dry cotton swabs before tape stripping the treated skin area.

Tape stripping procedure

Treated skin sites were tape-stripped with Tesa[®] tape using a standardized method previously described in detail [6, 8]. After removal of the delivery formulations, a flexible template of 5 cm x 7 cm with a rectangular aperture of 1.3 cm x 3.3 cm was fixed onto the treated skin surface with adhesive tape. A strip of Tesa[®] tape was placed on the skin surface exposed through the aperture, and pressure was applied perpendicularly to the adhering tape in a uniform manner using a hand roller. The tape was then manually removed, alternating the direction of stripping (elbow-to-wrist or wrist-to-elbow).

Experimental Design

Two sets of experiments were conducted to evaluate the influence of vehicle and application time on MBC penetration into the SC and the influence of vehicle to create a reservoir of MBC in the skin (substantivity).

Influence of Vehicle and Application Time on MBC Penetration

The influence of propylene glycol (F1) and mineral oil (F2) as vehicle, and the influence of the skin-contact time, on MBC penetration were investigated in five subjects (2 males/3 females). Three sites were dosed on each forearm such that each formulation was randomly applied three times to each subject. Each formulation was allowed to remain on the skin for three durations ($t=1\text{h}$, $t=3\text{h}$, and $t=6\text{h}$) before removal of residual formulation.

Influence of Vehicle on the Substantivity of MBC

Three formulations, PEG 400 (F3) [control], PEG 400 containing 10% Transcutol[®]GC (F4) and PEG 400 containing 50% Transcutol[®]GC (F5), were evaluated in ten subjects (5 males/5 females) for their ability to create a reservoir of MBC in the skin (substantivity). Each subject was treated with control (F3) and one other formulation: either F3/F4 (five subjects) or F3/F5 (five subjects). At time zero, each of the two formulations was applied to a single site on each forearm of every subject, randomized with respect to the location on the arm and left versus right arm. All formulations remained on the skin for one hour, and residual vehicle was then removed by dry swabbing. One treated site for each vehicle was stripped immediately after removal of the formulation (at one hour post application); the other site was stripped at seven hours after initial application, six hours after vehicle removal.

RESULTS

Influence of Vehicle and Application Time on MBC Penetration

The total mass of MBC penetrating into the SC on all the tape strips was summated from the data of each individual strip analysis as described in detail previously [6]. The first tape collected from each site of all the subjects was discarded due to potential drug/vehicle remaining on the skin surface. The data from this evaluation are depicted in Figure 2.

At all contact times investigated there was greater penetration of MBC into the SC from the propylene glycol than from the mineral oil vehicle. An ANOVA evaluation was conducted with the log-transformed results based on the analysis factors of “formulation”, “time” and “volunteer”. In addition, the combined effects of a) formulation – time, b) formulation – volunteer and c) time – volunteer were evaluated. The only statistical parameter that showed a significant effect ($p<0.05$) on MBC penetration was “formulation”. All other factors evaluated (time, volunteer, and combined effects) showed no significant effect.

The number of tape strips used to completely remove the stratum corneum was compared for the propylene glycol and mineral oil vehicles in the five subjects (Figure 3). A paired sample t-test was conducted to compare the means of the total number of tapes required for complete SC removal for all application durations. There is a statistically significant difference ($p=0.05$) between the number of tape strips required for complete SC removal in the presence of the propylene glycol and mineral oil vehicles, at each application duration.

Influence of Vehicle on the Substantivity of MBC

The total mass of MBC penetrating the SC after one hour of vehicle contact, and the mass remaining in the SC six hours after swabbing of residual formulation (seven hours after initial application), was analyzed as previously described. An ANOVA evaluation was conducted with the log-transformed results based on the analysis factors of “formulation”, “time” and “volunteer”. In addition, the combined effects of a) formulation – time, b) formulation – volunteer and c) time – volunteer were evaluated.

PEG 400 (F3) versus PEG 400 + 10% Transcutol®CG (F4)

There was no significant difference ($p<0.05$, all factors) in the mass of MBC found in the stratum corneum delivered from the PEG 400 formulation or from that containing 10% Transcutol®CG, either at 1- nor 7-hours after initial application (Figure 4).

PEG 400 (F3) versus PEG 400 + 50% Transcutol®CG (F5)

The comparison of the formulations containing 50% Transcutol®CG and the formulation without Transcutol®CG by means of the variance analysis was statistically significant for the factors “formulation”, “time interval” and “volunteer” ($p<0.05$). No significant effect was detected for the combined effects. Thus, there is a significant difference in MBC penetration in the presence or absence of 50% Transcutol®CG, both at 1-hour and at 7-hours post application (Figure 5). In addition, this comparison of formulations indicated a significant difference between individual test subjects (inter-individual distribution). This methodology is, therefore, capable of detecting differences in the extent of reservoir formation of the sunscreen when applied to the skin in different delivery vehicles.

CONCLUSIONS

The evaluations reported in this series of papers [6, 8, 10] provide a comprehensive evaluation of the optimized tape-stripping technique, the analysis of permeant and corneocyte abundance on tape strips, and the comparison of HPLC-extract and direct UV/VIS analysis of the strip samples. In addition, it has been shown that the fully validated UV/VIS method of analysis for skin tape strips collected from the optimized in vivo methodology is applicable to accurately monitoring the delivery of MBC from different topical vehicles. Importantly, the optimized methodology is capable of showing significantly-different extents of active delivery from the different vehicles where these exist, underscoring the potential use of the stripping protocol in topical bioequivalence evaluations. It must be stressed that the credence of this data obtained is based on a full analytical validation and verification of all aspects of the methodology – both analytical procedures and sample procurement methods – based on pharmaceutical industry standards. The facilitated handling of the tape strips, and the rapid means of analysis make this a very attractive method for sunscreen product development and formulation performance evaluation. Moreover, the analytical procedures, with appropriate modifications, should have equal applicability to other classes of topical drugs (e.g. topical antifungals or retinoids), and to other chemicals that may be important for agricultural or military monitoring (e.g. insecticides or chemical warfare agents).

REFERENCES

1. Schwarb FP, Gabard B, Ruffli T, Surber C. Percutaneous absorption of salicylic acid in man after topical administration of three different formulations. *Dermatology* 1999;198:44-51.
2. Treffel P, Gabard B. Skin penetration and sun protection factor of ultra-violet filters from two vehicles. *Pharm Res* 1996;13(5):770-774.
3. Jacobi U, Tassopoulos T, Surber C, Lademann J. Cutaneous distribution and localization of dyes affected by vehicles all with different lipophilicity. *Arch Dermatol Res* 2005;297(7):303-310.
4. Surber C, Smith EW. The mystical effects of dermatological vehicles. *Dermatology* 2005;210:157-168.
5. Date AA, Naik B, Nagarsenker MS. Novel drug delivery systems: Potential in improving topical delivery of antiacne agents. *Skin Pharmacol Physiol* 2006;19:2-16.

6. Tassopoulos T, Figueiredo V, Imanidis G, Smith EW, Surber C. Simultaneous spectrophotometric determination of a sunscreen agent relative stratum corneum tissue density in skin tape strips. II. Application of the method in Humans. Submitted. J Pharm Sci 2005.
7. Leopold C, Lippold BC. A new application chamber for skin penetration studies in vivo with liquid preparations. Pharm Res 1992;9(9):1215-1218.
8. Tassopoulos T, Figueiredo V, Imanidis G, Smith EW, Surber C. Simultaneous spectrophotometric determination of a sunscreen agent and relative stratum corneum tissue density in skin tape strips. I. Validation of analytical methodology. Submitted. J Pharm Sci 2005.
9. Guidance for Industry. E6 Good Clinical Practice: Consolidated Guidance. International Conference on the Harmonization of Technical Requirements for the Registration of Pharmaceuticals for Human Use, Center for Drug Evaluation and Research, Center for Biologics Evaluation and Research, Food and Drug Administration, U.S. Department of Health and Human Services, 1996, p 1-63.
10. Tassopoulos T, Figueiredo V, Imanidis G, Smith EW, Surber C. Simultaneous spectrophotometric determination of a sunscreen agent and relative stratum corneum tissue density in skin tape strips. III. Comparison of vehicle effects in Humans. Submitted. J Pharm Sci 2005.

Figure 1: Leopold glass application chamber.

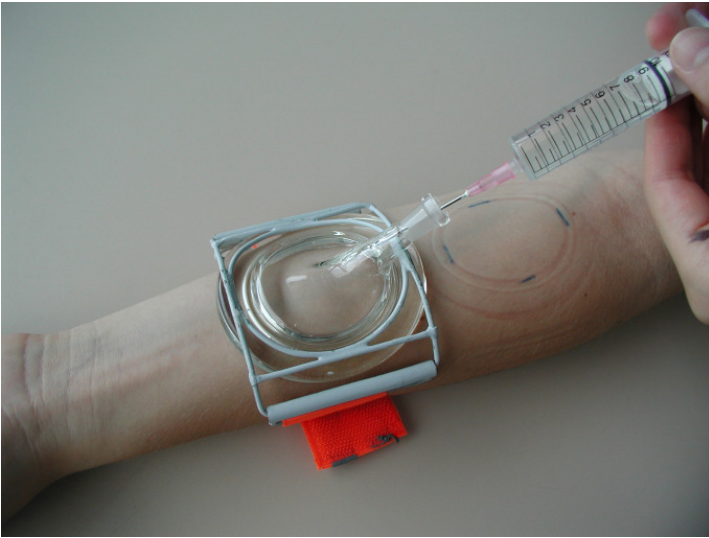


Figure 2: Total mass (μg) of MBC determined delivered from propylene glycol and mineral oil after 1h, 3h, and 6h of vehicle application ($\bar{x} \pm \text{SD}$; n=5).

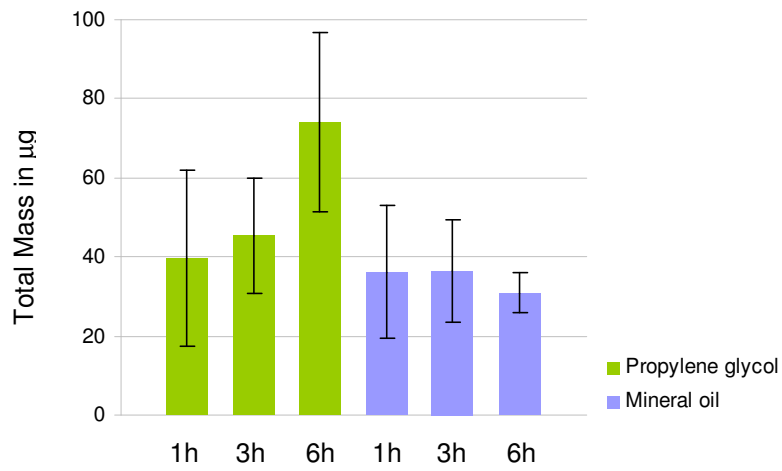
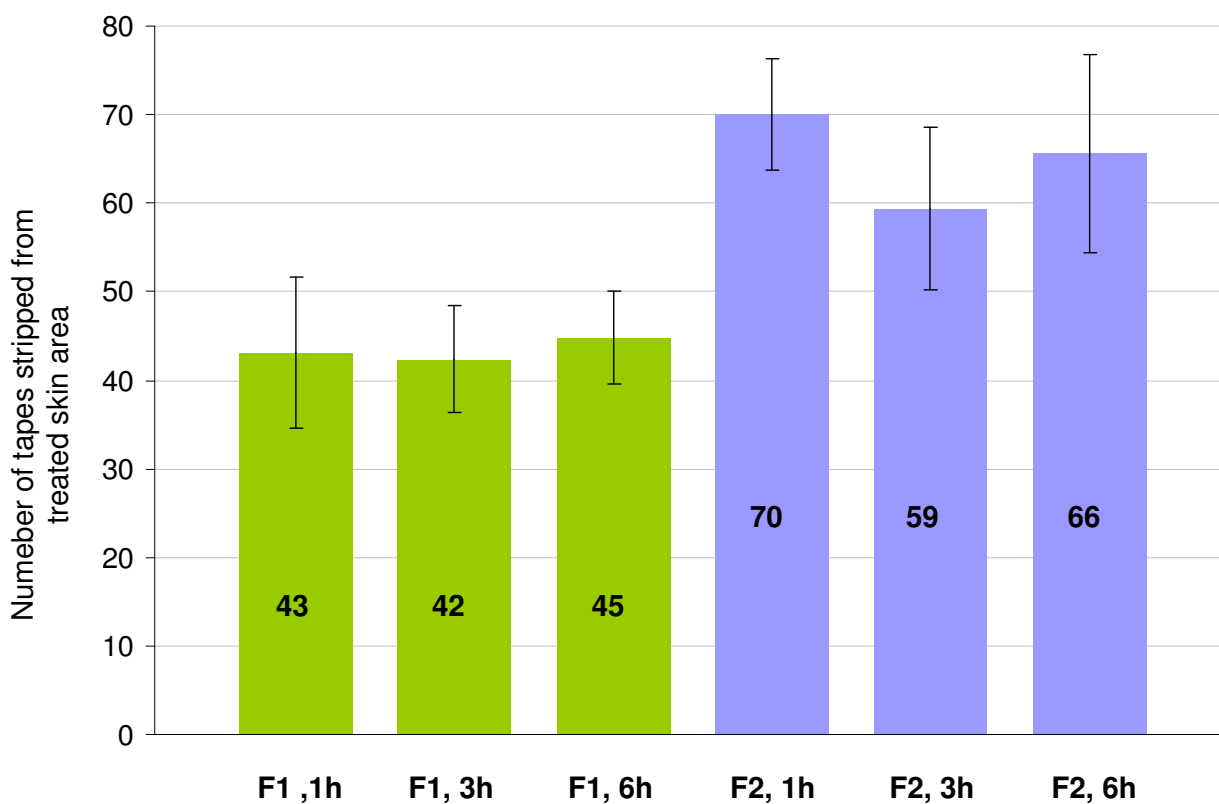


Figure 3. Number of tapes required to remove the stratum corneum after treatment with propylene glycol (F1) and mineral oil (F2), at different application durations.



Legend. n=5 (volunteers) for both formulations.

F1, 1h: $x = 43$; $SD = \pm 9$.

F1, 3h: $x = 42$; $SD = \pm 6$.

F1, 6h: $x = 45$; $SD = \pm 5$.

F2, 1h: $x = 70$; $SD = \pm 6$.

F2, 3h: $x = 59$; $SD = \pm 9$.

F2, 6h: $x = 66$; $SD = \pm 11$.

Figure 4: Total mass (μg) of MBC determined delivered from the formulations containing 0% and 10% Transcutol at 1 hour and 7 hours post application ($\bar{x} \pm \text{SD}$; $n=5$ except for PEG 400, 0h and PEG 400, 6h ($n=10$)).

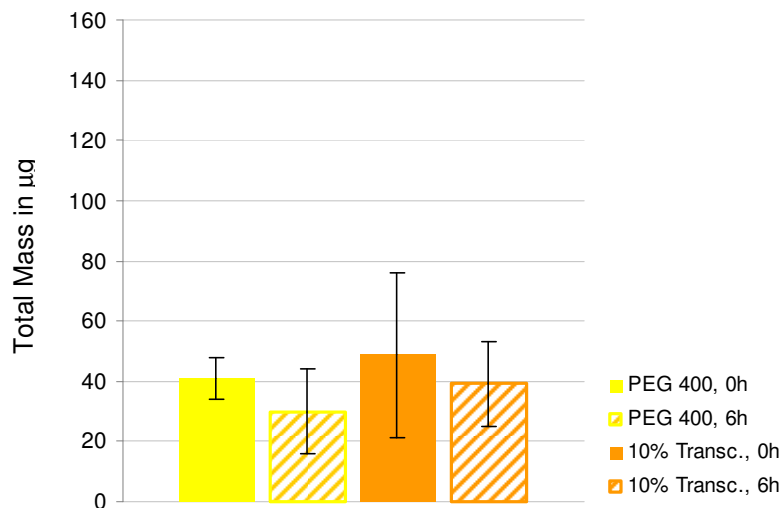


Figure 5: Total mass (μg) of MBC determined delivered from the formulations containing 0% and 50% Transcutol at 1 hour and 7 hours post application ($\bar{x} \pm \text{SD}$; $n=5$ except for PEG 400, 0h and PEG 400, 6h ($n=10$)).

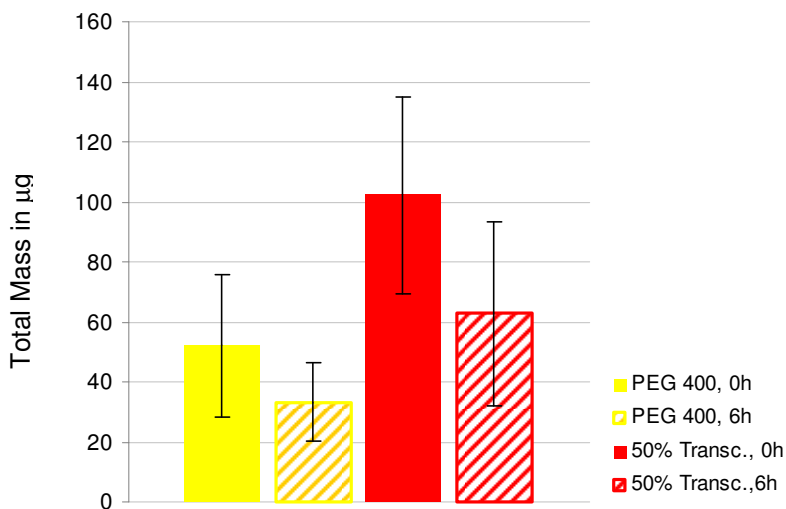


Table 1: Saturation solubility of MBC in different delivery vehicles

VEHICLE	ABBREVIATION	SATURATION SOLUBILITY	
Propylene glycol	F1	2.4 ± 0.1% (m/m)	24.4 ± 1.2 mg/mL
Mineral oil	F2	8.8 ± 0.7% (m/m)	76.3 ± 6.9 mg/mL
PEG 400	F3	7.6 ± 0.2% (m/m)	85.2 ± 3.6 mg/mL
PEG 400 + 10% Transcutol®GC	F4	9.4 ± 0.4% (m/m)	103.0 ± 4.3 mg/mL
PEG 400 + 50% Transcutol®GC	F5	19.6 ± 0.6% (m/m)	203.3 ± 5.8 mg/mL

9 Overall conclusion and future perspectives

Chemical sunscreens are the active ingredients in sunscreens and they reduce the amount of UV radiation reaching the skin by absorption. The concentration and combination of sunscreens in a formulation determine the efficacy of sunscreens as measured by the sun protection factor. To be effective the sunscreens should ideally remain on the skin surface or penetrate in the upper most layers of the stratum corneum (SC) after application. The vehicle influences both the sun protection factor and the extent of sunscreens agent penetration. In the present work, the SC penetration capacity of the model compound 3-(4-Methylbenzylidene)camphor (4-MBC), a commonly used sunscreens agent, from different delivery vehicles was investigated by tape skin stripping. The data of the stripping experiment were analyzed by an analytical method developed and validated for the simultaneous determination of the analyte and SC directly on tapes.

Validation of Analytical Methodology.

A commonly used method for analyte determination on tapes consists of sample extraction followed by HPLC analysis. However, this quantification method is time consuming and may involve loss of analyte. In order to relate the mass of permeant found on each strip to SC depth or volume, the mass of SC removed has to be determined. For SC determination several methods are described in the literature (e.g. weighing of tapes or determination of the protein content) that are laborious and susceptible to artefacts. The present spectrophotometric method comprises the advantage of a simultaneous determination of SC and analyte directly on the tape using simple sample handling procedures. With a modified UV/VIS spectrophotometer, the simultaneous determination of SC and at least one analyte on a tape with only one absorbance spectrum can be performed presuming different absorbance maxima of the analytes and no interferences with the tape matrix. The purpose of the first part of the present work was to develop and validate a simple and accurate spectrophotometric method for the simultaneous quantification of both 4-MBC and SC on tape strips. The validation parameters of the proposed spectrophotometric method were evaluated according to guidelines of the International Conference on Harmonization of Technical Requirements for Registration of Pharmaceuticals for Human Use (ICH) and compared to a conventional solvent extraction/HPLC method.

The following validation parameters were absolutely comparable to those of the HPLC method: linearity range, intermediate precision and repeatability, accuracy, detection limit

(DL) and quantitation limit (QL). In particular, DL und QL of the UV/VIS method were lower by approximately a factor 2 than DL and QL of the HPLC method. Statistical analysis of recovery data showed no difference in the amount of 4-MBC found by both methods. The direct spectrophotometric technique was demonstrated to be precise and sensitive enough for the accurate determination of low analyte concentrations on the tape strips as there was no loss of analyte in the sample handling protocol.

Application of the method in Humans.

The second part of the work consisted in a tape stripping experiment with the purpose of investigating 4-MBC delivery into the SC after application of a 2% and 4% emulsion for one hour in vivo. Both methods, UV/VIS spectroscopy and solvent extraction/HPLC, were applied for analysis of the tapes. The data obtained from the analytical methods were set in comparison to each other. The 4-MBC delivery from both formulations was evaluated.

The variability of the tape stripping data was minimized by optimization and standardization of the sample procurement. These issues centered mainly on the adhesivity of the tape used, the pressure of tape application by using a hand roller, the reproducibility of locating each sequential tape strip on exactly the same skin site by using a template, and the uniformity of the process of tape removal from the skin.

In order to compare the total amount of 4-MBC that had entered the SC, the data were evaluated as SC profiles and the 4-MBC abundance determined per tape and area of tape strip was summated in order to yield information of the total mass of compound delivered. In the profiles, the penetrated 4-MBC amount is presented versus either the tape strip number or the relative fraction of stratum corneum removed from the epidermis. The vehicle effect can be visualized by the thickness of the bars representing the relative amount of stratum corneum adhering to the tape. However, the interpretation of the amount of sunscreensing agent in the SC depicted as a funnel does not represent the real distribution of the compound and can thus be misleading. In order to compare the 4-MBC delivery from the 2% and 4% 4-MBC formulation, the data were calculated as total mass. The results show that the dosing strength of the formulations has a statistically significant influence on the penetration of 4-MBC. The higher 4-MBC delivery from the 4% 4-MBC formulation can be explained by the higher drug concentration and saturation degree in the vehicle. The 4-MBC abundance measured by UV/VIS spectroscopy showed an excellent correlation ($R^2 = 0.974$) with the solvent extraction/HPLC. This investigation confirmed that the accuracy and precision of the direct spectrophotometric method, combined with its ease of use, make this an ideal

analytical tool for rapidly processing the large data sets involved in dermatopharmacokinetic studies of sunscreens, contained in a variety of delivery systems.

Comparison of vehicle effects in Humans

The third part of the present work addresses the evaluation of the influence of delivery vehicle and application time on the penetration and substantivity of 4-MBC into the SC in vivo using the direct spectrophotometric method. The vehicle effect describes not only the influence of a delivery vehicle on the penetration due to its composition, but also the influence of a delivery vehicle due to the changes occurring in the formulation due to application (vehicle metamorphosis). These changes include: evaporation of volatile components, penetration of ingredients into the skin, or water uptake from the skin into the vehicle. All of these effects also depend on the individual and on the environmental conditions.

In this part, the influence of the following vehicles on 4-MBC penetration was investigated: (1) propylene glycol (PG) versus mineral oil (MO); (2) Polyethylene glycol 400 (PEG 400) vehicles containing 0%, 10% and 50% Transcutol[®]CG. In order to compare the influence of different vehicles on 4-MBC penetration into the SC, all vehicles investigated in the experiments were saturated 4-MBC-solutions thus obtaining constant thermodynamic activity of 4-MBC in all vehicles.

The vehicle effect of PG and MO on 4-MBC penetration could clearly be demonstrated. The experiment showed that the sunscreens agent delivery was significantly higher from the PG formulation than from the MO formulation, although the solubility of 4-MBC was approximately 3.5 times lower in the PG formulation than in the MO formulation. These observations point to the penetration enhancing effect of PG. A plausible hypothesis is that PG loosens the corneocytes and thereby alters the skin barrier function. This phenomenon was clearly demonstrated by the low number of tapes required to strip off the entire SC. The different application times (1hr, 3hrs and 6hrs) had no significant influence on the penetration of 4-MBC neither from the PG nor from the MO formulation.

Adding 10% Transcutol[®]CG to PEG 400 did not increase the total mass of 4-MBC penetrated compared to pure PEG 400 at one hour post application. Seven hours post vehicle application the total mass of 4-MBC in SC was the same as at one hour post application for both vehicles. An addition of 50% Transcutol[®]CG increased the 4-MBC solubility and consequently the total mass of penetrated 4-MBC almost proportionally to the solubility. Seven hours post application the total mass of 4-MBC was reduced compared to one hour

post application. The experiment confirmed that rate and extent of compound penetration, measured one hour post application, correlate with its solubility in the vehicle. PEG 400 is known to increase the solubility of a compound in the SC and thus retain it in the SC. Adding Transcutol[®]CG in a concentration of 10% did not result in changes in substantivity seven hours post application. For 50% Transcutol[®]CG, however, a difference in 4-MBC measured in the SC between one hour and seven hours post application could be confirmed by ANVOVA.

The findings of this experiment cannot readily be applied to commercial sunscreens because of the special conditions throughout this experiment such as vehicle application through the Leopold chamber, which affects the environmental conditions and thus the vehicle metamorphosis. They provide, however, useful insights into the influence of these studies parameters on the effectiveness of sunscreen formulations.

Future Perspectives

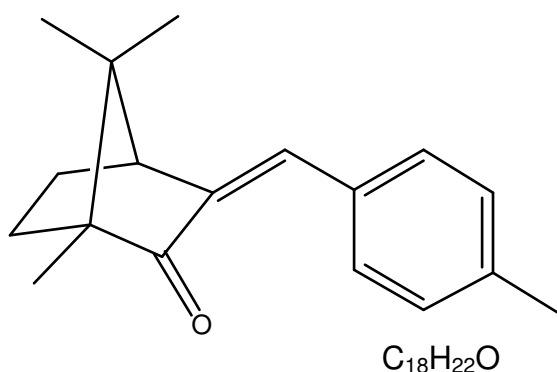
While conceptually simple, sunscreen formulations are quite complex, requiring careful selection and evaluation of UV filter and vehicle components. The facilitated handling of the tape strips and the rapid means of analysis render the spectrophotometric method a very attractive tool for sunscreen product development and formulation performance evaluation.

Future perspectives in the development of sunscreens include DNA repair enzymes or factors, which can induce the endogenous cellular DNA repair system such as topically applied pTT (thymidine dinucleotide). Thereby, the risk to develop UV-induced skin malignancies is markedly reduced. Forthcoming research also has the potential to develop sunscreens that can prevent UV-induced immune suppression and that can greatly enhance the ability to deflect the UV rays. In the research and development of new suncreening agents it is of great importance not to investigate only the effects of individual potential compounds, but to take into consideration the impact of the vehicle they will be embedded in. Recently, for the first time a clinical study was able to show the potential of a commercial sunscreen product to block UV-induced immunosuppression in healthy volunteers [245].

10 Appendix

10.1 Physical and Chemical Data for 4-Methylbenzylidene camphor

IUPAC name	1,7,7-trimethyl-3-[(4-methylphenyl)methylidene]norbornan-2-one
Other names	3-(4-Methylbenzylidene)-camphor; 3-(4-methylbenzylidene)-DL-camphor; 3-(4-Methylbenzylidene)bornan-2-one; Eusolex 6300; Neo Heliopan MBC; Parsol 5000; Uvinul MBC 95



Chemical structure

Molecular weight 254.37g/mol

Appearance white powder

Solubility	isopropanol	25 g in 100 mL
	ethanol	25 g in 100 mL
	glycerol	12 g in 100 mL
	propylene glycol	4 g in 100 mL
	water	0.00013 g in 100 mL
	vegetable oils	freely soluble

Specific absorbance 930-990 at 299 nm (1%, MeOH, 1 cm)

λ_{\max} ca. 300 nm

4-Methylbenzylidene camphor is a UVB filter with high absorptivity that is approved in the EU and is suitable for use in all major types of sunscreen products (o/w and w/o emulsions, gels and aerosols). Concentration up to 4% is recommended.

Table 8. Approval status of 4-MBC.

	EU	USA	Japan
4-MBC	+ (4%)	-	-

+ = provisionally or finally approved as a sunscreen agent (with max. concentration)

- = not approved

10.2 UV/VIS spectrophotometer specification

In order to guarantee the success of this project a special spectral device was necessary that measures the components fixed on the tape strips and integrates an area of about 1 cm² in the strips. Perkin Elmer produced this instrument with the following technical specifications:

- Double beam spectrometer
- Wavelength range 190-1100 nm
- Wavelength resolution 2 nm
- Measuring area ≥ 1cm²

10.2.1 Introduction

The measurements of the horny layer particles require a specific measurement set up. This set up has been realized on the basis of a Perkin-Elmer Lambda 35 UV/VIS spectrophotometer. The aim of this set-up is to provide a uniform measurement area of approximately 10 mm x 10 mm while keeping the operating functions and options of a standard UV/VIS spectrophotometer. In Berlin and Athens two instruments have been modified according to the instrument optics.

Lambda 35 is a high quality routine UV/VIS spectrometer with a wavelength range of 190-1100 nm and a standard resolution of 2 nm spectral bandwidth. The instrument is equipped with a serial RS-232C communications interface that allows full control of the instrument by PC software. The UV/VIS spectroscopy applications software package UVWinLab version 2.7 is part of the package.

10.2.2 Adaptations of Perkin-Elmer Lambda 35 UV/VIS-Spectrometer

The instrument has been adapted by Perkin Elmer (Ascanis OHG, D-88662 Überlingen, Mr. Liekmeier). A number of different approaches were tested by optical calculations and experimental set ups.

The spherical mirror within the common beam was replaced by a toroidal mirror of radius vertical $R_v=215.3$ mm and radius horizontal $R_h=275.6$ mm. Size and thickness of the mirror were approximately 25 mm x 25 mm and 14 mm, respectively. The modified optics increase the beam size at the sample position to a quadratic area of 14 mm x 14 mm without requirements for mechanical modifications on the instruments base or in the sample compartment. The main area of 10 mm x 10 mm covers 72% of the original energy. This range is selected for sample illumination by a quadratic beam mask of 10 mm x 10 mm aperture in front of the sample holder. The lens in front of the detectors was replaced by larger lenses with the same optical data.

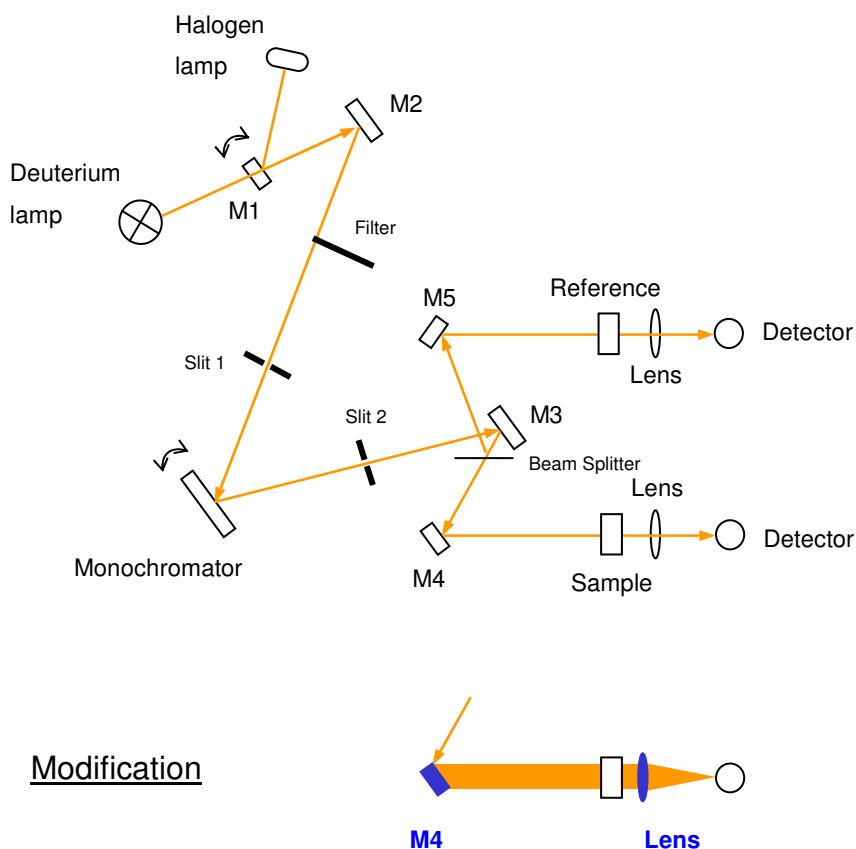


Figure 15. Optical diagram of sample beam using a lambda 35 spectrophotometer.

- Legend. M = mirror
M4 = toroidal mirror

The standard cell sample holders were replaced by specifically designed sample holders. These holders carry the metal rings used for the experimental tapes. The holder encloses the aperture mask and is adjustable to the beam in height and position.

Specification measurements showed that the loss of energy was 30% but that the typical specifications of the instruments are, nevertheless, valid. These specifications comprised noise, baseline stability and stray light data.

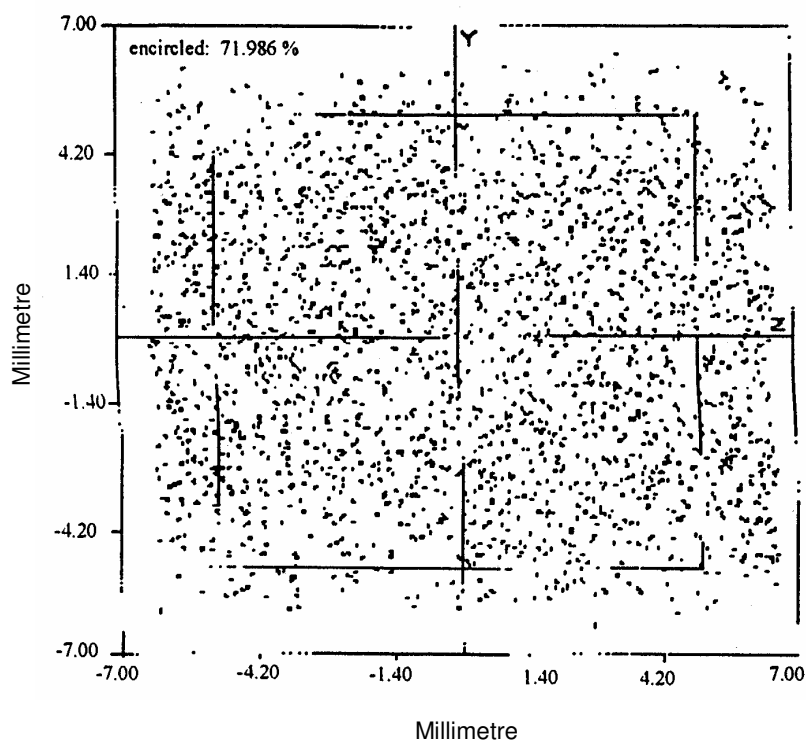


Figure 16. Pattern of light distribution produced by beam sample.

Legend. Modified parameters used to obtain the designated pattern of light distribution: 80% radius [mm] = 5.987; image dist. [mm] = 164.229; wavelength [nm] = 750.000 ; $(r_{100}-r_{80})/r_{80} = 44.4\%$; centre vert. [mm] = 0.023 ; centre hor. [mm] = 0.192 ; y-range [mm] = 12.679 ; z-range [mm] = 12.969.

The standard applications software UVWinLab version 2.7 controls the spectrophotometer. This application software package supplies all general functions necessary for the project applications. The two UV/VIS spectroscopic measuring systems were developed and manufactured by Perkin Elmer.

10.3 Selection of adhesive tape

10.3.1 Physicochemical properties of adhesive tapes

Selection of adhesive tape with appropriate properties is a necessary prerequisite for accurate dermatopharmacological studies based on stratum corneum stripping for determination of a drug concentration profile. If the tape is too aggressive removing large parts of the SC in only few strippings a profile of minor value would result. A tape that removes the stratum corneum in forty strips will then give a better profile. One relevant parameter for determination of a drug concentration profile is the relative depth of penetration which can be visualized after a large series of strippings.

Recently, Bashir et al. [3] analyzed the influence of the adhesive properties of tapes and their barrier as a possible source of variation in by measuring SC amount removal and TEWL. They concluded that the choice of tape influences the degree of barrier disruption as does the number of tape strips. Some tapes failed to increase TEWL after repeated stripping [3, 9]. The failure of these tapes to increase TEWL provides some evidence that the SC remains intact and that the water barrier is not significantly disrupted. The adhesiveness of the tape for particular components of the SC may serve as an explanation. Moreover, the tapes are not stripping components of the SC which are responsible for barrier maintenance e.g. ceramids, lipids and free fatty acids.

As already outlined (see section 7.3.4), the UV/VIS spectroscopy allows quantification of the SC removed and, at the same time to quantification of the sunscreensing agent.

The individual tape properties are responsible for the amount of SC removed.

The prerequisites of the tape used in the present experimental part were:

- a) non-absorbance in the ultraviolet wavelength range thus preventing interference with absorbance measured of the UV-filter, 4-MBC (λ_{\max} 299 nm) and
- b) sufficient removal of SC by each tape.

A first selection was performed based on the absorbance characteristics of different commercially available tapes.

Table 9. Physicochemical properties of selected adhesive tapes.

Tape trademark	Backing	Thickness	Adhesive	Absorbance ^a
Sellotape, Sellux	PP ^b	47µm	Acrylate	0.0707
D-Squame [®] Skin Sampling Discs	Polyester	100 µm	Polyacrylate ester	3.4127
Scotch [®] crystall clear 600	Acetate	62 µm	Synthetic acrylics	0.1791
Scotch [®] Book Tape 845	PP	85 µm	Synthetic acrylics	0.8977
Tesa [®] Pack 4024, Beiersdorf	PP	50 µm	Acrylate	0.0596
Tesa [®] Multifilm transparent 57315, Beiersdorf	PP	58 µm	Acrylate	0.0611
Tesa [®] Pack 4124, Beiersdorf	PVC ^c	60 µm	Natural rubber	1.1475

^a $\lambda = 299 \text{ nm}$

^b polypropylene

^c polyvinylchloride

The absorbance spectra are displayed in Figure 17.

The absorbance characteristics of the tapes revealed three candidates which were suitable for evaluation and comparison of further properties i.e. Sellux[®], Tesa[®] Pack 4024, and Tesa[®] Multifilm transparent 57315.

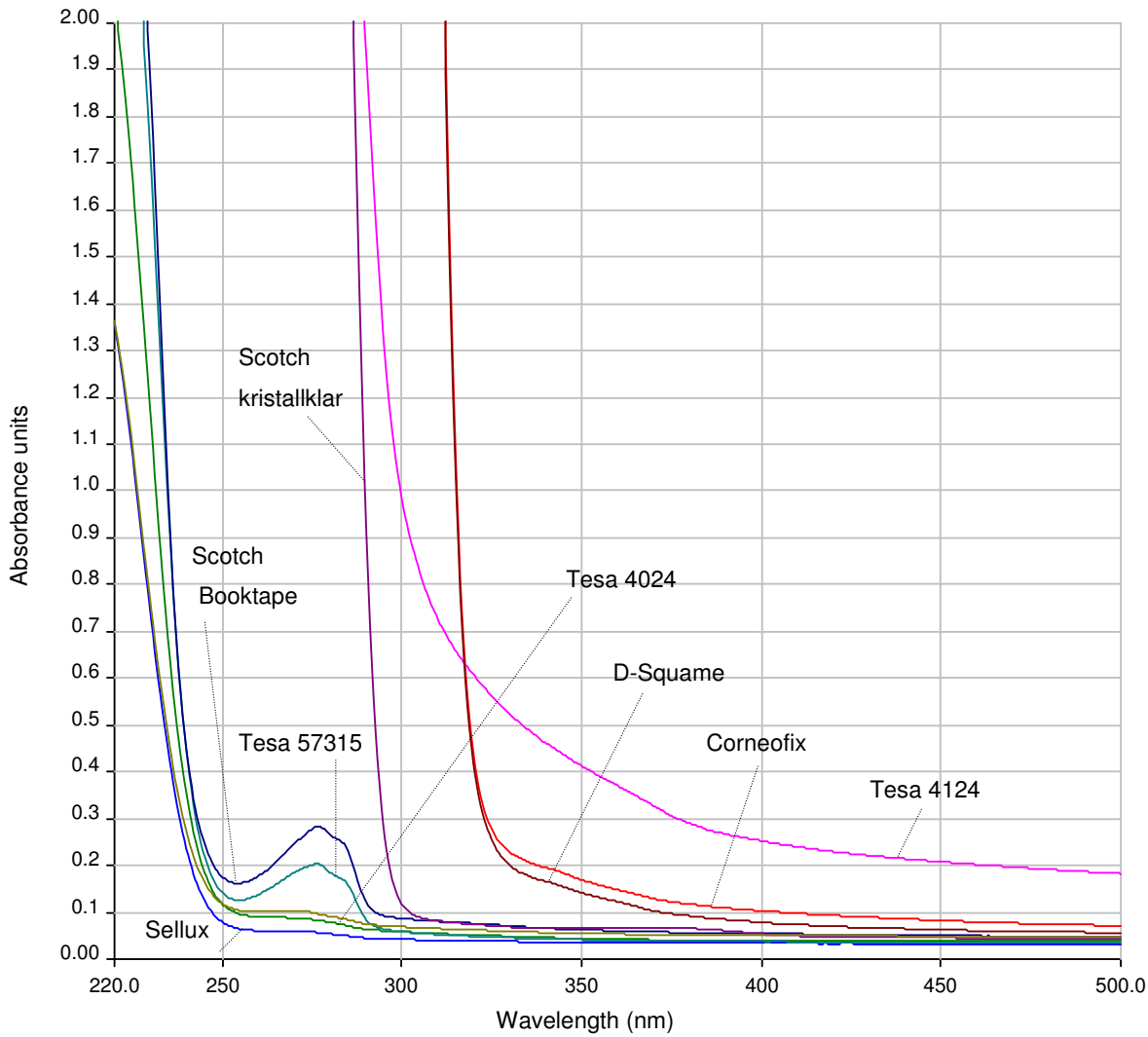


Figure 17. Absorbance spectra for different tape brands.

To ensure the completeness of SC removal, the transmission of SC material on the tape had to be above 97% at 430 nm. Two tape types which gave a transmission > 97% turned out to be painful and irritating (Sellotape® and Tesa® Multifilm transparent 57315; Table 10). With Tesa® Multifilm transparent 57315, 40 tapes were necessary to remove sufficient SC material to reach a transmission > 97%. However, the sensations during and after tape stripping were acceptable for the volunteers.

Table 10. Adhesive power criteria for selection of optimal tape.

Tape trademark	Number of tapes ^a	Transmission (%)	Sensation of last tape
Sellotape®, Sellux	45	97.10	painful, irritating
Tesa® Pack 4024, Beiersdorf	80	98.90	painful
Tesa® Multifilm transparent 57315, Beiersdorf	40	97.80	acceptable

^a number of tapes required to remove sufficient SC to reach a transmission of >97%.

10.4 Validation

Method validation is the process of proving that an analytical method is acceptable for its intended purpose. Various approaches to perform validation are known. The International Conference of Harmonization of the Technical Requirements for Registration of Pharmaceuticals for Human Use (ICH) guidelines [246] provide a framework for performing such validations. However, they provide only a basis for the validation parameters, their calculation and for their interpretation. Based on these parameters and requirements of the different guidelines, the design of these validation studies and the evaluation of their results can be adjusted to the individual analytical procedure in order to achieve an understanding of their real performance.

The UV/VIS spectrophotometric and the HPLC methods were validated in terms of performance characteristics such as specificity, linearity and range, detection limit, quantitation limit, precision (repeatability, intermediate precision) and accuracy. Statistical analysis of the data was used to demonstrate validity and justify the adequacy of the analytical procedures.

10.4.1 UV/VIS Method

10.4.1.1 UV/VIS spectrophotometric procedure

Spectrophotometric measurements of 4-MBC on the tape matrix were made using an UV-Spectrophotometer (Perkin Elmer Lambda 35); which was controlled by UV WinLab software (v 2.85), (Perkin Elmer, Überlingen, Germany). The optical chamber of the spectrophotometer was modified by the manufacturer to house a specialized sample holder that enabled monitoring of a rectangular incident light beam of 1 cm² area on each tape. Spectra of each tape were recorded between 220 and 500 nm.

10.4.1.2 The template

The validation of the UV/VIS method was performed directly on the tape by spiking it with standard solutions of different 4-MBC concentrations using a template (Figure 18). In order to define the spiking area a template (B) was stacked on every tape (A) yielding a spiking area

of 2.3 cm x 1.3 cm. The complex of tape and template (C) was fixed across a photographic slide frame (D), exposing the tape through the aperture.

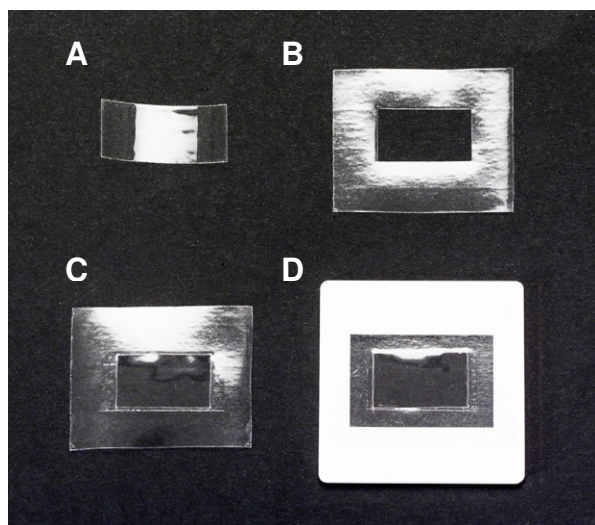


Figure 18. Composition of template.

Legend. A Tape
 B Template
 C Tape stacked on template
 D Tape and template fixed on photographic slide frame.

A colored, methanol solution was spiked on the tape area (Figure 19 A) in order to verify the distribution of the 4-MBC containing methanol solution on the tape. The homogeneously colored tape confirmed that the methanol solution was evenly distributed and that the solution was not running out of the area delimited by the template (Figure 19 B).

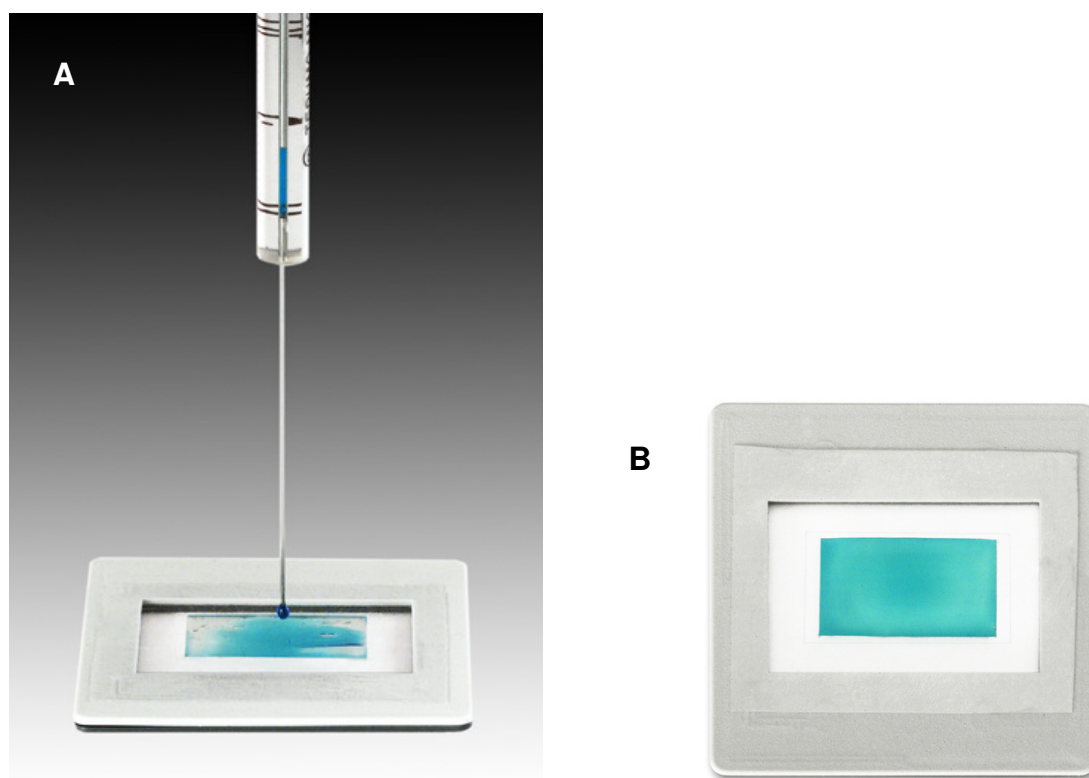


Figure 19. Standardization of spiking procedure.

Legend. A Spiking of template-tape with a colored, methanol 4-MBC solution.
B Visualization of distribution after spiking.

10.4.1.3 Specificity

To ensure that there was no interference of 4-MBC with the tape stripping matrix components (e.g. polymer film or adhesive) in the direct spectrophotometric monitoring method, tapes were spiked with a 25 μL standard methanol solution containing 0.0, 1.0 and 35.0 $\mu\text{g}/\text{cm}^2$ of 4-MBC. In addition, to demonstrate that the specificity of the analytical method was unaffected by the presence of corneocytes, tapes stripped from human forearm skin were similarly spiked. The methanol and 4-MBC solutions were allowed to evaporate completely under ambient conditions after spiking.

The specificity of the spectrophotometric methodology was assessed by recording and comparing absorbance spectra of untreated tapes, methanol-spiked tapes, 4-MBC/methanol-spiked tapes and 4-MBC/methanol-spiked tapes all of which were stripped from the skin. In each case, the tapes were mounted on a spectrophotometer recording frame and an absorbance spectrum for each tape was recorded between 220 and 500 nm.

10.4.1.3.1 The absorbance spectrum

The absorbance spectrum of 4-MBC reached a maximum at 297 nm. There was no interference between 4-MBC and the tape matrix or corneocytes. Due to SC adhering on the tape, the absorbance of 4-MBC was always calculated by three-wavelength analysis (Figure 20, Equation 4). Absorbance values are taken at three different wavelengths in order to evaluate the actual absorbance of the compound of interest.

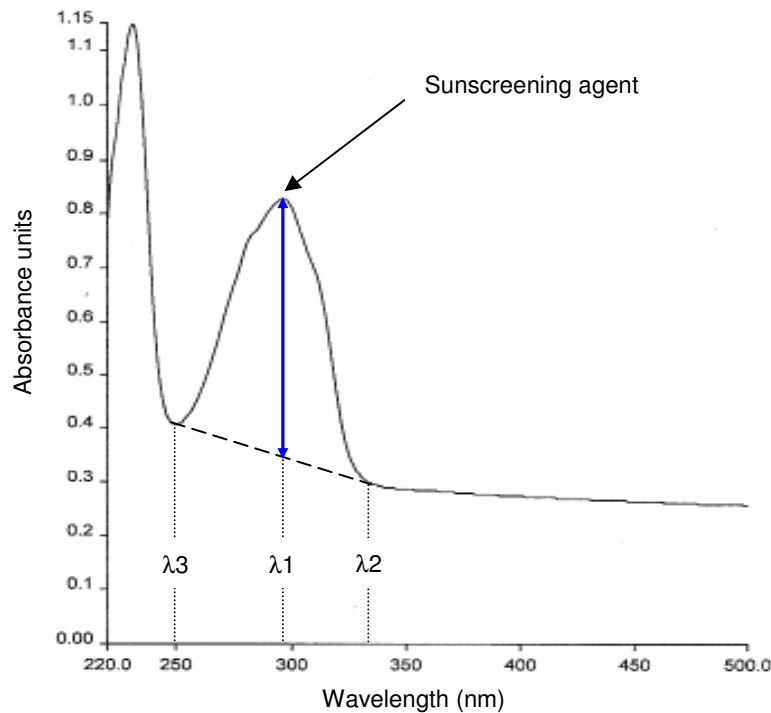


Figure 20. UV spectrum of a tape strip removed from the skin after treatment with a 4-MBC formulation.

Legend.

- λ 1 = wavelength at maximum peak absorbance
- λ 2 = wavelength at end of peak absorbance
- λ 3 = wavelength at beginning of peak absorbance.

$$A_{\text{xenobiotic}} = A(\lambda_1) - \frac{[A(\lambda_2) - A(\lambda_3)](\lambda_1 - \lambda_3)}{(\lambda_2 - \lambda_3)} - A(\lambda_3)$$

Equation 4. Calculation of 4-MBC absorbance by three wavelength analysis.

Legend. A = Absorbance units; for wavelength λ 1, λ 2 and λ 3 see legend Figure 20.

10.4.1.3.2 Influence of skin and time on the 4-MBC absorbance

The purpose of the following experiment was to investigate of the influence of SC adhering to the tape and the time on the absorbance of 4-MBC obtained from tape measurements.

Stripped tapes (with corneocytes) and blank tapes were spiked with 25 μL of 4-MBC standard solutions. The experiment was performed at three different concentration levels: 1, 5 or 35 $\mu\text{g}/\text{cm}^2$. Directly after evaporation of methanol, the absorbance of 4-MBC was measured at a wavelength of 299 nm. The measurement was repeated 24h and 48h later. For each concentrations 5 stripped and 5 blank tapes were spiked.

Results

The absorbance values and absorbance ratios are presented in Table 11. The absorbance ratios of are depicted in Figure 21.

Table 11. Absorbance values and absorbance ratios based on various concentrations of 4-MBC measured on tapes at various time points.

	4-MBC-concentrations ($\mu\text{g}/\text{cm}^2$) ^a					
	Stripped tapes (n=5)			Blank tapes (n=5)		
	1	5	35	1	5	35
Absorbance values						
0h	0.1213	0.5362	2.9159	0.0981	0.4910	2.9306
24h	0.1199	0.5331	2.9839	0.0977	0.4900	2.9299
48h	0.1195	0.5313	2.9789	0.0975	0.4882	2.9286
Absorbance ratios						
24:0	0.989	0.994	1.024	0.995	0.998	1.000
48:0	0.985	0.991	1.022	0.993	0.994	0.999
48:24	0.997	0.997	0.998	0.998	0.996	1.000

^a measured at 299 nm

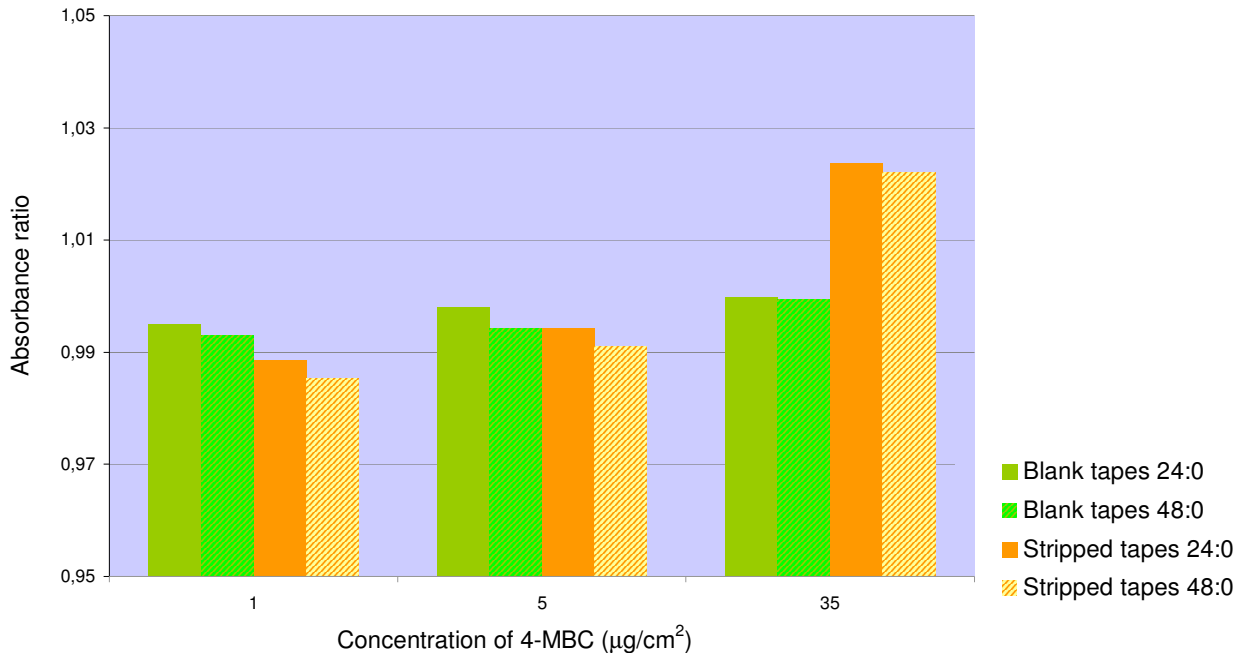


Figure 21. Absorbance ratios based on various concentrations of 4-MBC measured on tapes at various time points.

A paired sample t-test for the ratio 24:0 with stripped tapes and blank tapes at a concentration of $5 \mu\text{g}/\text{cm}^2$ confirmed that there was no statistically significant difference in the 4-MBC absorbance in the presence of skin. The t-test for the ratios 24:0 and 48:24 also revealed that time had no statistically significant influence on 4-MBC absorbance.

10.4.1.4 Linearity and Range

For the UV/VIS method two methanol solutions of 1.2 and 2.4 mg/mL 4-MBC were freshly prepared. Appropriate dilutions of these solutions gave concentrations of 0.024 mg/mL to 4.7 mg/mL (0.024, 0.12, 0.24, 0.36, 0.48, 0.60, 1.20, 1.80, 2.40, 3.00, 3.60, 4.20 and 4.68 mg/mL). Aliquots of 25 μL of these solutions were dosed onto tapes, yielding loading doses of 0.2, 1.0, 2.0, 3.0, 4.0, 5.0, 10.0, 15.0, 20.0, 25.0, 30.0, 35.0 and 39.0 $\mu\text{g}/\text{cm}^2$. A template was stacked on every tape that was used to define spiking area (2.3 cm x 1.3 cm) (see section 10.4.1.2). Two calibration curves (curve 1 and curve 2) were established ranging from 24 to 600 $\mu\text{g}/\text{mL}$ and 0.6 to 4.68 mg/mL corresponding to tape doses of 0.2-5.0 $\mu\text{g}/\text{cm}^2$ and 5.0-39.0 $\mu\text{g}/\text{cm}^2$, respectively. Three replicates were performed at each concentration level and linearity was evaluated for each curve. Spectral analysis was carried out and 4-MBC absorbance was calculated for each prepared tape (Equation 4) in order to assess the

linearity of the detector response in both concentration ranges.

Linear relationship was obtained between the absorbance and the concentration of 4-MBC. Both calibration curves were tested for linearity by means of the Mandel fitting test. Therefore, unweighted and weighted (weighting factors $1/x$ and $1/x^2$) linear regression models were compared with the quadratic regression model. Mandel's fitting test is commonly used to ascertain whether the chosen regression model adequately fits the data. The Mandel test value (F_{crit} , 95%) follows F-distribution and the significance of the test values can be calculated. If the Test-value is higher than F (95%) the quadratic regression model will be more significant.

The results in Table 12 show that the unweighted linear regression model can be accepted for calibration curve 1 at a 95% confidence level. For calibration curve 2, the linear and the linear $1/x$ weighted model must be rejected at the 95% confidence level. The best-fit equation for calibration curve 2 is the $1/x^2$ weighted linear regression.

Table 12. Mandel's fitting test for calibrations curves with the UV/VIS method

	Calibration curve 1			Calibration curve 2		
	s_y^2 ^a	F (95%)	Test value	s_y^2	F (95%)	Test value
Linear	4.963E-05	10.13	0.03	1.669E-03	6.61	8.59
Linear weighted $1/x$	1.290E-05		-2.21	1.912E-03		10.56
Linear weighted $1/x^2$	1.375E-06		-2.92	1.392E-03		6.33
Quadratic	6.543E-05			7.371E-04		

^a Residual variance

10.4.1.5 Agreement between nominal and measured 4-MBC concentrations

To assure the quality of the 4-MBC detection in the tape by UV/VIS spectroscopy the agreement between the nominal 4-MBC concentrations on spiked tapes and the actually measured 4-MBC concentrations was determined applying the linear regression model ($1/x^2$ weighted). Deviation between nominal and measured 4-MBC concentration was calculated according to Equation 5. Results are presented in Table 13.

$$\text{Deviation from nominal conc.} = \frac{(\text{nominal conc.} - \text{determined conc.})}{\text{nominal conc.}} \times 100$$

Equation 5. Calculation of deviation between nominal 4-MBC spiked on tapes and measured 4-MBC by UV/VIS spectroscopy.

Table 13. Deviation (%) between nominal and measured 4-MBC concentration (n=3, nominal samples at each concentration).

	Nominal conc. ($\mu\text{g}/\text{cm}^2$)	Deviation from nominal conc. (%)
	$1/x^2$ weighted linear	
Calibration curve 1	0.2	-0.62
	1.0	3.28
	2.0	2.07
	3.0	-0.30
	4.0	-4.76
	5.0	0.31
	\bar{x} (%)	0.00
	SD	2.77
Calibration curve 2	5.0	4.04
	10.0	-8.91
	15.0	0.00
	20.0	-1.57
	25.0	-1.64
	30.0	1.83
	35.0	2.30
	39.0	3.95
	\bar{x} (%)	0.00
	SD	4.23

Based on these results, the linear $1/x^2$ weighted regression model was used for interpolation of the absorbance data for all samples measured (calibration curve 1 and calibration curve 2) in these studies.

10.4.1.6 Exclusion of Matrix Effects in the Low Concentration Range

Theoretically, a calibration curve must pass through the origin (zero). In cases of matrix effects, a calibration curve may not pass through zero, indicating systematic errors in the methodology. To exclude a systematic error the confidence interval range of the y-intercept must include zero and the intercept should statistically not be distinguishable from zero at a defined level of confidence. This requirement is met at a 95% confidence interval ranging from $-1.97\text{E}-03$ to $+1.27\text{E}-03$ including zero (Table 14). It can therefore be assumed that there are no systematic errors at low 4-MBC concentration measurements.

Table 14 Regression parameters of calibration curve 1.

Regression equation ^a	r^b	SD ^c		S_r^d
		Slope	Intercept	
$y=0.0796 x - 3.566E-4$	1.000	1.232E-3	5.867E-4	1.173E-3

^a Peak area y vs appropriate concentration x in $\mu\text{g}/\text{cm}^2$; six standards

^b Correlation coefficient

^c Standard deviation of slope and of intercept

^d Standard error of estimate

10.4.1.7 Reference Calibration Curve

In contrast to HPLC procedures where a need of establishing daily calibration curves exist UV/VIS spectroscopy is little susceptible to instrument based interferences. It is therefore feasible to establish a representative calibration curve for the instrument for determining 4-MBC concentrations on the tape strips for the entire experimental period (6 weeks). Nonetheless, the "stability" of the determination of 4-MBC concentration was tested over a 4 week period and average regression parameters were determined from five curves using the Method Validation in Analytics - MVA software (Novia, Frankfurt am Main, Germany) (Table 15).

Table 15. Calibration equation for 4-MBC determination by UV/VIS spectroscopy.

Sample ($\mu\text{g}/\text{cm}^2$)	Regression equation ^a	r^b	SD ^c			S_r^d
4-MBC			Slope	Intercept		
0.2-5.0 (I)	$y=0.0796 x - 3.566\text{E-}4$	1.000	1.232E-3	5.867E-4	1.173E-3	
0.2-5.0 (II)	$y=0.0790 x + 2.918\text{E-}4$	0.999	1.291E-3	6.146E-4	1.229E-3	
0.2-5.0 (III)	$y=0.0808 x - 1.036\text{E-}4$	0.999	1.930E-3	9.189E-4	1.837E-3	
0.2-5.0 (IV)	$y=0.0772 x + 2.226\text{E-}3$	0.999	1.501E-3	7.149E-4	1.429E-3	
0.2-5.0 (V)	$y=0.0814 x + 1.545\text{E-}3$	1.000	1.083E-3	5.159E-4	1.031E-3	
Reference calibration curve 1	$y=0.0796 x - 7.205\text{E-}4$	0.999	7.561E-4	3.600E-4	1.609E-3	
5.0-39.0 (I)	$y=0.0714 x + 0.0562$	0.998	1.836E-3	2.101E-2	3.731E-2	
5.0-39.0 (II)	$y=0.0728 x + 0.0515$	0.999	1.394E-3	1.594E-2	2.832E-2	
5.0-39.0 (III)	$y=0.0740 x + 0.0450$	0.998	1.997E-3	2.285E-2	4.059E-2	
5.0-39.0 (IV)	$y=0.0752 x + 0.0358$	0.998	1.847E-3	2.113E-2	3.753E-2	
5.0-39.0 (V)	$y=0.0707 x + 0.0668$	1.000	4.977E-4	5.693E-3	1.011E-2	
Reference calibration curve 2	$y=0.0728 x + 0.0510$	0.998	7.010E-4	8.020E-2	3.185E-2	

^a Peak area y vs appropriate concentration x in $\mu\text{g}/\text{cm}^2$; six standards for calibration curve 1; eight standards for calibration curve 2

^b Correlation coefficient

^c Standard deviation of slope and of intercept

^d Standard error of estimate

The reference calibration curve 1 and 2 were used for all further measurements.

10.4.1.8 Lack-of-Fit Test

The lack-of-fit test is designed to determine the adequacy of the regression model for the description of the data. Significant lack-of-fit shows that the specified model does not adequately fit the response. Analysis of variance (ANOVA) with lack-of-fit test for the overall analysis of calibration curves 1 and 2 are shown in Table 16 and Table 17. Since the p value in the ANOVA table corresponding to F test for significance of regression is 0.0000, a statistically significant relationship appears between absorbance and concentration of 4-MBC. The p value for the lack-of-fit test is higher than 0.10. Therefore, the model appears to be adequate.

Table 16. ANOVA with lack-of-fit for overall analysis calibration curve 1.

Source	Sum of squares	Df	Mean squares	F-ratio	p value
Model	0.3798	1	0.3798	21803.98	0.0000
Residual	0.0015	88	0.0000		
Lack-of-fit	-0.0053	4	-0.0013	-16.28	1.0000
Pure error	0.0068	84	0.0001		
Total	0.3814	89			

Table 17. ANOVA with lack-of-fit for overall analysis calibration curve 2.

Source	Sum of squares	Df	Mean squares	F-ratio	p value
Model	0.2510	1	0.2510	22996.72	0.0000
Residual	0.0013	118	0.0000		
Lack-of-fit	-0.3925	6	-0.0654	-18.61	1.0000
Pure error	0.3938	112	0.0035		
Total	0.2523	119			

10.4.1.9 Detection Limit and Quantitation Limit

According to the ICH recommendations several methods were used for determining detection limit (DL) and quantitation limit (QL). These included:

1. calculation from noise ($DL=3.3 \cdot x_{\text{noise}}$, $QL=10 \cdot x_{\text{noise}}$)
2. calculation from standard deviation of the blank ($DL=3.3 \cdot SD_{\text{blank}}/\text{slope}$, $QL=10 \cdot SD_{\text{blank}}/\text{slope}$)
3. calculation from standard deviation of the y intercept ($DL=3.3 \cdot SD_{\text{intercept}}/\text{slope}$, $QL=10 \cdot SD_{\text{intercept}}/\text{slope}$)
4. calculation from residual standard deviation of the calibration line ($DL=3.3 \cdot s_y/\text{slope}$, $QL=10 \cdot s_y/\text{slope}$)

For determining the noise of the UV/VIS method blank tapes were spiked with methanol and the spectrum was recorded. The noise corresponds to the amplitude between the highest and the lowest signal.

Using the blank procedure, the corresponding calculation value was multiplied by the factors 3.3 and 10 for the DL and the QL, respectively. The calculations from the standard deviation of the blank, from the residual standard deviation and from the intercept were performed using the $(1/x^2)$ weighted linear regression parameters.

Results of the DL and QL of the UV/VIS method are summarized in Table 18. The DL and QL were quite different according to the respective calculation method. The DL and QL obtained from the calculation of the SD of the blank yielded the lowest values. The DL and QL for 4-MBC determined showed the highest value when using the residual standard deviation calculation. However, in order to be as objective as possible the residual standard deviation method was chosen for calculation of DL and QL of 4-MBC, yielding for calibration curve 1 values of 0.049 $\mu\text{g}/\text{cm}^2$ and 0.147 $\mu\text{g}/\text{cm}^2$ respectively. For calibration curve 2, QL was 5.22 $\mu\text{g}/\text{cm}^2$ using the residual standard deviation method.

Table 18. Detection and quantitation limit of the UV/VIS method.

Calculation method	Calibration curve 1		Calibration curve 2
	DL ($\mu\text{g}/\text{cm}^2$)	QL ($\mu\text{g}/\text{cm}^2$)	QL ($\mu\text{g}/\text{cm}^2$)
1. Signal-to-noise	1.76E-03	5.33E-03	5.33E-03
2. SD of the blank	1.73E-03	5.23E-03	5.23E-03
3. SD of the intercept	0.024	0.074	2.94
4. Residual SD	0.047	0.147	5.22

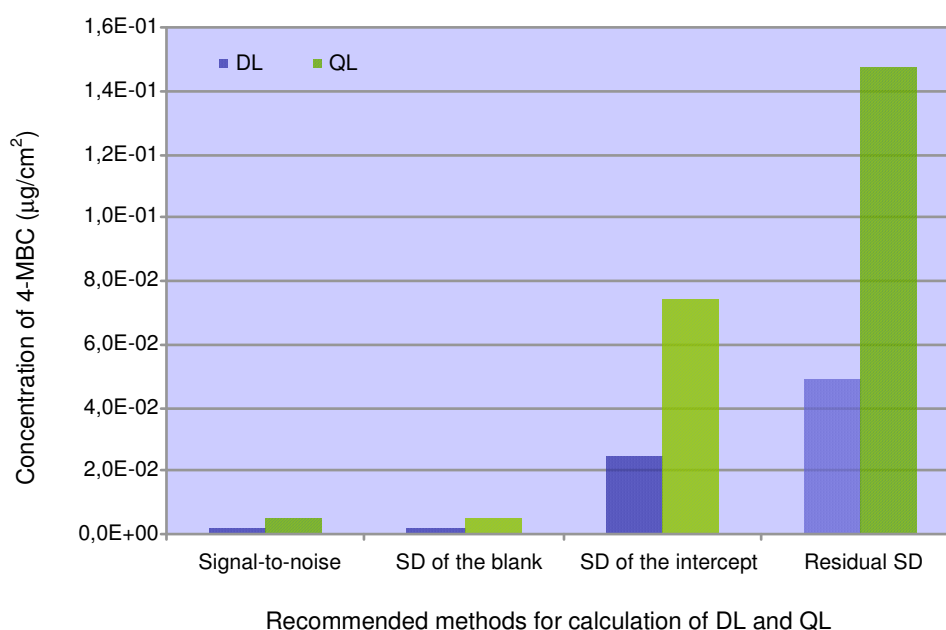


Figure 22. Discrepancies based on different recommendations of the ICH Guidelines for calculation of detection limit and quantitation limit for the UV/VIS method.

10.4.1.10 Repeatability and intermediate precision

For the estimation of the repeatability (intra-day variation) and intermediate precision (inter-day variation) of the UV/VIS method, the standard solutions of both calibration curves were used. Three replicates were performed at each concentration level to ensure the repeatability. The entire procedure was repeated on five different days to determine intermediate precision.

Both calibration curves 1 and 2 were studied separately to evaluate repeatability and intermediate precision of the UV/VIS method.

The precision parameters were calculated using the ratio of absorbance to concentration. All parameters of calibration curve 1 are listed in Table 19. The various levels of precision were calculated by means of ANOVA where the overall variation is divided into the contributions of intra-serial and inter-serial variance. There was no significant difference between the means at the 95% confidence level. The repeatability and the intermediate precision were 4.3% and 4.4% respectively. The coefficients of variation for the different series were lower or equal to 6.21%.

Table 19. Repeatability and intermediate precision with UV/VIS method for curve 1.

Series number ^a	1	2	3	4	5
CV	2.90%	3.00%	4.28%	6.21%	4.18%
\bar{x}	7.92E-02	7.93E-02	8.07E-02	7.99E-02	8.32E-02
Intra serial variance	1.19E-05				
Inter serial variance	8.13E-07				
Overall variance	1.27E-05				
Overall \bar{x}	8.05E-02				
Repeatability	4.29%				
Intermediate precision	4.43%				

^a for each series number, n=6

The precision parameters of calibration curve 2 are listed in Table 20. The coefficients of variation for the different series were lower or equal to 5.9%. The repeatability and the intermediate precision were 5.3% and 5.3%, respectively.

Table 20. Repeatability and intermediate precision with UV/VIS method for curve 2.

Seriesnumber ^a	1	2	3	4	5
CV	5.93%	4.98%	5.47%	4.76%	5.32%
\bar{x}	7.53E-02	7.63E-02	7.70E-02	7.77E-02	7.53E-02
Intra serial variance	1.63E-05				
Inter serial variance	-9.21E-07				
Overall variance	1.64E-05				
Overall \bar{x}	7.63E-02				
Repeatability	5.30%				
Intermediate precision	5.30%				

^a for each series number, n=8

Finally, Cochran's C test was performed to compare variances over the entire concentration range of each calibration curve. Since the p values for both curves were higher than 0.05 (p value curve 1 = 0.09, p value curve 2 = 1.0), there was no statistically significant difference for variances at the 95% confidence level.

10.4.1.11 Accuracy by comparison

As there was no extraction step accuracy can be obtained after precision, linearity and specificity have been established (ICH). Therefore, accuracy of the UV/VIS method was obtained by comparing the 4-MBC amounts measured directly on the tapes by UV/VIS spectroscopy with those measured by the HPLC method after extraction of 4-MBC from the tapes. The t-test allows the comparison of two analytical procedures (see section 10.5.5.1).

10.4.2 HPLC Method

10.4.2.1 Chromatographic conditions

4-MBC concentrations were assayed by HPLC using a Waters Alliance HPLC System (2690 Separations Module, 996 Photodiode Array Detector, Millenium³² software and a Symmetry Shield RP18 (2.1x 100 mm, 3.5 μ m particle size) column (all Waters Corporation, Millford, Massachusetts). The mobile phase consisted of 75% (v/v) methanol and 25% (v/v) water adjusted to the pH 4.8 with glacial acetic acid (approximately 0.01% v/v); the flow rate was set at 0.4 mL/min. The analytical column temperature was set at 35°C. Sample aliquots of

10 μ L were injected into the chromatograph and the principal wavelength for detection was set at 305 nm.

10.4.2.2 Specificity

To determine HPLC specificity, the tapes prepared as described in section 10.4.2.1 were extracted for 16 hours with 2.0 mL methanol in a stoppered, 50 mL-volumetric flask. Then, a filtered aliquot of this extraction solution was injected onto the HPLC column without further dilution. The spectra obtained from these injections were compared to the MBC spectrum from injection of a standard solution.

For the HPLC method, the retention time of 4-MBC was recorded at 4.33 ± 0.01 min. In the chromatograms of the tape extracts, skin components and tape material did not interfere with the peak of interest.

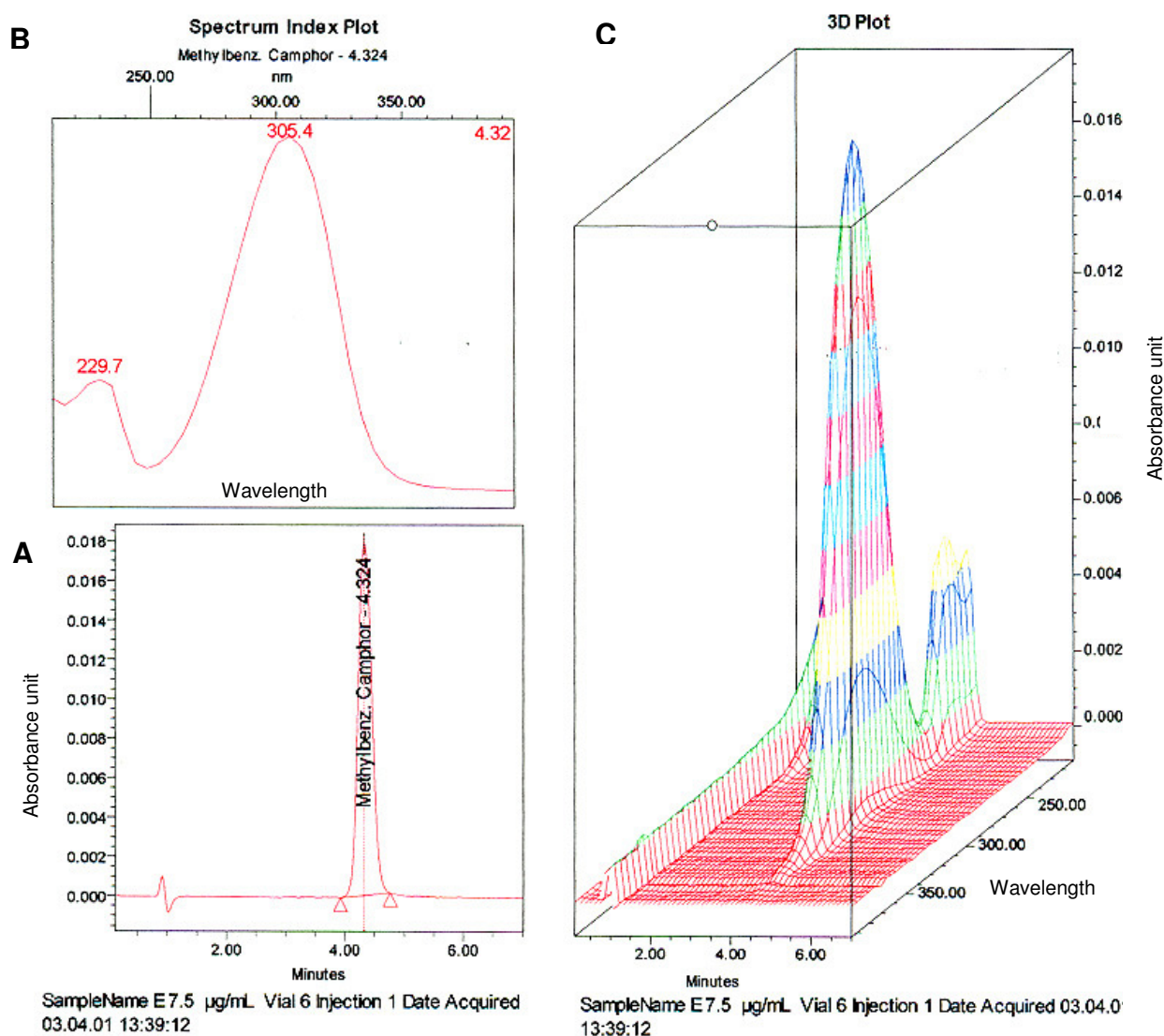


Figure 23. A Chromatogram; B Spectrum index plot and; C 3D plot.

10.4.2.3 Linearity and Range

The linearity of the HPLC method was evaluated by injecting six standard solutions with concentrations ranging from 0.5 - 10.0 $\mu\text{g/mL}$. Therefore, a stock solution was prepared by dissolving 100 mg of 4-MBC in 100 mL methanol. Appropriate dilutions of the stock solution gave standard solutions with concentrations of 0.5, 1.0, 2.5, 5.0, 7.5 and 10.0 $\mu\text{g/mL}$. Linear relationship was obtained between the peak area and the concentration.

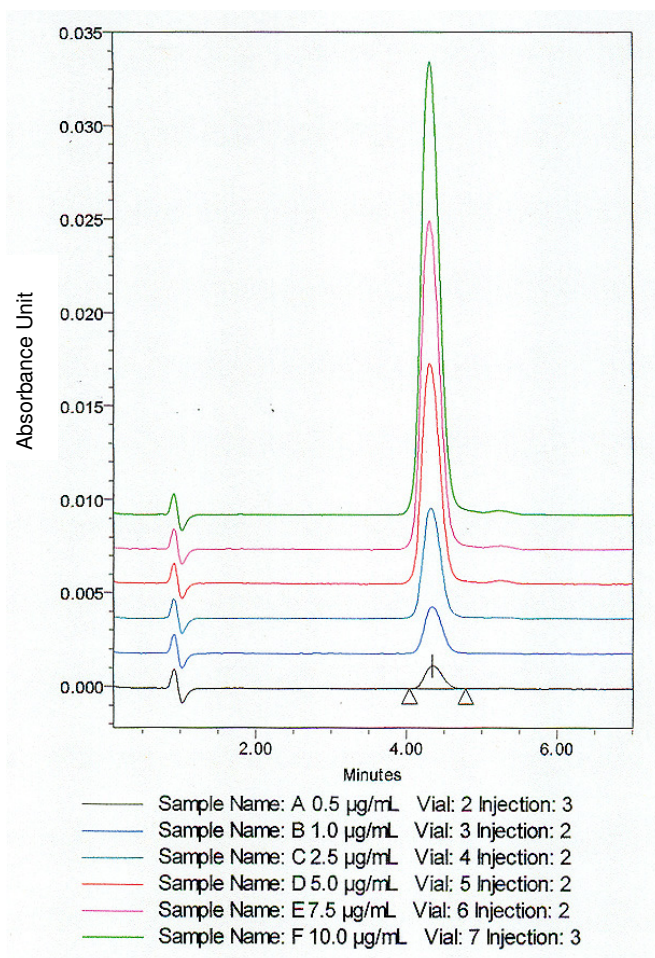


Figure 24. Chromatogram standards.

Table 21. Peak Summary with Statistics.

	Sample Name	Sample Type	Name	Retention Time (min)	Area	Concentration	Units
1	A 0.5 µg/mL	Standard	4-MBC	4.347	19'971	0.5	µg/mL
2	B 1.0 µg/mL	Standard	4-MBC	4.344	41'382	1.0	µg/mL
3	C 2.5 µg/mL	Standard	4-MBC	4.326	97'109	2.5	µg/mL
4	D 5.0 µg/mL	Standard	4-MBC	4.310	195'937	5.0	µg/mL
5	E 7.5 µg/mL	Standard	4-MBC	4.307	298'211	7.5	µg/mL
6	F 10.0 µg/mL	Standard	4-MBC	4.312	406'998	10.0	µg/mL

The Mandel fitting test tested the calibration curve for linearity. Therefore, the data was fitted to unweighted and weighted linear regression models with the weighting factors $1/x$ and $1/x^2$ and compared to the quadratic regression model.

With respect to the HPLC method, the results in Table 22 showed that the quadratic regression model can be rejected at the 95% confidence level, if a $1/x$ weighted linear regression model is used.

Table 22. Mandel's fitting test HPLC method.

	s_y^2 ^a	F (95%)	Test value
Linear	1.039E+07	10.13	32.72
Linear weighted $1/x$	3.427E+06		8.80
Linear weighted $1/x^2$	6.643E+05		-0.71
Quadratic	1.162E+06		

^a Residual variance

The equation of the $1/x$ weighted linear regression, the correlation coefficient (r) and the standard error of the estimates (S_r) of the calibration line are given in Table 23, along with the standard deviations of the slope and the intercept.

The y intercept of the calibration curve was statistically equal to zero since the p value was 0.28.

Table 23. Calibration equation for 4-MBC determination by HPLC.

Sample ($\mu\text{g/mL}$)	Regression equation ^a	r ^b	SD ^c	S_r ^d	
4-MBC			Slope	Intercept	
0.5-10.0	$y=3954 x + 549$	1.000	358	940	1851

^a Peak area y vs appropriate concentration x in $\mu\text{g/mL}$; six standards

^b Correlation coefficient

^c Standard deviation of slope and of intercept

^d Standard error of estimates

10.4.2.4 Detection Limit and Quantitation Limit

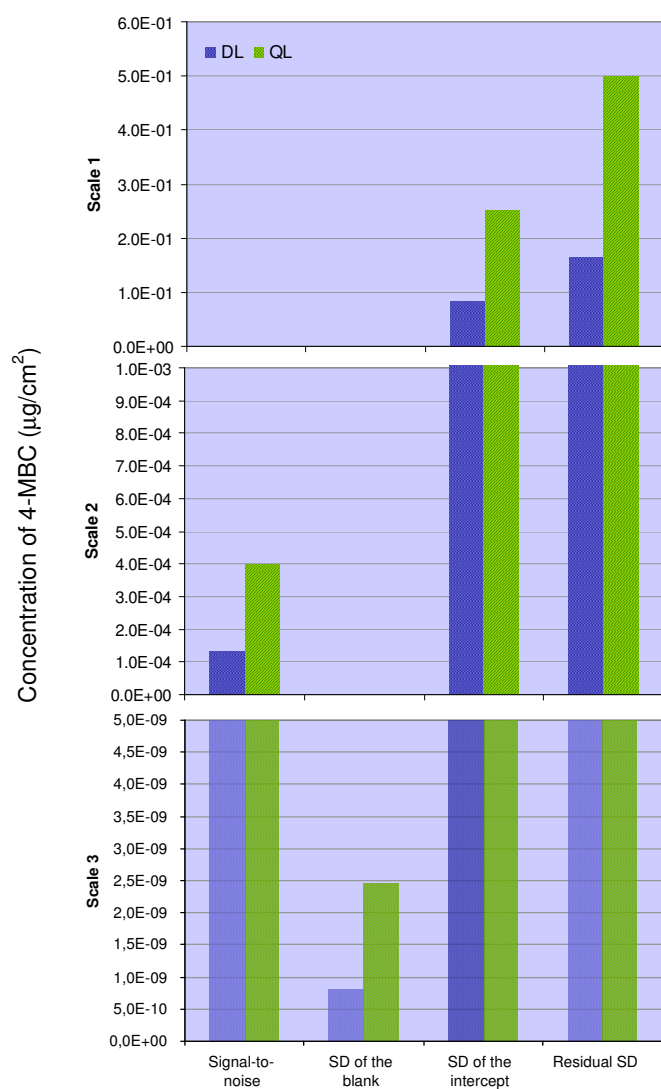
The DL and QL were evaluated according to the different methods described in section 10.4.1.9.

The noise of the HPLC method was measured between the highest and the lowest signal of a blank (methanol) injection.

Results of the DL and QL of the HPLC method are summarized in Table 24. The DL and QL were quite different according to the calculation method used. The DL and QL obtained from the calculation of the SD of the blank yielded the lowest values. The DL and QL for 4-MBC determined using the residual standard deviation calculation showed the highest values. Using the residual standard deviation method, DL and QL were calculated at a concentration of 0.164 and 0.498 $\mu\text{g/mL}$, respectively.

Table 24. Detection limit and quantitation limit of the HPLC method.

Calculation method	DL ($\mu\text{g/mL}$)	QL ($\mu\text{g/mL}$)
1. Signal-to-noise	1.32E-04	3.98E-04
2. SD of the blank	8.13E-10	2.46E-09
3. SD of the intercept	0.835	0.253
4. Residual SD	0.164	0.498



Recommended methods for calculation of DL and QL

Figure 25. Discrepancies based on different recommendations of the ICH Guidelines for calculation of detection limit and quantitation limit for the HPLC method.

10.4.2.5 Repeatability and Intermediate Precision

In order to evaluate the repeatability of the HPLC method, three replicates of each concentration level of the calibration curve were injected onto the HPLC system. The entire procedure was repeated on different days to test intermediate precision.

The precision parameters were calculated based on the ratio of area and concentration. Precision parameters are listed in Table 25. The coefficients of variation for the different

series were found to be 4.79%, 2.40% and 2.15% respectively. There was no significant difference between the means at a 95% confidence level. The repeatability and the intermediate precision were both 3.35%. These results were acceptable for the quantification of 4-MBC by HPLC.

Table 25. Repeatability and intermediate precision of the HPLC method.

Series number ^a	1	2	3
CV	4.79%	2.40%	2.15%
\bar{x}	4.02E+04	3.99E+04	3.94E+04
Intra serial variance	1.78E+06		
Inter serial variance	-1.53E+05		
Overall variance	1.78E+06		
Overall \bar{x}	3.98E+04		
Repeatability	3.35%		
Intermediate precision	3.35%		

^a for each series number, n=6

Cochran's C test was performed in order to compare variances over the entire concentration range. Since the p value was higher than 0.05 (p value = 0.12), there was no statistically significant difference among the variances at the 95% confidence level.

10.4.2.6 Accuracy by recovery

The accuracy of the HPLC method was calculated from the recovery yield between the value found with a calibration curve and the true value of 4-MBC spiked on a tape. The accuracy was determined by spiking skin-stripped tapes with known amounts of 4-MBC at concentrations of 1.17, 4.66 and 34.97 $\mu\text{g}/\text{cm}^2$. 4-MBC was extracted for 16 hours with 2.0 mL methanol in a stoppered, 50 mL-volumetric flask. After appropriate dilution, the 4-MBC concentration in the extracts were assayed by the HPLC procedure described in section 10.4.2.1. The accuracy was calculated from the recovery yield between the value found with a calibration curve and the true value spiked on the skin-stripped tape.

Recoveries were determined at three concentration levels. The recovery for 4-MBC was 91.9% at a concentration of 1.17 $\mu\text{g}/\text{cm}^2$. Recoveries were found to be 96.1% and 90.9%, for concentrations of 4.66 and 34.97 $\mu\text{g}/\text{cm}^2$ respectively. The recovery data are summarized in

Table 26. The mean recovery ($\bar{x}_{\text{recovery}}$) of 4-MBC from spiked tapes was 93% (95% confidence interval = 86.1% to 99.8%). From the recovery rates, it can be concluded that this extraction procedure provides a reliable quantitative determination of the UV filter in tape extracts.

Table 26 Recoveries of 4-MBC on spiked tapes.

Amount added ($\mu\text{g}/\text{cm}^2$)	Amount found ($\mu\text{g}/\text{cm}^2$) $\bar{x} \pm \text{SD}$ (n = 6)	Recovery (%)	$\bar{x}_{\text{recovery}}$ (%)	CI ^a (95%)
1.17	1.08 \pm 0.01	91.9		
4.66	4.49 \pm 0.07	96.1	92.7	86.1 - 99.8
34.97	31.79 \pm 0.65	90.9		

^a CI = confidence interval

10.5 Experiment 1

In Experiment 1, the penetration of 4-MBC from a 2% and 4% standard formulation was investigated by tape stripping. Preparation of the test area (volar aspect of the forearm), vehicle application and the tape stripping procedure as well as environmental conditions were standardized. The amount of 4-MBC and the thickness of SC in each single tape were simultaneously determined by the previously validated UV/VIS spectroscopic method. In addition, the amount of 4-MBC in each single tape was verified by the validated HPLC assay.

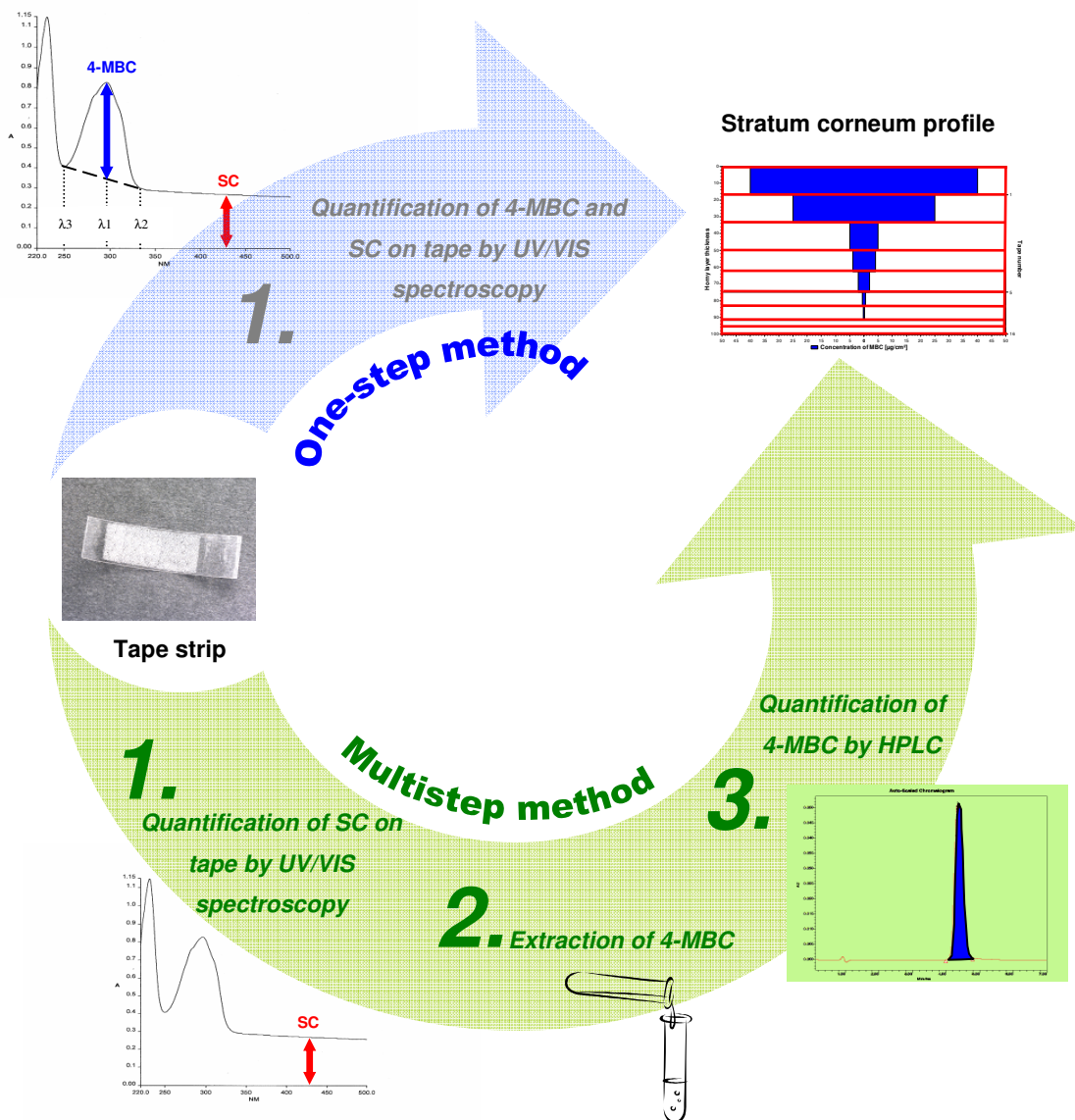


Figure 26. Scheme illustrating distribution of 4-MBC in SC obtained by a new, direct one-step spectroscopic method vs an established, multistep method.

10.5.1 4-MBC Sunscreen formulation

The sunscreen used was a formulation based on the proposed Standard P3 formulation of the COLIPA Guidelines [101] for sun protection factor measurement. The sunscreen was an o/w emulsion. As 4-MBC solubility in water is low, the major part of the UV filter will be diluted in the oil phase.

10.5.1.1 Ingredients

Solubility of 4-MBC in Tegosoft TN was investigated prior to producing 4-MBC formulations. At room temperature and under constant stirring, 40% (w/w) 4-MBC could still be solved in Tegosoft TN. 50% (w/w) 4-MBC was no longer soluble in Tegosoft TN.

The emulsion formulation used as the delivery vehicle for the sunscreen in these experiments was a modified P3 standard formulation from the COLIPA guidelines [101]. The ingredients of the emulsion are listed in Table 27.

Table 27. Composition of 4-MBC sunscreen formulations tested.

Component	Percent (%)
4-MBC	2.00 or 4.00
Tegosoft TN	15.00
Emulgade F	3.15
KOH (10% sol)	1.50
Carbopol 934	0.30
Ethanol absolutum	8.00
Water	70.05 or 68.05
Total	100.00

The 4-MBC and potassium hydroxide were obtained from Merck KgaA, D-64271 Darmstadt, Germany; Tegosoft TN (C12-15 Alkyl benzoate) from Goldschmidt AG, D-45127 Essen, Germany; Emulgade F (Cetearyl alcohol & PEG-40 castor oil & sodium cetearyl sulfate) from Cognis Deutschland GmbH, D-40551, Düsseldorf, Germany; Carbopol 934 (Carbomer) from Noveon Inc., Cleveland-OH 44141, USA; Ethanol absolutum from Fluka, Buchs, Switzerland. All the components of the oil phase (4-MBC, Emulgade F and Tegosoft TN) were melted together at 90°C over a water bath. Carbopol was dispersed in water at 16'000 rpm during approximately 30 seconds with an Ultra Turrax agitator (IKA Ultra Turrax T25 Basic with IKA

Dispergierer S25N25F) and was also heated to 90°C using a water bath. The aqueous solution was then slowly added to the oil phase with continuous stirring (200 rpm) using a stirring motor (type IKA Eurostardigital / IKA RW 28 Basic). The ethanol was added when the emulsion had cooled to a temperature of 40°C. The emulsion was then homogenized with the Ultra Turrax (16 000 rpm) during one minute and finally stirred (50 rpm) during 30 minutes until room temperature was reached. The mass of the final formulation was checked and brought up to the final volume with water during the final stirring phases. The emulsion phase stability was checked by centrifuging (15 min at 5000rpm). In addition, the microscopic aspect and pH of the formulations were tested. The emulsions were homogeneous and stable after centrifuging. The microscopic examination confirmed a monodisperse appearance for both emulsion concentrations without the presence of any crystals. The pH was measured at 6.6 for the 4% 4-MBC formulation and 7.0 for the 2% 4-MBC formulation.

10.5.1.2 Stability testing

Table 28. Stability tests of 2% and 4% 4-MBC formulations.

19.4.2001	Start	2 Weeks			6 Weeks			3 Months			6 Months
		5 °C	RT	43 °C	5 °C	RT	43 °C	5 °C	RT	43 °C	RT
2% 4-MBC											
Phase stability		1		1	1		1	1		1	
Color		white *		white *	white *		white *	white *		white *	
Microscopy		1a		1a	1a		1a	1a		1a	
Skin feel / Stickiness		1a		1a	1a		1a	1a		1a	
Odor		1		1	1		1	1		1	
pH value 25 °C	0.00	6.61		6.53	6.54		6.533	6.59		6.59	
Viscosity (Brookfield RVT) Value at 25 °C in Cps, after 30s											

19.4.2001	Start	2 Weeks			6 Weeks			3 Months			6 Months
		5 °C	RT	43 °C	5 °C	RT	43 °C	5 °C	RT	43 °C	RT
4% 4-MBC											
Phase stability		1		1	1		1	1		1	
Color		white *		white *	white *		white *	white *		white *	
Microscopy		1a		1a	1a		1a	1a		1a	
Skin feel / Stickiness		1a		1a	1a		1a	1a		1a	
Odor		1		1	1		1	1		1	
pH value 25 °C	0.00	6.6		6.56	6.57		6.6	6.41		6.57	
Viscosity (Brookfield RVT) value at 25 °C in Cps, after 30s											

Phase Stability

1: Stable
2: slightly inhomogenous
3: begins to separate
4: clearly separating
5: separated

Microscopy

1: monodisperse
2: polydisperse
a) No Crystals
b) Crystals

Odor

1: good
2: acceptable
3: bad

Skin Feel and Stickiness

1: not oily
2: slightly oily
3: oily
a: non sticky
b: slightly sticky
c: sticky

10.5.2 Determination of 4-MBC concentration in formulation

10.5.2.1 *Material*

Chromatograph	Waters Alliance HPLC System (2690 Separations Module, 996 Photodiode Array Detector, Millenium ³² Software (all Waters Corporation, Millford, Massachusetts))
Column	Symmetry Shield RP18 (2.1x 100 mm, 3.5 µm particle size)
Mobile phase	75% (v/v) methanol, 25% (v/v) water and glacial acetic acid (approximately 0.01% v/v) at 0.4 mL/min
Volume of injection	10 µL
Detection wavelength	Absorbance at 305 nm

10.5.2.2 *Method*

4-MBC was extracted from the formulation with methanol. This included the weighing of an appropriate amount (1 g) of formulation in a 100 mL volumetric flask and adding methanol (ca. 90 mL). The volumetric flask was then placed in an ultrasonic bath during 5 minutes. As soon as the solution had cooled down to room temperature (24°C) methanol was added to the mark. The solution was filtered through a 0.45 µm membrane (Nylon GyroDisc, Orange Scientific, Braine l' Alleud, Belgium). Then, 0.5 mL of the filtered solution was diluted to 50 mL (volumetric flask) with methanol. 4-MBC concentrations were assayed by HPLC.

The extraction procedure was performed in a triplicate with both formulations (4% and 2% 4-MBC).

10.5.2.3 *Results*

The concentrations were determined with the validated HPLC method. The 4-MBC concentration in the 4% and 2% formulation was 3.89% and 1.97% respectively.

10.5.3 Study Design for Experiment 1

Five human volunteers, three males and two females aged 24-29 participated in the study. The volunteers were all naive to topical drug therapy.

The compounded emulsions containing 4-MBC were randomly applied to the volar surfaces of the forearms. One arm of each subject was treated with a 2% formulation (F1) and the other arm with a 4% formulation (F2). In each case, 90 mg of the product was applied to the skin with a 1 mL syringe and spread over an area of 45 cm² with a gloved finger, to give a topical application dose of 2 mg/cm². One hour after formulation application, an area of 4.03 cm² of the dosed skin sites were stripped.

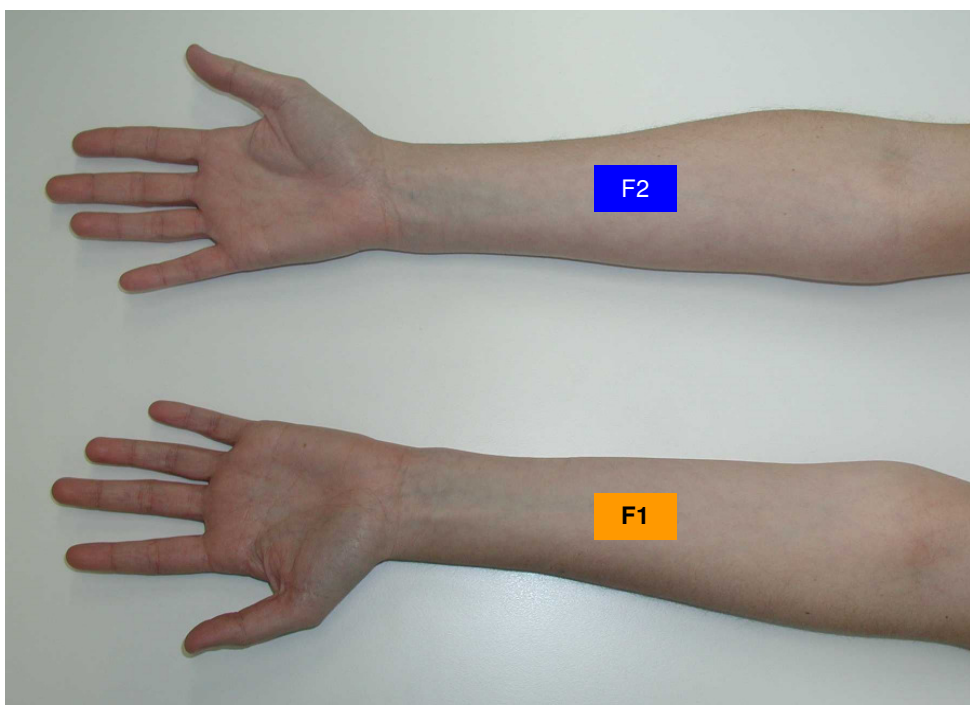


Figure 27. Treatment scheme for test person for Experiment 1.

Legend. F1=2% 4-MBC formulation;
F2=4% 4-MBC formulation.

10.5.4 Tape stripping procedure

The formulation application area on each arm was delineated by taping a flexible template on the skin. The template had a rectangular aperture of 1.3 cm x 3.1 cm, thereby exposing a constant skin area for each sequential tape stripping and ensuring consistent removal of stratum corneum from exactly the same formulation application site. The long axis of the

template was fixed along the midline of the forearm to ensure intimate contact with the skin and to simplify the subsequent stripping procedure. Tape stripping was carried out with Tesa tape (Multi-Film Kristall-Klar[®] 57315 tape, Tesa, Beiersdorf, Hamburg, Germany) of 1.5 cm width. A strip of adhesive tape (larger than the aperture of the template) was placed on the skin area exposed through the template aperture. Pressure was then applied perpendicularly to the adhering tape in a uniform manner using a hand roller that supplied a gravitational weight of 140 g/cm² to the skin. The roller was uniformly passed over the tape 10 times at each stripping, thus compensating for any inconsistency issues of pressure application as described in previous papers [247, 248]. The tape (with adhering corneocytes) was then manually removed from the skin by pulling, using firm, rapid and uniform tension. The direction of tape removal (elbow-to-wrist or wrist-to-elbow) was alternated with each tape in order to strip the stratum corneum in a consistent manner (Figure 28).

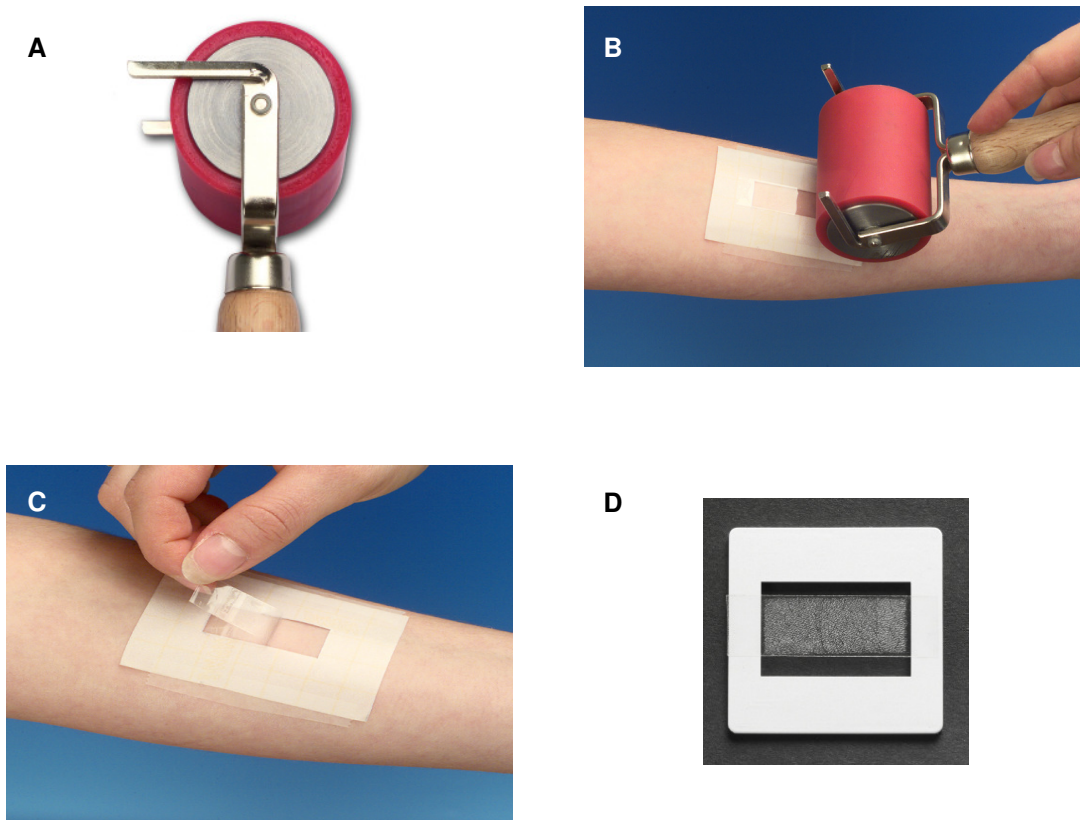


Figure 28. Demonstration of tape stripping.

Legend. Tapes are pressed by a roll (A) on the skin defined by a template with a pressure of 140 g/cm² (B); they are then stripped (C) to be finally fixed onto a photographic slide frame (D).

Once removed from the skin, each tape was fixed across a photographic slide frame, exposing the tape and adhering corneocytes through the aperture. This frame size could easily be accommodated in the solid-sample holder of the spectrophotometer (Lambda 35

with custom modification to monitor an incident light path area of 1 cm², Perkin Elmer Instruments, Überlingen, Germany).

Stripping with sequential tapes was carried out in this manner at each skin test site to remove the entire stratum corneum layer. The absorbance of every tenth tape/corneocyte sample was measured at 430 nm to determine the transmission through the specimen in relation to blank tape. Stripping of the skin stopped when transmission at 430 nm approached 97% (representing almost complete removal of the stratum corneum).

Once all the tape strips had been collected from each test site, samples were allowed to equilibrate for 24 hours before being scanned for absorbance potential between 220 and 500 nm and were then extracted for HPLC analysis as described above.

10.5.5 Results

10.5.5.1 Correlation of UV/VIS spectroscopy with HPLC (Accuracy by comparison)

All 4-MBC concentrations measured directly on the tapes by the UV/VIS method were compared to results obtained from HPLC. As the first tape strip always contains the largest 4-MBC quantity, which is much higher than in the following tape strips, its influence on the regression curve is too large. Therefore, the first tape was not used for calculating the regression equation. Table 29 lists the number of tape strips used for the correlation of the 4-MBC concentrations which were measured by the UV/VIS method and the one found by the HPLC method.

Table 29. Correlation of the 4-MBC concentration found by UV/VIS spectroscopy and HPLC without including the first tape.

Volunteer	Age (Sex ^a)	Formulation ^b	Number of tapes for correlation	Regression equation ^c	r ^{2d}
1	24 (f)	F1	12	$y = 1.0068x + 0.0573$	0.976
		F2	23	$y = 1.0493x + 0.0620$	0.976
2	26 (m)	F1	10	$y = 0.9654x + 0.0055$	0.997
		F2	12	$y = 1.0866x + 0.0418$	0.997
3	29 (m)	F1	16	$y = 0.9001x + 0.0673$	0.995
		F2	13	$y = 1.6846x + 0.5995$	0.910
4	25 (f)	F1	13	$y = 0.8207x + 0.1327$	0.999
		F2	24	$y = 1.0282x + 0.0239$	0.994
5	25 (m)	F1	10	$y = 0.8768x + 0.1005$	0.982
		F2	19	$y = 1.1583x + 0.0143$	0.974

^a (f) female, (m) male

^b F1 2% 4-MBC formulation, F2 4% 4-MBC formulation

^c 4-MBC concentration measured by UV/VIS spectroscopy vs concentration measured after 4-MBC extraction by HPLC

^d correlation coefficient

In order to determine if there was no difference between the two analytical methods, the data were subjected to null hypothesis using the paired sample t-test. However, this hypothesis gave a p value > 0.05 (p value 0.167), proving that there was no significant difference between the UV/VIS and the HPLC method.

Statistical data analysis of the correlation was performed by using a paired-sample t-test where data collected in pairs is compared. In the paired-sample t-test the data was analyzed by calculating the difference between each value in each pair of observations. The null hypothesis is rejected if the mean for the paired differences is not equal to 0 for a given alpha. Since the p value was higher than 0.05 (p value 0.167) the null hypothesis cannot be rejected at the 95% confidence level.

Table 30 shows a frequency tabulation dividing the range of the paired differences into equal width intervals. The number of data values were counted in each interval. The frequencies show the number of data values in each interval while the relative frequencies show the proportions in each interval. Both Table 30 and the histogram in Figure 29 showed that

97.55% of the data fell within one interval, again indicating that there were no significant differences between the two analytical methods.

Table 30. Frequency tabulation.

Class	Lower Limit	Upper Limit	Midpoint	Frequency	Relative Frequency	Cumulative Frequency	Cum. Rel. Frequency
At or below		-9.0		0	0.0000	0	0.0000
1	-9.0	-7.3	-8.2	1	0.0061	1	0.0061
2	-7.3	-5.7	-6.5	0	0.0000	1	0.0061
3	-5.7	-4.0	-4.8	0	0.0000	1	0.0061
4	-4.0	-2.3	-3.2	0	0.0000	1	0.0061
5	-2.3	-0.7	-1.5	2	0.0123	3	0.0184
6	-0.7	1.0	0.2	159	0.9755	162	0.9939
7	1.0	2.7	1.8	0	0.0000	162	0.9939
8	2.7	4.3	3.5	1	0.0061	163	1.0000
9	4.3	6.0	5.2	0	0.0000	163	1.0000
Above		6.0		0	0.0000	163	1.0000

$$\bar{x} = -0.079, \text{SD} = 0.723$$

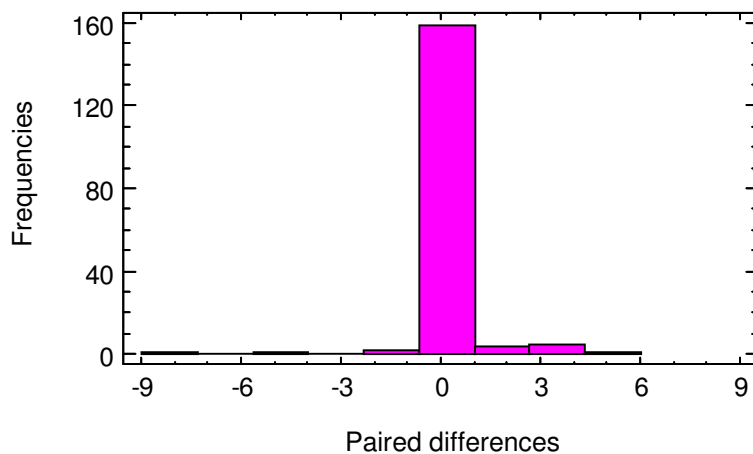
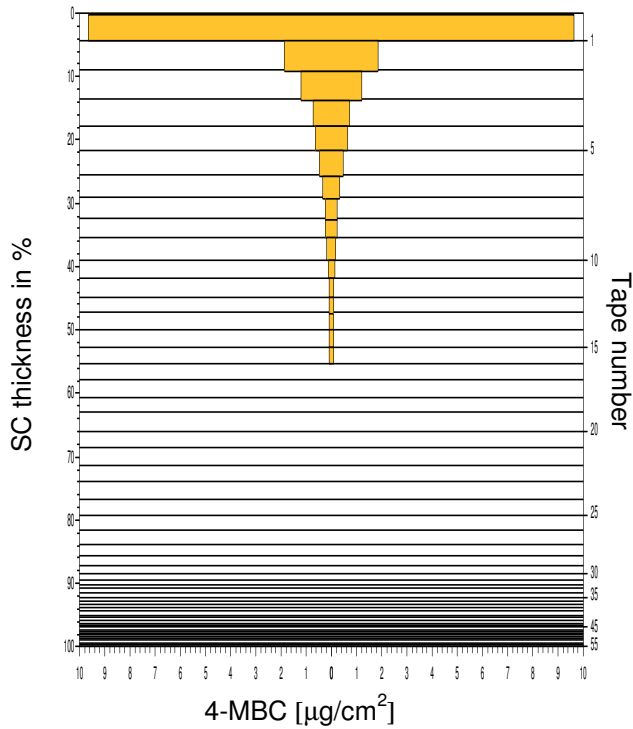


Figure 29. Histogram showing distribution of paired differences for data from UV/VIS vs HPLC.

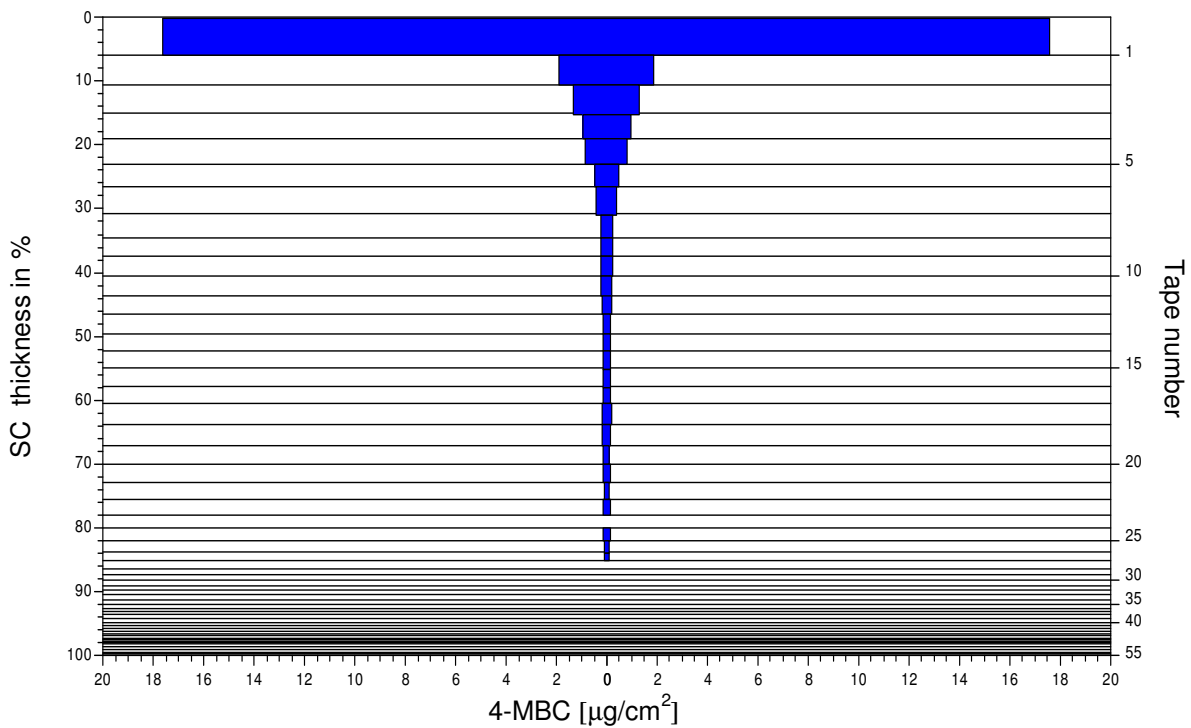
10.5.5.2 Stratum Corneum Profiles

Volunteer 1

2% 4-MBC formulation, $AUC_{conc-sc} = 33.21$ (without first tape)

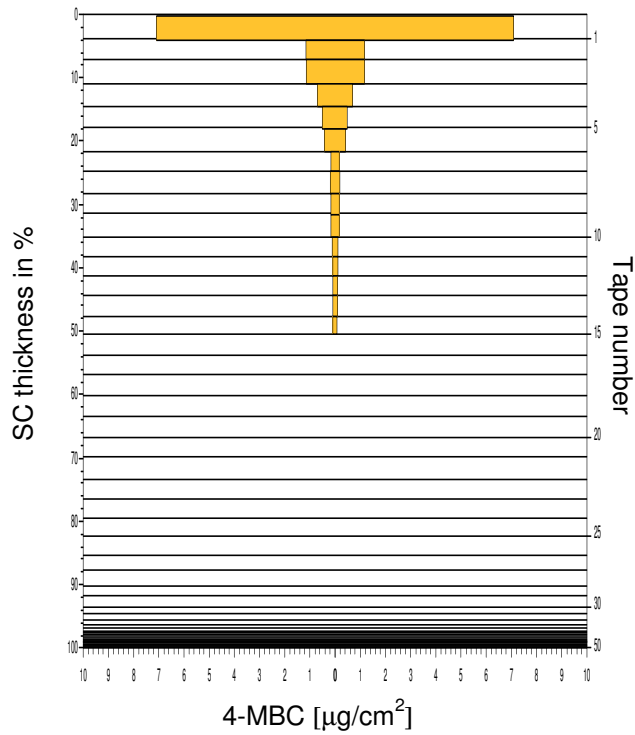


4% 4-MBC formulation, $AUC_{conc-sc} = 76.32$ (without first tape)

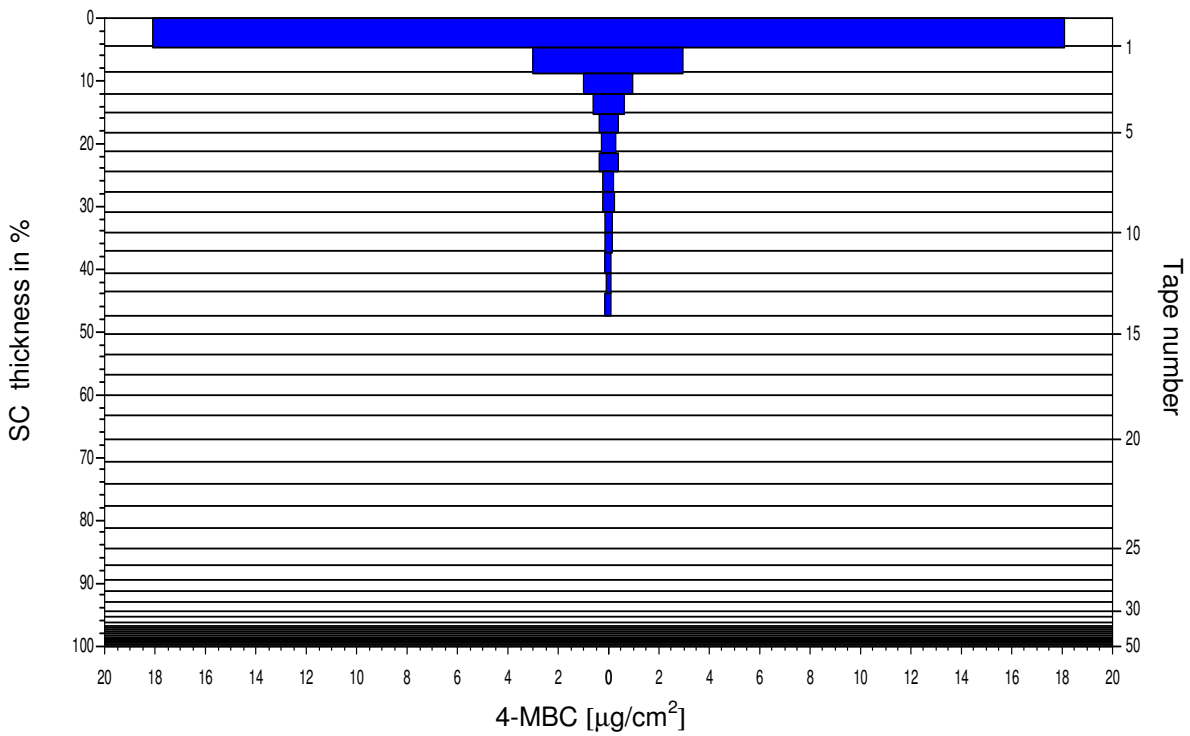


Volunteer 2

2% 4-MBC formulation, $AUC_{\text{conc-sc}} = 63.61$ (without first tape)

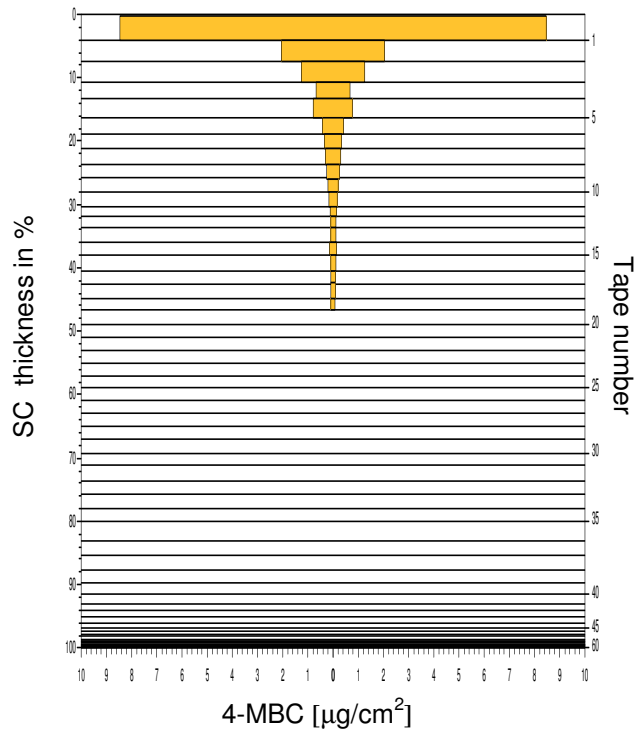


4% 4-MBC formulation, $AUC_{\text{conc-sc}} = 101.95$ (without first tape)

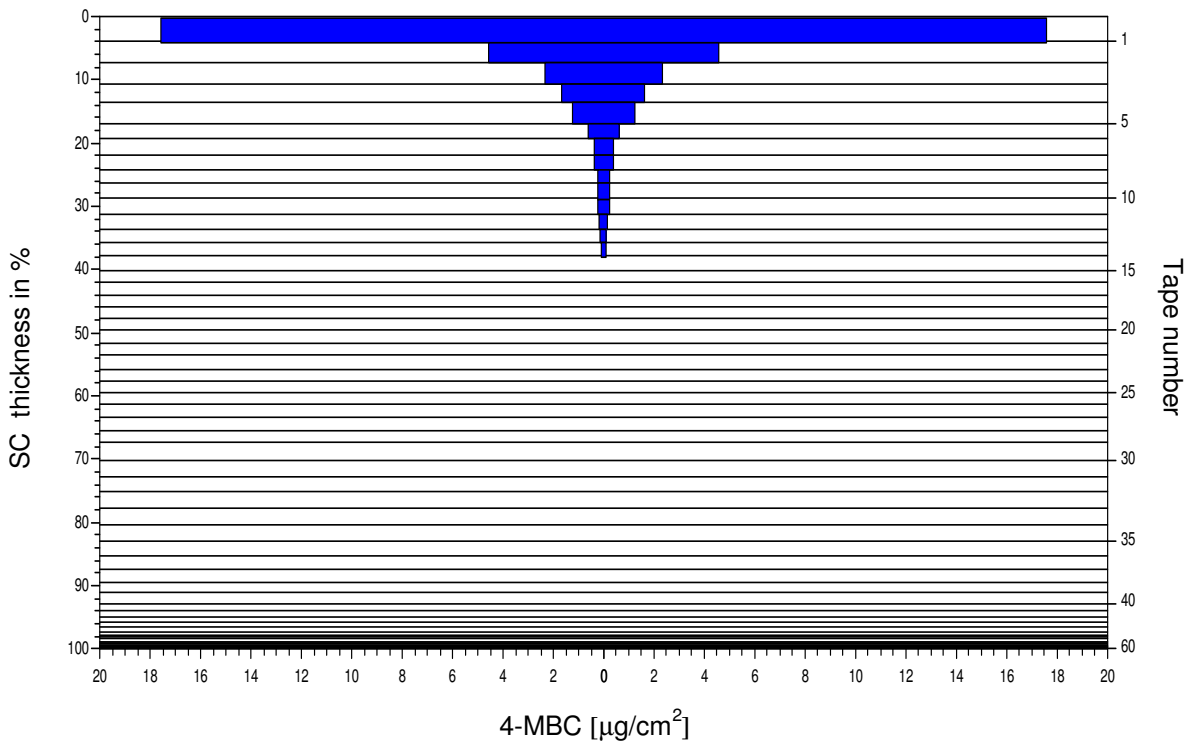


Volunteer 3

2% 4-MBC formulation, $AUC_{conc-sc} = 62.54$ (without first tape)

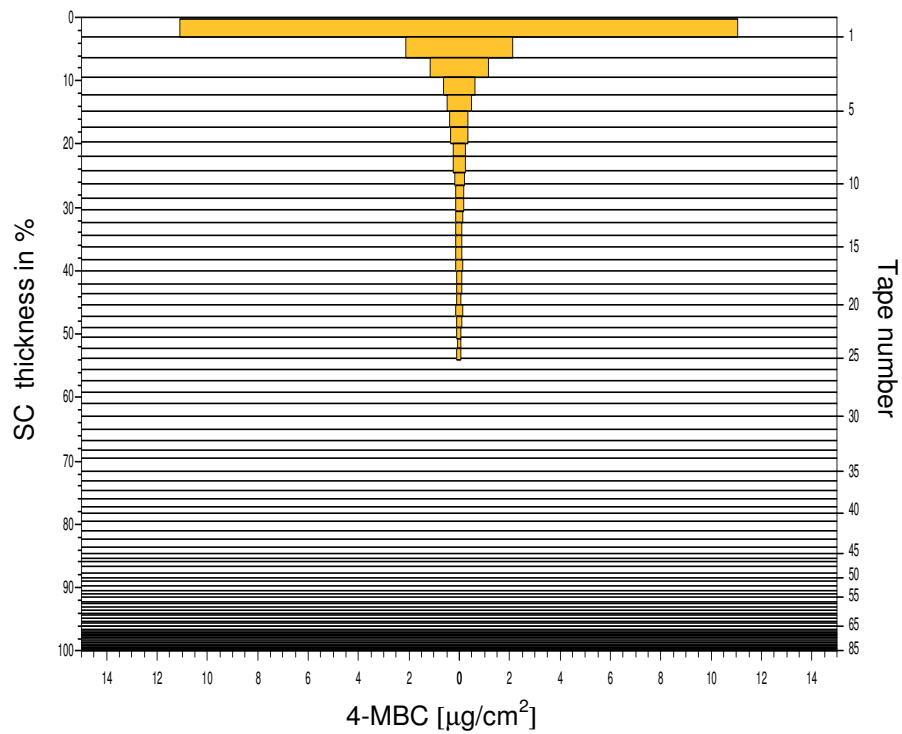


4% 4-MBC formulation, $AUC_{conc-sc} = 104.46$ (without first tape)

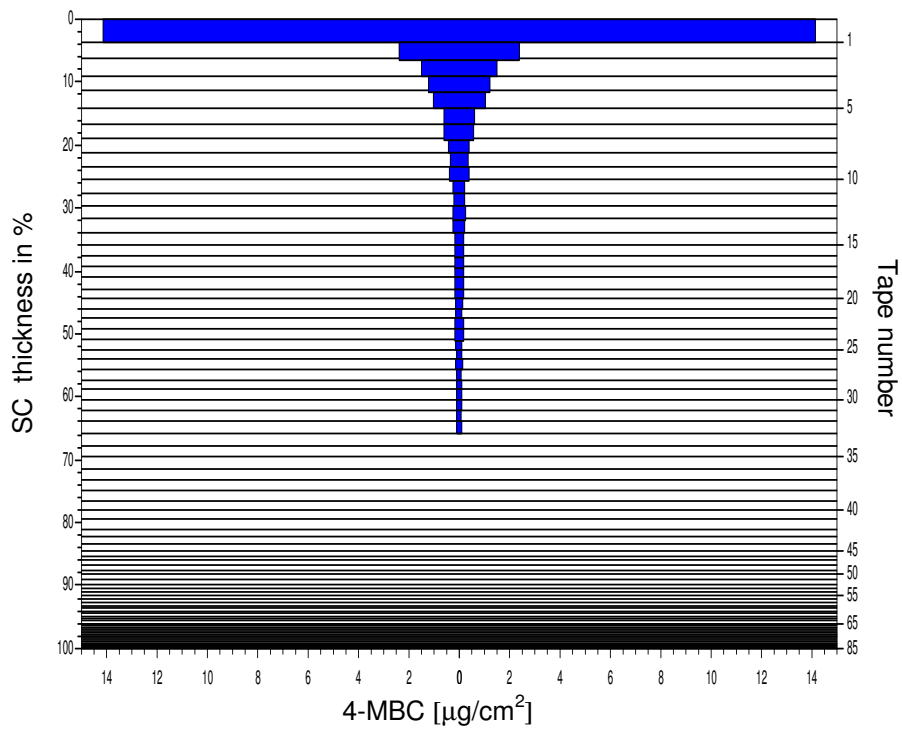


Volunteer 4

2% 4-MBC formulation, $AUC_{\text{conc-sc}} = 43.97$ (without first tape)

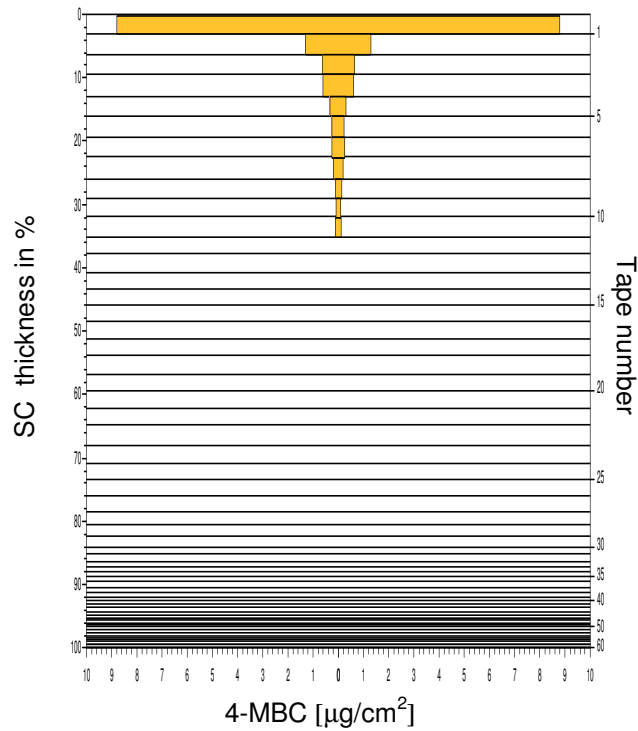


4% 4-MBC formulation, $AUC_{\text{conc-sc}} = 56.41$ (without first tape)

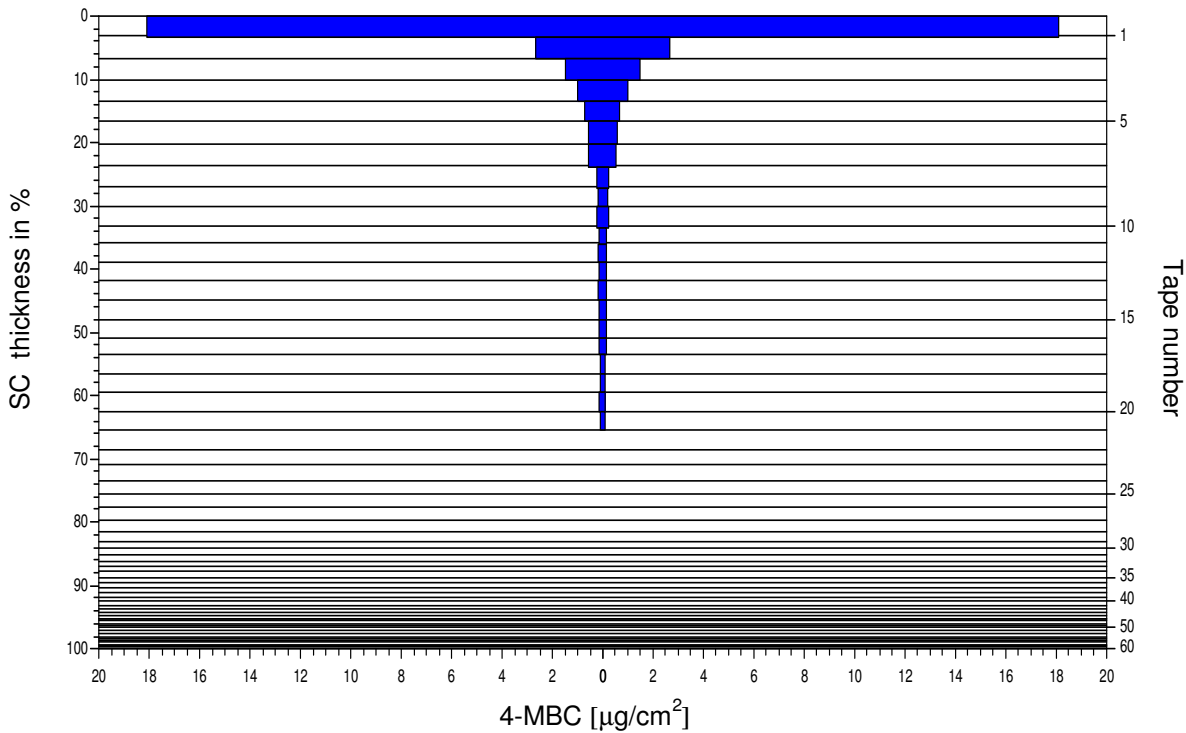


Volunteer 5

2% 4-MBC formulation, $AUC_{\text{conc-sc}} = 55.02$ (without first tape)



4% 4-MBC formulation, $AUC_{\text{conc-sc}} = 74.15$ (without first tape)



10.5.5.3 Amount of 4-MBC penetrating the SC (results calculated by the UV/VIS method)

The amount of 4-MBC amount penetrating into the SC was calculated as area under the curve of the concentration in the SC ($AUC_{\text{conc-sc}}$). The 4-MBC concentration ($\mu\text{g}/\text{cm}^2$) found in one tape was multiplied by the stripped skin area (cm^2) to obtain the total mass (μg) of compound in one tape. Adding up the total mass of 4-MBC of each tape strip gave the $AUC_{\text{conc-sc}}$ corresponding to total compound delivered to the skin.

In Figure 30 - Figure 32 the volunteers' $AUC_{\text{conc-sc}}$ are presented calculated with all the tapes, discarding the first tape and discarding tape 1-4.

Statistical analysis of the data were performed with Statgraphics®PLUS 5 software (Manugistic, Inc., Rockville, Maryland, USA). Differences in the $AUC_{\text{conc-sc}}$ between the two formulations were statistically analyzed at 95% confidence with multifactor ANOVA.

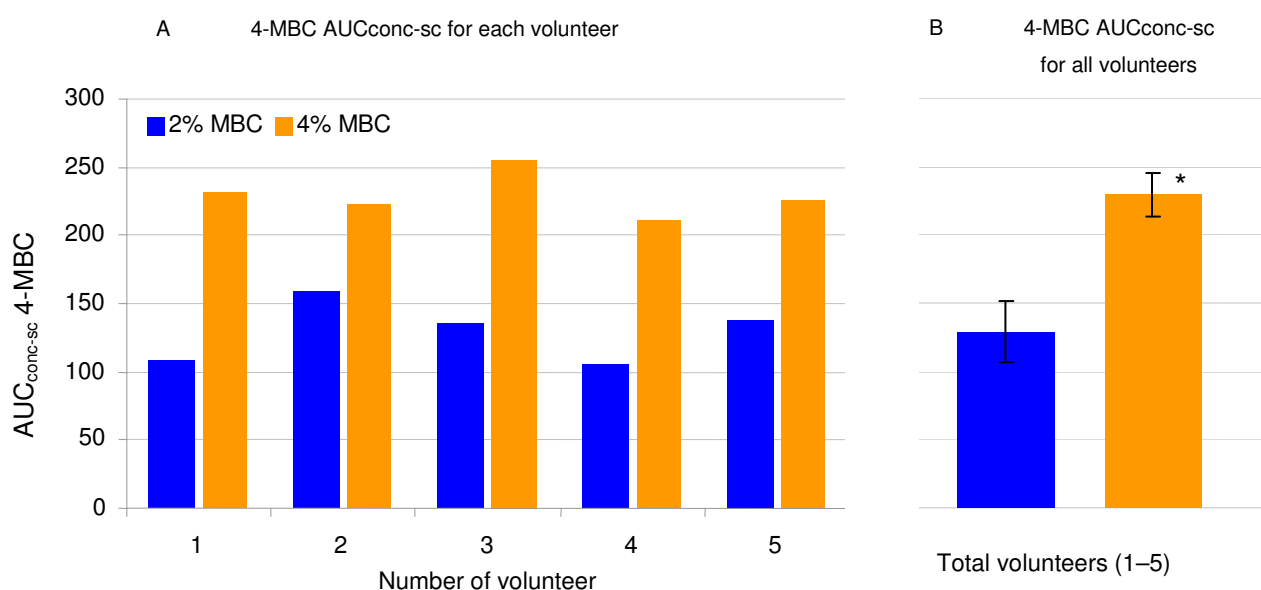


Figure 30. $AUC_{\text{conc-sc}}$ for tape strips from individual (A) and from all volunteers (B).

Legend. B $\bar{x} \pm \text{SD}$ (n=5) expressed as $AUC_{\text{conc-sc}}$ in $\mu\text{g}/\text{tape}$; * $p < 0.05$. A significant difference in the $AUC_{\text{conc-sc}}$ between the 2% and 4% formulations were found.

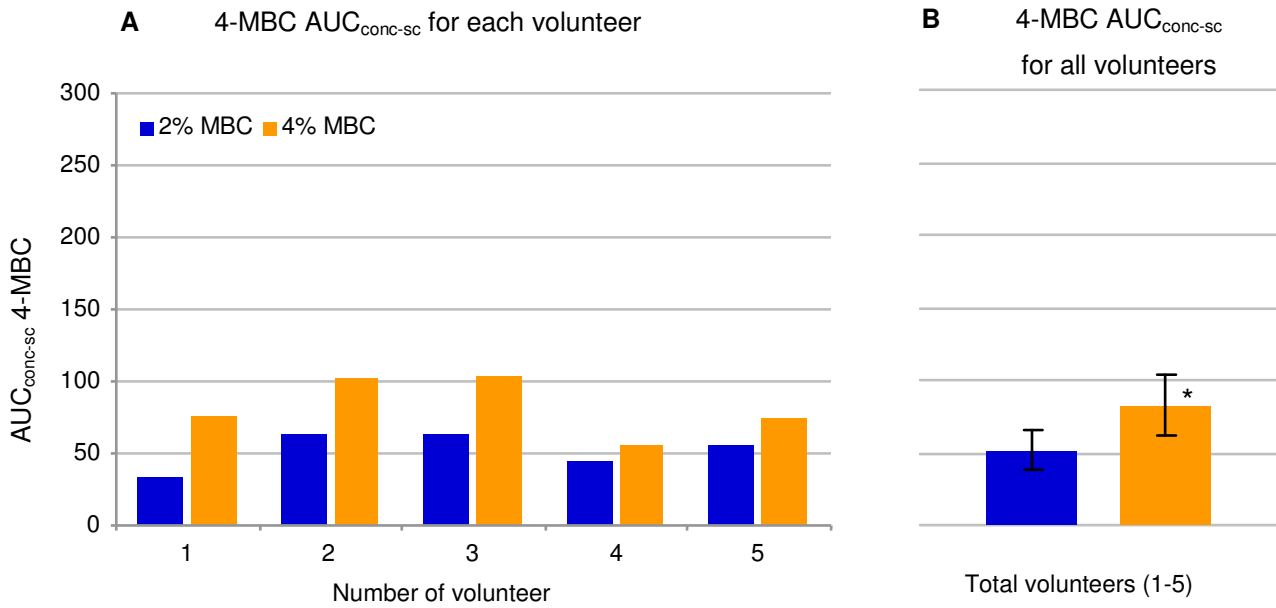


Figure 31. AUC_{conc-sc} without including the first tape strip from individual (A) and from all volunteers (B).

Legend. B $\bar{x} \pm SD$ (n=5) expressed as AUC_{conc-sc} in $\mu\text{g}/\text{tape}$; * p < 0.05. A significant difference in the AUC_{conc-sc} between the 2% and 4% formulations were found.

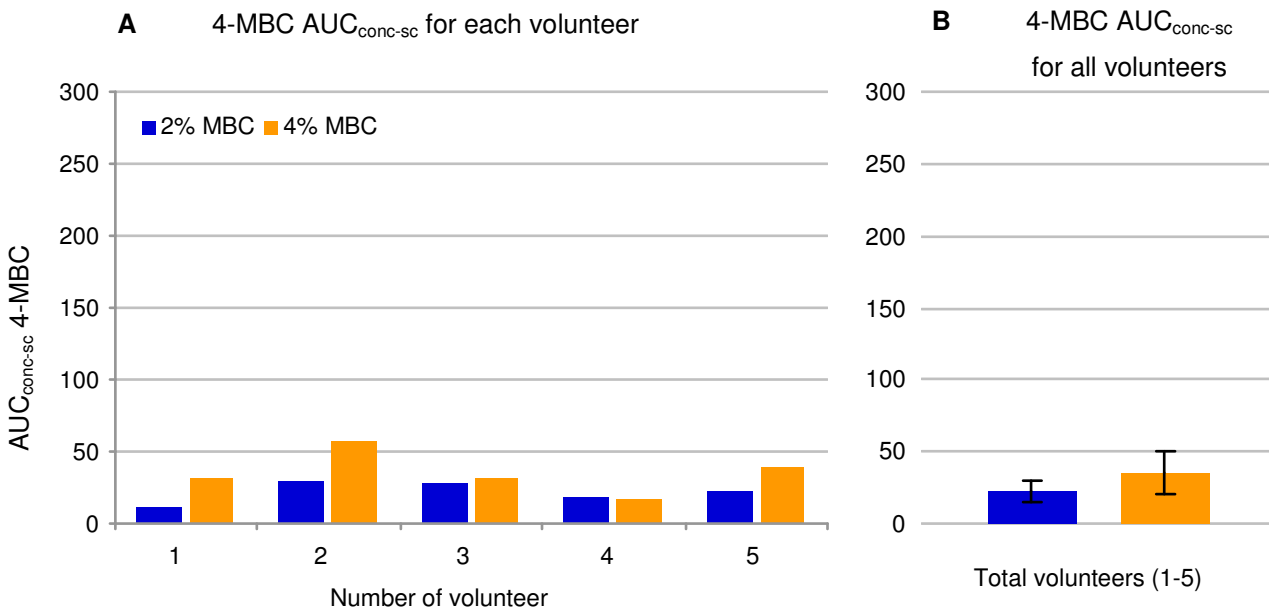


Figure 32. AUC_{conc-sc} without including tape strips 1-4 from individual (A) and from all volunteers (B).

Legend. B $\bar{x} \pm SD$ (n=5) expressed as AUC_{conc-sc} in $\mu\text{g}/\text{tape}$, p > 0.05. If tapes 1-4 were discarded, no statistically significant difference in the AUC_{conc-sc} between the 2% and 4% formulations were found.

10.6 Experiment 2

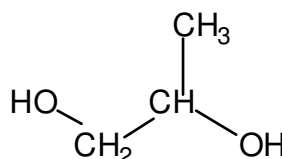
The purpose of Experiment 2 was to determine how the penetration of 4-MBC into SC was affected by the vehicle and duration of application. Therefore, saturated solutions (thermodynamic activity = 1) of 4-MBC in different vehicles (mineral oil and propylene glycol) were applied on the volar forearm of 5 volunteers for a time period of 1, 3 and 6 hours. SC samples were collected by standardized tape stripping. Absorption of 4-MBC and corneocytes on the tapes were determined simultaneously using two different wavelength (297 nm and 430 nm respectively) by the validated UV/VIS spectroscopic method. Distribution profiles of 4-MBC in SC were then assessed and an ANOVA was conducted with the logarithmic $AUC_{\text{conc-sc}}$.

10.6.1 Vehicles

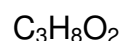
10.6.1.1 Propylene glycol

IUPAC Name 1,2-Propanediol

Molecular weight 74.13



Chemical structure



Properties

Propylene glycol (PG) belongs to the class of dialcohols some of which are widely used in cosmetics and in dermatological formulations. Of the two PGs, 1,2-propanediol is used far more often than 1,3-propanediol. PG and 1,2-propanediol are synonyms. PG is characterized as an odorless, viscous liquid; it is readily miscible with water, acetone, chloroform and essential oils; in addition, it is soluble in ether. The isotonic concentration is 2% in water. It is very hygroscopic in higher concentrations.

PG is an important part of the vehicle for most transdermal formulations. In fact, the penetration of corticosteroids is often greatly enhanced by PG. PG also potentiates the penetration of other drugs e.g. minoxidil, methotrexate, diclofenac, norfloxacin etc. In cosmetic vehicles, PG has been shown to increase the penetration of allantoin [249].

PG is believed to act by increasing drug solubility in the skin.

PG's importance as a cosolvent for lipophilic drugs and potential enhancers such as Azone and fatty acids has been acknowledged but the literature provides conflicting results as to whether this molecule is able to increase skin permeability.

The alteration of the barrier function includes affecting the bilayer structure of the intercellular lipids and/or the keratinocytes, especially α -keratin structure. It is questionable whether the increased drug uptake, based on higher partitioning into the SC as a consequence of solvent penetration, could be considered to be an enhancing action since the intact skin structure is not changed. This effect, directed at the increase of the solution capacity within the SC, is supposed to be the main effect of PG.

Based on numerous experiments, the action of solvents such as PG was attributed to a pure cosolvent effect. Maximizing the thermodynamic activity of a drug on the vehicle PG contributes to increased drug uptake in the skin. The permeation of many drugs, especially of very lipophilic molecules, was shown to be unaffected when they were applied in PG as compared to a standard vehicle. Therefore, the effects of PG were explained by differences in drug solubility on the donor site etc. [250].

10.6.1.2 Mineral oil

IUPAC name	Hydrocarbon oils
Formula	Unspecified
Molecular weight	-

Properties

Following application of mineral oil (MO) to the skin, the intercellular space is relatively uniformly filled with a smooth-appearing amorphous material, presumably the MO. Intercellular spaces were occasionally focally dilated. The MO appeared to have little effect other than a "spacer" separating corneocytes [251].

10.6.2 Determination of solubility of 4-MBC in vehicles

The formulations were prepared freshly for every volunteer.

10.6.2.1 Material

- UV/VIS-spectrophotometer, Lambda Bio 20, Perkin Elmer, Norwalk, CT, 06859 USA, serial # 101N7062724; UVWinLab Software V2.85. 04
- Magnetic stirrer, N.ZIVY & CIE SA, 4104 Oberwil, Switzerland
- Pharmacopoeial thermometer (from -2 to +50 °C), Ph. Helv., 1994, SCS3120.
- Water-bath WTE var 3185
- Labofuge I, Haereus Christ, Laborgeräte AG, Zürich, Switzerland, serial # 00100581.

10.6.2.2 Method

The saturation solubility of 4-MBC in MO and PG was determined at 33 °C i.e. skin temperature. An excess amount of 4-MBC was added to each vehicle. The suspensions were kept in sealed glass flasks, stirred magnetically and allowed to equilibrate in a thermostat water bath maintaining the sample temperature at 33 ± 1 °C for 24h. The saturated solutions were centrifuged at 4000rpm for 10 min. The supernatant solution was diluted with methanol and analyzed by UV spectroscopy at 299 nm.

10.6.2.3 Results

The solubility of 4-MBC in MO and PG is presented in Figure 33. The small standard deviations ensure the reproducibility of the preparation of the formulation.

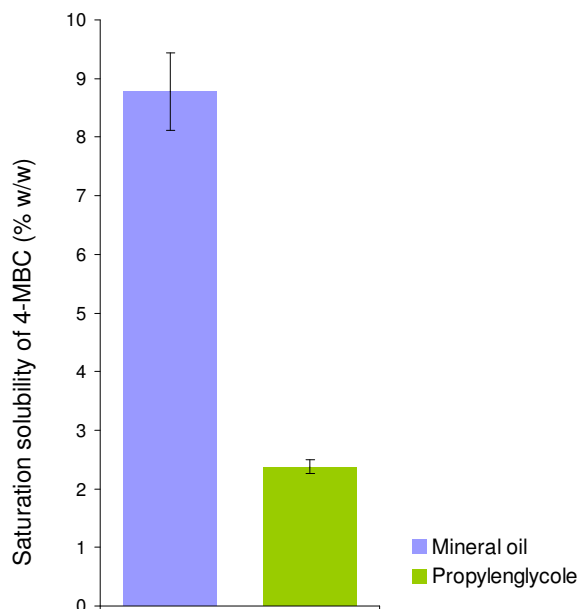


Figure 33. Saturation solubility of 4-MBC in mineral oil and in propylene glycol.

Legend. Saturation solubility was measured at 33°C; n=5 for both solvents.

Mineral oil: $x = 8.7$; $SD = \pm 0.7$.

Propylene glycol: $x = 2.6$; $SD = \pm 0.1$.

10.6.3 Study Design for Experiment 2

All suitable test persons for this series of studies were selected according to inclusive and exclusive criteria (see section 10.6.4).

Due to their liquid form, the formulations were applied to the skin of the test persons' forearms by means of an application chamber (Figure 34). Each test person was treated with both formulations.

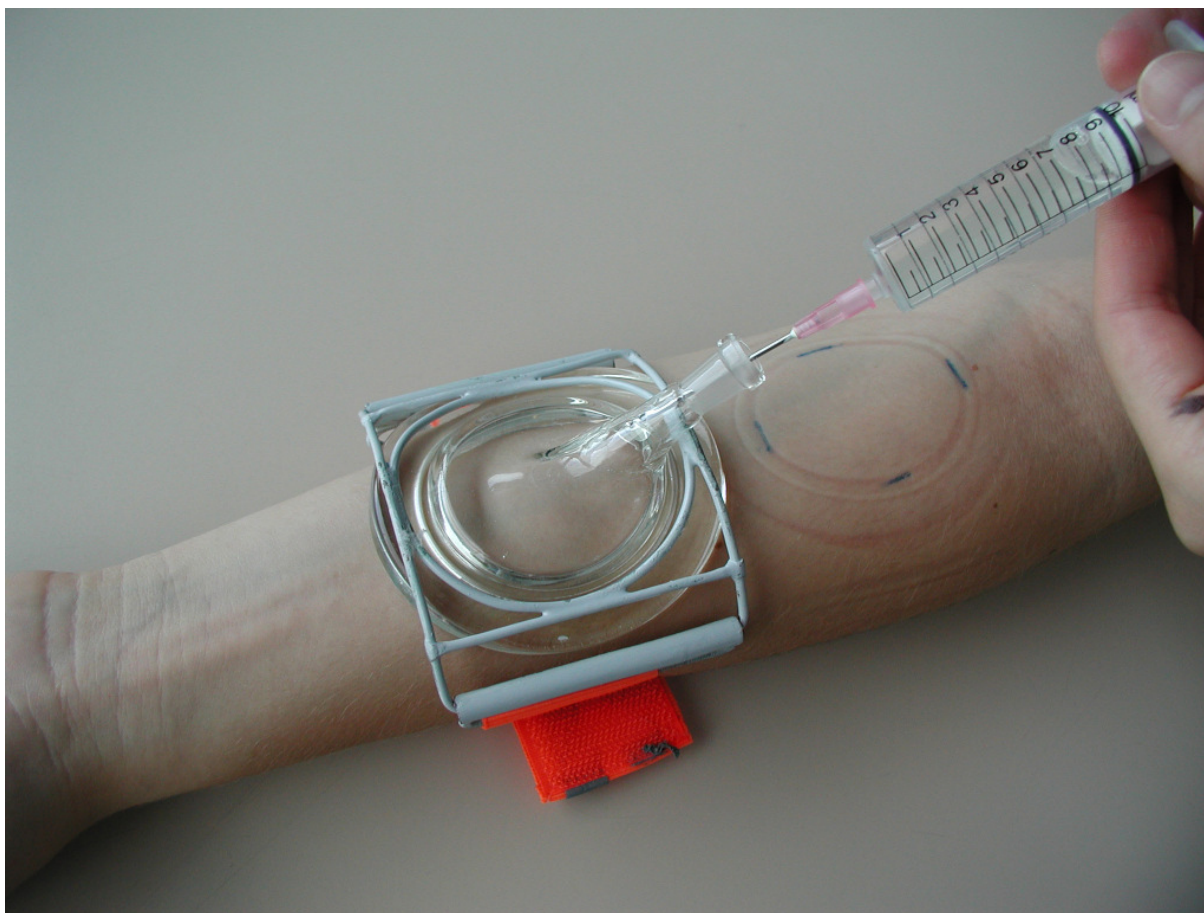


Figure 34. Application chamber.

The penetration of 4-MBC was measured for each formulation on three different patches of application at three different times (Figure 36, Table 31). At $t = 1, 3$ and 6 h the application chambers were removed. The extra amount of formulation was removed with a dry cotton swab and the penetration of 4-MBC was measured by means of the tape stripping method. Based on the data thus gained, the $AUC_{\text{conc-sc}}$ of 4-MBC was calculated.

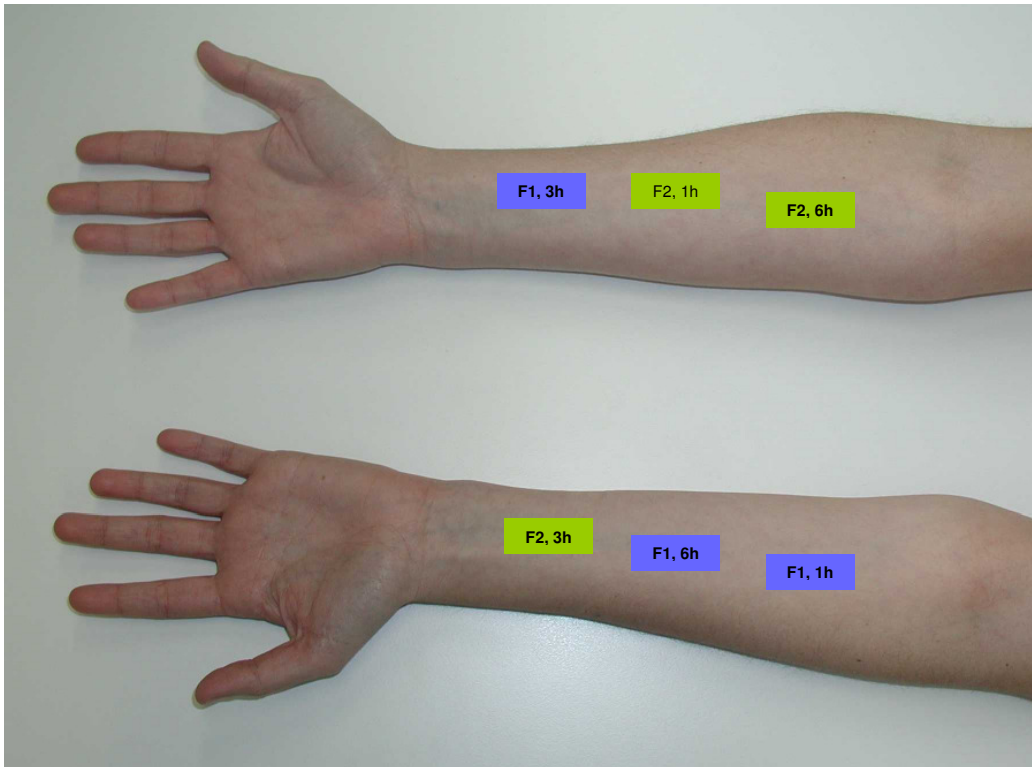


Figure 35. Treatment scheme for test person with different formulations (F) for Experiment 2.

- Legend.
- F1, 1h = mineral oil saturated with 4-MBC applied to skin for 1 hour.
 - F1, 3h = mineral oil saturated with 4-MBC applied to skin for 3 hours.
 - F1, 6h = mineral oil saturated with 4-MBC applied to skin for 6 hours.
 - F2, 1h = propylene glycol saturated with 4-MBC applied to skin for 1 hour.
 - F2, 3h = propylene glycol saturated with 4-MBC applied to skin for 3 hours.
 - F2, 6h = propylene glycol saturated with 4-MBC applied to skin for 6 hours.

Table 31. Scheme for a test person for Experiment 2.

	F 1	F 2
t = 1 h	F1, 1h	F2, 1h
t = 3 h	F1, 3h	F2, 3h
t = 6 h	F1, 6h	F2, 6h

F= formulation
t= duration of application of formulation

In summary, each test person undergoes 6 measurements, the two formulations at three different application durations each. The application duration of the treatment varies with regard to the three patches on each arm (arm A: t = 1, 3 and 6 h, arm B: t = 1, 3 and 6 h), where the duration on the arm was chosen at random. One duration of application per person was tested simultaneously with respect to both formulations.

10.6.4 Inclusion Exclusion Criteria

Before entering the study, the skin of the volunteer had to first be examined by a Dermatologist who then had to confirm the eligibility of the volunteer for entrance into the study providing the Inclusion and Exclusion Criteria below were met.

10.6.4.1 Inclusion Criteria

Volunteers who

- are between 18 and 35 years old
- have Caucasian skin type
- are willing to participate into the study.

10.6.4.2 Exclusion Criteria

Volunteers who

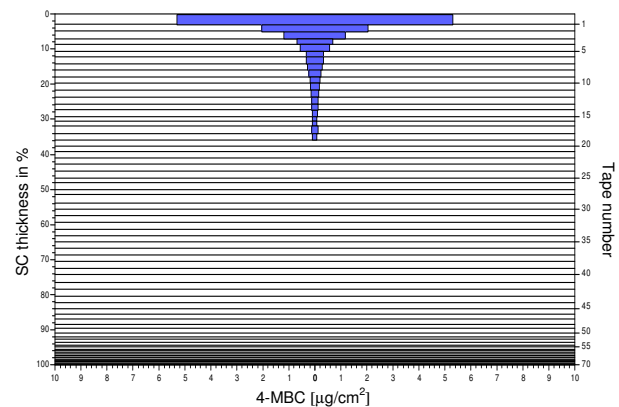
- do not want to participate or who are unable to understand and/or sign the consent form
- have acute inflammations of the skin
- have other diseases or allergies
- are pregnant or lactating
- have limited abilities to register and/or judge their circumstances
- are participating in other ongoing studies
- have a positive HIV-Test.

10.6.5 Results

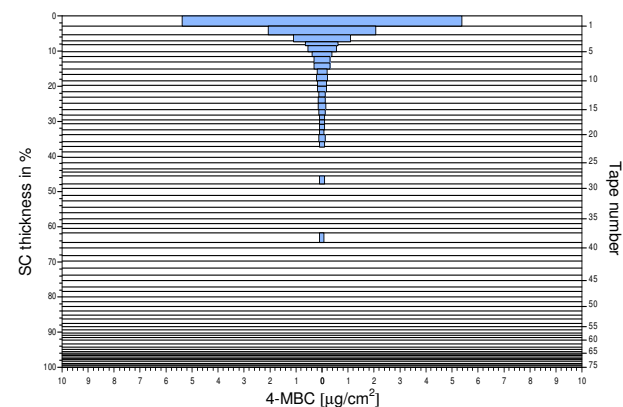
10.6.5.1 Stratum Corneum Profiles

Volunteer 1

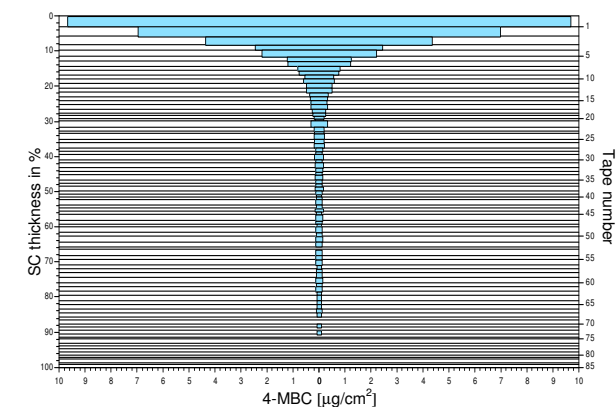
Mineral oil 1h, $AUC_{\text{conc-sc}} = 41.12$



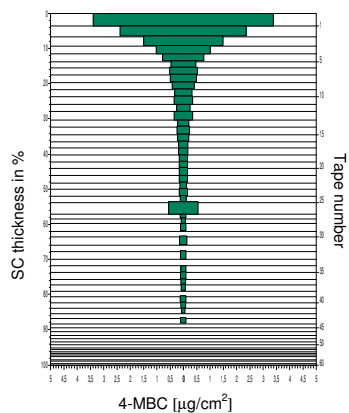
Mineral oil 3h, $AUC_{\text{conc-sc}} = 43.67$



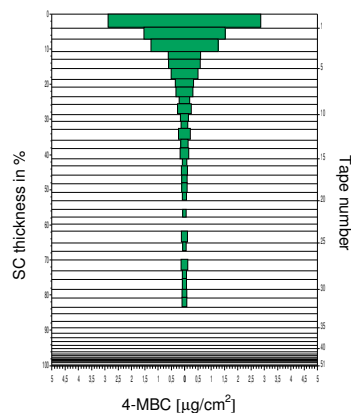
Mineral oil 6h, $AUC_{\text{conc-sc}} = 180.75$



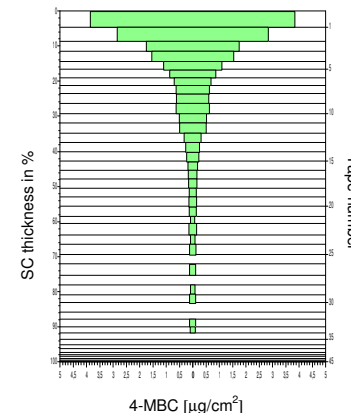
Propylene glycol 1h, $AUC_{\text{conc-sc}} = 75.48$



Propylene glycol 3h, $AUC_{\text{conc-sc}} = 45.39$

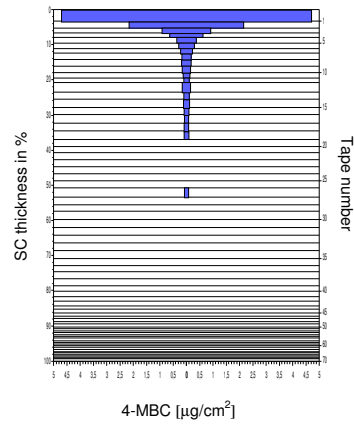


Propylene glycol 6h, $AUC_{\text{conc-sc}} = 85.58$

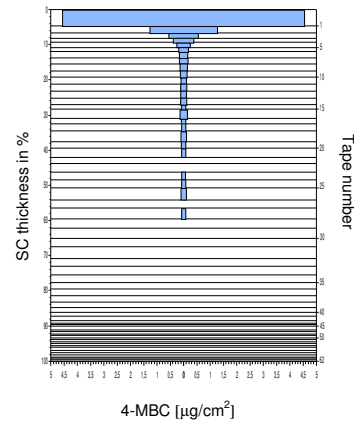


Volunteer 2

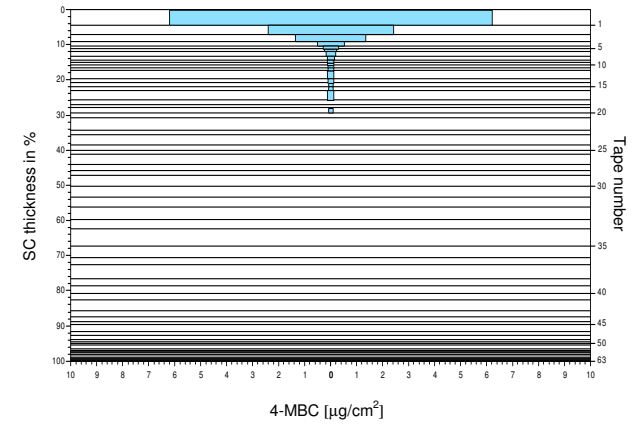
Mineral oil 1h, $AUC_{\text{conc-sc}} = 36.41$



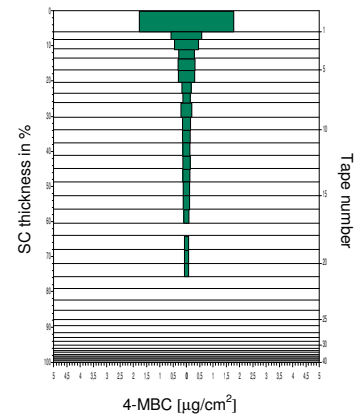
Mineral oil 3h, $AUC_{\text{conc-sc}} = 27.79$



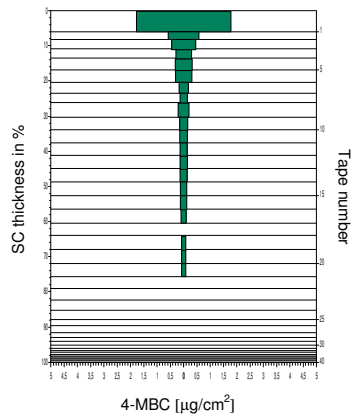
Mineral oil 6h, $AUC_{\text{conc-sc}} = 36.32$



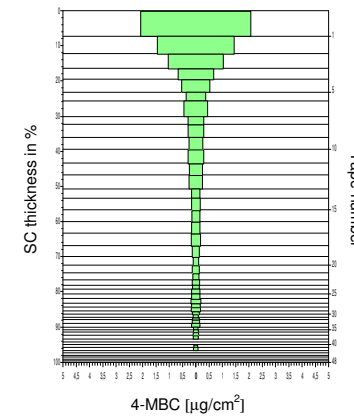
Propylene glycol 1h, $AUC_{\text{conc-sc}} = 22.04$



Propylene glycol 3h, $AUC_{\text{conc-sc}} = 47.21$

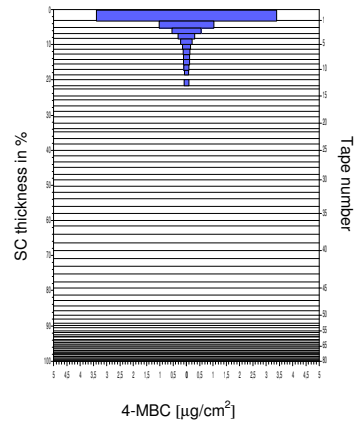


Propylene glycol 6h, $AUC_{\text{conc-sc}} = 57.45$

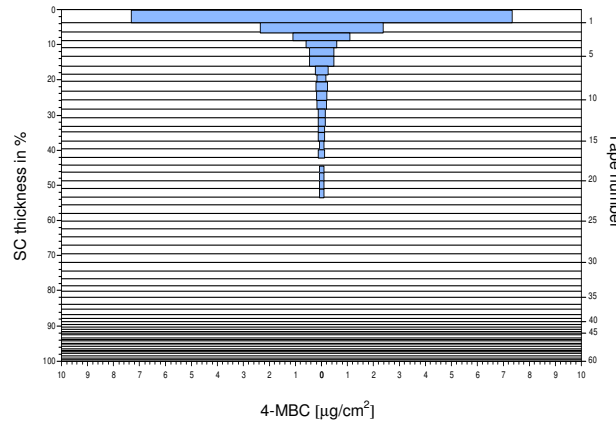


Volunteer 3

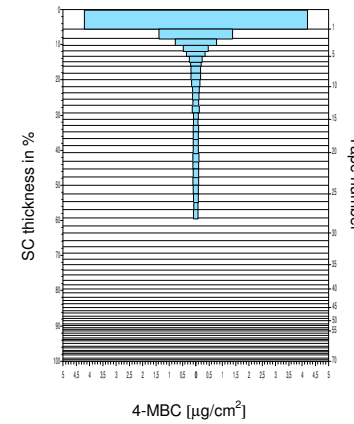
Mineral oil 1h, $AUC_{\text{conc-sc}} = 17.12$



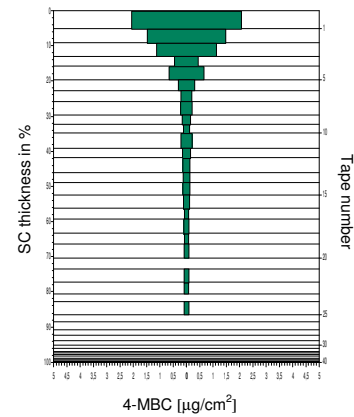
Mineral oil 3h, $AUC_{\text{conc-sc}} = 41.62$



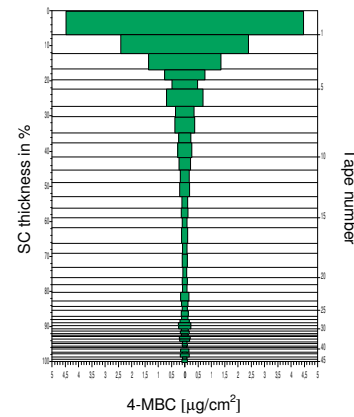
Mineral oil 6h, $AUC_{\text{conc-sc}} = 34.36$



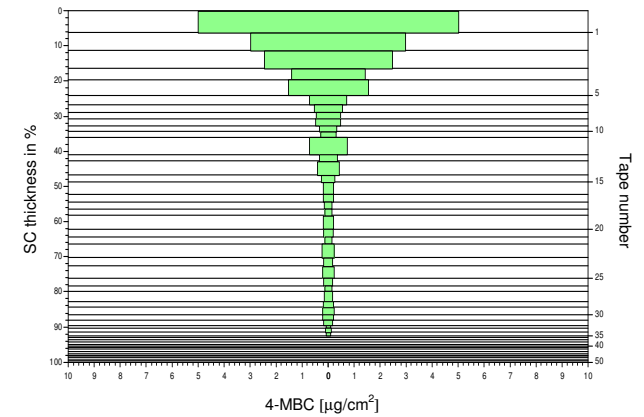
Propylene glycol 1h, $AUC_{\text{conc-sc}} = 36.65$



Propylene glycol 3h, $AUC_{\text{conc-sc}} = 68.09$

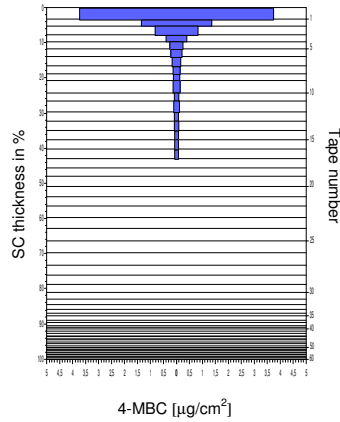


Propylene glycol 6h, $AUC_{\text{conc-sc}} = 97.93$

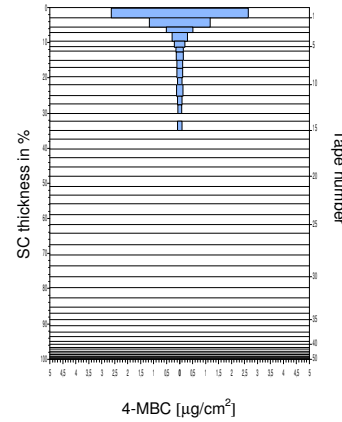


Volunteer 4

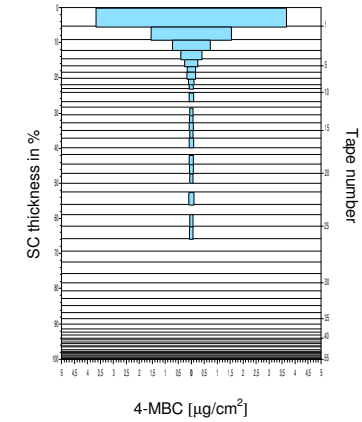
Mineral oil 1h, $AUC_{\text{conc-sc}} = 25.12$



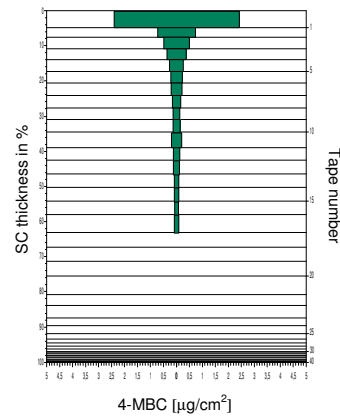
Mineral oil 3h, $AUC_{\text{conc-sc}} = 18.84$



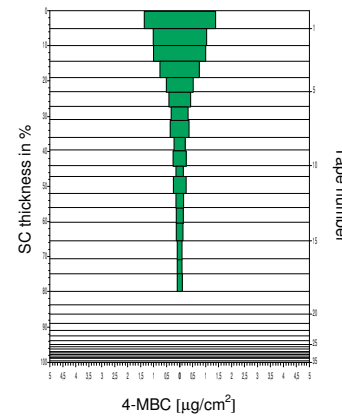
Mineral oil 6h, $AUC_{\text{conc-sc}} = 26.50$



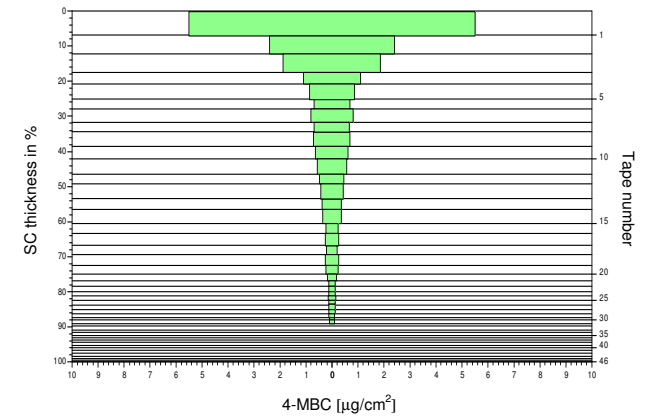
Propylene glycol 1h, $AUC_{\text{conc-sc}} = 20.89$



Propylene glycol 3h, $AUC_{\text{conc-sc}} = 35.57$

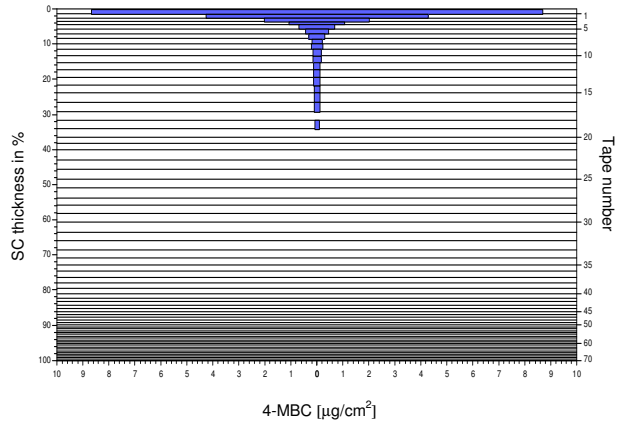


Propylene glycol 6h, $AUC_{\text{conc-sc}} = 86.16$

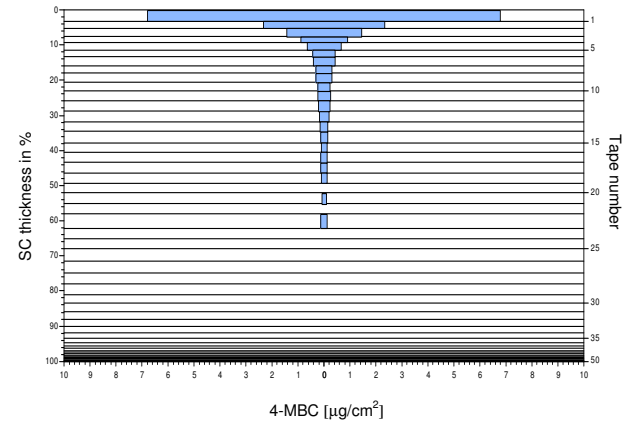


Volunteer 5

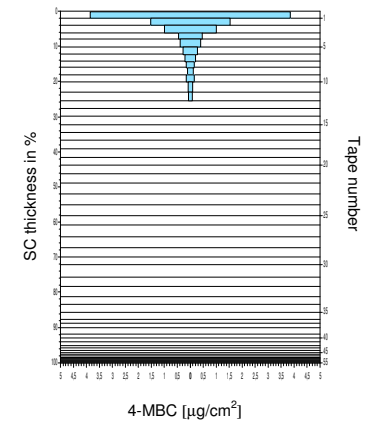
Mineral oil 1h, $AUC_{\text{conc-sc}} = 61.11$



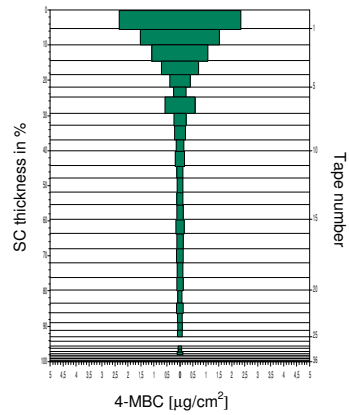
Mineral oil 3h, $AUC_{\text{conc-sc}} = 50.98$



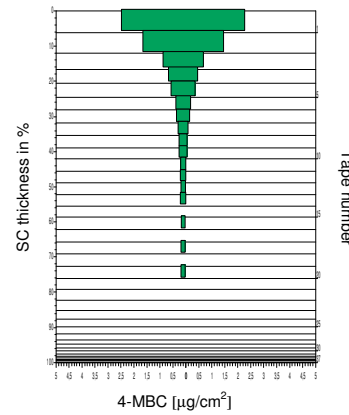
Mineral oil 6h, $AUC_{\text{conc-sc}} = 26.59$



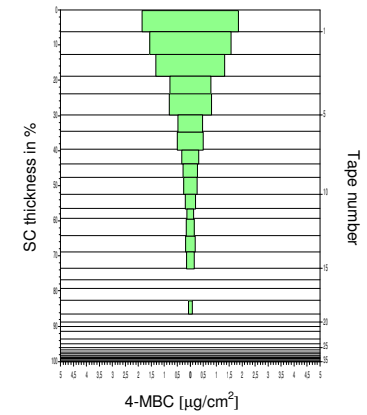
Propylene glycol 1h, $AUC_{\text{conc-sc}} = 42.91$



Propylene glycol 3h, $AUC_{\text{conc-sc}} = 30.24$



Propylene glycol 6h, $AUC_{\text{conc-sc}} = 43.17$



10.6.5.2 Results for Experiment 2: $AUC_{conc-sc}$

For the calculation of the $AUC_{conc-sc}$, the first tape collected was discarded due to potential drug remaining on the skin surface.

Table 32. $AUC_{conc-sc}$ -values for Experiment 2.

Volunteer No.	Age (Sex ^a)	Mineral oil (F1)			Propylene glycol (F2)		
		1h	3h	6h	1h	3h	6h
1	26 (m)	41.12	43.67	180.75	75.48	45.39	85.58
2	22 (m)	36.41	27.79	36.32	22.04	47.21	57.45
3	30 (f)	17.12	41.62	34.36	36.65	68.09	97.93
4	25 (f)	25.12	18.84	26.50	20.89	35.57	86.16
5	27 (f)	61.11	50.98	26.59	42.91	30.24	43.17
\bar{x}		36.17	36.58	60.90	39.59	45.30	74.06
SD		16.82	12.99	67.14	22.17	14.53	22.80

^a (f) female, (m) male

10.6.5.3 Statistical analysis of results for Experiment 2

An ANOVA was conducted with the results of both experiments, based on the main factors of formulation, time and volunteer. In addition, the analysis included the impact of interaction, consisting of formulation x time, formulation x volunteer and time x volunteer.

The variance analysis presumes an equal distribution on the different factor levels. In general, the relative standard deviation tends to be more independent (variance coefficients) from the factor levels than the absolute standard deviations with regard to concentration measurement. In this case, the equality of the absolute dispersion can be calculated when taking the logarithm of the data. This transformation was applied to these data.

Table 33. Logarithmic AUCconc-sc values for Experiment 2.

Volunteer No.	Mineral oil (F1)			Propylene glycol (F2)		
	1h	3h	6h	1h	3h	6h
1	1.61	1.64	2.26	1.88	1.66	1.93
2	1.56	1.44	1.56	1.34	1.67	1.76
3	1.23	1.62	1.54	1.56	1.83	1.99
4	1.40	1.28	1.42	1.32	1.55	1.94
5	1.79	1.71	1.42	1.63	1.48	1.64

The variance analysis excluded the extreme value (volunteer 1, F1, 6h).

The factor formulation showed a significant impact ($p < 0.05$) on the amount of 4-MBC which penetrated the stratum corneum. The factors of time and volunteer as well as interaction showed no significant impact.

This experiment leads to the conclusion that more 4-MBC penetrated the skin from PG than from MO.

Table 34. ANOVA for 4-MBC amount in SC from F1 and F2 in Experiment 2 – Type III Sum of Squares.

Source	Sum of Squares	Df	Mean square	F-ratio	p value
main effects					
A: formulation	0.1821	1	0.1821	11.25	0.0122
B: time	0.0780	2	0.0390	2.41	0.1598
C: volunteer	0.1298	4	0.0324	2.00	0.1983
interactions					
AB	0.1295	2	0.0647	4.00	0.0694
AC	0.1416	4	0.0354	2.19	0.1724
BC	0.2665	8	0.0333	2.06	0.1786
residual	0.1133	7	0.0162		
total	1.1358	28			

All F-ratios are based on the residual mean square error

10.6.5.4 Number of tapes stripped

The number of tape strips used to remove the stratum corneum was compared for MO and PG. A paired sample t-test was used to compare the mean ($n=5$) total number of tapes stripped for every site of application. There is a statistically significant ($p=0.05$) difference between MO and PG vehicles required for complete SC removal at every duration of application. More tapes (67 tapes (mean value over all durations of application)) were necessary to strip the whole stratum corneum of test sites that had previously been treated

with MO. Skin that had been treated with PG was completely stripped using fewer tapes (45 tapes (mean value over all experiments)) (Figure 36).

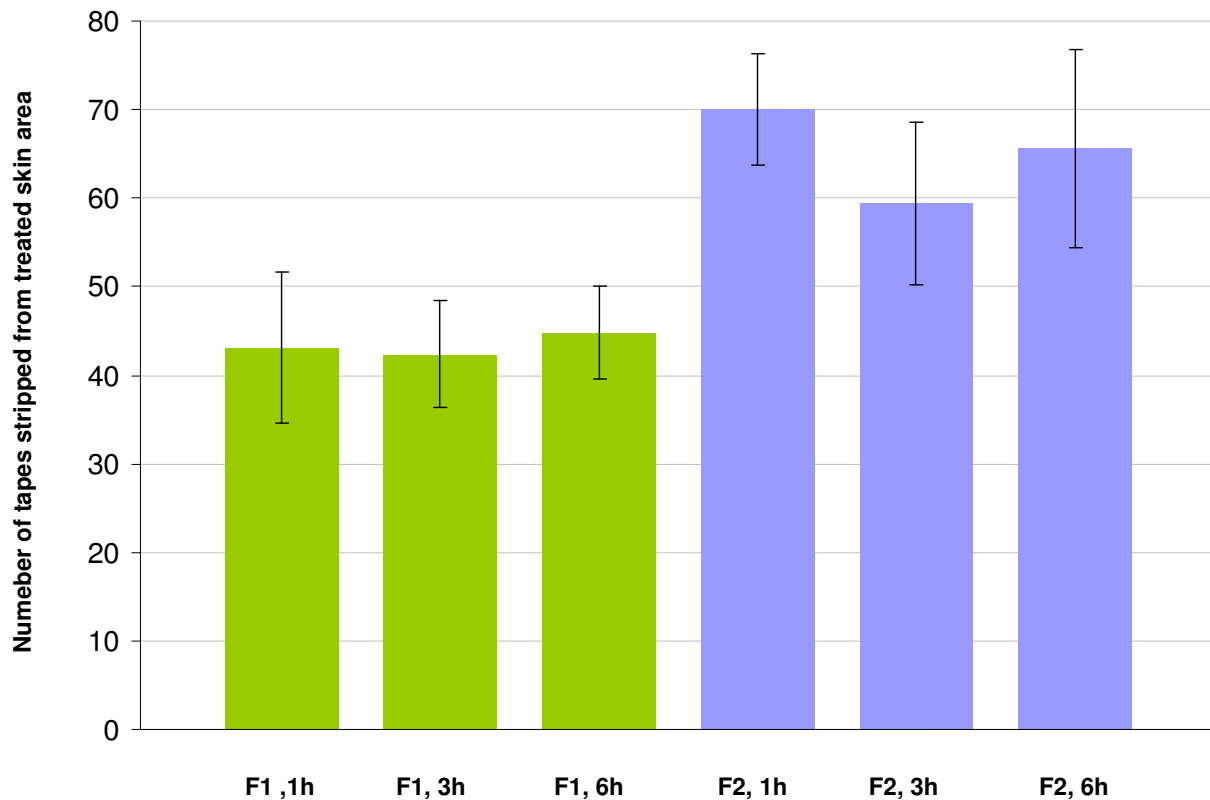


Figure 36. Number of tapes removed from skin treated with mineral oil (F1) and propylene glycol (F2) after different durations of application.

Legend. n=5 (volunteers) for both formulations.

F1, 1h: $x = 43$; $SD = \pm 8$.

F1, 3h: $x = 42$; $SD = \pm 11$.

F1, 6h: $x = 45$; $SD = \pm 10$.

F2, 1h: $x = 70$; $SD = \pm 11$.

F2, 3h: $x = 60$; $SD = \pm 14$.

F2, 6h: $x = 66$; $SD = \pm 11$.

10.7 Experiment 3

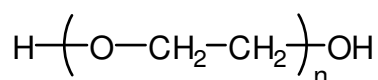
The effect of the penetration enhancer Transcutol[®]CG on the substantivity of 4-MBC in the SC was investigated on the volar forearm of 10 volunteers. After one hour of skin contact with saturated 4-MBC (thermodynamic activity = 1) in Polyethylene glycol 400 containing 0%, 10% and 50% Transcutol[®]CG, tape stripping immediately and after 6 hours. SC samples were collected by standardized tape stripping. Absorption of 4-MBC and corneocytes on the tapes was determined simultaneously at 297 nm and 430 nm, respectively, by the validated UV/VIS spectroscopic method. Distribution profiles of 4-MBC in SC were assessed and an ANOVA was conducted with the logarithmic $AUC_{\text{conc-sc}}$.

10.7.1 Vehicles

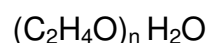
10.7.1.1 Polyethylene glycol 400

IUPAC name Poly(oxy-1,2-ethanediyl), α -hydro- ω -hydroxy-

Molecular weight 380-420



Chemical structure



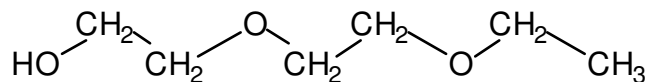
Properties

Polyethylene glycol (PEG) polymers are available in a variety of molecular weights. These materials are water-soluble and neither hydrolyze nor support mold growth. Thus, PEGs are ideal bases for washable ointments and can be formulated to provide either soft or hard consistencies. PEGs dissolve in water to form clear solutions. They are also soluble in organic solvents such as mineral oil and produce formulations that are more substantive to the skin [252].

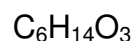
10.7.1.2 *Transcutol*[®]CG

IUPAC name Diethylene glycol monoethyl ether

Molecular weight 134.2



Chemical structure



Properties

Transcutol[®]CG is a hygroscopic liquid that is freely miscible with both polar and non-polar solvents. *Transcutol*[®]CG has been recognized as a potential transdermal permeation enhancer due to its non-toxicity, biocompatibility with skin and excellent solubilizing properties. However, *Transcutol*[®]CG has also been reported to increase the skin accumulation of topically applied compounds without a concomitant increase in transdermal permeation [185].

Transcutol[®]CG enhances penetration of several compounds prostaglandins, morphine base, and oestradiol [187]. It has been suggested that *Transcutol*[®]CG may enhance drug flux across SC by diffusing into it and altering its solubility parameters. Diffusion cell data show that *Transcutol*[®]CG can increase drug flux without an apparent change in lag time. This implies that *Transcutol*[®]CG acts by altering the solubility of a permeant in the skin [187]. This mechanism was demonstrated for the model compound, cyanophenol.

Transcutol[®]CG is a vehicle used as a solvent/cosolvent in cosmetic and topical preparations and has been shown to form cutaneous depots in the skin with corticosteroids [186] and griseofulvin [188, 190].

10.7.2 Determination of 4-MBC solubility

10.7.2.1 Method

The saturation solubility of 4-MBC in PEG 400 (F1), PEG 400 with 10% *Transcutol*[®]CG (F2) and PEG 400 with 50% *Transcutol*[®]CG (F3) was determined as described in section 10.6.2.2.

10.7.2.2 Material

- UV/VIS-spectrophotometer, Perkin Elmer, Lambda Bio 20 serial # 101N7062724; UVWinLab Software V2.85. 04
- Magnetic stirrer, N.ZIVY & CIE SA, 4104 Oberwil, Switzerland
- Pharmacopoeial thermometer (from -2 to +50 °C), Ph. Helv., 1994, SCS3120.
- Water-bath WTE var 3185
- Labofuge I, Haereus Christ, Laborgeräte AG, Zürich, Switzerland, serial # 00100581.

10.7.2.3 Results

The influence of Transcutol®CG as a cosolvent is clearly visible in Figure 37. Adding 50% Transcutol®CG to PEG 400 augments the 4-MBC solubility greatly.

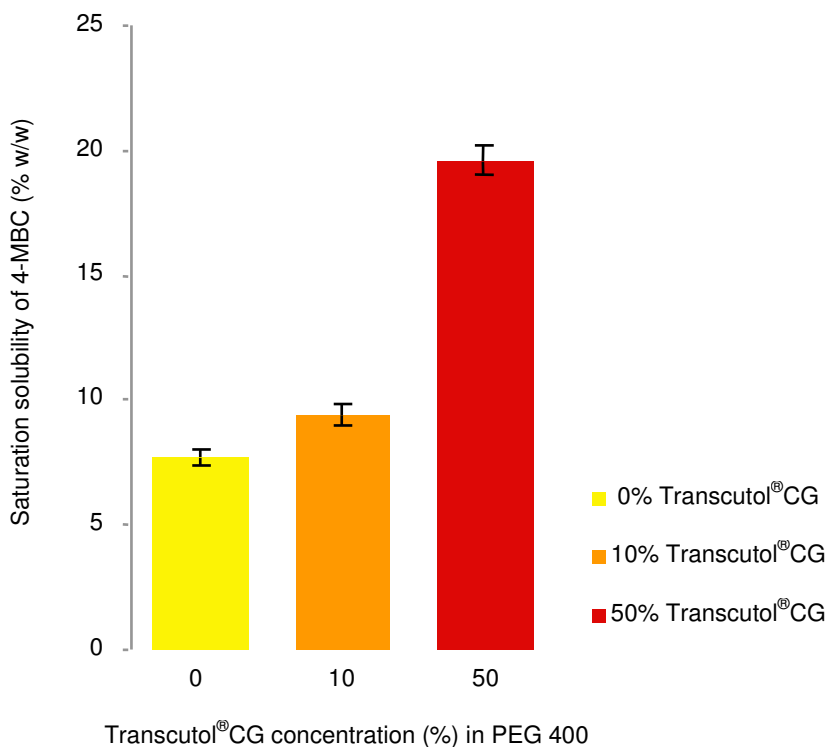


Figure 37. Effect of Transcutol®CG concentration on the saturation solubility of 4-MBC.

Legend. The saturation solubility of 4-MBC was measured at 33 °C; n=10 for 0%, n=5 for 10% and; n= 5 for 50% Transcutol®CG in polyethylene glycol 400.

0% Transcutol®CG : $x = 7.7$; $SD = \pm 0.4$.

10% Transcutol®CG: $x = 9.4$; $SD = \pm 0.4$.

50% Transcutol®CG: $x = 19.6$; $SD = \pm 0.6$.

10.7.3 Study Design for Experiment 3

All suitable test persons for this series of studies were selected according to inclusive and exclusive criteria (see section 10.6.4).

Three formulations (F1, F2 and F3) were tested. Each of the three formulations contained 4-MBC in a saturated concentration. Each test person was treated with two formulations (F1 and F2 or F3) and each candidate received F1 application. Twice within one hour each formulation was applied to the skin of the forearm by means of an application chamber. Both application chambers were removed from both arms after one hour. The extra amount of formulation was removed with a dry cotton swab. The penetration of 4-MBC was measured on one arm immediately after application chamber removal (TI = 0 h) and on the other arm six hours later (TI = 6 h) (Table 35, Figure 38).

Table 35. Scheme for two test persons for Experiment 3.

		F 1	F 2	F 3
volunteer	TI = 0 h	F1, 0h	F2, 0h	
	TI = 6 h	F1, 6h	F2, 6h	
volunteer	TI = 0 h	F1, 0h		F3, 0h
	TI = 6 h	F1, 6h		F3, 6h

F= formulation

TI= Time interval between the moment of formulation removal and the tape stripping phase

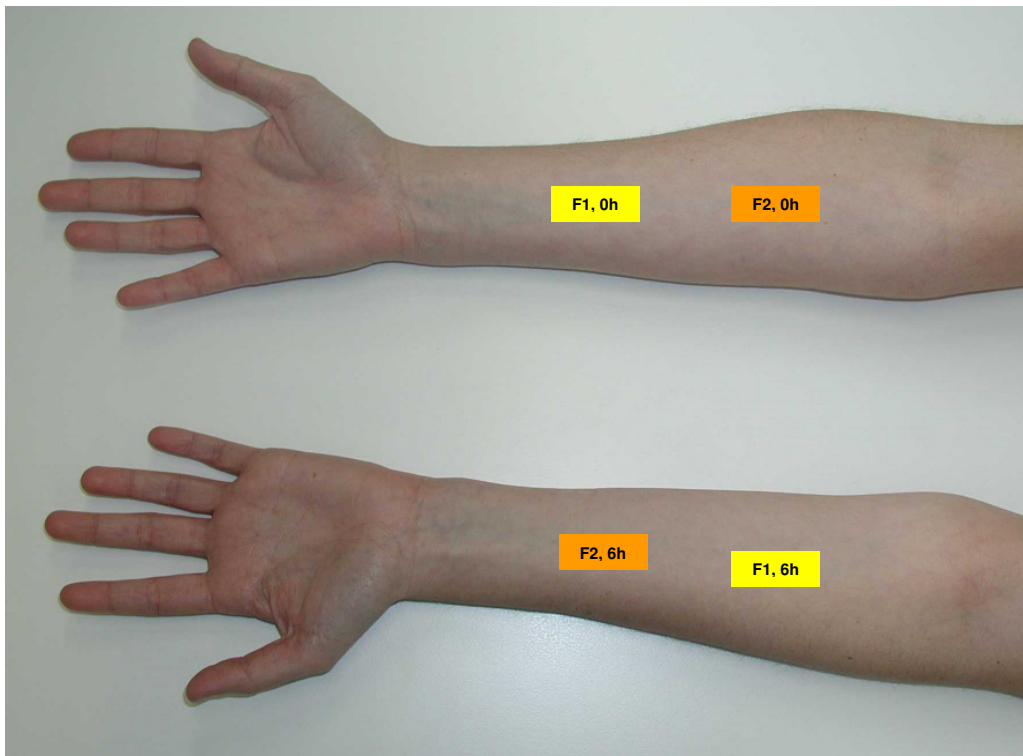


Figure 38. Treatment scheme for test person with different formulations (F).

Legend. F1, 0h = skin treated with PEG 400 saturated with 4-MBC and stripped directly after removing the formulation.
F1, 6h = skin treated with PEG 400 saturated with 4-MBC and stripped 6 hours after removing the formulation.
F2, 0h = skin treated with 10% Transcutol[®]CG in PEG 400 saturated with 4-MBC and stripped directly after removing the formulation.
F2, 6h = skin treated with 10% Transcutol[®]CG in PEG 400 saturated with 4-MBC and stripped 6 hours after removing the formulation.

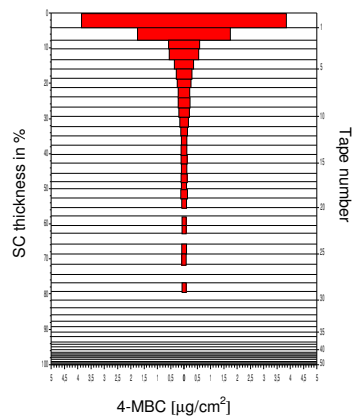
On each arm two patches were treated during different time intervals (arm A: F1/TI = 0 h, F2/TI = 6 h, Arm B: F2/TI = 0 h, F1/TI = 6 h), and the time intervals on the arm were chosen at random. Two patches were treated simultaneously, one on each arm. 4 measurements were taken for each test person, the two formulations both at two different time intervals.

10.7.4 Results

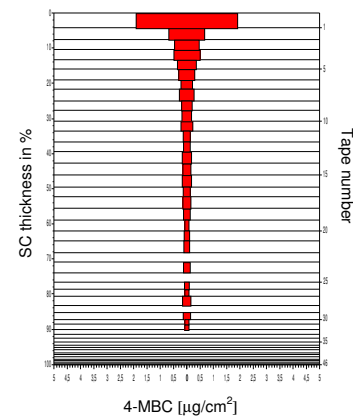
10.7.4.1 Stratum Corneum Profiles

Volunteer 1

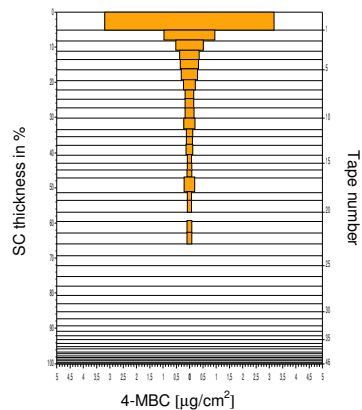
PEG 400, TI=0h, $AUC_{\text{conc-sc}} = 35.80$



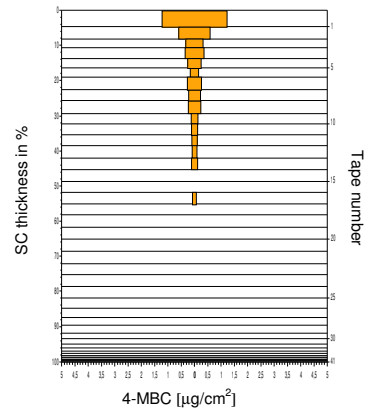
PEG 400, TI=6h, $AUC_{\text{conc-sc}} = 33.09$



Transcutol[®]CG 10%, TI=0h, $AUC_{\text{conc-sc}} = 27.19$

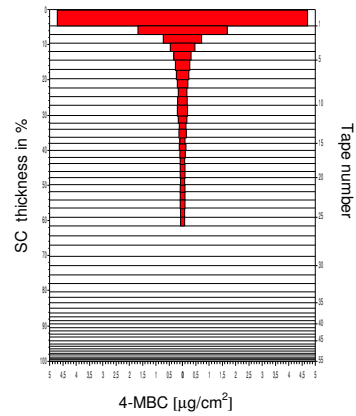


Transcutol[®]CG 10%, TI=6h, $AUC_{\text{conc-sc}} = 17.89$

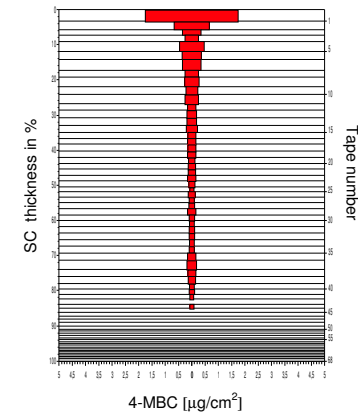


Volunteer 2

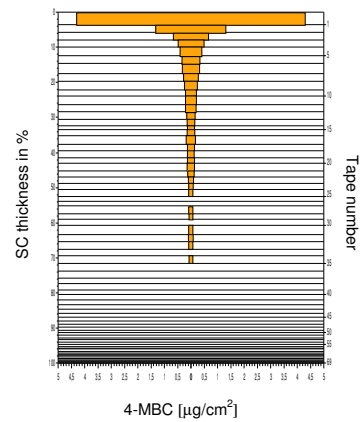
PEG 400, TI=0h, $AUC_{\text{conc-sc}} = 35.45$



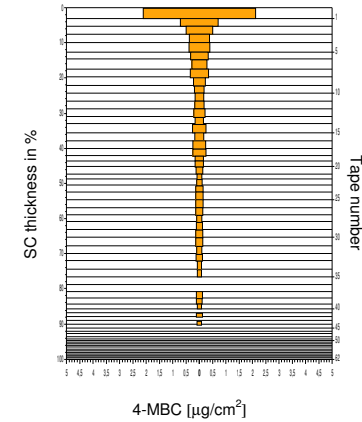
PEG 400, TI=6h, $AUC_{\text{conc-sc}} = 44.83$



Transcutol[®]CG 10%, TI=0h, $AUC_{\text{conc-sc}} = 40.25$

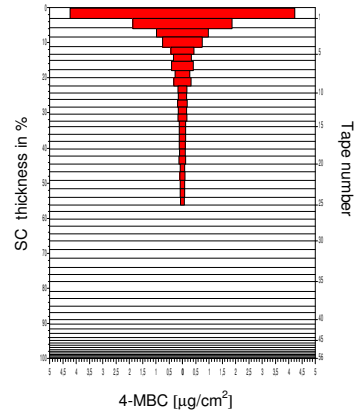


Transcutol[®]CG 10%, TI=6h, $AUC_{\text{conc-sc}} = 40.22$

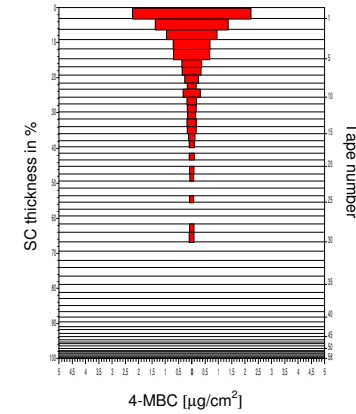


Volunteer 3

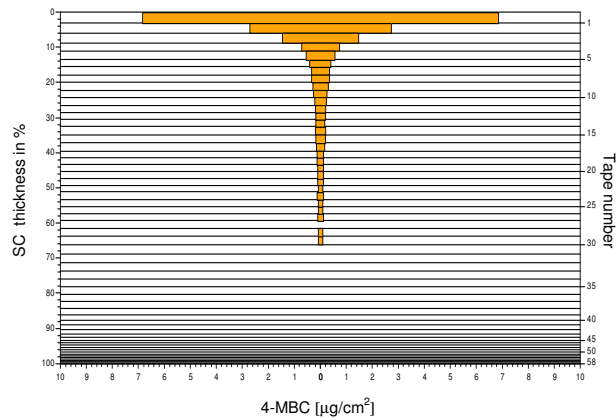
PEG 400, TI=0h, $AUC_{\text{conc-sc}} = 43.67$



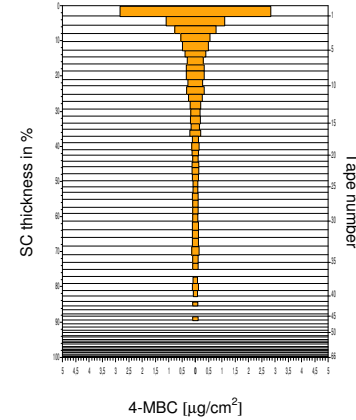
PEG 400, TI=6h, $AUC_{\text{conc-sc}} = 40.19$



Transcutol[®]CG 10%, TI=0h, $AUC_{\text{conc-sc}} = 57.15$

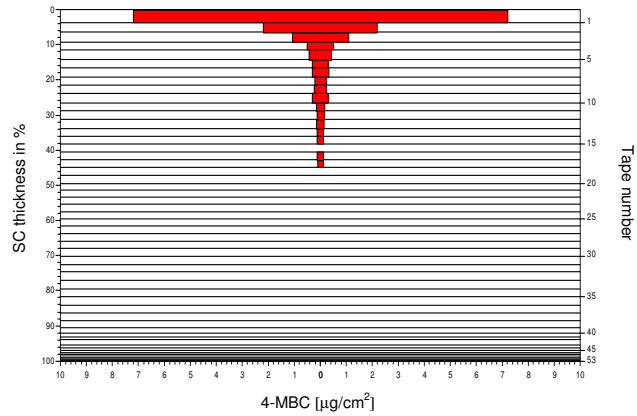


Transcutol[®]CG 10%, TI=6h, $AUC_{\text{conc-sc}} = 51.56$

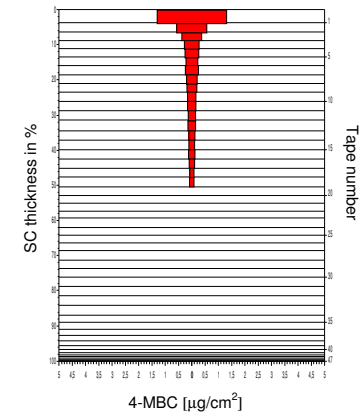


Volunteer 4

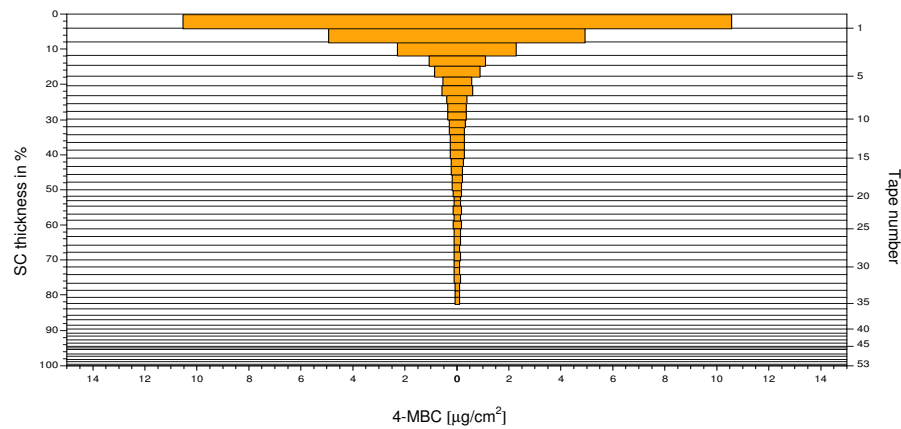
PEG 400, TI=0h, $AUC_{\text{conc-sc}} = 38.65$



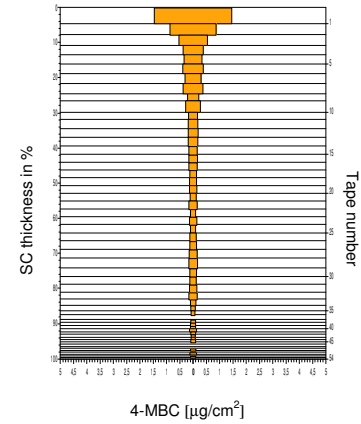
PEG 400, TI=6h, $AUC_{\text{conc-sc}} = 20.90$



Transcutol®CG 10%, TI=0h, $AUC_{\text{conc-sc}} = 92.38$

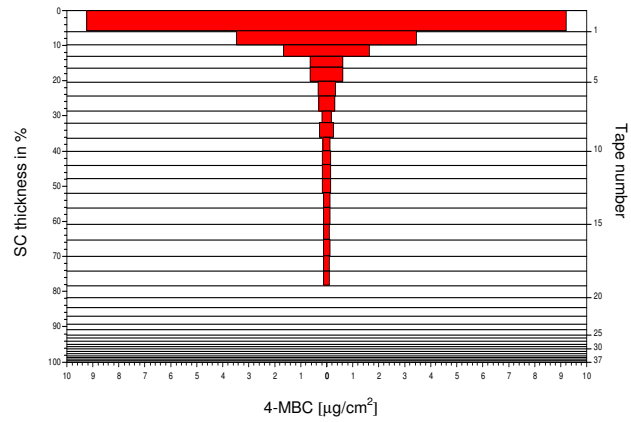


Transcutol®CG 10%, TI=6h, $AUC_{\text{conc-sc}} = 49.14$

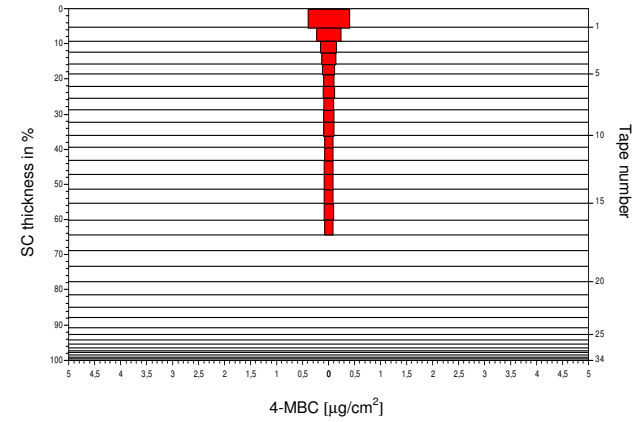


Volunteer 5

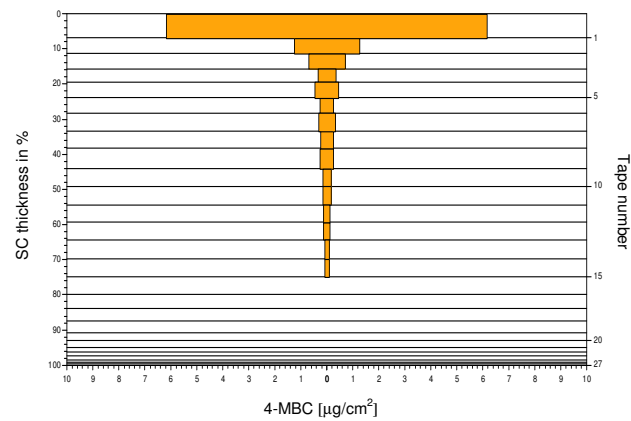
PEG 400, TI=0h, $AUC_{\text{conc-sc}} = 51.97$



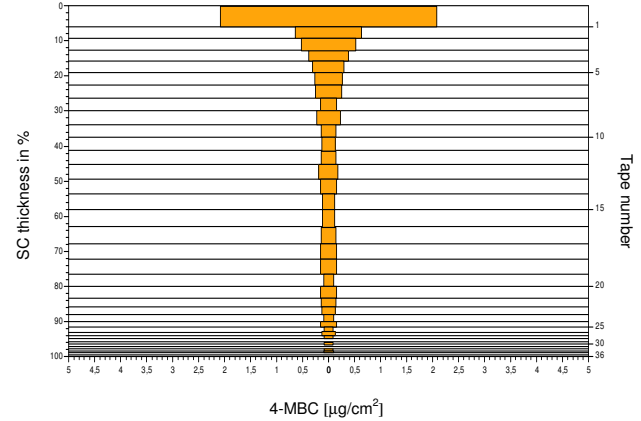
PEG 400, TI=6h, $AUC_{\text{conc-sc}} = 10.30$



Transcutol[®]CG 10%, TI=0h, $AUC_{\text{conc-sc}} = 27.03$

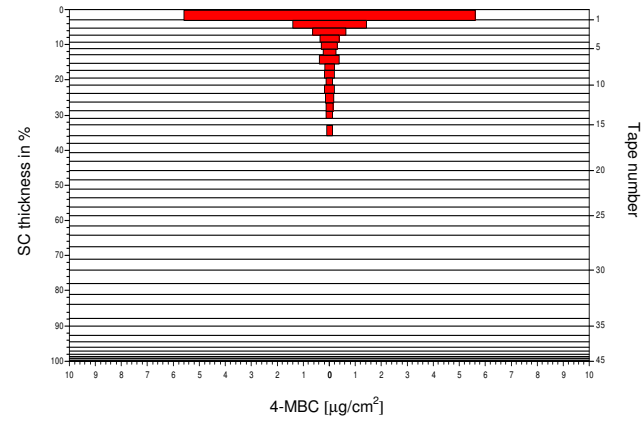


Transcutol[®]CG 10%, TI=6h, $AUC_{\text{conc-sc}} = 32.81$

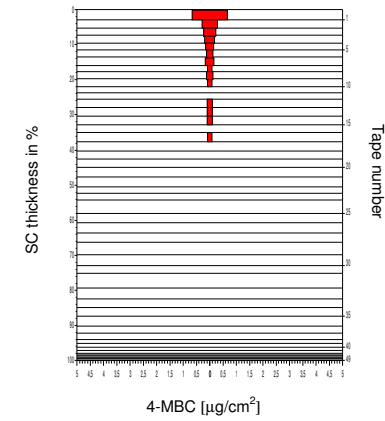


Volunteer 6

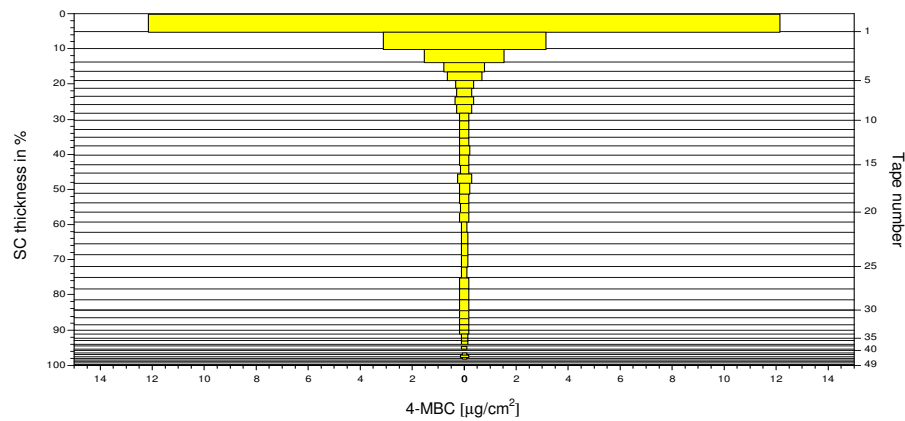
PEG 400, TI=0h, $AUC_{\text{conc-sc}} = 27.13$



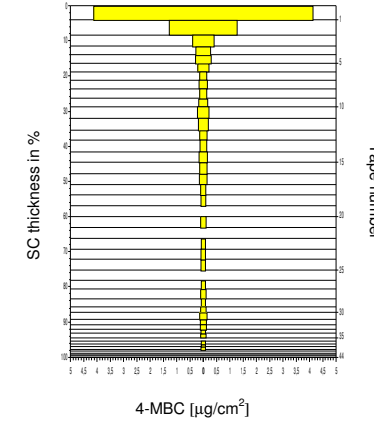
PEG 400, TI=6h, $AUC_{\text{conc-sc}} = 10.67$



Transcutol®CG 50%, TI=0h, $AUC_{\text{conc-sc}} = 71.87$

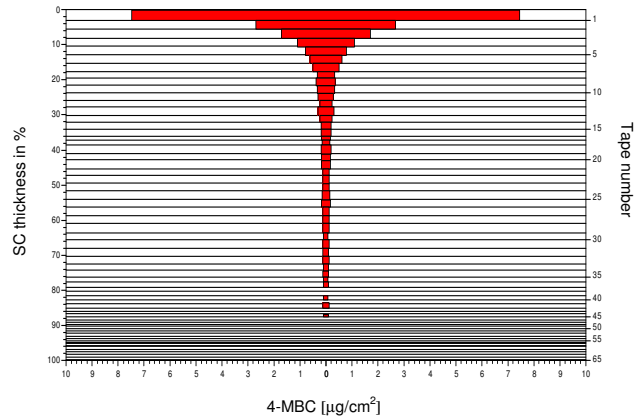


Transcutol®CG 50%, TI=6h, $AUC_{\text{conc-sc}} = 34.55$

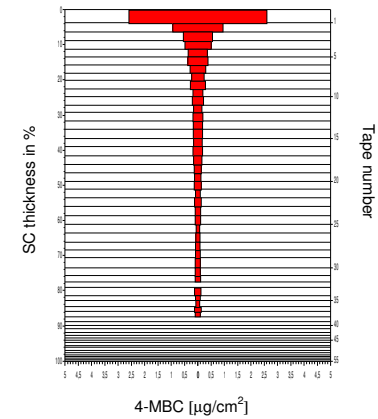


Volunteer 7

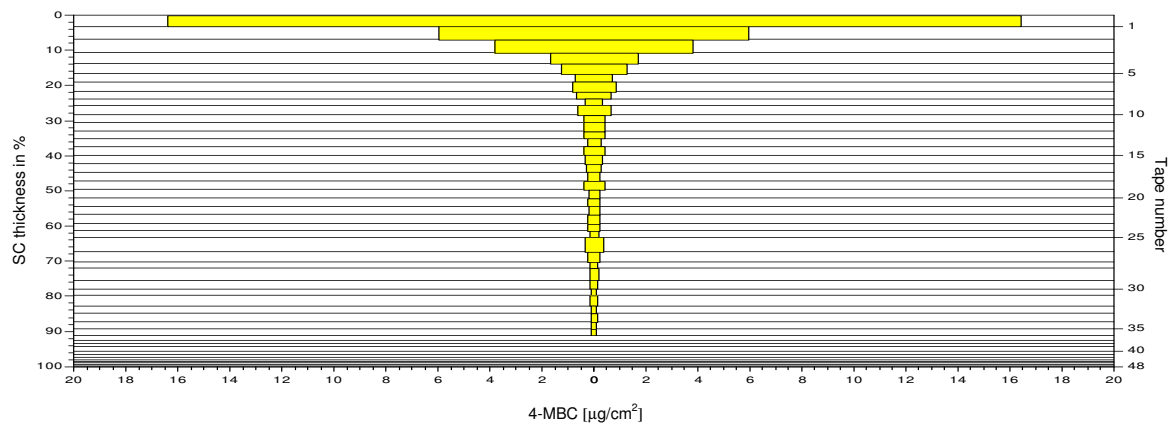
PEG 400, TI=0h, $AUC_{\text{conc-sc}} = 76.45$



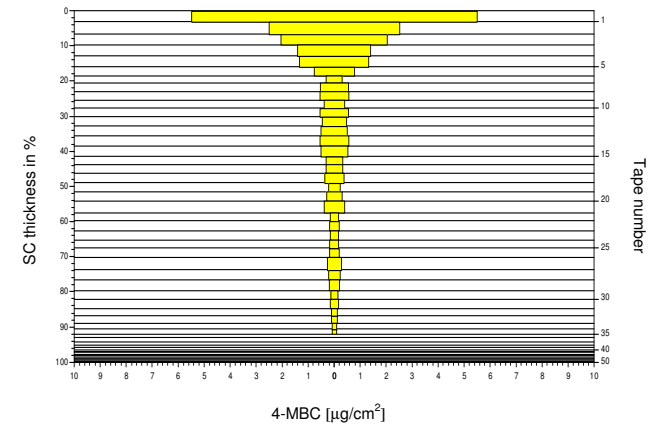
PEG 400, TI=6h, $AUC_{\text{conc-sc}} = 42.03$



Transcutol®CG 50%, TI=0h, $AUC_{\text{conc-sc}} = 131.24$

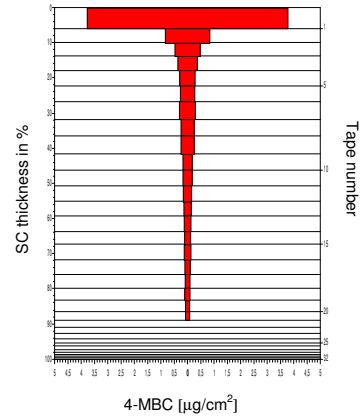


Transcutol®CG 50%, TI=6h, $AUC_{\text{conc-sc}} = 99.18$

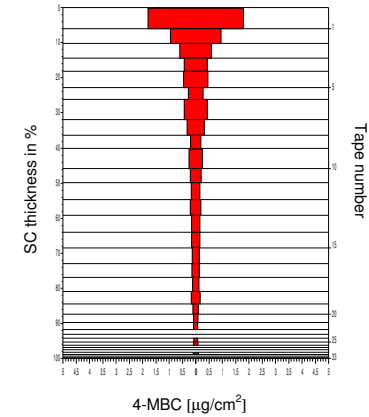


Volunteer 8

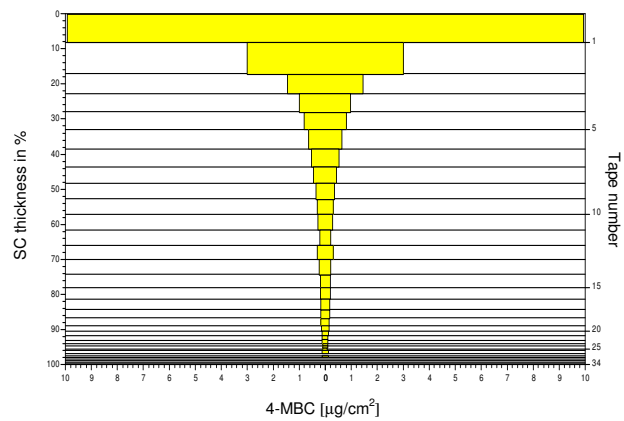
PEG 400, TI=0h, $AUC_{\text{conc-sc}} = 26.62$



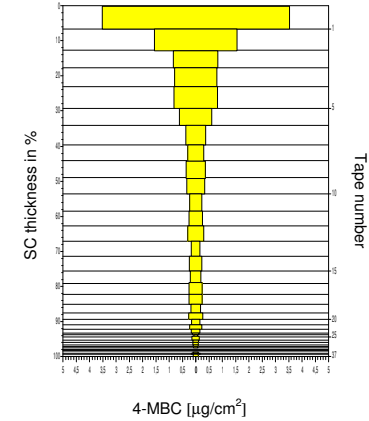
PEG 400, TI=6h, $AUC_{\text{conc-sc}} = 34.95$



Transcutol®CG 50%, TI=0h, $AUC_{\text{conc-sc}} = 67.62$

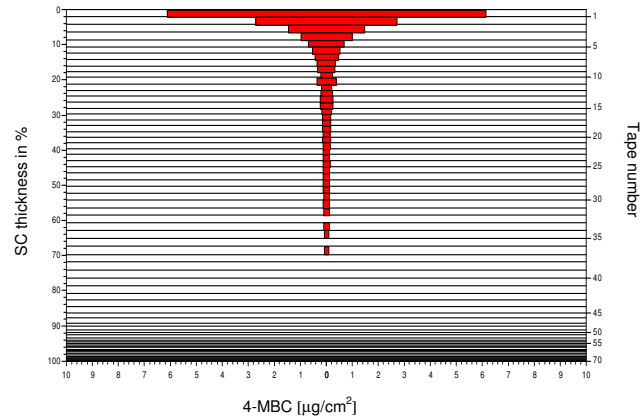


Transcutol®CG 50%, TI=6h, $AUC_{\text{conc-sc}} = 59.15$

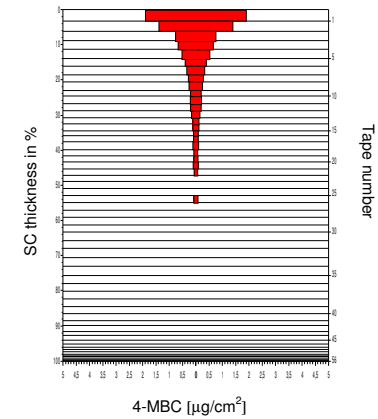


Volunteer 9

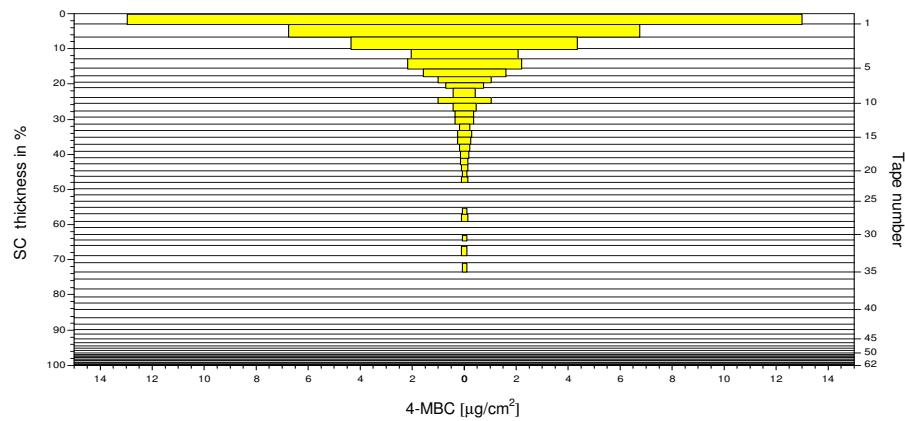
PEG 400, TI=0h, $AUC_{\text{conc-sc}} = 68.72$



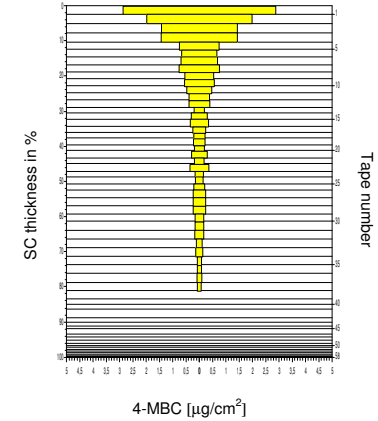
PEG 400, TI=6h, $AUC_{\text{conc-sc}} = 37.55$



Transcutol[®]CG 50%, TI=0h, $AUC_{\text{conc-sc}} = 138.60$

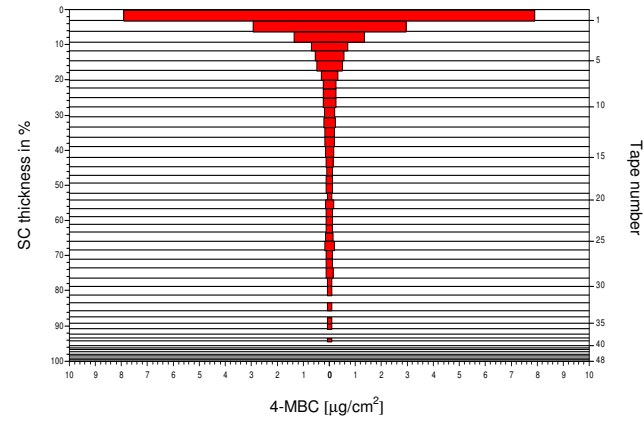


Transcutol[®]CG 50%, TI=6h, $AUC_{\text{conc-sc}} = 88.37$

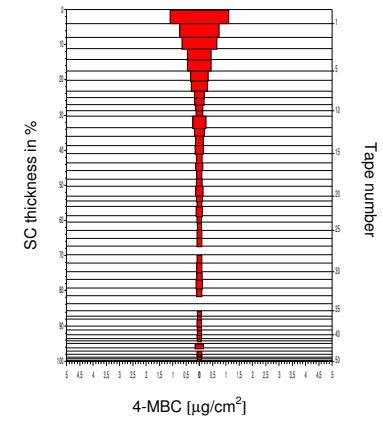


Volunteer 10

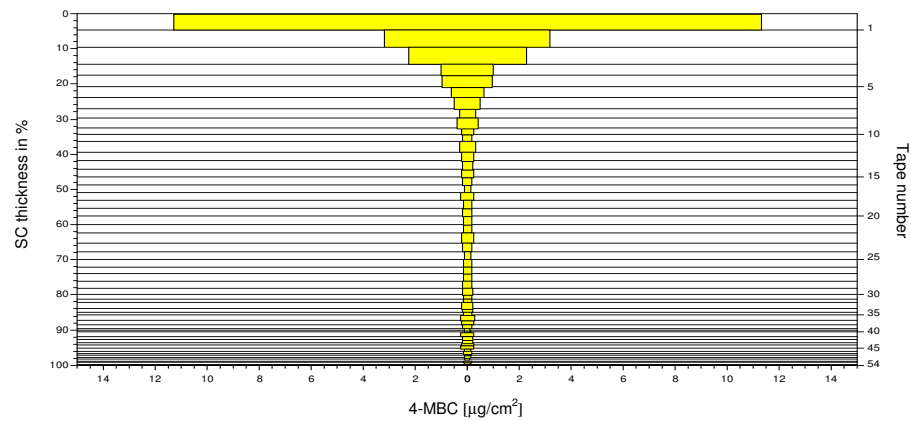
PEG 400, TI=0h, $AUC_{\text{conc-sc}} = 61.67$



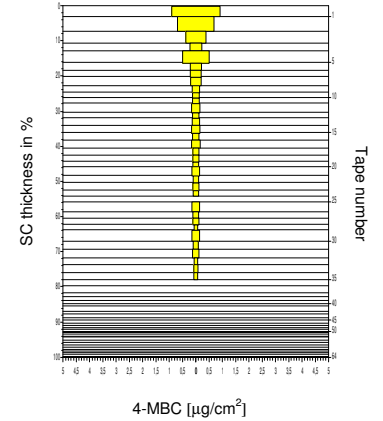
PEG 400, TI=6h, $AUC_{\text{conc-sc}} = 41.42$



Transcutol®CG 50%, TI=0h, $AUC_{\text{conc-sc}} = 101.71$



Transcutol®CG 50%, TI=6h, $AUC_{\text{conc-sc}} = 32.32$



10.7.4.2 Results for Experiment 3: $AUC_{conc-sc}$

For the calculation of the $AUC_{conc-sc}$, the first tape collected was discarded due to potential drug remaining on the skin surface.

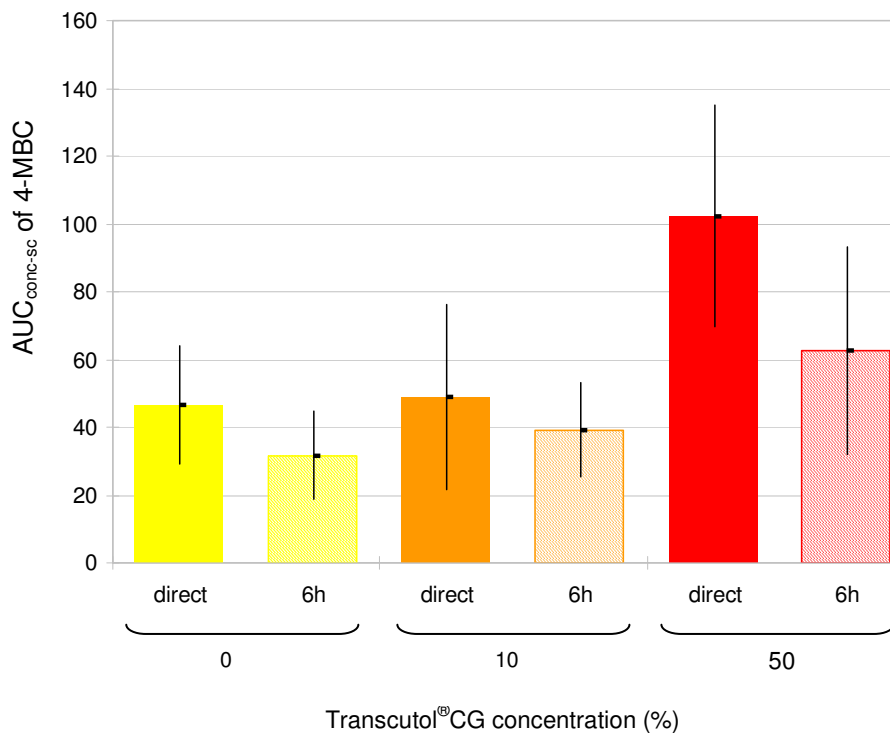


Figure 39. $AUC_{conc-sc}$ -values of 4-MBC after treating skin with PEG 400 formulations containing various concentrations of Transcutol®CG.

Legend. $\bar{x} \pm SD$ expressed as $AUC_{conc-sc}$ in $\mu\text{g}/\text{tape}$, $n=5$ except for 0% Transcutol®CG ($n=10$).

10.7.4.3 Statistical Analysis of results for Experiment 3

In Experiment 3, two variance analyses were conducted, one for F2 vs F1, one for F3 vs F1.

Table 36. Logarithmic AUCconc-sc-values of Experiment 3.

volunteer	0% Transcutol®CG		10% Transcutol®CG		50% Transcutol®CG	
	TI = 0h	TI = 6h	TI = 0h	TI = 6h	TI = 0h	TI = 6h
1	1.55	1.52	1.43	1.25	-	-
2	1.55	1.65	1.60	1.65	-	-
3	1.64	1.60	1.76	1.71	-	-
4	1.56	1.32	1.97	1.69	-	-
5	1.72	1.01	1.43	1.52	-	-
6	1.43	1.03	-	-	1.86	1.54
7	1.88	1.62	-	-	2.12	2.00
8	1.43	1.54	-	-	1.83	1.77
9	1.84	1.57	-	-	2.14	1.95
10	1.79	1.62	-	-	2.01	1.51

10.7.4.3.1 Formulation with 10% Transcutol®CG vs formulation with 0% Transcutol®CG

None of the examined main factors showed a significant impact on the amount of 4-MBC which penetrated the stratum corneum ($p > 0.05$).

No interaction could be traced ($p > 0.05$).

Thus, no difference with respect to the penetrated 4-MBC amount could be deduced from this constellation of experiments between the formulations 0% Transcutol®CG and 10% Transcutol®CG at any time.

Table 37. ANOVA for 4-MBC amount in SC from 0% and 10% Transcutol®CG formulations in Experiment 3 – Type III Sum of Squares.

Source	Sum of Squares	Df	Mean square	F-ratio	p value
main effects					
A: fomulation	0.0370	1	0.0370	0.99	0.3762
B: time intervall	0.0871	1	0.0871	2.33	0.2015
C: volunteer	0.2318	4	0.0580	1.55	0.3406
interactions					
AB	0.0168	1	0.0168	0.45	0.5390
AC	0.1676	4	0.0419	1.12	0.4571
BC	0.1033	4	0.0258	0.69	0.6356
residual	0.1495	4	0.0374		
total	0.7931	19			

All F-ratios are based on the residual mean square error.

10.7.4.3.2 Formulation with 50% Transcutol®CG vs formulation with 0% Transcutol®CG

The comparison of the formulation containing 50% Transcutol®CG and the formulation without Transcutol®CG by means of the variance analysis was statistically showed for the factors formulation ($p < 0.05$), time interval ($p < 0.05$) and volunteer ($p < 0.05$). However, no significant data arose in the test for interaction.

However, an addition of 50% Transcutol®CG caused a significant change in the amount of penetrating 4-MBC. The impact of the factor time interval shows that the amount of 4-MBC in the stratum corneum at TI = 6 h was significantly different from TI = 0 h. In contrast to other variance analyses, this comparison of formulations indicated a major difference among individual test persons (inter-individual distribution).

Table 38. ANOVA for 4-MBC amount in SC from 0% and 50% Transcutol®CG formulations in Experiment 3 - Type III Sum of Squares.

Source	Sum of Squares	Df	Mean Square	F-ratio	p value
main effects					
A: formulation	0.4440	1	0.4440	43.80	0.0027
B: time intervall	0.2376	1	0.2376	23.44	0.0084
C: volunteer	0.5174	4	0.1294	12.76	0.0151
interactions					
AB	0.0020	1	0.0647	0.20	0.6799
AC	0.0908	4	0.0354	2.24	0.2270
BC	0.0938	4	0.0333	2.31	0.2182
residual	0.0406	4	0.0162		
total	1.42628	19			

All F-ratios are based on the residual mean square error.

10.8 Calculation of intra–individual variance for determination of number of volunteers

In a clinical test that involves a topical formulation a test person is often treated on different skin patches (placebo and verum). Both formulations are tested on a candidate. Subsequently, a calculation of a number of volunteers is necessary in order to conduct such a pair experiment. Still the inter–individual dispersion has no influence on such a test constellation.

The intra-individual variance σ^2 can be estimated by the results of the variance analyses as average Mean Square Error (the Mean Square Errors of the three variance analyses are assessed together with the degrees of freedom for the average calculation). Departing from a proportional, relevant difference D between two formulations, the selectivity can be calculated by means of this variance for a given test scope (nomogram [253]) which means one can discern the probability based on which a certain impact occurs with a definite number n of test persons. The proportional difference D has to be recalculated to the difference δ of the natural logarithmic values when applying the nomogram. On the other hand, the nomogram permits the assessment of the required test scope based on the calculated impact and the determined selectivity.

Our estimated value for the intra-individual standard deviation σ equals 0.434. The required test scope can be read from the nomogram for definite, proportional differences at different selectivity.

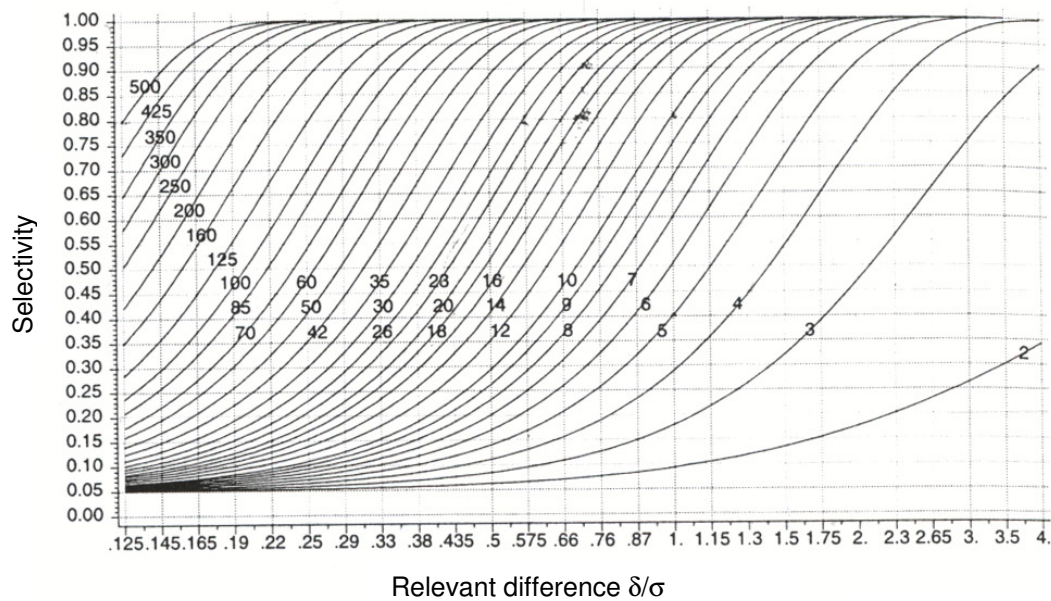


Figure 40. Nomogramm for determination of number of volunteers needed in a population to obtain statistical significance for results.

Table 39. Values read in the nomogram in order to assess the test scope based on known, relevant difference, D and selectivity.

	δ^b	δ/σ^c	selectivity					
			20%	40%	50%	60%	80%	100%
D^a =10%	0.095	0.22	30	55	85	110	180	500
D=20%	0.182	0.42	9	18	23	30	46	125
D=30%	0.262	0.60	6	10	13	16	25	60
D=40%	0.336	0.78	4	7	9	10	15	42
D=50%	0.405	0.93	4	6	7	8	12	26
D=60%	0.470	1.08	3	5	6	7	9	20
D=70%	0.530	1.22	3	4	5	6	7	16
D=80%	0.588	1.35	3	4	5	5	7	14
D=90%	0.642	1.48	3	4	4	5	6	12
D=100%	0.693	1.60	3	4	4	4	5	10

^a Relevant difference between 2 formulations

^b Difference of the natural logarithmic values

^c Relevant difference

11 References

1. Draft - Guidance for Industry. Topical dermatological drug product NDAs and ANDAs- In vivo bioavailability, bioequivalence, in vitro release, and associated studies. Center for Drug Evaluation and Research, Food And Drug Administration, U.S. Department of Health and Human Services, 1998, p 1-19.
2. Surber C, Schward FP, Smith EW. Tape-Stripping technique. In: Bronaugh RL, Maibach HI, eds. Percutaneous Absorption. 3rd ed. New York: Marcel Dekker; 1999. p. 395-425.
3. Bashir SJ, Chew A-L, Anigbogu A, Dreher F, Maibach HI. Physical and physiological effects of stratum corneum tape stripping. *Skin Res Technol* 2001;7:40-48.
4. Caron D, Queille-Roussel C, Shah VP, Schaefer H. Correlation between the drug penetration and the blanching effect of topically applied hydrocortisone creams in human beings. *J Am Acad Dermatol* 1990;23(3):458-462.
5. Henn U, Surber C, Schweitzer A, Bieli E. D-Squame adhesive tapes for standardized stratum corneum stripping. In: Brain KR, James VJ, Walters KA, eds. Prediction of Percutaneous Penetration; 1993; La Grande Motte, Languedoc, France: STS Publishing; 1993. p. 477-481.
6. Treffel P, Gabard B. Skin penetration and sun protection factor of ultra-violet filters from two vehicles. *Pharm Res* 1996;13(5):770-774.
7. Lotte C, Wester RC, Rougier A, Maibach HI. Racial differences in the in vivo percutaneous absorption of some organic compounds: a comparison between black, Caucasian and Asian subjects. *Arch Dermatol* 1993;284:456-459.
8. Dreher F, Arens A, Hostynek JJ, Mudumba S, Ademola J, Maibach HI. Colorimetric method for quantifying human stratum corneum removed by adhesive-tape-stripping. *Acta Derm Venereol* 1998;78(3):186-189.
9. Tsai J-C, Weiner ND, Flynn GL, Ferry J. Properties of adhesive tapes used for stratum corneum stripping. *Int J Pharm* 1991;72:227-231.
10. Martin E, Neillissen-Subnel MTA, De Haan FHN, Boddé HE. A critical comparison of methods to quantify stratum corneum removed by tape stripping. *Skin Pharmacol* 1996;9:69-77.
11. Kalia YN, Alberti I, Sekkat N, Curdy C, Naik A, Guy RH. Normalization of stratum corneum barrier function and transepidermal water loss in vivo. *Pharm Res* 2000;17(9):1148-1150.
12. Weigmann H-J, Lademann J, Meffert H, Schaefer H, Sterry W. Determination of the horny layer profile by tape stripping in combination with optical spectroscopy in visible range as a prerequisite to quantify percutaneous absorption. *Skin Pharmacol Appl Skin Physiol* 1999;12(1-2):34-35.
13. Lindemann U, Weigmann H-J, Schaefer H, Sterry W, Lademann J. Evaluation of the pseudo-absorption method to quantify human stratum corneum removed by tape stripping using the protein absorption. *Skin Pharmacol Appl Skin Physiol* 2003;16(4):228-236.
14. Weigmann H-J, Lindemann U, Antoniou C, Tsirikas GN, Stratigos AI, Katsambas A, et al. UV/VIS absorbance allows rapid, accurate, and reproducible mass determination of corneocytes removed by tape stripping. *Skin Pharmacol Appl Skin Physiol* 2003;16(4):217-227.
15. Schaefer H, Redelmeier TE. Structure and dynamics of the skin barrier. In: *Skin barrier: principles of percutaneous absorption*. Basel: Karger; 1996. p. 1-20.
16. Elias PM. Epidermal lipids, barrier function, and desquamation. *J Invest Dermatol* 1983;80:44s-49s.
17. Marks R, Barton SP. The significance of size and shape of corneocytes. In: Marks R, Plewig G, eds. *Straum corneum*. Berlin: Springer; 1983. p. 175-180.
18. Rawlings AV, Scott IR, Harding CR, Browser PA. Stratum corneum moisturization at the molecular level. *J Invest Dermatol* 1994;103:731-740.

11 References

19. Reichert U, Michels, Schmidt R. The cornified envelope: A key structure of terminally differentiating keratinocytes. In: Darmon M, Blumenberg M, eds. *The keratinocytes*. San Diego: Academic Press; 1993. p. 107-150.
20. Wertz PW, Swartzendruber DC, Kitko DJ, Madison KC, Downing DT. The role of the corneocyte lipid envelopes in cohesion of the stratum corneum. *J Invest Dermatol* 1989;93:169-172.
21. Wertz PW, Madison KC, Downing DT. Covalently bound lipids of the stratum corneum. *J Invest Dermatol* 1989;92:107-150.
22. Nemes Z, Steinert PM. Bricks and mortar of the epidermal barrier. *Exp Mol Med* 1999;31:5-19.
23. Dale BA, Holbrook KA, Steinert PM. Assembly of stratum corneum basic protein and keratin filaments in macrofibrils. *Nature* 1978;276:729-731.
24. Chapman SJ, Walsh A. Desmosomes, corneosomes and desquamation. *Arch Derm Res* 1990;282:304-310.
25. Serre G, Mils V, Haftek M. Identification of late differentiation antigens of human cornified epithelia, expressed in re-organized desmosomes and bound to cross-linked envelope. *J Invest Dermatol* 1991;97:1061-1072.
26. Haftek M, Serre G, Mils V, Thivolet J. Immunocytochemical evidence of the possible role of keratinocyte cross-linked envelopes in stratum corneum cohesion. *J Histochem Cytochem* 1991;30:153-158.
27. Warner RR, Myers MC, Taylor DA. Electron probe analysis of human skin: determination of the water concentration profile. *J Invest Dermatol* 1988;90(2):218-224.
28. von Zglinicki T, Lindberg M, Roomans GM, Forslind B. Water and ion-distribution profiles in human skin. *Acta Derm Venereol* 1993;73:340-343.
29. Kligman AM. Hydration injury to human skin: a view from the horny layer. In: Kanerva L, Elsner P, Wahlberg JE, Maibach HI, eds. *Handbook of occupational dermatology*. Berlin: Springer; 2000. p. 76-80.
30. Walters KA, Roberts M. The structure and function of the skin. In: Walters KA, ed. *Dermatological and transdermal formulations*. New York, Basel: Marcel Dekker, Inc.; 2002. p. 1-39.
31. Scheuplein RJ, Blank IH. Permeability of the skin. *Physiol Rev* 1971;51:702-747.
32. Blank IH. Further observations on factors which influence the water content of the stratum corneum. *J Invest Dermatol* 1953;21:259.
33. Elias PM, Friend DS. The permeability barrier in mammalian epidermis. *J Cell Biol* 1975;65:180-191.
34. Michaels AS, Chandrasekaran SK, Shaw JE. Drug permeation through human skin: Theory and in-vitro experimental measurements. *Am Inst Chem Eng* 1975;21(5):985-996.
35. Potts RO, Guy RH. Lipids alone account for stratum corneum permeability. *J Invest Dermatol* 1991;96:579.
36. Ward AJ, du Reau C. The essential role of lipid bilayers in the determination of stratum corneum permeability. *Int J Pharm* 1991;74:137.
37. Potts RO, Francoeur ML. The influence of stratum corneum morphology on water permeability. *J Invest Dermatol* 1991;96:120-130.
38. Wertz PW, Downing DT. Stratum corneum: biological and biochemical considerations. In: Hadgraft J, Guy RH, eds. *Transdermal drug delivery: developmental issues and research initiatives*. New York: Marcel Dekker; 1989. p. 1-22.
39. Suhonen TM, Bouwstra JA, Urtti A. Chemical enhancement of percutaneous absorption in relation to stratum corneum structural alterations. *J Control Release* 1999;59:149-161.
40. Matoltsy AG, Downes AM, Sweeney TM. Studies of the epidermal water barrier. Part II. Investigation of the chemical nature of the water barrier. *J Invest Dermatol* 1968;50:19-26.
41. Sweeney TM, Downing DT. The role of lipids in the epidermal barrier to water diffusion. *J Invest Dermatol* 1970;55:135-140.
42. Squier CA, Cox P, Wertz PW. Lipid content and water permeability of skin and oral mucosa. *J Invest Dermatol* 1991;96:123-126.

11 References

43. Vickers CFH. Existence of reservoir in the stratum corneum. *Arch Dermatol* 1963;88(July):72-75.
44. Barry Bw. *Dermatological formulations: Percutaneous absorption*. New York: Marcel Dekker; 1983.
45. Fritsch W, Stoughton RB. The effect of temperature and humidity on the penetration of C14 acetylic acid in excised human skin. *J Invest Dermatol* 1963;41:307-311.
46. Mackenzie AW, Stoughton RB. Method for comparing percutaneous absorption of steroids. *Arch Dermatol* 1962;86:608-610.
47. Vickers CFH. Stratum corneum reservoir for drugs. In: Montagna W, Van Scott EJ, Stoughton RB, eds. *Advances in biology of the skin; Pharmacology and the skin*. New York: Appleton-Century-Crofts; 1972. p. 177-189.
48. Stoughton RB. Dimethylsulfoxide (DMSO) induction of a steroid reservoir in human skin. *Arch Dermatol* 1965;91:657-660.
49. Stoughton RB. Hexachlorophene deposition in human stratum corneum. *Arch Dermatol* 1966;94(Nov):646-648.
50. White SH, Mirejovsky D, King GI. Structure of lamellar lipid domains and corneocyte envelopes of murine stratum corneum: an x-ray diffraction study. *Biochemistry* 1988;27:3725-3732.
51. Bouwstra JA, Dubbelaar FER, Gooris GS, Ponc M. The lipid organization in the skin barrier. *Acta Derm Venereol* 2000;208(Suppl):23-30.
52. Kitson N, Thewalt J, Lafleur M, Bloom M. A model membrane approach to the epidermal permeability barrier. *Biochemistry* 1994;33:6707-6715.
53. Gay CL, Guy RH, Golden GM, Mak VHW, Francoeur ML. Characterization of low temperature (i.e., <65°C) lipid transitions in human stratum corneum. *J Invest Dermatol* 1994;103:233-239.
54. Moore DJ, Rerek ME. Insights into the molecular organization of lipids in the skin barrier from infrared spectroscopy studies of stratum corneum lipid models. *Acta Derm Venereol* 2000;208(Suppl):16-22.
55. Pilgram GSK. A close look at the stratum corneum lipid organization by cryoelectron diffraction: Significance of the barrier function of human skin. Amsterdam: Leiden University; 2000.
56. Behne M, Uchida Y, Seki T, de Montellano PO, Elias PM, Holleran WM. Omega-hydroxyceramides are required for corneocyte envelope (CLE) formation and normal epidermal permeability barrier function. *J Invest Dermatol* 2000;114:185-192.
57. Bouwstra JA, Gooris GS, Cheng K, Weerheim A, Bras W, Ponc M. Phase behavior of isolated skin lipids. *Journal of lipid research* 1996;37:999-1011.
58. Bouwstra JA, Gooris GS, Dubbelaar FER, Weerheim AM, IJzerman AP, Ponc M. Role of ceramide 1 in the molecular organization of the stratum corneum lipids. *Journal of lipid research* 1998;39:186-196.
59. Bouwstra JA, Cheng K, Gooris GS, Weerheim A, Ponc M. The role of ceramides 1 and 2 in the stratum corneum lipid organisation. *Biochim Biophys Acta* 1996;1300:177-186.
60. Breathnach AS, Goodman T, Stolinky C, Gross M. Freeze-fracture replication of cells of stratum corneum of human epidermis. *J Anat* 1973;114(1):65-81.
61. Swartzendruber DC, Wertz PW, Kitko DJ, Madison KC, Downing DT. Molecular models of the intercellular lipid lamellae in mammalian stratum corneum. *J Invest Dermatol* 1989;92(2):251-257.
62. Holman BP, Spies F, Boddé HE. An optimized freeze-fracture replication procedure for human skin. *J Invest Dermatol* 1990;94(3):332-335.
63. Wertz PW, Downing DT. Acylglucosylceramides of pig epidermis: structure determination. *Journal of lipid research* 1983;24(6):753-758.
64. Bouwstra JA, Gooris GS, van der Spek JA, Lavrijsen S, Bras W. The lipid and protein structure of mouse stratum corneum: a wide and small angle diffraction study. *Biochim Biophys Acta* 1994;1212:183-192.
65. Bouwstra JA, Gooris GS, Bras W, Downing DT. Lipid organization in pig stratum corneum. *Journal of lipid research* 1995;36:685-695.

11 References

66. Bouwstra JA, Gooris GS, Salomons-de Vries MA, van der Spek JA, Bras W. Structure of human stratum corneum as function of temperature and hydration. A wide angle X-ray diffraction study. *Int J Pharm* 1992;84:205-216.
67. Bouwstra JA, Gooris GS, van der Spek JA, Bras W. Structural investigations of human stratum corneum by small angle x-ray scattering. *J Invest Dermatol* 1991;97:1004-1012.
68. Norlén L. Skin barrier structure and function: the single gel phase model. *J Invest Dermatol* 2001;117(4):830-836.
69. Chapman SJ, Walsh A, Jackson SM, Friedmann PS. Lipids, proteins and corneocyte adhesion. *Arch Derm Res* 1991;283:167-173.
70. Suzuki Y, Nomura J, Hori J, Koyama J, Takahashi M, Horii I. Detection and characterization of endogeneous protease associated with desquamation of stratum corneum. *Arch Derm Res* 2003;285:372-377.
71. Hansson L, Strömquist M, Bäckman A, Wallbrandt P, Carlstein A, Egelrud T. Cloning, expression, and characterization of stratum corneum chymotryptic enzyme. *J Biol Chem* 1994;269:19420-19426.
72. Brattsand M, Egelrud T. Purification, molecular cloning, and expression of human stratum corneum trypsin-like serine protease with possible function in desquamation. *J Biol Chem* 1999;274:30033-30040.
73. Rawlings A, Harding C, Watkinson A, Bank J, Ackerman C, Sabin R. The effect of glycerol and humidity on desmosome degradation in stratum corneum. *Arch Derm Res* 1995;287(5):457-464.
74. King IA, Tabiwo A, Purkis P, Leigh I, Magee AI. Expression of distinct desmocollin isoforms in human epidermis. *J Invest Dermatol* 1993;100(4):373-379.
75. Eckholm IE, Brattsand M, Egelrud T. Stratum corneum tryptic enzyme in normal epidermis: a missing link in the desquamation process? *J Invest Dermatol* 2000;114:56-63.
76. Egelrud T. Desquamation. In: Lodén M, Maibach HI, eds. *Dry skin and moisturizers*. Boca Raton: CRC Press; 2000. p. 109-117.
77. Sato J, Denda M, Nakanishi J, Nomura J, Koyama J. Cholesterol sulfate inhibits proteases that are involved in desquamation of stratum corneum. *J Invest Dermatol* 1998;111:189-193.
78. Lindberg M, Forslind B. The skin as a barrier. In: Lodén M, Maibach HI, eds. *Dry skin and moisturizers*. Boca Raton: CRC Press; 2000. p. 27-37.
79. Stick C, Pielke L. Die Zusammensetzung der solaren UV-Strahlung im Tagesverlauf. *Aktuelle Derm* 1998;24:159-163.
80. Roberts M. Exposure to the sun. In: Auerbach PS, Geehr RS, eds. *Management of wilderness and environmental emergencies*. 2nd ed. St. Louis: Mosby-Year Book; 1989.
81. Norris PG, Gange RW, Hawk JL. Acute effects of ultraviolet radiation on the skin. In: Freedberg IM, Austen KF, Eisen AZ, Wolff K, Fitzpatrick TB, eds. *Fitzpatrick's dermatology in general medicine*. 4th ed. New York: McGraw-Hill; 1993. p. 1651-1657.
82. Farr PM, Diffey BL. The erythema response of human skin to ultraviolet radiation. *Br J Dermatol* 1985;113:65-70.
83. Cadet J, Berger M, Douki T, Morin B, Raoul S, Ravanat JL, et al. Effects of UV and visible radiation on DNA final base damage. *Biol Chem* 1997;378:1275-1286.
84. Steger H, Roza L, Vink AA, Grewe M, Ruzicka T, Grether-Beck S, et al. Enzyme plus light therapy to repair DNA damage in ultraviolet-B-irradiated human skin. *Proc Natl Acad Sci USA* 2000;97(4):1790-1795.
85. Aberer W, Schuler G, Stingl G, Hönigsman H, Wolff K. Ultraviolet light depletes surface markers on Langerhans cells. *J Invest Dermatol* 1981;76:781-794.
86. Koulu L, Jansen CT, Viander M. Effect of UVA and UVB irradiation on human Langerhans cell membrane markers defined by ATPase activity and monoclonal antibodies (OKT 6 and anti-Ia). *Photodermatol* 1985;2:339-346.
87. Koulu L, Soderstrom KO, Jansen CT. Relation of antipsoriatic and Langerhans cell depleting effects of systemic psoralen photochemotherapy: a clinical, enzyme, histochemical, and electron microscopic study. *J Invest Dermatol* 1984;82:591-593.

11 References

88. Ashwoth J, Kahan MC, Breathnach L. PUVA therapy decreases HLA-DR, CD1a+ Langerhans cells and epidermal cell antigen-presenting capacity in human skin, but flow cytometrically-sorted residual HLA-Dr + CD1a+ Langerhans cells exhibit normal alloantigen presenting function. *Br J Dermatol* 1989;120:329-339.
89. Ullrich SE. Modulation of immunity by ultraviolet radiation: key effects on antigen presentation. *J Invest Dermatol* 1995;105:30S-36S.
90. Cooper KD, Fox P, Neises G, Katz SI. Effects of ultraviolet radiation on human epidermal cell antigen presentation: initial depression of Langerhans cell-dependent function is followed by the appearance of T6DR+ cells that enhance epidermal alloantigen presentation. *J Immunol* 1985;134(1):129-137.
91. Kim TY, Kripke ML, Ullrich SE. Immunodepression by factors released from UV-irradiated epidermal cells: selective effects on the generation of contact and delayed hypersensitivity after exposure to UVA and UVB radiation. *J Invest Dermatol* 1990;94:26-32.
92. Gibbs NK, Norval M, Traynor NJ, Wolf M, Johnson BA, Crosby J. Action spectra for the trans to cis photoisomerization of urocanic acid in vitro and in mouse skin. *Photochem photobiol* 1993;57:584-590.
93. Kaplan LA. Suntan, sunburn and sun protection. *J Wilderness Med* 1992;3:173-196.
94. Harber LC, DeLeo VA, Prystowsky JH. Intrinsic and extrinsic photoprotection against UVB and UVA radiation. In: Lowe NJ, Shaath N, eds. *Sunscreens: development, evaluation and regulatory aspects*. New York: Marcel Dekker; 1990. p. 359-378.
95. de Marly D. *The history of Haute-couture: 1850-1950*. London: Batsford; 1980.
96. Ananthaswamy HN, Loughlin SM, Cox P, Evans RL, Ullrich SE, Kripke ML. Sunlight and skin cancer: Inhibition of p53 mutations in UV irradiated mouse by sunscreens. *Nat Med* 1997;3(5):510-514.
97. Rosenstein BS, Phelps RG, Weinstock MA, Bernstein JL, Gordon ML, Rudikoff D, et al. p53 mutations in basal cell carcinomas arising in routine users of sunscreens. *Photochem photobiol* 1999;70(5):798-806.
98. Duteil L, Queille-Roussel C, Loesche C, Verschoore M. Assessment of the effects of a sunblock stick in the prevention of solar-simulating ultraviolet light-induced herpes labialis. *J Dermatol Treat* 1998;9:11-14.
99. Schaefer H, Moyal D, Fourtanier A. State of the art sunscreens for prevention of photodermatoses. *J Dermatol Sci* 2000;23 Suppl 1(Mar):S62-74.
100. US Department of Health EaW, Food and Drug Administration. Sunscreen products for over-the-counter human use. *Fed Reg* 1978;43:38206-38269.
101. COLIPA Sun protection test method. European Cosmetic, Toiletry and Perfumery Association (COLIPA). Brussels, Belgium 1994: 1-72.
102. Ferguson J. European guidelines (COLIPA) for evaluation of sun protection factors. In: Lowe NJ, Shaath N, Pathak MA, eds. *Sunscreens: development, evaluation and regulatory aspects*. 2nd ed. New York: Marcel Dekker; 1997. p. 513-525.
103. Sayre RM, Powell J, Rheins LA. Product application technique alters the sun protection factor. *Photodermatol Photoimmunol Photomed* 1991;8(5):222-224.
104. Morrison R, Boyd R. *Organic chemistry*. 3rd ed. Boston: Allyn & Bacon; 1973.
105. Sayre RM, Killias N, Roberts RL, Baqer A, Sadiq I. Physical sunscreens. *J Soc Cosmet Chem* 1990;41(2):103-109.
106. Lademann J, Weigmann H-J, Rickmeyer C, Berthelme H, Schaefer H, Mueller G, et al. Penetration of titanium dioxide microparticles in a sunscreen formulation into the horny layer and the follicular orifice. *Skin Pharmacol Appl Skin Physiol* 1999;12:247-256.
107. Guidance for Industry, Bioavailability and bioequivalence studies for orally administered drug products - General considerations. Food and Drug Administration, U.S. Department of Health and Human Services, 2000: 1-28.
108. Zatz JL. Optimizing skin delivery. *Cosmetics & Toiletries* 2000;115:31-35.
109. Zatz JL. Scratching the surface: Rationale and approaches to skin permeation. In: Zatz JL, ed. *Skin permeation, Fundamentals and application*. Wheaton, IL: Allured Publishing Corp.; 1993. p. 11-31.

11 References

110. Howes D, Guy RH, Hadgraft J, Heylings J, Hoeck U, Kemper F, et al. Methods for assessing percutaneous absorption: European centre for the validation of alternative methods (ECVAM); 1996.
111. Watkinson AC, Brain KR, Walters KA, Hadgraft J. Prediction of the percutaneous penetration of ultra-violet filters used in sunscreen formulations. *Int J Cosmet Sci* 1992;14:265-275.
112. Hagedorn-Leweke U, Lippold BC. Absorption of sunscreens and other compounds through human skin in vivo: Derivation of a method to predict maximum fluxes. *Pharm Res* 1995;12(9):1354-1360.
113. Fernandez C, Nielloud F, Fortuné R, Vian L, Marti-Mestres G. Benzophenone-3: rapid prediction and evaluation using non-invasive methods of in vivo human penetration. *J Pharm Biomed Anal* 2002;28:57-63.
114. Yano T, Nakagawa A, Tsuji M, Noda K. Skin permeability of various non-steroidal anti-inflammatory drugs in man. *Life Science* 1986;49:1043-1050.
115. Hayden CGJ, Roberts MS, Benson HAE. Systemic absorption of sunscreen after topical application. *Lancet* 1997;350:863-864.
116. Hany J, Nagel R. Nachweis von UV-Filtersubstanzen in Muttermilch. *Deutsche Lebensmittel-Rundschau* 1995;91(11):341-345.
117. Schlumpf M, Cotton B, Conscience M, Haller V, Steinmann B, Lichtensteiger W. In vitro and in vivo estrogenicity of UV screens. *Environ Health Perspect* 2001;109(3):239-244.
118. Comotto L, Bussi R. Unpublished data.
119. Bachmann S, Hellwig J. Unpublished data.
120. Bech-Thomsen N, Wulf HC. Sunbathers' application of sunscreen is probably inadequate to obtain the sun protection factor assigned to the preparation. *Photodermatol Photoimmunol Photomed* 1992/93;9:242-244.
121. Potts RO, Buras EM, Chrisman DA. Changes with age in the moisture content of human skin. *J Invest Dermatol* 1984;82:97-100.
122. Potts RO, Buras EM. In vivo changes in the dynamic viscosity of human stratum corneum as a function of age and ambient moisture. *J Soc Cosmet Chem* 1985;36:169-176.
123. Pochi PE, Strauss JS, Downing DT. Age-related changes in sebaceous gland activity. *J Invest Dermatol* 1979;73:108-111.
124. Lavker RM, Zheng P, Dong G. Morphology of aged skin. In: Gilchrist BA, ed. *Dermatologic Clinics: The aging skin*. Philadelphia: W. A. Saunders; 1986. p. 379-389.
125. Ryan TJ. Cutaneous circulation. In: Goldsmith LA, ed. *Biochemistry and Physiology of the Skin*. New York: Oxford University Press; 1983. p. 817-877.
126. Roskos KV, Maibach HI, Guy RH. The effect of aging on percutaneous absorption in man. *J Pharmacokinet Biopharm* 1989;17(6):617-630.
127. Weigand DA, Gaylor JR. Irritant reaction in negro and caucasian skin. *South Med J* 1974;67(5):548-551.
128. Johnson LC, Corah NL. Racial differences in skin resistance. *Science* 1960;139:766-767.
129. Reinertson RP, Wheatley VR. Studies on the chemical composition of human epidermal lipids. *J Invest Dermatol* 1959;32:49-59.
130. Berardesca E, Maibach HI. Racial differences in sodium lauryl sulphate induced cutaneous irritation: black and white. *Contact Dermatitis* 1987;17:12-17.
131. Williams RL, Thakker KM, John V, Lin ET, Gee WL, Benet LZ. Nitroglycerin absorption from transdermal systems: formulation effects and metabolic concentrations. *Pharm Res* 1991;8:744-749.
132. Lotte C, Rougier A, Wilson DR, Maibach HI. In vivo relationship between transepidermal water loss and percutaneous penetration of some organic compounds in man: Effect of anatomic site. *Arch Derm Res* 1987;279:351-356.
133. Feldmann RJ, Maibach HI. Regional variation in percutaneous penetration of ¹⁴C cortisol in man. *J Invest Dermatol* 1967;48(2):181-183.

11 References

134. Wester RC, Maibach HI. Regional variation in percutaneous absorption. In: Bronaugh RL, Maibach HI, eds. *Percutaneous absorption*. Basel: Marcel Dekker; 1989. p. 111-120.
135. Cummings EG. Temperature and concentration effects on penetration of N-octylamine through human skin in situ. *J Invest Dermatol* 1969;53:64-70.
136. Katz M, Poulsen BJ. Absorption of drugs through skin. In: Brodie BB, Gillette JR, eds. *Handbook of Experimental Pharmacology*. New York: Springer; 1971. p. 103-174.
137. Blank IH, Scheuplein RJ. The epidermal barrier. In: Rook AJ, Champion RH, eds. *Progress in the biological sciences in relation to dermatology*. Cambridge: University Press Cambridge; 1964. p. 245-261.
138. Bucks D, Maibach H. Occlusion does not uniformly enhance penetration in vivo. In: Bronaugh RL, Maibach H, eds. *Percutaneous absorption: drugs - cosmetics - mechanisms - methodology*. 3rd ed. New York: Marcel Dekker; 1999. p. 81-105.
139. Feldmann RJ, Maibach HI. Penetration of ¹⁴C hydrocortisone through normal skin: the effect of stripping and occlusion. *Arch Derm Res* 1965;91:661-666.
140. Cronin E, Stoughton RB. Percutaneous absorption, regional variations and the effect of hydration and epidermal stripping. *Br J Dermatol* 1964;74:265.
141. Malkinson FD. Permeating of the stratum corneum. In: Montagna W, Lobitz WC, Jr, eds. *The epidermis*. New York: Academic Press; 1964.
142. Riviere JE. Biological factors in absorption and permeation. In: Zatz JL, ed. *Skin permeation, Fundamentals and application*. Wheaton, IL: Allured Publishing Corp.; 1993. p. 113-126.
143. Behl CR, Flynn GL, Kurihara T, Harper N, Smith H, Higuchi WI, et al. Hydration and percutaneous absorption: I. Influence of hydration on alkanol permeation through hairless mouse skin. *J Invest Dermatol* 1980;75:346-352.
144. Corcuff P, Leveque JL. Corneocyte changes after acute UV irradiation and chronic solar exposure. *Photodermatol* 1988;5:110-115.
145. Maibach HI. *In vivo* percutaneous penetration of corticoids in man and unresolved problems in their efficacy. *Dermatologica* 1976;152, (Suppl. 1):11-25.
146. Levy G. The clay feet of bioequivalence testing. *J Pharm Pharmacol* 1995;47(12A):975-977.
147. Brown S, Diffey B. The effect of applied thickness on sunscreen protection: in vivo and in vitro studies. *Photochem photobiol* 1986;44(4):509-513.
148. Stokes R, Diffey B. How well are sunscreen users protected? *Photodermatol Photoimmunol Photomed* 1997;13:186-188.
149. Stenberg C, Larkö O. Sunscreen application and its importance for the sun protection factor. *Arch Dermatol* 1985;121:1400-1402.
150. Diffey BL, Grice J. The influence of sunscreen type on photoprotection. *Br J Dermatol* 1997;137(1):103-105.
151. Dupuis D, Rougier A, Roguet R, Lotte C, Kalopissis G. In vivo relationship between horny layer reservoir effect and percutaneous absorption in human and rat. *The Journal of Investigative Dermatology* 1984;82:353-356.
152. Wulf HC, Stender I-M, Lock-Andersen J. Sunscreens used at the beach do not protect against erythema: a new definition of SPF is proposed. *Photodermatol Photoimmunol Photomed* 1997;13:129-132.
153. Gottlieb A, Bourget TD, Lowe NJ. Sunscreens: Effects of amounts of application of sun protection factors. In: Lowe NJ, Schaath NA, Pathak MA, eds. *Sunscreens: Development, Evaluation and Regulatory Aspects*. New York: Marcel Dekker, Inc.; 1997. p. 583-588.
154. Autier P, Boniol M, Severi G, Doré J-F. Quantity of sunscreen used by European students. *Br J Dermatol* 2001;144:288-291.
155. Lynfield YL, Schechter BA. Choosing and using a vehicle. *J Am Acad Dermatol* 1984;10:56-59.
156. Rhodes LE, Diffey BL. Fluorescence spectroscopy: a rapid, noninvasive method for measurement of skin surface thickness of topical agents. *Br J Dermatol* 1997;136:12-17.

11 References

157. Grecnis PW, Stokes R. An evaluation of photographic methods to demonstrate the uniformity of sunscreen applied to the skin. *J Audiov Media Med* 1999;22(4):171-177.
158. Loesch H. Pitfalls in sunscreen application. *Arch Dermatol* 1994;130(may):665-666.
159. Azurdia RM, Pagliaro JA, Diffey BL, Rhodes LE. Sunscreen application by photosensitive patients is inadequate for protection. *Br J Dermatol* 1999;140:255-258.
160. Pruijm B, Green A. Photobiological aspects of sunscreen re-application. *Australas J Dermatol* 1999;40(1):14-18.
161. Schneider J. The teaspoon rule of applying sunscreen. *Arch Derm Res* 2002;138:838-839.
162. Taylor S, Diffey B. Simple dosage guide for suncreams will help users. *BMJ* 2002;324:1526.
163. Auton TR, Westhead DR, Woollen BH, Scott RC, Wilks MF. A physiologically based mathematical model of dermal absorption. *Hum Exp Toxicol* 1994;13:51-60.
164. Dupuis D, Rougier A, Roguet R, Lotte C. The measurement of the stratum corneum reservoir: a simple method to predict the influence of vehicles on in vivo percutaneous absorption. *Br J Dermatol* 1986;115:233-238.
165. Gupta VK, Zatz JL, Rerek M. Percutaneous absorption of sunscreens through Micro-Yucatan pig skin in vitro. *Pharm Res* 1999;16:1602-1607.
166. Fernandez C, Marti-Mestres G, Ramos J, Maillols H. LC analysis of benzophenone-3: II application to determination of 'in vitro' and 'in vivo' skin penetration from solvents, coarse and submicron emulsions. *J Pharm Biomed Anal* 2000;24:155-165.
167. Yener G, Hadgraft J, Pugh JW. Penetration of two sunscreens in various formulations through a synthetic membrane as compared to human skin in vitro. *Acta Pharmaceutica Turcica* 1998;XXXX(1):27-32.
168. Walters KA, Watkinson AC, Brain KR. In vitro skin permeation evaluation: the only realistic option. *Int J Cosmet Sci* 1998;20:307-316.
169. Kurul E, Hekimoglu S. Skin permeation of two different benzophenone derivatives from various vehicles. *Int J Cosmet Sci* 2001;23:211-218.
170. Jiang R, Roberts MS, Collins DM, Benson HAE. Absorption of sunscreens across human skin: an evaluation of commercial products for children and adults. *Br J Clin Pharmacol* 1999;48:635-637.
171. Lowe NJ, Weingarten D, Wortzman M. Sunscreens and phototesting. *Clin Dermatol* 1988;6:40-49.
172. Patel NP, Highton PM, Moy RL. Properties of topical sunscreen formulation. *J Der Surg Oncol* 1992;18:316-320.
173. Kaidbey KH. Substantivity and water resistance of sunscreens. In: Lowe NJ, Shaath N, eds. *Sunscreens: development, evaluation and regulatory aspects*. New York: Marcel Dekker; 1990.
174. Bottari F, Nannipieri E, Saettone MF, Serafini MF, Vitale D. Substantivity of sunscreens: a study on the interaction of four alkyl 4-aminobenzoates with keratin. *J Soc Cosmet Chem* 1978;29:353-363.
175. Saettone MF, Giannaccini B, Morganti C, Persi A, C. C. Substantivity of sunscreens: an appraisal of some quaternary ammonium sunscreens. *Int J Cosmet Sci* 1986;8:9-25.
176. Willis I, Kligman AM. Aminobenzoic acid and its esters. The quest for more effective sunscreens. *Arch Dermatol* 1970;102(4):405-417.
177. Goddard ED. Substantivity through cationic substitution. *Cosmetics & Toiletries* 1987;102:71-80.
178. Hagedorn-Leweke U, Lippold BC. Accumulation of sunscreens and other compounds in keratinous substrates. *Eur J Pharm Biopharm* 1998;46:215-221.
179. Saettone MF, Alderigi C, Giannaccini B, Anselmi C, Rossetti MG, Scotton M, et al. Substantivity of sunscreens - preparation and evaluation of some quaternary ammonium benzophenone derivatives. *Int J Cosmet Sci* 1988;10:99-109.
180. Monti D, Saettone MF, Centini M, Anselmi C. Substantivity of sunscreens - in vitro evaluation of the transdermal permeation characteristics of some benzophenone derivatives. *Int J Cosmet Sci* 1993;15:42-52.

11 References

181. Lorenzetti OJ, Boltralik J, Busby E, Fortenberry B. The influence of protein vehicles on the penetrability of sunscreens. *J Soc Cosmet Chem* 1975;26:593-609.
182. Felton LA, Wiley CJ, Godwin DA. Influence of hydroxypropyl- β -cyclodextrin on the transdermal permeation and skin accumulation of oxybenzone. *Drug Dev Ind Pharm* 2002;28(9):1117-1124.
183. Menon GK, Lee SH, Roberts MS. Ultrastructural effects of some solvents on the stratum corneum and other skin components: evidence for an extended mosaic partitioning model of the skin barrier. In: Roberts MS, Walters KA, eds. *Dermal absorption and toxicity assessment*. New York: Marcel Dekker; 1998. p. 727-751.
184. Munro DD. The relationship between percutaneous absorption and stratum corneum retention. *Br J Dermatol* 1969;81:92-97.
185. Godwin DA, Kim N-H, Felton LA. Influence of Transcutol CG on the skin accumulation and transdermal permeation of ultraviolet absorbers. *Eur J Pharm Biopharm* 2001;53:23-27.
186. Panchagnula R, Ritschel WA. Development and evaluation of an intracutaneous depot formulation of corticosteroids using transcutol as a cosolvent: In-vitro, ex-vivo rat studies. 1991;43:609-614.
187. Harrison JE, Watkinson AC, Green DM, Hadgraft J, Brain K. The relative effect of Azone and Transcutol on permeant diffusivity and solubility in human stratum corneum. *Pharm Res* 1996;13(4):542-546.
188. Yazdaniyan M, Chen E. The effect of diethylene glycol monoethyl ether as a vehicle for topical delivery of ivermectin. *Vet Res Commun* 1995;19(4):309-319.
189. Munro DD, Stoughton RB. Dimethylacetamide (DMAC) and dimethylformamide (DMFA) effect on percutaneous absorption. *Arch Dermatol* 1965;92(5):585-586.
190. Ritschel WA, Hussain AS. In vitro skin penetration of griseofulvin in rat and human skin from an ointment dosage form. *Arzneimittelforschung* 1988;38(11):1630-1632.
191. Nannipieri E, Carelli V, Di Colo G, Giorgi I, Serafini MF. Vehicle influence on the permeation of a highly lipophilic molecule. An in vitro technique to evaluate skin-vehicle interactions. *Int J Cosmet Sci* 1990;12:21-31.
192. Samour, Carlos M, Krauser, Scott F, inventors; MacroChem Corporation (Lexington, MA), assignee. Cationic film-forming polymer compositions, and the use thereof in topical agents delivery system and method of delivering agents to the skin. United States patent 5807957. 1998.
193. Hansenne I, Rick DW, inventors; Societe L'Oreal, S.d. (Paris, FR), assignee. Enhanced SPF sunscreen (sprayable) formulations comprising interpolymers of PVP/dimethiconylacrylate/polycarbonyl/polyglycol ester patent Appl. No. 791734. 2002.
194. Frater G, Schwarzenbach R, Van Oycke SFM, inventors; Givaudan-Roure Corporation (Clifton, NJ), assignee. Organosiloxane compounds patent 5 403 944 (Appl. No. 960384). 1995.
195. Wissing SA, Müller RH. A novel sunscreen system based on tocopherol acetate incorporated into solid lipid nanoparticles. *Int J Cosmet Sci* 2001;23:233-243.
196. Epstein WL, Shah VP, Riegelman S. Griseofulvin levels in stratum corneum. Study after oral administration in man. *Arch Dermatol* 1972;106:344-348.
197. Wallace SM, Shah VP, Epstein WL, Greenberg J, Riegelman S. Topically applied antifungal agents. *Arch Dermatol* 1977;113:1539-1542.
198. Faergemann J, Zehender H, Jones T, Maibach HI. Terbinafine levels in serum, stratum corneum, dermis-epidermis (without stratum corneum, hair, sebum and eccrine sweat). *Acta Derm Venereol* 1991;71(4):322-326.
199. Faergemann J, Zehender H, Denouel J, Millerioux L. Levels of terbinafine in plasma, stratum corneum, dermis-epidermis (without stratum corneum), sebum, hair and nails during and after 250 mg terbinafine orally once per day for four weeks. *Acta Derm Venereol* 1993;73(4):305-309.
200. Faergemann J, Laufen H. Levels of fluconazole in serum, stratum corneum, epidermis-dermis (without stratum corneum) and eccrine sweat. *Clin Exp Dermatol* 1993;18(2):102-106.

11 References

201. Marks R, Dawber RPR. Skin surface biopsy: an improved technique for examination of the horny layer. *Br J Dermatol* 1971;84:117-123.
202. Whiting DA, Bisset EA. The investigation of superficial fungal infections by skin surface biopsy. *Br J Dermatol* 1974;91:57-65.
203. Sheth NV, McKeough MB, Spruance SL. Measurement of stratum corneum drug reservoir to predict the therapeutic efficacy of topical iododeoxyuridine for herpes simplex. *J Invest Dermatol* 1987;89:598-602.
204. Öhman H, Vahlquist A. In vivo studies concerning a pH gradient in human stratum corneum and upper epidermis. *Acta Derm Venereol* 1994;74(5):375-379.
205. Lückner P, Nowak H, Stüttgen G, Werner G. Penetrationskinetik eines Tritium-markierten 9 alpha-Fluor-16 methylen-prednisolonesters nach epicutaner Applikation beim Menschen. *Arzneimittelforschung* 1968;18(1):27-29.
206. Tsai JC, Cappel MJ, Flynn GL, Weiner ND, Kreuter J, Ferry J. Drug and vehicle deposition from topical applications: use of *in vitro* mass balance technique with minoxidil solutions. *J Pharm Sci* 1992;81(8):736-743.
207. Tojo K, Lee ARC. A method for predicting steady-state rate of skin penetration in vivo. *J Invest Dermatol* 1989;92(1):105-108.
208. Eriksson G, Lamke L. Regeneration of human epidermal surface and water barrier function after stripping. A combined study with electron microscopy and measurement of evaporative loss. *Acta Derm Venereol* 1971;51(3):169-178.
209. Wilhelm D, Elsner P, Maibach HI. Standardized trauma (tape-stripping) in human vulvar and forearm skin. Effects on transepidermal water loss, capacitance and pH. *Acta Derm Venereol* 1991;71(2):123-126.
210. Downes AM, Matoltsy AG, Sweeney TM. Rate of turnover of the stratum corneum in hairless mice. *J Invest Dermatol* 1967;49(4):400-405.
211. Pinkus H. Examination of the epidermis by the strip method of removing horny layers. II. Biometric data on regeneration of human epidermis. *J Invest Dermatol* 1951;16:431-447.
212. Monash S. Location of the superficial epithelial barrier to skin penetration. *J Invest Dermatol* 1957;29:367-376.
213. Monash S, Blank IH. Location and reformation of the epithelial barrier to water vapor. *Arch Dermatol* 1958;78:710-714.
214. Moon KC, Wester RC, Maibach HI. Diseased skin models in the hairless guinea pig: *in vivo* percutaneous absorption. *Dermatologica* 1990;180:8-12.
215. Reed JT, Ghadially R, Elias PM. Skin type, but neither race nor gender, influence epidermal permeability barrier function. *Arch Dermatol* 1995;131(10):1134-1138.
216. Rougier A, Dupuis D, Lotte C, Maibach H. Stripping method for measuring percutaneous absorption in vivo. In: Bronaugh RL, Maibach HI, eds. *Percutaneous absorption*. 2nd ed. New York: Marcel Dekker; 1989. p. 415.
217. Rougier A, Rallis M, Krien P, Lotte C. In vivo percutaneous absorption: a key role for stratum corneum/vehicle partitioning. *Arch Dermatol* 1990;282:498-505.
218. Feldmann RJ, Maibach HI. Absorption of some organic compounds through the skin in man. *J Invest Dermatol* 1970;54:399-404.
219. Feldmann RJ, Maibach HI. Percutaneous penetration of some pesticides and herbicides in man. *Toxicol Appl Pharmacol* 1974;28:126-132.
220. Feldmann RJ, Maibach HI. Percutaneous penetration of steroids in man. *J Invest Dermatol* 1969;52(1):89-94.
221. Shah VP, Flynn GL, Yacobi A, Maibach HI, Bon C, Fleischer NM, et al. Bioequivalence of topical dermatological dosage forms - methods of evaluation of bioequivalence. AAPS/FDA Workshop on 'Bioequivalence of Topical Dermatological Dosage Forms - Methods of Evaluating Bioequivalence', September 4-6, 1996, Bethesda, Md. *Skin Pharmacol Appl Skin Physiol* 1998;11:117-124.
222. Shah S, Hare D, Dighe SV, Williams RL. Bioequivalence of topical dermatological products. In: Shah VP, Maibach HI, eds. *Topical drug bioavailability, bioequivalence and penetration*. New York: Plenum Press; 1993. p. 393-413.
223. Shah S. Challenges in evaluating bioequivalence of dermatological products. In: Surber C, Elsner P, Bircher AJ, eds. *Exogenous dermatology*. Basel: Karger; 1995. p. 152-157.

11 References

224. Shah VP, Flynn GL, Guy RH, Maibach H, Schaefer H, Skelly JP, et al. In vivo percutaneous penetration/absorption, Washington D.C., May 1989. *Pharm Res* 1991;8(8):1071-1075.
225. Huang YC, Lesko L, Schwartz P, Williams RL. Topical and transdermal generic products: regulatory issues and resolution. In: Brain KR, James VJ, Walters KA, eds. *Prediction of percutaneous penetration*; 1993. p. 463-472.
226. Shah VP. Topical dermatological drug product NDAs and ANDAs: in vivo bioavailability, bioequivalence, in vitro release, and associated studies. *Food and Drug Administration* 1998:1-19.
227. Coderch L, De Pera M, Perez-Cullell N, Estelrich J, de la Maza A, Parra JL. The effect of liposomes on skin barrier structure. *Skin Pharmacol Appl Skin Physiol* 1999;12:235-246.
228. Coderch L, Oliva M, Pons M, de la Maza A, Manich AM, Parra JL. Percutaneous penetration of liposomes using the tape stripping technique. *Int J Pharm* 1996;139:197-203.
229. van Hoogdalem EJ. Assay of erythromycin in tape strips of human stratum corneum and some preliminary results in man. *Skin Pharmacol* 1992;5:124-128.
230. van der Valk PG, Maibach HI. A functional study of the skin barrier to evaporative water loss by means of repeated cellophane-tape stripping. *Clin Exp Dermatol* 1990;15(3):180-182.
231. King CS, Barton SP, Nicholls S. The change in properties of the stratum corneum as a function of depth. *Br J Dermatol* 1979;100:165-172.
232. van der Molen RG, Spies F, van 't Noordende JM, Boelsma E, Mommaas M, Koerten HK. Tape stripping of human stratum corneum yields cell layers that originate from various depths because of furrows in the skin. *Arch Derm Res* 1997;289:514-518.
233. Surber C, Henn U, Bieli E, Schwarb FP, Gabard B, Ruffli T. Skin tape stripping: Is this technique adequate to explore principles of dermatopharmacokinetics? *Dermatology* 1999, in preparation.
234. Weigand DA, Gaylor JR. Removal of stratum corneum in vivo: an improvement on the cellophane tape stripping technique. *J Invest Dermatol* 1973;60(2):84-87.
235. Bommannan DB, Potts RO, Guy RH. Examination of stratum corneum barrier function in vivo by infrared spectroscopy. *J Invest Dermatol* 1990;95:403-408.
236. Kalia YN, Pirot F, Guy RH. Homogeneous transport in a heterogenous membrane: water diffusion across human stratum corneum. *Biophys J* 1996;71:2692-2700.
237. Pirot F, Kalia YN, Stinchcomb AL, Keating G, Bunge A, Guy RH. Characterization of the permeability barrier of human skin in vivo. *Proc Natl Acad Sci USA* 1997;94:1562-1567.
238. Pershing LK, Lambert L, Wright DE, Shah VP, Williams RL. Topical 0.05% bethamethasone dipropionate. *Arch Derm Res* 1994;130(6):740-747.
239. Pershing LK, Corlett JL, Lambert LD, Poncelet CE. Circadian activity of topical 0.05% betamethasone dipropionate in human skin in vivo. *J Invest Dermatol* 1994;102(5):734-739.
240. Fiedler M, Meier WD, Hoppe U. Texture analysis of the surface of human skin. *Skin Pharmacol* 1995;8:252-265.
241. Higo N, Naik A, Bommannan DB, Potts RO, Guy RH. Validation of reflectance infrared spectroscopy as a quantitative method to measure percutaneous absorption in vivo. *Pharm Res* 1993;10(10):1500-1506.
242. Rougier A, Dupuis D, Lotte C, Roguet R, Wester RC, Maibach HI. Regional variation in percutaneous absorption in man: measurement by the stripping method. *Arch Derm Res* 1986;278:465-469.
243. Pershing LK, Silver BS, Krueger GG, Shah VP, Skelley JP. Feasibility of measuring the bioavailability of topical betamethasone dipropionate in commercial formulations using drug content in skin and a skin blanching bioassay. *Pharm Res* 1992;9:45-51.
244. Wester RC, Maibach HI. Percutaneous absorption of drugs. *Clin Pharmacokinet* 1992;23(4):253-266.

11 References

245. Schiller M, Brzoska T, Bohm M, Metze D, Scholzen TE, Rougier A, et al. Solar-simulated ultraviolet radiation-induced upregulation of the melanocortin-1 receptor, proopiomelanocortin, and alpha-melanocyte-stimulating hormone in human epidermis in vivo. *J Invest Dermatol* 2004;122(2):468-476.
246. Guidance for Industry. Q2B Validation of analytical procedures: Methodology. International Conference on the Harmonization of Technical Requirements for the Registration of Pharmaceuticals for Human Use, Center for Drug Evaluation and Research, Center for Biologics Evaluation and Research, Food And Drug Administration, U.S. Department of Health and Human Services, 1996, p 1-10. Available from: URL: <http://www.fda.gov/cder/guidance/1320fnl.pdf>
247. Lademann J, Weigmann H-J, Lindemann U, Audring H, Antoniou C, Tsirikas G, et al. Investigations on the influence of furrows and wrinkles when quantifying penetration of drugs and cosmetics by tape stripping. In: Walters KA, ed. *Perspectives in Percutaneous Penetration*; 2002; Juans-Les Pins, Antibes; 2002. p. 49.
248. Loffler H, Dreher F, Maibach HI. Stratum corneum adhesive tape stripping: influence of anatomical site, application pressure, duration and removal. *British Journal of Dermatology* 2004;151(4):746-752.
249. Hannuksela M. Glycols. In: Maibach HI, ed. *Dry Skin and Moisturizers, Chemistry and Function*. Boca Raton, London, New York, Washington D.C.: CRC Press; 2000. p. 413- 419.
250. Bendas B, Neubert R, Wohrab W. Propylene Glycol. In: Maibach HI, ed. *Percutaneous Penetration Enhancers*. Boca Raton: CRC Press; 1995. p. 61-77.
251. Warner RR, Boissy YL. Effect of moisturizing products on the structure of lipids in the outer stratum corneum of humans. In: Maibach HI, ed. *Dry Skin and Moisturizers, Chemistry and Function*. Boca Raton, London, New York, Washington D.C.: CRC Press; 2000. p. 349-369.
252. Epstein H, Simion FA. Emulsion-based skincare products: Formulating and measuring their moisturizing benefits. In: Maibach HI, ed. *Handbook of cosmetic science and technology*. Basel: Marcel Dekker, Inc.; 2001. p. 511-529.
253. Trampisch HJ, Windeler J, Ehle B, Lange S. *Medizinische Statistik*. Berlin Heidelberg New York: Springer-Verlag; 1997.

12 Curriculum vitae

Personal data

Name Tatiana Fässler Tassopoulos
Place and date of birth Athens, 8 November, 1973
Citizen of Basel (BS)

Education / Experience

1979 - 1982 Primary School at École française de Nairobi, Kenya
1982 - 1984 Primary School at École française de Bâle, Basel, Switzerland
1984 - 1992 High School at Gymnasium Bäumlhof, Basel, Switzerland
Graduation (Matura) Type B (Latin and English)
1992 - 1997 School of Pharmacy, University of Basel, Switzerland
Master's Degree in Pharmaceutical Sciences
1994 - 1995 Pharmacy apprenticeship, Sonnen-Apotheke, Basel, Switzerland
1996 - 1998 Substituting pharmacist, Kirschgarten-Apotheke, Basel,
Switzerland
1998 Substituting pharmacist, St. Chrischona-Apotheke, Riehen,
Switzerland
1998 Substituting pharmacist, Apotheke Höschgasse, Zürich,
Switzerland
1999 Pharmacist, Division of Clinical Relations, Institute of Hospital
Pharmacy, University Hospital, Basel, Switzerland
1999 - 2006 PhD study at the Institute of Hospital Pharmacy and the
Department of Dermatology, University Hospital, Basel,
Switzerland
2003 - 2004 Director of Medical Relations
Laboratoire Pharmaceutique La Roche-Posay,
Département Cosmétique Active (Suisse) SA,
Groupe L'Oréal, Neuenhof, Switzerland

During my academic education I attended lectures and practical courses given by the following professors and lecturers:

Barras J-P, Bartels HC, Bienz KA, Bruppacher R, Durrer H, Eckert V, Erb P, Guentert TW, Haag D, Hädener A, Haefeli W, Haegeli A, Hersberger K, Hofbauer KG, Hunziker W, Iberg N, Imanidis G, Kress A, Leuenberger H, Maître L, Marbet GA, Meyer E, Meyer J, Meyer UA, Moroni C, Nicholls J, Oelhafen P, Pfeilschifter JM, Schaffner W, Scholer A, Seiler H, Séquin U, Sigel H, Spornitz UM, Stöckel KM, Tamm C, Van de Waterbeemd J, Weiss P, v Hahn H, Zuberbühler AD.